การสังเคราะห์สารประกอบกลูโคซิลจิบเบอเรลลิน (GA)
และการศึกษาหน้าที่ของเอนไซม์ GA เบตากลูโคซิเดสจากข้าว

นางหยานหลิง หัว

SYNTHESES OF GIBBERELLIN (GA) GLUCOSYL

CONJUGATES AND FUNCTIONAL STUDIES

OF RICE GA β–GLUCOSIDASE

Yanling Hua

A Thesis Submitted in Partial Fulfillment of the Requirements for the

Degree of Doctor of Philosophy in Biochemistry

Suranaree University of Technology

Academic Year 2012

SYNTHESES OF GIBBERELLIN (GA) GLUCOSYL CONJUGATES

AND FUNCTIONAL STUDIES OF RICE GA β-GLUCOSIDASE

Suranaree University of Technology has approved this thesis submitted in partial fulfillment of the requirements for the Degree of Doctor of Philosophy.

Thesis Examining Committee

_____

(Assoc. Prof. Dr. Jatuporn Wittayakun)

Chairperson

_____

(Prof. Dr. James R. Ketudat-Cairns)

Member (Thesis Advisor)

_____

(Dr. Prasat Kittakoop)

Member

_____

(Assoc. Prof. Dr. Mariena Ketudat-Cairns)

Member

_____

(Asst. Prof. Dr. Jaruwan Siritapetawee)

Member

_____   _____

(Prof. Dr. Sukit Limpijumnong)   (Assoc. Prof. Dr. Prapun Manyum)

Vice Rector for Academic Affairs   Dean of Institute of Science

หยานหลิง หัว : การสังเคราะห์สารประกอบกลูโคซิลจิบเบอเรลลิน (GA) และการศึกษา
หน้าที่ของเอนไซม์ GA เบตากลูโคซิเดสจากข้าว (SYNTHESES OF GIBBERELLIN (GA)
GLUCOSYL CONJUGATES AND FUNCTIONAL STUDIES OF RICE GA β-
GLUCOSIDASE) อาจารย์ที่ปรึกษา : ศาสตราจารย์ ดร.เจมส์ เกตุทัต-คาร์นส์, 157 หน้า.

เพื่อตรวจหาเอนไซม์เบตา-ดี-กลูโคซิเดสที่สามารถไฮโดรไลส์สารประกอบจิบเบอเรลลิน
(gibberellins, GA) จากข้าว สารประกอบจิบเบอเรลลิน 9 ชนิด ได้แก่ acetylated และ deacetylated
gibberellin GA_4 glucosyl ester (GA_4-Glc) acetylated และ deacetylated GA_3 glucosyl ester GA_4
methyl ester GA_3 methyl ester 3-O-β-D-glucopyranosyl gibberellin A_3 methyl ester 13-O-β-D-gluco-
pyranosyl gibberellin A_3 methyl ester และ β-D-glucopyranosyl gibberellin A_4 methyl ester
ถูกสังเคราะห์ขึ้น และ โครงสร้างของสารเหล่านี้ถูกวิเคราะห์ด้วย NMR และ LC-MS spectrometry

เพื่อตรวจหาเอนไซม์ GA เบตา-ดี-กลูโคซิเดสจากข้าว เอนไซม์เบตา-ดี-กลูโคซิเดสสกัดจากต้น
และใบของข้าวที่มีอายุ 10 วัน และแยกให้บริสุทธิ์ด้วย 7 ขั้นตอนแล้วตรวจหาเอนไซม์โดยการตรวจวัด
การย่อยสลายของ p-nitrophenyl β-D-glucopyranoside (pNPGlc) และ GA_4-Glc พบเอนไซม์ไกลโคไซด์
ไฮโดรเลส ตระกูล family 1 glycoside hydrolase (GH1) ที่สามารถย่อย GA_4-Glc ได้คือเอนไซม์
OS4BGlu13 เบตากลูโคซิเดส ซึ่งพิสูจน์ได้โดยการวิเคราะห์ด้วยวิธี LC-MS ของเปปไทด์ที่ได้จากการ
ย่อยของเอนไซม์ทริปซิน

แนวทางที่สองที่ใช้ตรวจหาเอนไซม์ GA เบตา-ดี-กลูโคซิเดสคือการทดสอบการย่อยสลาย
pNPGlc และ GA_4-Glc โดยเอนไซม์ไกลโคไซด์ไฮโดรเลสตระกูล GH1 ซึ่งเป็นเอนไซม์สายผสม
จากข้าว 5 ชนิด ได้แก่ Os3BGlu6 Os3BGlu7 (BGlu1) Os4BGlu12 Os3BGlu18 และ Os9BGlu31
พบว่า เอนไซม์ Os3BGlu6 มีความสามารถสูงสุดในการย่อยสลาย GA_4-Glc เพื่อเปรียบเทียบกลไก
การย่อยสลายของเอสเทอร์ (ester) และไกลโคไซด์ และการศึกษาการจับของ GA_4-Glc โดยเอนไซม์
เอนไซม์ Os3BGlu6 และเอนไซม์กลายพันธุ์ที่มีการดัดแปลงกรดอะมิโน M251N E178Q E178A
E394D และ E394Q ถูกสร้างขึ้นมาเพื่อทดสอบการย่อยสลายของ pNPGlc และ GA_4-Glc พบว่า
เอนไซม์กลายพันธุ์ Os3BGlu6 M251N สามารถย่อยสลาย pNPGlc ได้ร้อยละ 52 และ GA_4-Glc ได้
ร้อยละ 89 เมื่อเปรียบเทียบกับเอนไซม์ดั้งเดิม Os3BGlu6 เอนไซม์กลายพันธุ์ที่ตำแหน่งแอซิด-เบส
E178Q และ E178A ไม่สามารถย่อยสลาย pNPGlc ได้ แต่ยังคงสามารถย่อยสลาย GA_4-Glc ได้ร้อยละ 13
และ ร้อยละ 22 ตามลำดับเมื่อเทียบกับเอนไซม์ดั้งเดิม เอนไซม์กลายพันธุ์ที่ตำแหน่ง นิวคลีโอไฟล์
E394D และ E394Q ไม่สามารถย่อยสลายได้ทั้ง pNPGlc และ GA_4-Glc

การทดสอบการโยกย้ายหมู่น้ำตาลของเอนไซม์ Os3BGlu6 ดั้งเดิมและเอนไซม์กลายพันธุ์
พบว่าเอนไซม์ Os3BGlu6 E178Q และ E178A สามารถสร้างผลผลิตจากการเคลื่อนย้ายหมู่น้ำตาลได้
เมื่อ pNPGlc หรือ GA_4-Glc เป็นน้ำตาลหมู่ให้และเอไซด์เป็นหมู่รับ ซึ่งแยกผลิตภัณฑ์ที่ได้ออกจากกัน
ด้วย HPLC และวิเคราะห์ด้วย NMR และ mass spectrometry ของผลผลิตที่ได้ตรงกับ β-D-gluco-

pyranosyl azide การทำงานของเอนไซม์กับค่าพีเอชสำหรับการเคลื่อนย้ายหมู่น้ำตาลระหว่างเอไซด์และ GA$_4$-Glc ถูกทดสอบในบัฟเฟอร์โซเดียมอะซิเตทและ MES พบว่าเอนไซม์ Os3BGlu6 E178Q และ E178A มีค่าพีเอชเหมาะสมต่อการทำงานในบัฟเฟอร์ MES คล้ายกัน แต่มีค่าพีเอชเหมาะสมที่แตกต่างกันในบัฟเฟอร์โซเดียมอะซิเตท โดยพบว่าไอออนอะซิเตททำงานเป็นนิวคลีโอไฟล์ ซึ่งทำให้เอนไซม์สามารถกลับมาทำหน้าที่ของการไฮโดรไลลิสได้ การปรับความเข้มข้นของน้ำตาลหมู่ให้ GA$_4$-Glc และน้ำตาลหมู่รับโซเดียมเอไซด์เพื่อทดสอบผลกระทบต่อการเคลื่อนย้ายหมู่น้ำตาล พบว่าโซเดียมเอไซด์ที่ความเข้มข้นสูงสามารถยับยั้งการทำงานของเอนไซม์ Os3BGlu6 E178Q แต่ไม่มีผลต่อการทำงานของเอนไซม์ Os3BGlu6 E178A เมื่อความเข้มข้นของโซเดียมเอไซด์เพิ่มขึ้นถึง 400 mM การย่อยสลายและการเคลื่อนย้ายหมู่น้ำตาลของเอนไซม์ Os3BGlu6 และเอนไซม์กลายพันธุ์ ยืนยันกลไกการทำงานของเอนไซม์และหน้าที่ของกรดอะมิโน M251 E178 และ E394 ต่อการทำงานของเอนไซม์

สาขาวิชาชีวเคมี   ลายมือชื่อนักศึกษา_____

ปีการศึกษา 2555   ลายมือชื่ออาจารย์ที่ปรึกษา_____
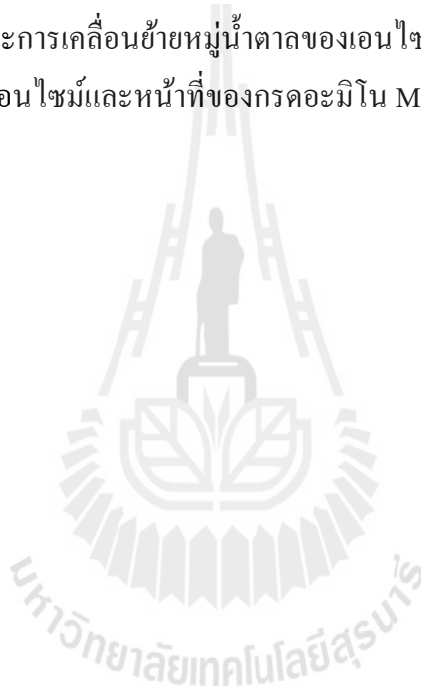
YANLING HUA : SYNTHESES OF GIBBERELLIN (GA) GLUCOSYL
CONJUGATES AND FUNCTIONAL STUDIES OF RICE GA β–
GLUCOSIDASE. THESIS ADVISOR : PROF. JAMES R. KETUDAT-CAIRNS,
Ph.D. 157 PP.

GIBBERELLIN/GIBBERELLIN A_4-GLUCOSYL ESTER/β-GLUCOSIDASE/RICE
/RECOMBINANT EXPRESSION/TRANSGLUCOSYLATION

In order to monitor the extraction of β-D-glucosidases that can hydrolyze gibberellin (GA) conjugates from rice, 9 GA conjugates, which included acetylated and deacetylated gibberellin GA_4 glucosyl esters (GA_4-Glc), acetylated and deacetylated GA_3 glucosyl esters, GA_4 methyl ester, GA_3 methyl ester, 3-O-β-D-glucopyranosyl gibberellin A_3 methyl ester, 13-O-β-D-glucopyranosyl gibberellin A_3 methyl ester and β-D-gluco-pyranosyl gibberellin A_4 methyl ester, were synthesized. Their structures were identified with nuclear magnetic resonance spectroscopy (NMR) and liquid chromatography-mass spectrometry (LC-MS).

To identify a GA β-D-glucosidase from rice, ten-day rice seedling shoots and leaves were extracted and the β-D-glucosidase activities were purified with seven purification steps. The fractions were monitored for hydrolysis of *p*-nitrophenyl β-D-glucopyranoside (*p*NPGlc) and GA_4-Glc. A family 1 glycoside hydrolase with relatively high activity to hydrolyze GA_4-Glc, Os4BGlu13 β-glucosidase, was identified in the final fraction by LC-MS of peptides generated by tryptic digestion.

In a second approach to identify a GA β-D-glucosidase, five recombinantly expressed rice GH1 enzymes, Os3BGlu6, Os3BGlu7 (BGlu1), Os4BGlu12, Os3BGlu18 and Os9BGlu31, were tested for relative hydrolysis activities toward *p*NPGlc and GA_4-Glc. Os3BGlu6 was found to have the highest hydrolysis activity to GA_4-Glc among these

enzymes. To compare the mechanism of hydrolysis of esters and glycosides and study GA$_4$-Glc binding, Os3BGlu6 and its mutants M251N, E178Q, E178A, E394D and E394Q were produced and their kinetic parameters for hydrolysis of pNPGlc and GA$_4$-Glc determined. The relative activities of Os3BGlu6 M251N were 52% for pNPGlc, 89% for GA$_4$-Glc compared to its wild type. The acid-base mutants E178Q and E178A were unable to hydrolyze pNPGlc, but maintained 13% and 22% of their activities toward GA$_4$-Glc compared to their wild type, respectively. The nucleophile mutants E394D and E394Q were found to completely lose hydrolytic activity for both pNPGlc and GA$_4$-Glc.

The transglucosylation activities were studied for Os3BGlu6 and its mutants. Both Os3BGlu6 E178Q and E178A could produce transglucosylation products when pNPGlc or GA$_4$-Glc was used as donor and sodium azide as acceptor. The prominent transglucosylation product was isolated by HPLC, and identified by NMR and mass spectra as β-D-glucopyranosyl azide. The activities versus pH profiles for transglucosylation of azide with GA$_4$-Glc donor were determined in sodium acetate and MES buffers. The Os3BGlu6 E178Q and E178A mutants showed similar optimum pH ranges in MES buffer, but different optimum pH in sodium acetate buffer. The acetate ion was found to act as a nucleophile in the reaction to rescue the hydrolysis activity. The concentrations of GA$_4$-Glc donor and sodium azide acceptor were varied to test their effects on transglucosylation kinetics. High concentrations of sodium azide were found to inhibit the reaction for Os3BGlu6 E178Q, but not for Os3BGlu6 E178A when the concentration of Na-azide was increased up to 400 mM. The hydrolysis and transglucosylation activities for Os3BGlu6 and its mutants confirmed its retaining catalytic mechanism, and the roles of the residues M251, E178 and E394 in the catalytic process.

School of Biochemistry   Student's signature_____

Academic Year 2012   Advisor's signature_____

ACKNOWLEDGEMENTS

Lastly, my deepest gratitude will go to my husband, Prof. Dr. Yupeng Yan, for taking over my family work, unconditionally supporting my study and work, encouraging me and advising me whenever I met a problem, to make my dream become true.

Yanling Hua

CONTENTS

CONTENTS (Continued)

CONTENTS (Continued)

CONTENTS (Continued)

CONTENTS (Continued)

LIST OF TABLES

LIST OF FIGURES

LIST OF FIGURES (Continued)

LIST OF FIGURES (Continued)

LIST OF FIGURES (Continued)

LIST OF FIGURES (Continued)

LIST OF FIGURES (Continued)

LIST OF FIGURES (Continued)

LIST OF ABBREVIATIONS

ABA	Abscissic acid
ABA-GE	Abscisic acid-glucose ester
Abg	*Agrobacterium faecalis* β-glucosidase
AtBG1	*Arabidopsis* β-glucosidase
Å	Ångstrom, a unit of length equal to 1×10^{-10} m
A_{405}	Absorbance at 405 nm
Abs	Absorbance
ABTS	2,2'-Azinobis-3-ethylbenthaiazolinesulfonic acid
ACN	Acetonitrile
Ag_2O	Silver oxide
API-ES	Atmospheric pressure ionization-electro spray
bp	Base pairs
BSA	Bovine serum albumin
°C	Degrees Celsius
CBB	Coomassie brilliant blue
$CDCl_3$	Deuterated chloroform
cDNA	Complementary deoxynucleic acid
$CHCl_3$	Chloroform
CH_2Cl_2	Methylene dichloride
CV	Column Volume (s)
Diazald	*p*-Toluenesulphonylmethylnitrosamide

LIST OF ABBREVIATIONS (Continued)

DIMBOAGlc	2-O-β-D-glucopyranosyl-4-hydroxy-7-methoxy-1,4-benzoxaxin-3-one
DMSO	Dimethyl sufoxide
DMSO-d_6	Dimethy sulfoxide containing 6 deuterium atoms
DNA	Deoxynucleic acid
DNase	Deoxyribonuclease
dNPGlc	2,4-Dinitrophenyl β-D-glucoside
dNTPs	Deoxynucleoside triphosphates
DP	Degree of polymerization
E. coli	*Escherichia coli*
EDTA	Ethylenediamine tetraacetate
ESI-MS	Electrospray ionization-mass spectrometry
EtOAc	Ethyl acetate
2F-DNPG (dNP2FGlc)	2′,4′-Dinitrophenyl-2-deoxy-2-fluoro-β-D-glucopyranoside
G2F	2-Deoxy-2-fluoro-α-D-glucopyranoside
GA_n	Gibberellin A_n
GA_3	Gibberellic acid
GA_3-Glc	GA_3-glucosyl ester
GA_3-OMe	Gibberellin methyl esters of GA_3
GA_3-OMe-Glc	β-D-glucopyranosyl gibberellin A_3 methyl ester
GA_3-OMe-Glc-Ac_4	Tetra acetylated β-D-glucopyranosyl gibberellin A_3 methyl ester
GA_3-OMe-3-O-Glc	3-O-β-D-glucopyranosyl gibberellin A_3 methyl ester

LIST OF ABBREVIATIONS (Continued)

GA$_3$-OMe-13-O-Glc	13-O-β-D-glucopyranosyl gibberellin A$_3$ methyl ester
GA$_4$-Glc	GA$_4$-glucosyl ester
GA$_4$-OMe	Gibberellin methyl esters of GA$_4$
GC-MS	Gas chromatography–mass spectrometry
GH	Glycoside hydrolase
GH1	Glycoside hydrolase family 1
Glc	Glucose
h	Hour(s)
HEWL	Egg-white lysozyme
HPLC	High performance liquid chromatography
IAA	Indole-3-acetic acid
IAA-GE	Indole-3-acetic acid-glucosyl ester
IMAC	Immobilized metal affinity chromatography
IPTG	Isopropyl thio-β-D-galactoside
JA	Jasmonic acid JA
kb	Kilo base pair(s)
kDa	Kilo Dalton(s)
KLrP	Klotho-related protein
LB	Luria-Bertani lysogeny broth
LC-MS	Liquid chromatography-mass spectrometry
MALDI-TOF	Matrix-assisted laser desorption/ionization-time-of-flight
MeOH	Methanol
MES	2-Morpholinoethanesulfonic acid

LIST OF ABBREVIATIONS (Continued)

min	Minute(s)
(m, μ, n)g	(milli, micro, nano) Gram(s)
(m, μ)l	(milli, micro) Liter(s)
(m, μ)M	(milli, micro) Molar(s)
(m, μ, f)mol	(milli, micro, femto) Mole(s)
MW	Molecular weight
MWCO	(Membrane) molecular-weight-cut-off
N	Normal (concentration)
N_2	Nitrogen gas
Na_2HPO_4	Disodium hydrogen phosphate
NaCl	Sodium chloride
NAG2FGlcF	2-Acetamido-2-deoxy-β-D-glucopyranosyl-(1→4)-2-deoxy-2-fluoro-β-D-glucopyranosylfluoride
$NaHCO_3$	Sodium bicarbonate
NaOMe	Sodium methoxide
Na_2CO_3	Sodium carbonate
Na_2HPO_4	Disodium hydrogen phosphate
Na_2SO_4	Sodium sulphate
NH_4HCO_3	Ammonium bicarbonate
$(NH_4)_2SO_4$	Ammonium sulphate
nm	nanometer(s)
NMR	Nuclear magnetic resonance
OD	Optical density

LIST OF ABBREVIATIONS (Continued)

OsTAGG1	Rice tuberonic acid glucoside-hydrolyzing β–D-glucosidase 1
PAGE	Polyacrylamide gel electrophoresis
PCR	Polymerase chain reaction
PEG	Polyethylene glycol
PGO assay	Peroxidase/glucose oxidase-based assay
PMSF	Phenylmethylsulfonylfluoride
*p*NP	*para*-Nitrophenyl
*p*NPGlc	*p*-Nitrophenyl-β-D-glucopyranoside
*p*NPTGlc	*p*-Nitrophenyl-β-D-thioglucopyranoside
PVDF	Polyvinylidene fluoride
qMS/MS	Tandem quadrupole mass spectrometer
RNA	Ribonucleic acid
RNase	Ribonuclease
RP-HPLC	Reversed phase HPLC
rpm	Rotations per minute
s	Second(s)
SbDhr1	Sorghum β-glucosidase Dhr1
SDS	Sodium dodecyl sulfate
SIM	Selective ion monitoring
SPE	Solid Phase Extraction
TA	Tuberonic acid
TAG	Tuberonic acid glucoside

LIST OF ABBREVIATIONS (Continued)

TEMED	N,N′,N″,N‴-tetramethylethyllenediamine
TEV	Tobacco etch virus
TFA	Trifluoroacetic acid
TLC	Thin-layer chromatography
TMS	Tetramethylsilane
Tris	Tris-(hydroxymethyl)-aminoethane
Tris-HCl	Tris(hydroxymethyl)aminomethane hydrochloride
UPLC	The ultra-performance liquid chromatography
UV	Ultraviolet
v/v	Volume/volume
w/v	Weight/volume
ZmGlu1	Maize β-glucosidase Glu1

CHAPTER I

INTRODUCTION

1.1 Overview of Gibberellins

1.1.1 Gibberellin classification, functions and applications

The gibberellins (GAs) are a class of plant hormones that play important roles in various plant growth phenomena, including seed germination, stem elongation, flower development, etc. They are highly functionalized diterpenoids and are distributed widely in plants, fungi and bacteria. Gibberellins were first isolated from the pathogenic fungus *Gibberella fujikuroi*, from which they derive their name. The presence of large quantities of GAs as secondary metabolites in this fungus leads to the extensive overgrowth of infected rice plants.

The gibberellins are classified on the basis of structure as well as function. Naturally occurring tetracyclic diterpenoid acids with structures based on the ent-gibberellane carbon skeleton (Figure 1.1) are named GA_1 to GA_n in the order of their discovery (Phinney, 1983; Tamura, 1990).

Among the 136 known GAs, only a few are biologically active. These include GA_1, GA_3, GA_4, GA_5, GA_6 and GA_7 (Figure 1.2). Gibberellic acid (GA_3), which was the first gibberellin to be structurally characterized, has been widely used to regulate plant growth and development. For example, GA_3 is widely used in the grape-growing industry as a hormone to induce the production of larger bundles and bigger grapes, especially for Thompson seedless grapes.
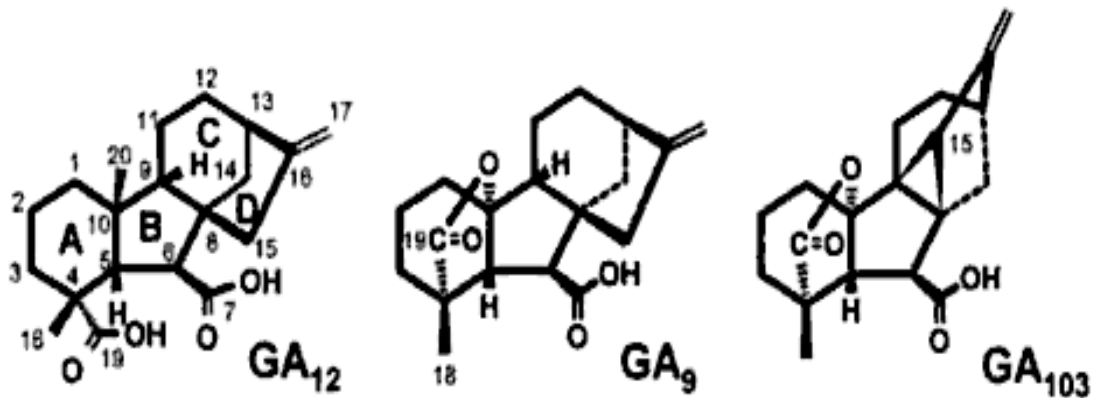
Figure 1.1 Structures of gibberellins with different levels of structural complexity. GA_{12} is a C20-GA with the ent-gibberellane skeleton; GA_9 is the simplest C19-GA, which has an ent-20-norgibberellane skeleton; and GA_{103} has an extra cyclopropane ring (Sponsel and Hedden, 2004).
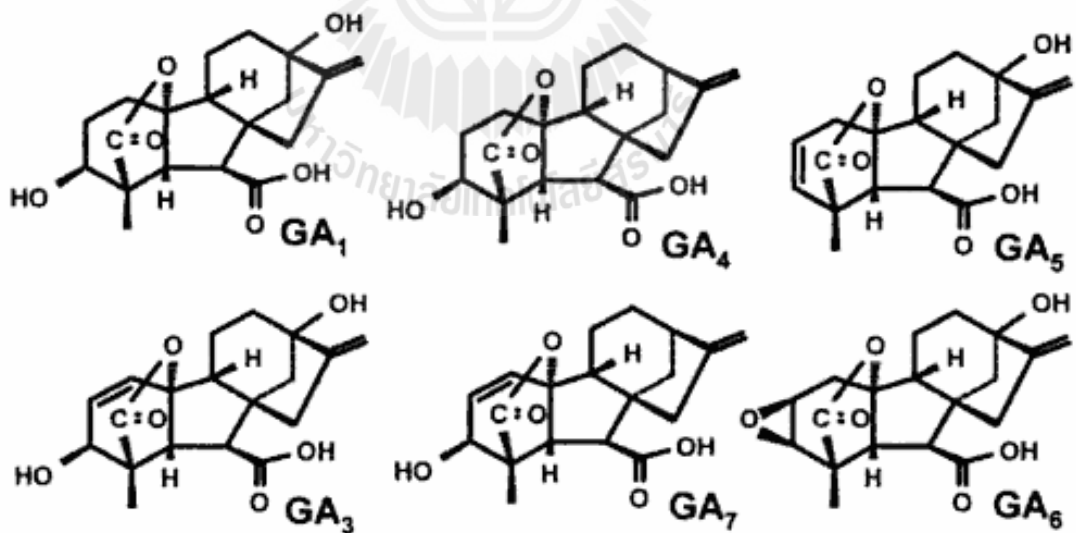
Figure 1.2 The structures of the main growth-active GAs (Sponsel and Hedden, 2004).

Active gibberellins show many physiological effects, each depending on the type of gibberellin present, as well as the species of plant. Gibberellins have been found to be involved in many physiological processes (Davies, 1995; Mauseth, 1991; Raven et al.,

1992; Salisbury and Ross, 1992). They stimulate stem elongation by stimulating cell division and elongation. They stimulate bolting /flowering in response to long days. They also break seed dormancy in some plants that require stratification or light to induce germination. They stimulate enzyme (α-amylase) production in germinating cereal grains for mobilization of seed reserves. GAs also induce maleness in dioecious flowers (sex expression). They can cause parthenocarpic (seedless) fruit development and delay senescence in leaves and citrus fruits.

The bioactive GAs exist in the plants together with many inactive GAs and their glucosyl conjugates, which may be inactive precursors or deactivation products of the active forms. The concentrations of bioactive GAs in plants are in the range of 10^{-11}-10^{-9}g /g fresh weight, depending on the tissue and species, and are closely regulated by the GA biosynthetic and catabolic pathways (Sponsel and Hedden, 2004).

Occurrence of GAs in plants, fungi and bacteria has been widely studied (MacMillan, 2002). The data show the widespread natural occurrence of GAs in 128 plants, 7 fungi and 7 bacteria. GA_1 is the most widespread (86 plants) and its precursors in the early 13-hydroxylation pathway occur with increasing frequency from GA_{53} (35 plants) to GA_{44} (44 plants) to GA_{19} (75 plants) to GA_{20} (80 plants). A similar increasing sequence of occurrence of the members of the non-early 13-hydroxylation precursors to GA_4 and GA_9 is evident, namely, GA_{12} (21 plants) to GA_{15} (25 plants) to GA_{24} (25 plants) to GA_9 (50 plants) and GA_4 (54 plants). Gibberellin GA_3, the major GA of *Gibberella fujikuroi*, has now been shown to occur in 45 plants, but not in rice (*Oryza sativa*). At least 12 GAs were found in rice so far, as shown in Table 1.1.

Table 1.1 Occurrence of gibberellins in rice (*Oryza sativa*) (MacMillan, 2002).

Gibberellin	Tissue	Reference
GA_1	immature seeds	Kobayashi et al. (1984)
GA_1	shoots and roots	Kurogoshi et al. (1979)
GA_1	ears	Suzuki et al. (1981)
GA_4	immature seeds, ears	Kobayashi et al. (1984)
GA_4	spikelets	Kobayashi et al. (1988)
GA_9	immature seeds, ears	Kobayashi et al. (1984)
GA_{17}	spikelets	Kobayashi et al. (1988)
GA_{19}	immature seeds	Kobayashi et al. (1984)
GA_{19}	spikelets	Kobayashi et al. (1988)
GA_{19}	roots, shoots, ears	Kurogochi et al. (1979)
GA_{20}	immature seeds, ears	Kobayashi et al. (1984)
GA_{20}	spikelets	Kobayashi et al. (1988)
GA_{24}	immature seeds, ears	Kobayashi et al. (1984)
GA_{29}	immature seeds, ears	Kobayashi et al. (1984)
GA_{29}	shoots, ears	Kobayashi et al. (1988)
GA_{34}	seeds, ears	Kobayashi et al. (1984)
GA_{34}	spikelets	Kobayashi et al. (1988)
GA_{44}	immature seeds, ears	Kobayashi et al. (1984)
GA_{51}	immature seeds, ears	Kobayashi et al. (1984)
GA_{53}	immature seeds, ears	Kobayashi et al. (1984)
GA_{53}	spikelets	Kobayashi et al. (1988)

1.1.2 Conjugation of gibberellins

Gibberellins exist in plants both as the free acids and in conjugated forms. After the isolation and identification of the first gibberellin, GA_1, from higher plants (MacMillan and Suter, 1958), many GA-conjugates were discovered. The first GA-conjugate, GA_8-2-O-β-D-glucoside, was isolated and characterized from maturing fruits of *Phaseolus coccineus* (Schreiber et al., 1967, 1970; Sembdner et al., 1968). After that, a

series of GA glucosyl conjugates have been isolated and structurally elucidated (Sembdner et al., 1994). Beside these glucosyl conjugates, acyl (Schreiber et al., 1966) and alkyl (Hemphill et al., 1973) GA derivatives have also been found in plants, although their biological significance is less well understood. Today, the conjugation process is considered to be an important aspect of GA metabolism in plants. Gibberellin conjugates may play an important role in the control of growth in higher plants in that they are potential metabolites of the GA biosynthetic pathways.

The most common GA conjugates isolated from plants are GA glucosyl conjugates, in which the GAs are connected to glucose. GA glucosyl conjugates can be divided into two groups, ethers and esters. In glucosyl ethers (or O-glucosides), the glucose is linked to a hydroxyl group of the GA skeleton, while in glucosyl esters, the glucose is attached via the GA-C-7-carboxyl group. For those glucosyl conjugates that have been characterized so far, β-D-glucopyranose is found as the only structural form of the conjugating sugar moiety (Schneider and Schliemann, 1994).

Table 1.2 lists some isolated and structurally elucidated GA glucosyl conjugates and some additional conjugates (Sembdner et al., 1994). For the GA-O-glucosides, the glucose moiety can be linked either to the 2-O-, 3-O-, 11-O-, 13-O- or 17-O-position of the parent GA (Figure 1.3, Sembdner et al., 1994). For the GA glucosyl esters, the glucose is attached via the GA-C-7-carboxyl group (Figure 1.3, Sembdner et al., 1994).

Table 1.2 Naturally occurring GA conjugates (Sembdner et al., 1994).

Conjugate	Plant source
GA-O-glucosides	
GA_1-3-O-glucoside	*Dolichos lablab, Hordeum vulgare , Phaseolus coccineus, Zea mays*
GA_1-13-O-glucoside	*Phaseolus coccineus*
3-epi-GA_1-3-O-glucoside	*Phaseolus coccineus*
GA_3-3-O-glucoside	*Pharbitis nil, Quamoclit pennata*
16,17-H_2, 16,17-dihydroxy-GA_4-17-O-glucoside	*Oryza sativa*
GA_5-13-O-glucoside	*Phaseolus coccineus*
GA_8-2-O-glucoside	*Althea rosea, Hordeum vulgare, Pharbitis nil, Phaseolus coccineus, Phaeolus vulgaris, Zea mays*
GA_{20}-13-O-glucoside	*Hordeum vulgate, Pisum sativum, Triticum aestivum, Zea mays*
GA_{26}-2-O-glucoside	*Pharbitis nil*
GA_{27}-2-O-glucoside	*Pharbitis nil*
GA_{29}-2-O-glucoside	*Hordeum vulgate, Pharbitis nil, Phaseolus coccineus, Pisum sativum, Zea mays*
GA_{29}-13-O-glucoside	*Hordeum vulgare, Pisum sativum, Zea mays*
GA_{35}-11-O-glucoside	*Cytisus scoparius*
GA β-D-glucopyranosyl esters	
GA_1 glucosyl ester	*Phaseolus vulgaris*
GA_4 glucosyl ester	*Phaseolus vulgans*
GA_5 glucosyl ester	*Pharbitis purpurea*
GA_9 glucosyl ester	*Picea sitchensis, Pseudotsuga menziesii, Pinus concorta*
GA_{37} glucosyl ester	*Phaseolus vulgaris*
GA_{38} glucosyl ester	*Phaseolus vulgans*
GA_{44} glucosyl ester	*Pharbitis purpurea*
GA alkyl esters	
GA_1 *n*-propyl ester	*Cucumis sativus*
GA_3 *n*-propyl ester	*Cucumis sativus*
GA_1 methyl ester	*Lygodium japonicum*
GA_{73} methyl ester	*Lygodiumjaponicum*
GA_{88} methyl ester	*Lygodium japonicum*
GA acyl derivatives	
GA_3-3-O-acetate	*Gibberella fujikuroi*
GA_{39}-3-O-isopentanoate	*Cucurbita maxima*
GA-related conjugate	
Gibberethione	*Pharbitis nil*
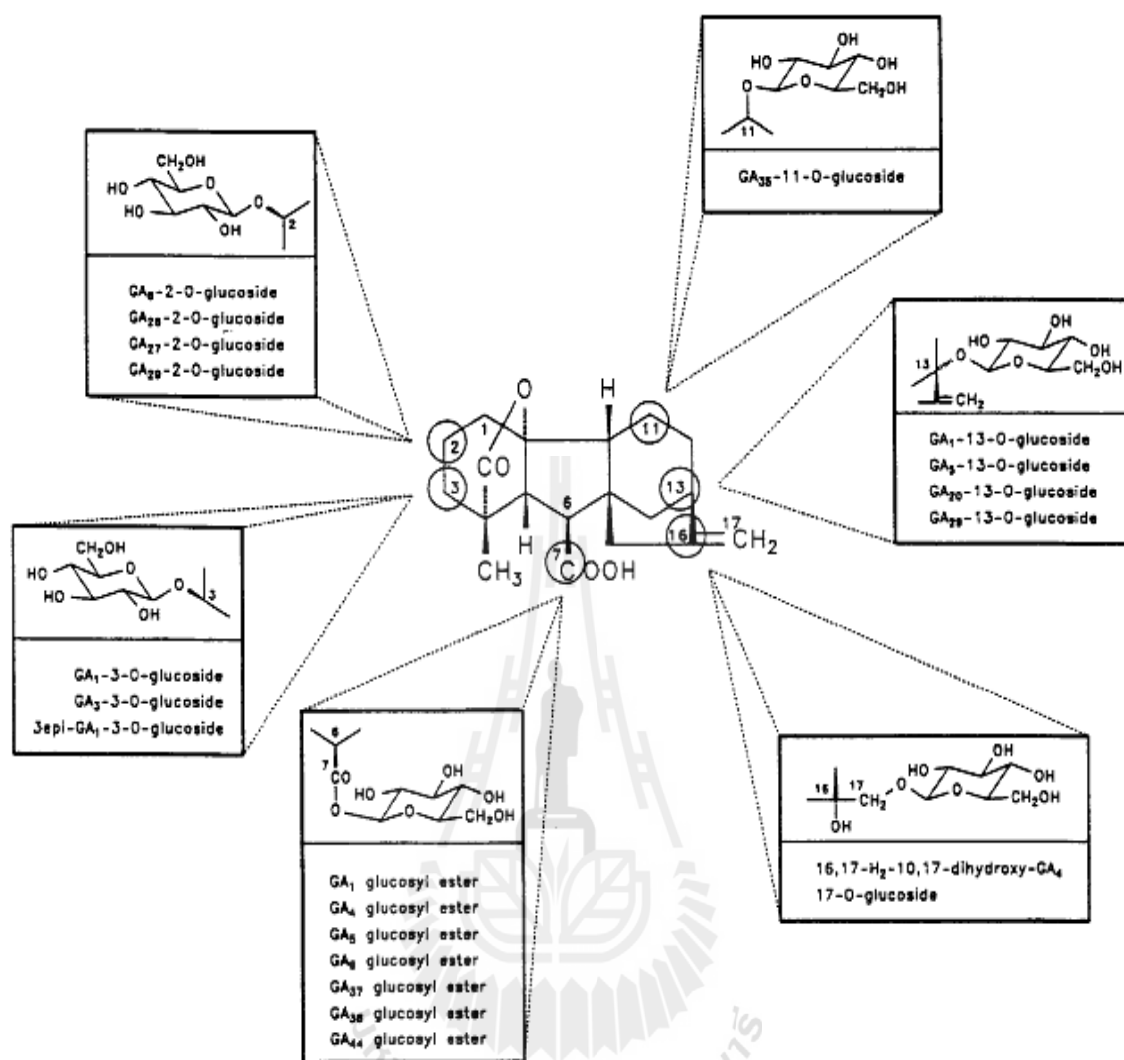
Figure 1.3 The structures of GA glucosyl conjugates (Sembdner et al., 1994).

It has been suggested that GA glucosyl esters are deactivated GAs that can be enzymatically reconverted to active GAs, thus serving as a reserve form of biologically active GAs (Schneider, 1983). After [^{13}C]GA$_{20}$-glucosyl ester was injected into light-grown maize seedlings, the metabolites, [^{13}C]GA$_{20}$, [^{13}C]GA$_{29}$, [^{13}C]GA$_{20}$-13-O-glucoside, [^{13}C]GA$_{29}$-2-O-glucoside, [^{13}C]GA$_{8}$ and [^{13}C]GA$_{8}$-2-O-glucoside were identified in the extracts of the seedlings made 24 h after the injection. This showed that the endogenous hydrolysis by the seedling of the introduced conjugate and its reconjugation led to the three new glucosides (Schneider et al., 1992, see Figure 1.4). In

rice, the glucosyl esters of GA_1, GA_2, GA_4, GA_8 and GA_{34} have been found after application of [^{3}H] GA_4 to seedlings (Koshioka et al., 1988).
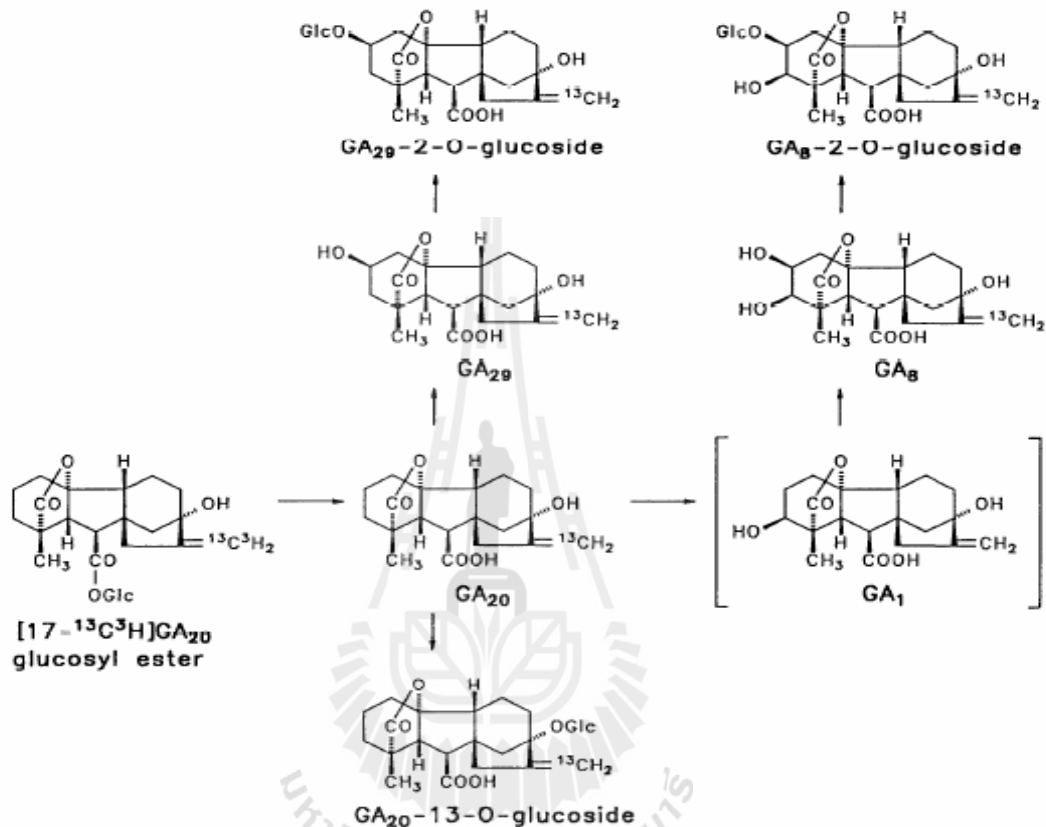
Figure 1.4 Presumptive biosynthetic pathway for ^{13}C-labelled metabolites identified by GC-MS after feeding [17-^{13}C] GA_{20} glucosyl ester to seedlings of *Zea mays* (GA_1 could not be detected, Schneider et al., 1992).

During the conjugation step, in which GAs are converted to GA glucosyl conjugates, the biological activity is reduced or totally lost, but the increased polarities of GA glucosyl conjugates are considered to favor GA conjugates being deposited into the vacuole (Sembdner et al., 1994). From the occurrence of GA glucosyl conjugates in the bleeding sap of trees, it has been suggested that these conjugates may possibly have a function in long-distance GA transport (Dathe et al., 1978, 1982). It also has been suggested that the glucosyl moiety of GA conjugates may cause a distorted orientation of

the GA molecule within the membrane, which prohibits the appropriate binding to an assumed receptor (Stoddart and Venis, 1980). Because GA glucosyl conjugates tend to form and accumulate during the seed maturation period, it has been proposed that this group of compounds may function as storage products (Lenton et al., 1991, 1993). However, this theory applies only to conjugates of biologically active GAs, where hydrolysis, for example during early stages of seed germination, releases free GAs prior to *de novo* GA biosynthesis.

For the biologically inactivated GAs, for example, 2-β-hydroxylated GAs, conjugation may be a step within the process of further catabolism (Sembdner et al., 1994, Schneider et al., 2002). GA glucosyl conjugates are easily formed and hydrolyzed in the plants, which means, reversible deactivation/activation of GAs may be linked to the regulation of free GA pools. The physiological roles of GA glucose conjugates are still not clear and need to be studied and clarified further.

1.1.3 Synthesis of gibberellin glucosyl conjugates

Since the quantities of endogenous gibberellin glucosyl conjugates are very low in plants, it is difficult to get enough pure compounds for structure identification. Therefore, the partial synthesis of these conjugates has been performed for the following purposes: 1, to get large enough quantities of GA conjugates for structure identification and bioactivity tests; 2, to synthesize labeled compounds for use as internal standards in chromatographic analysis and as substrates in metabolic studies; and 3, to produce new compounds as standards for uncharacterized native conjugates by modifying known endogenous structures (Schneider and Schliemann, 1994).

GA-O-glucosides were synthesized by glucosylation of gibberellins under Koenigs-Knorr conditions (Shreiber et al., 1969, Schneider et al., 1974, 1977, 1984, 1989, Figure 1.5). The Koenigs-Knorr glucosylation has the advantage of stereo-

selectivity, which produces only the β-D-glucopyranosyl structure. GA β-D-gluco-pyranosyl esters were synthesized either by the Koenigs-Knorr reaction (Shreiber et al., 1969; Hiraga et al., 1974; Schneider et al., 1984, Figure 1.6) or by a base catalyzed reaction (Schneider et al., 1994). The most crucial step of the synthesis is to remove acetyl groups from the sugar moiety, without splitting the glycosyl ester linkage. Successful deacetylation has been achieved with 0.02 N sodium methoxide in methanol at -10°C for an hour (Hiraga et al., 1974).
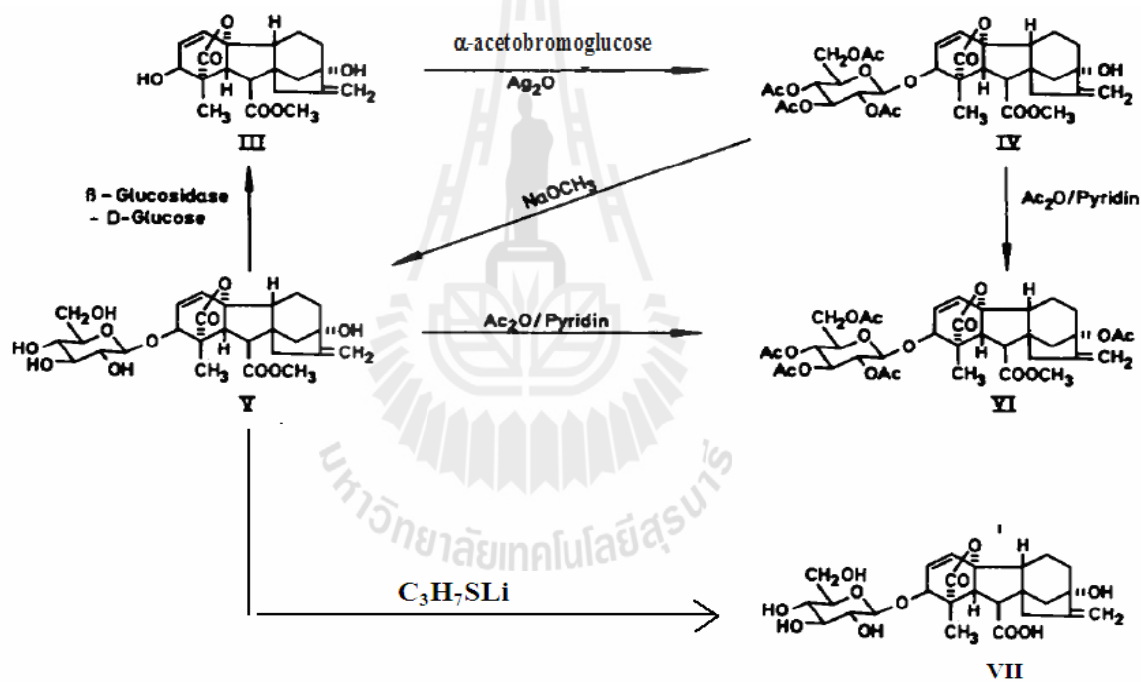
Figure 1.5 GA glucoside syntheses (Schneider et al., 1977).
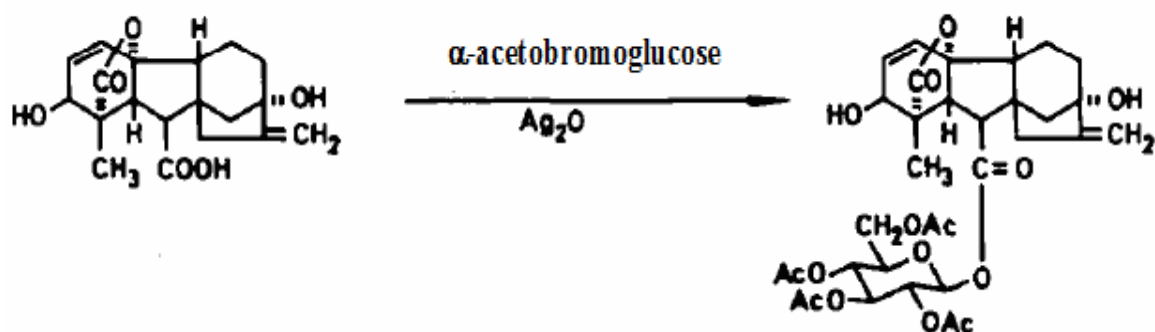
Figure 1.6 GA β-D-glucopyranosyl ester synthesis (Shreiber et al., 1969).

To synthesize labeled GA glucosyl conjugates, [17-^{13}C], [17-^{2}H$_2$], or [17-^{13}C,^{3}H] GAs can be used as starting material. The reaction will proceed in the same manner as unlabeled GAs (Schneider et al., 1990; Fuchs and Schneider, 1996). The glucose moiety can also be labeled by using [6-^{2}H$_2$] glucose as starting material (Schneider et al., 1990). The metabolism of both the parent GA and glucose could be followed by detecting the labeled GAs and GA conjugates in the plants.

1.1.4 Analysis of gibberellins and their conjugates

In order to understand the metabolism of gibberellins in the plants, we should know the concentrations of gibberellins, as well as their conjugates, in the plants. The active form of the hormone is important, but their metabolites and precursors are also important, because they often give us clues for understanding the regulation of hormone action and metabolism. Since the concentrations of gibberellins and their conjugates are very low in the plant, highly sensitive instruments are required. Gas chromatography-mass spectrometry (GC-MS), Liquid chromatography-mass spectrometry (LC-MS) and LC-MS/MS are usually used for the analysis.

Due to the broad range of polarities of GA conjugates, sample preparation is extremely difficult. It is difficult to analyze free GAs, GA-O-glucosides and GA glucosyl esters simultaneously, since no method can extract them all in high enough quantities for chromatographic analysis. The extraction method usually includes the first step to extract GA conjugates and GAs with methanol, and a second step to separate GA-glucosyl esters from GAs and GA-O-glucosides by ion exchange chromatography, for example with a DEAE-Sephadex column (Schneider et al., 1992, 1993). The esterified GAs will be mainly found in the neutral fractions. All free GAs and GA-O-glucosides will be mainly found in the acidic fractions because of their carboxylic acid groups on the GA rings.

Further purification of these fractions depends on the final analytical method used and on the target compound of the analysis. Reverse phase HPLC (RP-HPLC) and derivatization are usually used for the continued purification. GAs and their glucosyl conjugates can be analyzed by GC-MS by preparing their trimethylsilyl (TMS) derivatives (Yokota et al., 1975). However, the limited mass range of the average benchtop GC-MS (approx. 800 m/z) is a problem, because the molecular weights of TMS derivatives of sugar conjugates are above the limit of the mass range. Thus, permethylation has been introduced for GA-O-glucoside analysis. This method can produce stable and smaller molecular size permethylated GA-O-glucosides, which are suitable for GC-MS analysis (River et al., 1981; Schneider et al., 1987, 1992; Senns et al., 1998). The permethylation method also has other advantages in that the method can be used directly with the acidic fraction after DEAE-Sephadex chromatography and the corresponding derivatives of free GAs and GA-O-glucosides can be separated easily as groups by RP-HPLC. GC-MS has good sensitivity for permethylated GA-O-glucosides. About 1 ng of compound is sufficient for a full scan spectrum with GC-MS (Schmidt et al., 1988). The selective ion monitoring (SIM) mode can also be used to monitor extracts for the occurrence of endogenous compounds, since this method can offer higher sensitivity than the scan mode. Permethylation cannot be applied to GA glycosyl esters as these conjugates undergo transesterification resulting in permethylated aglycones (Schneider and Schliemann, 1994).

LC-MS and LC-MS/MS techniques have provided new prospects for the investigation of polar and high-molecular-mass compounds without prior derivatization or hydrolysis. GA glucosyl esters can be detected by LC-electrospray ionization (ESI) MS in both positive and negative ion modes (Schneider and Schmidt, 1996). In the positive mode, the abundant $[M+Na]^+$ ion will be detected and enable sugar esters to be recognized from their molecular masses; another important fragment is the Na^+ adduct of the

aglycone, [M+Na-sugar]$^+$, which will be useful for the aglycone identification (Figure 1.7, Schneider and Schmidt, 1996). Under the negative mode, the molecular ion [M-H]$^-$ is weak but the [M-sugar]$^-$ ion, which represents the aglycone moiety, will be the base peak and enable us to identify the aglycone easily (Figure 1.8).

Compound	[M + K]$^+$	[M + Na]$^+$	[M + Na − sugar]$^+$	[M + H − sugar]$^+$	[M + H − sugar − H$_2$O]$^+$	[M + H − sugar − H$_2$O − HCOOH]$^+$
GA$_3$GlcE (1)	547 (15)	531 (90)	369 (30)	347 (2)	329 (58)	283 (100)
GA$_3$GalE (2)	547 (20)	531 (80)	369 (10)	347 (20)	329 (95)	283 (100)
GA$_3$XylE (3)	517 (4)	501 (10)	369 (10)	347 (8)	329 (42)	283 (100)
GA$_3$AraE (4)	517 (15)	501 (45)	369 (20)	347 (10)	329 (43)	283 (100)
ABAGlcE (5)	465 (10)	449 (75)	287 (100)	265 (2)	247 (4)	–

Figure 1.7 Diagnostic ions *(m/z)* and their relative abundances (% of highest peak in parentheses) in positive-ion ESI mass spectra of glycosyl esters of GA$_3$ and abscissic acid (ABA) (Schneider and Schmidt, 1996).

Compound	[M − H]$^-$	a	b
GA$_3$GlcE (1)	507 (1)	387 (26)	345 (100)
GA$_3$GalE (2)	507 (5)	387 (24)	345 (100)
GA$_3$XylE (3)	477 (8)	387 (8)	345 (100)
GA$_3$AraE (4)	477 (4)	387 (25)	345 (100)
ABAGlcE (5)	425 (4)	305 (10)	263 (100)

Figure 1.8 Diagnostic ions *(m/z)* and their relative abundances (% of highest peak in parentheses) in negative-ion ESI mass spectra of glycosyl esters of GA$_3$ and ABA, and the scheme of sugar ester fragmentation (Schneider and Schmidt, 1996).

The sensitivity of GA-glycosyl ester analysis by LC-MS has been studied by Schneider and Schmidt (1996). Under the positive ion condition, GA_3 glycosyl ester can be detected at about 100 ng with the SIM mode *(m/z* 283). Under the negative ion mode, about 10 ng is needed for the GA_3 glycosyl ester to be detected with the SIM mode *(m/z* 345).

Hitoshi Sakakibara's group developed a highly sensitive and high-throughput method for the simultaneous analysis of 43 molecular species of cytokinins, auxins, abscissic acid (ABA) and gibberellins with the new generation of LC-MS/MS (Kojima et al., 2009). They used an automatic liquid handling system for solid phase extraction, which enabled them to treat a large number of samples without handling mistakes. The ultra-performance liquid chromatography (UPLC) coupled with a tandem quadrupole mass spectrometer (qMS/MS) equipped with an ESI interface also provided the highest sensitivity compared to other LC-MS systems. In order to improve the detection limit of negatively charged compounds, such as gibberellins, they derivatized the fractions containing auxin, ABA and gibberellins with bromocholine, which has a quaternary ammonium functional group (Figure 1.9). Therefore, the negatively charged compounds were converted to positively charged and analyzed with other originally positively charged compounds in a single run. This modification, called "MS-probe", greatly increased the quantification limits of gibberellins and reduced the time for analysis. The quantification limits can reach 1 fmol for GA_1 and 5 fmol for GA_4. This method can be used to analyze more than 180 plant samples simultaneously.
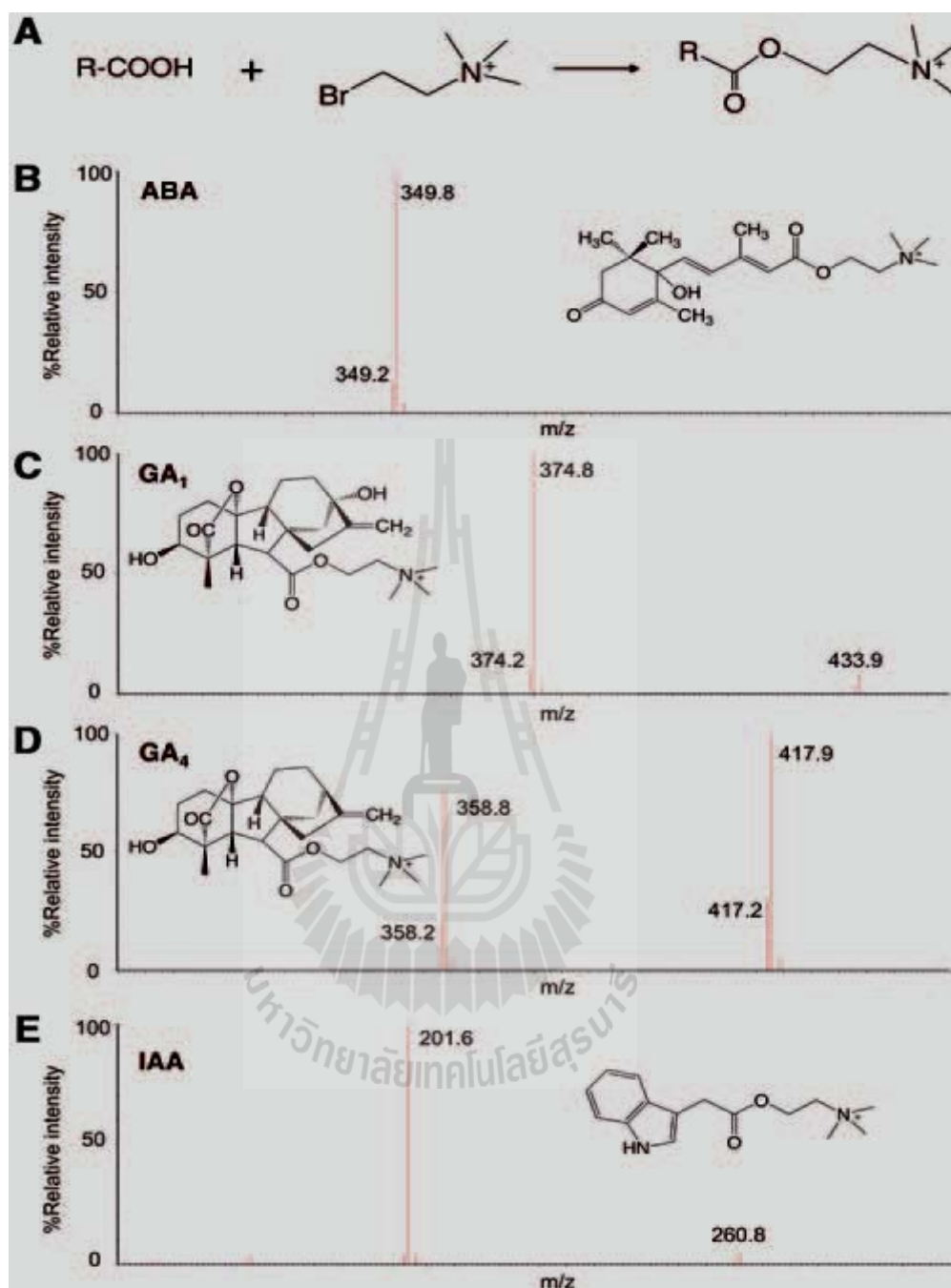
Figure 1.9 Phytohormone detection by MS-probe derivatization. (A) MS-probe derivatization. (B-E) Structures of derivatized products and their fragmentation patterns for ABA (B), GA$_1$ (C), GA$_4$ (D) and indole-3-acetic acid (IAA) (E) that were analyzed with a Quattro Premier XE (Waters) in the positive ion mode (Kojima et al., 2009).

1.2 Overview of β-D-Glucosidases

1.2.1 β-D-Glucosidases and their functions

Beta-glucosidases (β-D-glucopyranoside glucohydrolases, E.C. 3.2.1.21) are enzymes that hydrolyze the β-O-glycosidic bond at the anomeric carbon of a glucose moiety to release nonreducing terminal glucosyl residues from glycosides and oligosaccharides. These enzymes are found essentially in all living organisms and have been implicated in a diversity of roles, such as biomass conversion in microorganisms (Fowler, 1993) and activation of defense compounds (Poulton, 1990; Duroux et al., 1998), phytohormones (Brzobohatý et al., 1993; Falk and Rask, 1995), lignin precursors (Dharmawardhana et al., 1995), aromatic volatiles (Mizutani et al., 2002), and metabolic intermediates (Barleben et al., 2005) by releasing glucose blocking groups from their inactive glucosides in plants. To achieve specificity for these various functions, different β-glucosidases must bind to distinct aglycones with a wide variety of structures, in addition to the glucose of the substrate.

β-Glucosidases have been classified into glycoside hydrolase (GH) families GH1, GH3, GH5, GH9, GH30 and GH116, based on their amino acid sequences and structural similarity (Henrissat, 1991; Henrissat and Davies, 1997; Cantarel et al., 2009; Ketudat Cairns and Esen, 2010; Cobucci-Ponzano et al., 2010), while other β-glucosidases remain to be classified. The GH1, GH5 and GH30 β-glucosidases fall in GH Clan A, which consists of proteins with $(\beta/\alpha)_8$-barrel structures. In contrast, the active site of GH3 enzymes comprises two domains, while GH9 enzymes have $(\alpha/\alpha)_6$ barrel structures. The mechanism by which GH1 enzymes recognize and hydrolyze substrates with different specificities remains an area of intense study.

1.2.2 Phytohormone β-D-glucosides and their β-D-glucosidases

Among β-D-glucosidase functions in plants, the function of phytohormone activation is very important and has attracted many peoples' interests. Phytohormone glucosyl conjugates are ubiquitous in plants, including those of GA, ABA, cytokinins, auxins, jasmonic acid derivatives and others, and β-glucosidases that hydrolyze these conjugates have been found in several plants (Schliemann 1984; Lee et al., 2006; Kai et al., 2007; Wakuta et al., 2010).

ABA is a phytohormone critical for plant growth, development, and adaptation to various stress conditions. Plants have to adjust ABA levels constantly to respond to changing physiological and environmental conditions (Lee et al., 2006). For example, cellular ABA levels increase significantly during seed maturation and under abiotic stress. In contrast, ABA levels are decreased during germination. When ABA is applied to plants, it causes rapid stomatal closure and thus reduces water loss via transpiration. Water stress causes a rapid increase in the ABA content of plants. Evidence has accumulated that this increase in ABA is attributable to *de novo* synthesis. Aside from the *de novo* synthesis pathway of abscisic acid, biologically inactive abscisic acid-glucose ester (ABA-GE) constitutes a reserve or stored form of ABA. An *Arabidopsis* β-glucosidase (AtBG1) has been found to hydrolyze ABA-GE to form free ABA, and this enzyme was found to be essential to proper response to drought stress and delay in seed germination, despite the fact that other ABA-GE hydrolyzing enzymes were detected.

The plant hormone indole-3-acetic acid (IAA) is also an important signal molecule that regulates growth and development in plants. The concentration of free IAA at the tissue or cellular level is controlled through a fine balance of the activities of biosynthesis, metabolism, and inter-cellular or -tissue transport, referred to as IAA homeostasis (Kai et al., 2007). Similar to ABA, IAA can also form indole-3-acetic

acid-glucosyl ester (IAA-GE) as an inactive and stored form. IAA-GE can also be hydrolyzed by IAA-glucose hydrolase to give active indole-3-acetic acid form.

Jasmonic acid (JA), which is a member of the oxylipins, is an essential compound involved in regulating responses to stresses, such as insect herbivory and pathogenic attack in plants (McConn et al., 1997; Vijayan et al., 1998). In addition, JA is involved in plant growth and development, including root growth, fruit ripening, and pollen maturation (Staswick et al., 1992; Fan et al., 1998; Stintzi and Browse, 2000; Wasternack, 2007). Numerous genes have been previously identified that are either inducible or down-regulated by JA (Sasaki et al., 2001; Wierstra and Kloppstech, 2000), suggesting that it might be an important signaling molecule for plants in response to environmental changes and development.

Tuberonic acid (TA, 12-hydroxyjasmonic acid) and its glucoside (TAG) were isolated as tuber-inducing compounds from potato (Koda et al., 1988; Yoshihara et al., 1989). These compounds were reported to be biosynthesized from JA by hydroxylation and subsequent glycosylation (Figure 1.10), and to be found in various plant species. A recent study suggested that TAG generated from JA transmits a signal from the damaged parts to the undamaged parts of the plant (Seto et al., 2009) and demonstrated that TA contributes to the down-regulation of the expression of JA biosynthetic genes, such as *LOX*, *AOS* and *OPR*, which are JA-inducible. Furthermore, they demonstrated that some housekeeping genes, such as *RBCS*, *CAB8* and *TUB*, are also strongly down-regulated (Miersch et al., 2007). These data suggest the importance of TAG glucosidase as a regulator of TA levels according to environmental conditions.

Recently, one β-glucosidase which can hydrolyze tuberonic acid β-D-glucoside to tuberonic acid was purified from rice panicles, and it was named as OsTAGG1 (Wakuta et al., 2010). The *in vivo* hydrolysis of TAG into TA in rice plants was also described (Figure 1.10).
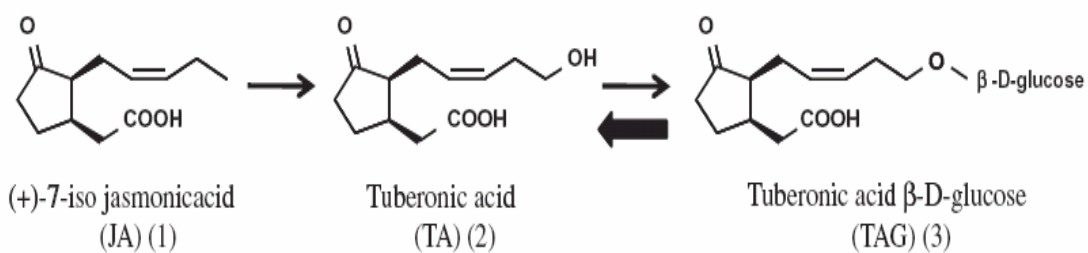
Figure 1.10 Metabolism of jasmonic acid (1) focusing on TA (2) and TAG (3). The narrow arrows indicate TAG (3) biosynthesis. JA (1) is metabolized to TA (2) by hydroxylation at the C-12 position and then glucosylated to produce TAG (3). The bold arrow shows the reverse pathway generating TA (2) from TAG (3), as described in the study of Wakuta et al. (2010).

β-Glucosidases have been proposed to hydrolyze the GA conjugates to active GAs, but not much research into their actions has been reported yet. Schliemann reported in 1984 that β-glucosidases extracted from mature rice seeds and seedlings have different hydrolytic activities toward GA_8-2-O-glucoside, GA_3-3-O-glucoside and GA_3-glucosyl ester, but he did not purify and characterize the β-glucosidases, so the enzymes that can hydrolyze the GA conjugates are still unknown. Furthermore, the substrate specificity of β-glucosidase to GA conjugates and how β-glucosidase binds to GA conjugates has yet to be reported.

1.2.3 β-D-Glucosidase hydrolysis mechanisms

β-D-Glucosidases can hydrolyze glycosidic bonds between non-reducing terminal glucosyl residues and alcohols of various structures. Two mechanisms have been proposed for glycoside hydrolase reactions: one is a retaining mechanism and the other is an inverting mechanism.

1.2.3.1 Retaining mechanism

The retaining mechanism involves a covalent glucosyl-enzyme intermediate that is formed and cleaved with acid/base catalytic assistance via oxocarbenium ion-like transition states. The mechanism has been proposed by Koshland since 1953 and includes two steps for the reaction (Figure 1.11a). The retaining glycosidases generally have a pair of essential carboxylic acid residues (Asp or Glu) located on the opposite sides of the bottom of the enzyme active site; they are normally about 5.5 Å apart (Zechel and Withers, 2000). In the first step, one of the carboxyl groups acts as a general acid catalyst to protonate the glycosidic oxygen, while the other carboxylic acid residue acts as a nucleophile to attack the anomeric carbon and form a covalent glucosyl-enzyme intermediate, which cleaves the C-O bond at the anomeric carbon to displace the aglycone group. The glycosyl-enzyme intermediate formed in this step, referred to as the glycosylation step, has an anomeric configuration opposite to that of the starting material. The second step, the deglycosylation step, involves the hydrolytic breakdown of the glycosyl-enzyme intermediate. The carboxylate that first acted as an acid catalyst now acts as a base to abstract a proton from the incoming nucleophile, normally a water molecule. The water molecule attacks the anomeric center of the sugar, and a second oxocarbenium ion-like transition state forms, as the carboxylate residue departs. The product is a hemi-acetal that has the same anomeric configuration as the starting material (Rempel and Withers, 2008). β-Glucosidases from families GH1, GH3, GH5, GH30 and GH116 use this retaining mechanism (Ketudat Cairns and Esen, 2010; Cobucci-Ponzano et al., 2010).
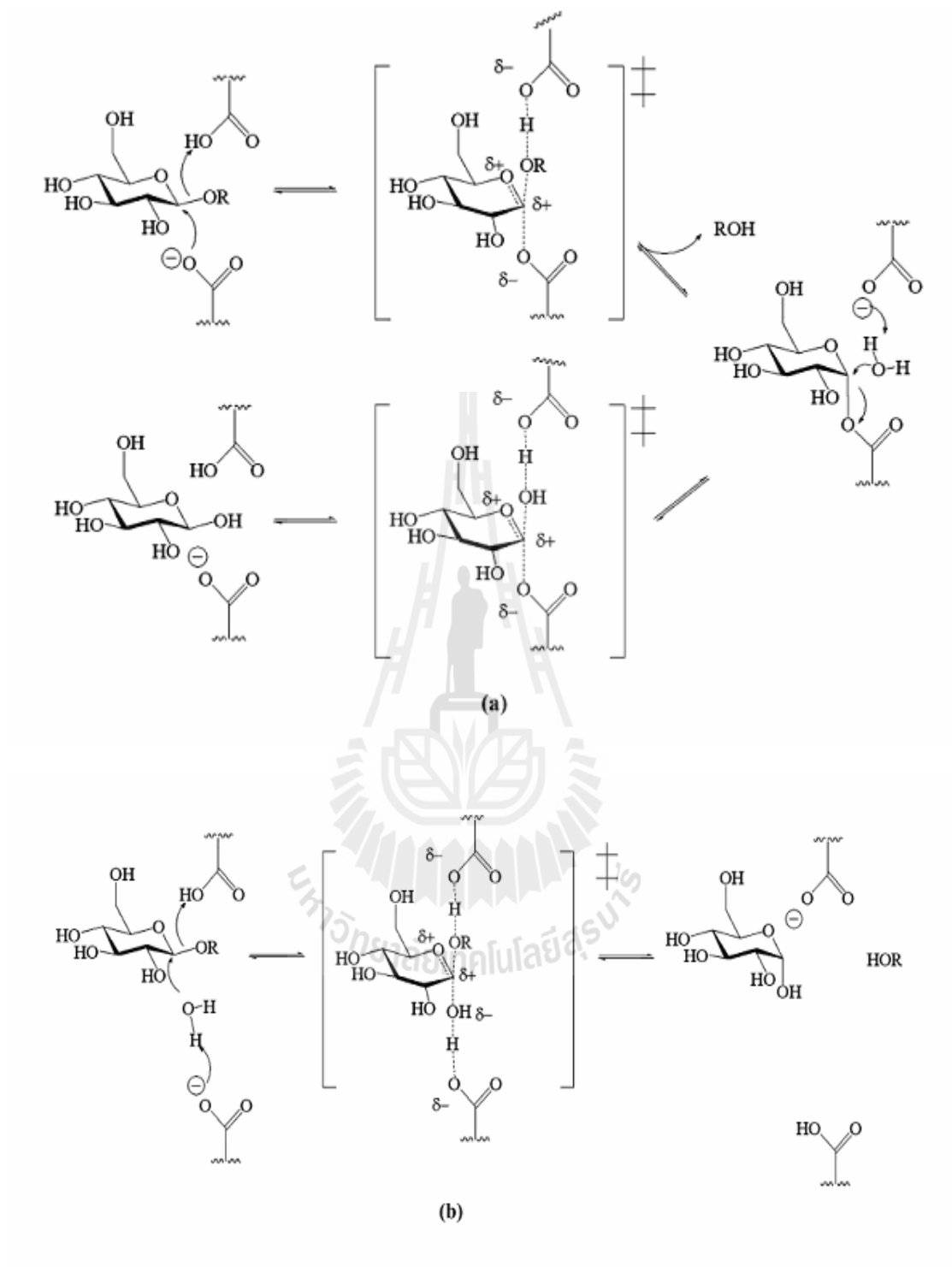
Figure 1.11 β-D-Glucosidase hydrolysis mechanisms. (a): Retaining mechanism; (b): Inverting mechanism (Rempel and Withers, 2008).

1.2.3.2 Inverting mechanism

The inverting mechanism includes a single oxocarbenium ion-like transition state (Figure 1.11b). There are also two carboxylic acid residues (Asp or Glu) in the inverting glycosidases, but they will be located around 10 Å apart on opposite sides of the active site (Zechel and Withers, 2000). One carboxylic acid acts as a general base to remove a proton from the incoming nucleophile-water, during its attack at the anomeric carbon. The other carboxylic acid acts as a general acid residue, protonating the departing aglycone oxygen atom and assisting in its departure from the anomeric center. This reaction is also called a single displacement mechanism (Koshland, 1953); bond-making and bond-breaking steps proceed through a single oxocarbenium ion-like transition state. The sugar product is a hemi-acetal that has the opposite configuration at the anomeric center to that of the starting material. β-Glucosidases from family GH9 are inverting enzymes that follow this mechanism (Park et al., 2002; Qi et al., 2008).

1.2.4 Covalent inhibitors of β-D-glucosidases

The glucosidase inhibitors include two groups: noncovalent and covalent (Rempel and Withers, 2008). Noncovalent inhibitors usually bind to the glucosidases reversibly and must be maintained at sufficient concentrations to occupy the active site much of the time to be effective in an organism. Thus, both high affinity binding and high specificity must be achieved. Noncovalent inhibitors have the greatest potentials as therapeutics, and have been extensively studied (Asano, 2003; Butters et al., 2003; de Melo et al., 2006). Covalent inhibitors form covalent bonds with the enzyme, so the active site is blocked or some important residues are modified, so that the enzyme cannot function properly and loses its activity. Covalent inhibitors have attracted many researchers' interests, since they are important tools in the determination of mechanisms of oligosaccharide processing. Covalent inhibitors can be used to identify the active site residues of the enzyme by

identification of the modified residues by mass spectrometry of proteolytic peptides or co-crystallization of the inhibitor with the wild enzyme and study of the complex structure and interactions between inhibitor and enzyme (Czjzek et al., 2001; Seshadri et al., 2009).

Among noncovalent inhibitors, those most often used for studies of glycosidases are substrate analogues and transition state analogues. One group of substrate analogues is thio-glycosides, which are often used to crystallize with the wild type enzymes to detect its active site and interactions between the substrate and enzyme in the Michaelis complex formed before the reaction (Figure 1.12; Czjzek et al., 2001). The replacement of the oxygen of the scissile bond with sulfur prevents hydrolysis by most β-glucosidases.

Of the covalent inhibitors, the group most successfully used with glycosidases is 2-deoxy-2-fluoro-glycosides (Rempel and Withers, 2008). Like the *p*NP-thio-glycoside, the 2-deoxy-2-fluoro-glycoside can form complexes with the enzyme and many crystal structures of these complexes have been solved by X-ray crystallography. Because the electron withdrawal by the 2-fluoro group destabilizes the transition states of both the glycosylation and deglycosylation steps of the retaining mechanism, the enzyme may be trapped in either the Michaelis complex or the covalent intermediate, depending of the leaving group ability of the substrate aglycone and enzyme properties. The use of good leaving groups with low pKa, like 2,4-dinitrophenolate or fluoride, helps to allow the glycosylation step to proceed to trap the enzyme in the covalent intermediate. One example of such a structure is that of the covalent complex of rice BGlu1 (also called Os3BGlu7) β-D-glucosidase, which has oligosaccharide hydrolysis and transglycosylation activity, with 2-deoxy-2-fluoro-β-D-glucopyranoside (G2F) from Chuenchor et al. (2008) (Figure 1.13). The structure showed that the sugar was close to a glycerol molecule that was positioned as an acceptor for transglycosylation by interactions with E176, the catalytic acid/base, and Y131. In total, five hydrogen bonds were formed between G2F and amino acids. The O3 atom of G2F is hydrogen bonded to W441 $N^{\varepsilon1}$, and Q29 $O^{\varepsilon1}$,

while the O4 atom forms hydrogen bonds with Q29 $N^{\varepsilon 2}$ and E440 $O^{\varepsilon 1}$, and O6 interacts

with $O^{\varepsilon 2}$ of E440. A hydrophobic stacking interaction between glucose and the indole ring

of W433 is conserved with other GH1 β-glucosidases. The nucleophile E386 is rotated

~60° around the C^{α} to C^{β} bond with respect to the free enzyme in order to form the

glycosyl–enzyme complex.
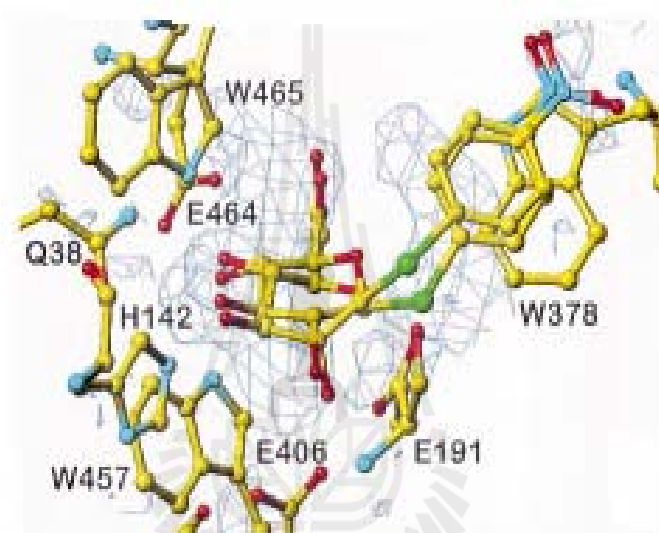
Figure 1.12 The view of the active-site residues with the experimental electron density

(Fo-Fc map, contoured at 2σ) for the *p*-nitrophenyl β-D-thioglucoside (*p*NPTGlc)

molecule in the active site of maize β-glucosidase ZMGlu1. The two superimposed

models of the inhibitor, in the ${}^{4}C_1$ chair and the ${}^{1}S_3$ skew-boat conformations, are equally

compatible with the observed electron density. The experimental electron density probably

also accounts for other intermediate conformations. The figure was produced with

TURBO (Czjzek et al., 2001).
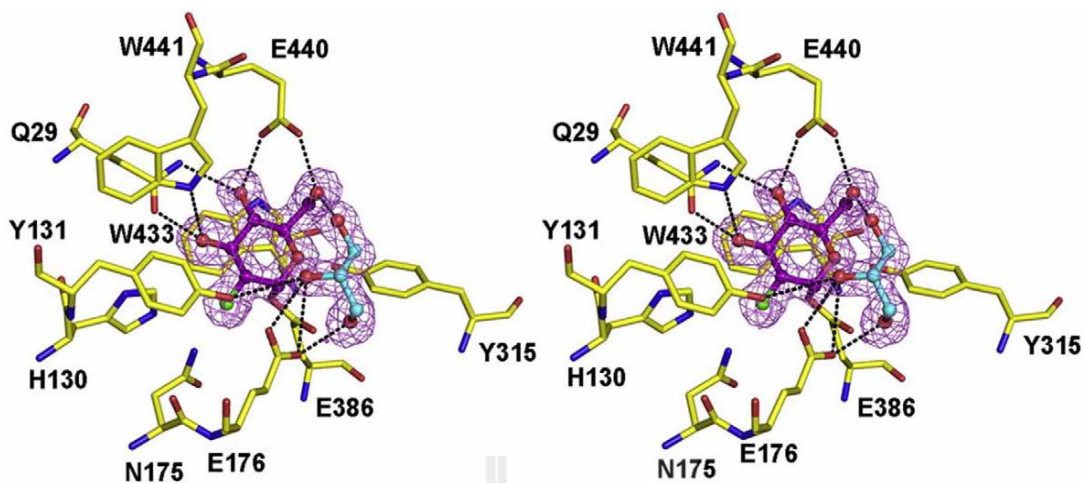
Figure 1.13 Stereoview of the protein-ligand interactions in the active site of the BGlu1-G2F complex. The amino acid residues surrounding G2F are presented in stick representation, with carbon yellow, nitrogen blue, oxygen red, and fluoride green. G2F and glycerol (GOL) are drawn in ball and stick representation in the same colors, except carbon atoms are purple and cyan, respectively. The purple ‖Fo‖-‖Fc‖ omit map for G2F and GOL is shown contoured at 3 σ. Hydrogen bonds between the protein and the glycone at subsite −1 and glycerol at subsite +1 are drawn as broken black lines (Chuenchor et al., 2008).

Another important structure is the covalently bound glycosyl-enzyme intermediate of hen egg-white lysozyme (HEWL) with 2-acetamido-2-deoxy-β-D-glucopyranosyl-(1→4)-2-deoxy-2-fluoro-β-D-glucopyranosylfluoride (NAG2FGlcF, Figure 1.14; Vocadlo et al., 2001). This structure supported the double-displacement mechanism via a covalent intermediate (Figure 1.15), as first proposed by Koshland (1953), whereas lysozyme was previously thought to act through a noncovalent intermediate.
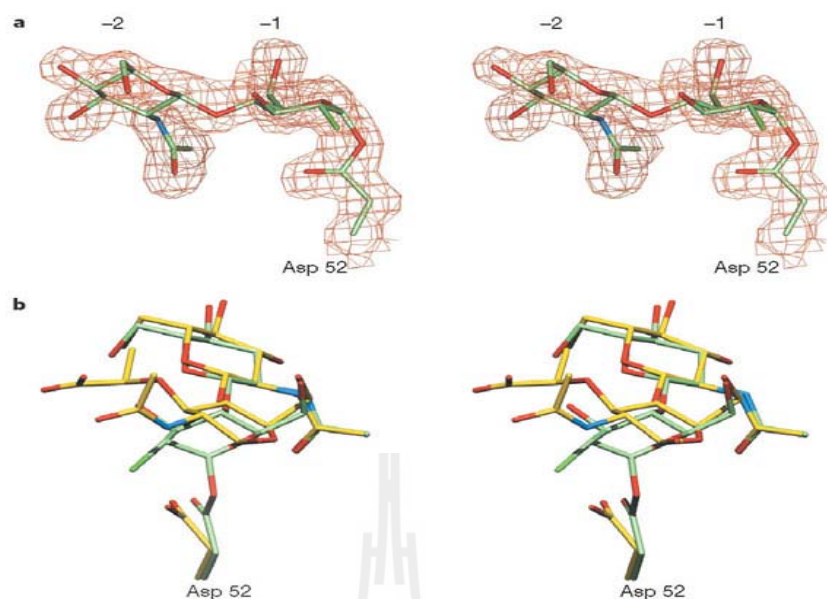
Figure 1.14 Structure of the covalent intermediate in the HEWL reaction. **a**, Maximum likelihood/σ_A-weighted $2F_O$ - F_C electron density for the covalent glycosyl-enzyme intermediate of HEWL, contoured at 0.4 electrons per Å^3. **b**, Overlap of the HEWL covalent intermediate and the product complex with MGM. Formation of the intermediate is accompanied by an approximate 45° rotation around χ_1 of Asp 52. MGM represents NAM-NAG-NAM trisaccharide. NAM represents 2-acetamido-2-deoxy-3-O-lactyl-glucopyranoside; NAG represents 2-acetamido-2-deoxy glucopyrano-side (Vocadlo et al., 2001).
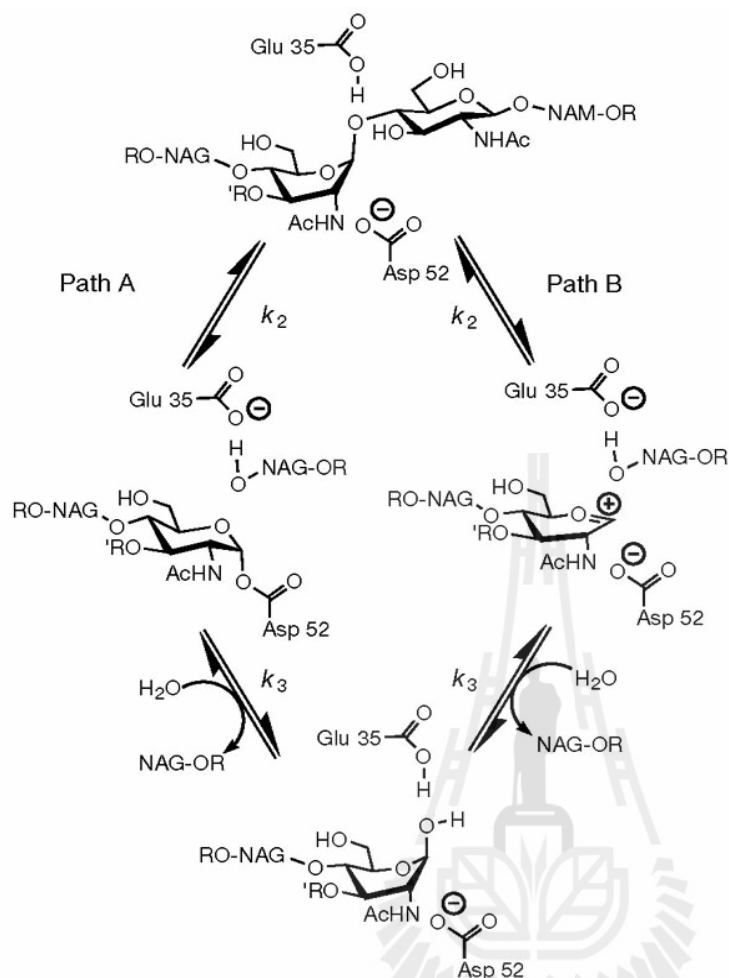
Figure 1.15 Two possible catalytic mechanisms for HEWL. Path A; the Koshland mechanism; path B; the Phillips mechanism. R, oligosaccharide chain; R', peptidyl side chain (Vocadlo et al., 2001).

1.2.5 The acid/base and nucleophile mutants of β-D-glucosidases

Acid/base and nucleophile mutants of β-D-glucosidases play very important roles in the study of the enzyme's active site and substrate specificity. Since these mutants usually cannot hydrolyze the native substrate of their wild type enzyme, the native substrates can often be crystallized bound to the mutant enzyme. These complexes allow identification of the interactions between the substrate and enzyme active site in the Michaelis complex formed before the reaction (Czjzek et al., 2000; Chuenchor et al., 2011). They can sometimes also allow accumulation of the covalent intermediate of the

native sugar. One good example is the study of the human crytosolic β-glucosidase (Noguchi et al., 2008).

Human cytosolic β-glucosidase, also known as klotho-related protein (KLrP, GBA3), is an enzyme that hydrolyzes a wide variety of β-D-glucosides, including synthetic aryl glycosides (4-nitrophenyl and 4-methylumebelliferyl monoglycosides), dietary flavonoids, isoflavones glucosides, and glucosylceramides (Berrin et al., 2002, 2003; Tribolo et al., 2007; Hayashi et al., 2007) and belongs to the GH1 family. The crystal structures of KLrP have been reported by two groups independently (Tribolo et al., 2007; Hayashi et al., 2007) and have a $(\beta/\alpha)_8$ barrel structure, in common with other GH1 enzymes. The crystal structures and site-directed mutagenesis identified Glu165 and Glu373 as the catalytic acid/base and nucleophile, respectively. Noguchi et al. (2008) reported the crystal structure of the covalent glucosyl-enzyme intermediate of the KLrP mutant E165Q (KLrPE165Q), in which the glucose was covalently bound to the nucleophile Glu373 (Figure 1.16), in the covalent intermediate expected for the retaining mechanism. In this figure, the density clearly showed a covalent linkage between the C1 atom of the glucose and the nucleophile Glu373 Oε1 atom (1.3 Å). The glucose ring was firmly stabilized by an extensive hydrogen bond network, basically identical to that observed in the KLrP/Glc product complex (Hayashi et al., 2007). The glycosyl-enzyme intermediate was trapped by co-crystallization of the general acid/base mutant, KLrPE165Q, with an activated sugar donor, *p*-nitrophenyl β-D-glucopyranoside (*p*NPGlc). The presence of such a good leaving group (*p*NP moiety) overcame the lack of general acid catalysis, allowing formation of the glycosyl-enzyme intermediate (Figure 1.17). This glucosyl-enzyme intermediate structure reveals the double displacement mechanism of the retaining β-glycosidase and suggests the stabilization mechanism of the transition state through the sugar 2-hydroxyl oxygen (Figure 1.17).
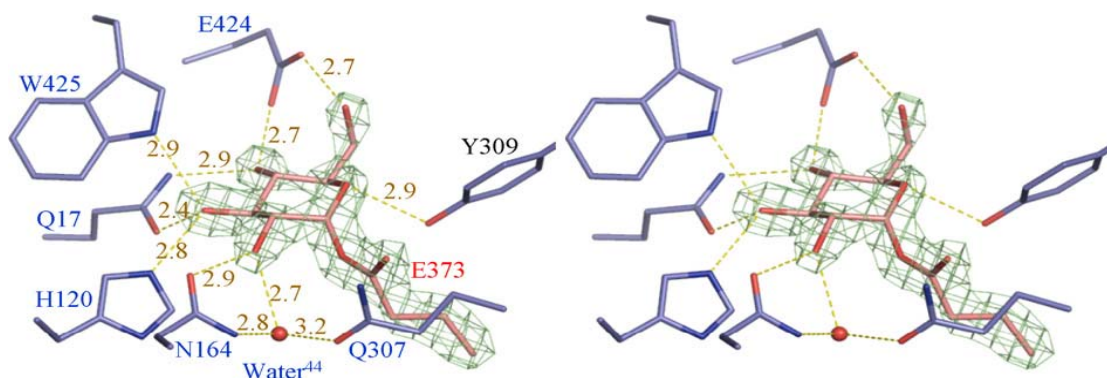
Figure 1.16 Stereo view of the electron density maps (Omit F_o–F_c map contoured at 4σ) of the active site of KLrPE165Q trapped as a covalent glucosyl-enzyme intermediate. Hydrogen bonds are represented by yellow dotted lines with the distance (in Å) (from Noguchi et al., 2008).
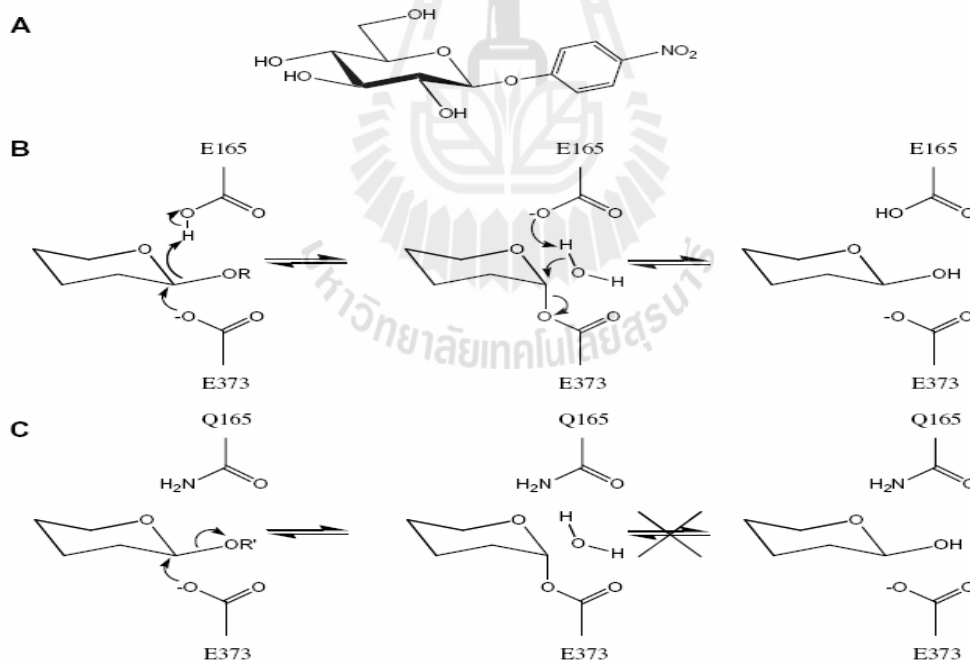
Figure 1.17 Mechanism of trapping of glycosyl intermediate in the human cytoplasmic β-D-glucosidase E165Q acid/base mutant. (A) The structure of pNPGlc. (B) The hydrolysis mechanism of the retained β-glycosidase (R represent aryl or ceramide moieties). (C) The trapping of a glucosyl-enzyme intermediate with a general acid/base mutant (R′ represents an activated leaving group: e.g., pNP) (Noguchi et al., 2008).

Due to the double-displacement mechanism for retaining β-glucosidases, the hydrolysis activities of the mutants of these enzymes in which the acid/base or nucleophile is removed can be rescued by small nucleophiles, leading to the transglycosylation (Rye and Withers, 2000; Wang et al., 1994, 1995). For the acid/base mutant of *Agrobacterium faecalis* β-glucosidase (AbgE170G), the hydrolysis of 2,4-dinitrophenyl β-D-glucoside (dNPGlc), which has a leaving group that does not require protonation (pKa = 3.96), lost its pH dependence from 7 to 9 and could be rescued by various small nucleophiles, such as azide, which produced β-D-glucosyl azide (Wang et al., 1995). This verified E170 as the catalytic acid/base and was consistent with the double displacement mechanism in which the role of the catalytic acid has been removed. Similarly, conversion of the Abg catalytic nucleophile to a small nonnucleophilic amino acid, i.e., Ala, Ser or Gly, resulted in an inactive enzyme that could be rescued by azide or fluoride to form α-D-glucosides, thereby converting a retaining enzyme to an inverting enzyme (Wang et al., 1994).

Alternatively, the use of α-fluoroglucoside, in which the fluoride replaces the enzyme nucleophile in the covalent intermediate, allowed transfer of a β-linked glucosyl moiety onto a sugar or other alcohol. Since these nucleophile mutants have low hydrolytic activity, but relatively high transferase activity, they were designated glycosynthases (Ly and Withers, 1999). The nucleophile mutant of rice BGlu1 β-glucosidase (E414G) showed high transglucosylation activity to synthesize oligosaccharides, when α-fluoroglucoside was used as donor and *p*NP-cellobioside as acceptor (Figure 1.18, Hommalai et al., 2007). Both the acid/base and the nucleophile mutants have potential uses in glycoconjugate synthesis.
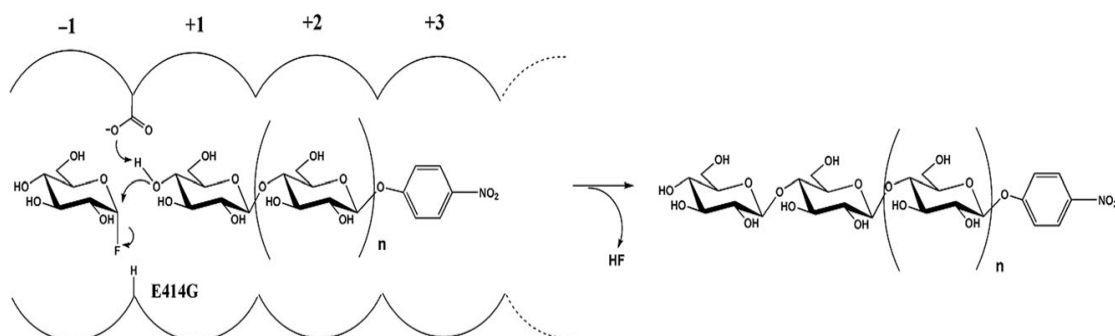
Figure 1.18 Transglucosylation reaction catalyzed by rice BGlu1 E414G glycosynthase (Hommalai et al., 2007).

1.2.6 β-D-Glucosidase substrate specificity

The substrate specificity is very important for the function of the β-D-glucosidases. Because plants possess a large number of β-D-glucosidases, an understanding of the mechanism of substrate specificity is important for predicting the diverse physiological functions of these proteins. The conformational change in the glucose moiety prior to nucleophilic attack and the determinants of binding and deformation of the glucose moiety in subsite -1 are well documented for certain glycoside hydrolases, but how β-D-glucosidases recognize their substrates and interact with them, specifically at the aglycone moiety, is still unclear. Several recent studies that have provided some insights, however (Cicek et al., 2000; Czjzek et al., 2000, 2001; Verdoucq et al., 2003, 2004; Sue et al., 2006; Barleben et al., 2005; Chuenchor et al., 2008, 2011).

Sorghum β-glucosidase Dhr1 (SbDhr1) and maize β-glucosidase Glu1 (ZmGlu1) have been selected to study the aglycone specificity, because they have significantly different behaviors in terms of substrate specificity, even though they share 72% amino acid sequence identity (Cicek et al., 2000). The SbDhr1 has strict specificity for its natural substrate dhurrin (*p*-hydroxy-(S)-mandelonitrile-β-D-glucoside), but the ZmGlu1 hydrolyzes a broad spectrum of substrates in addition to its natural substrate DIMBOAGlc (2-O-β-D-glucopyranosyl-4-hydroxy-7-methoxy-1,4-benzoxaxin-3-one), but not dhurrin.

Structural data from enzyme-substrate complexes showed that the modes of aglycone binding are different for SbDhr1 and ZmGlu1 (Verdoucq et al., 2004). In ZmGlu1, aromatic stacking interactions are dominant in the aglycone-binding pocket, so this enzyme can bind and hydrolyze a number of β-D-glucosides which have different aromatic aglycones (Czjzek et al., 2000, 2001). In contrast, in the aglycone-binding site of SbDhr1, Asn259, Phe261 and Ser462 tightly bind its natural substrate dhurrin, and thereby determine a single position of the aglycone moiety within the aglycone binding pocket (Figure 1.19). The tight binding of the aglycone moiety of dhurrin promotes the stabilization of the reaction intermediate in which the glycone moiety is in a deformed $^1S_3$ conformation within the glycone-binding site, ready for nucleophilic attack to occur (Verdoucq et al., 2004). Compared with the broad specificity of maize β-D-glucosidase, this different binding mode explains the narrow specificity of sorghum dhurrinase-1.
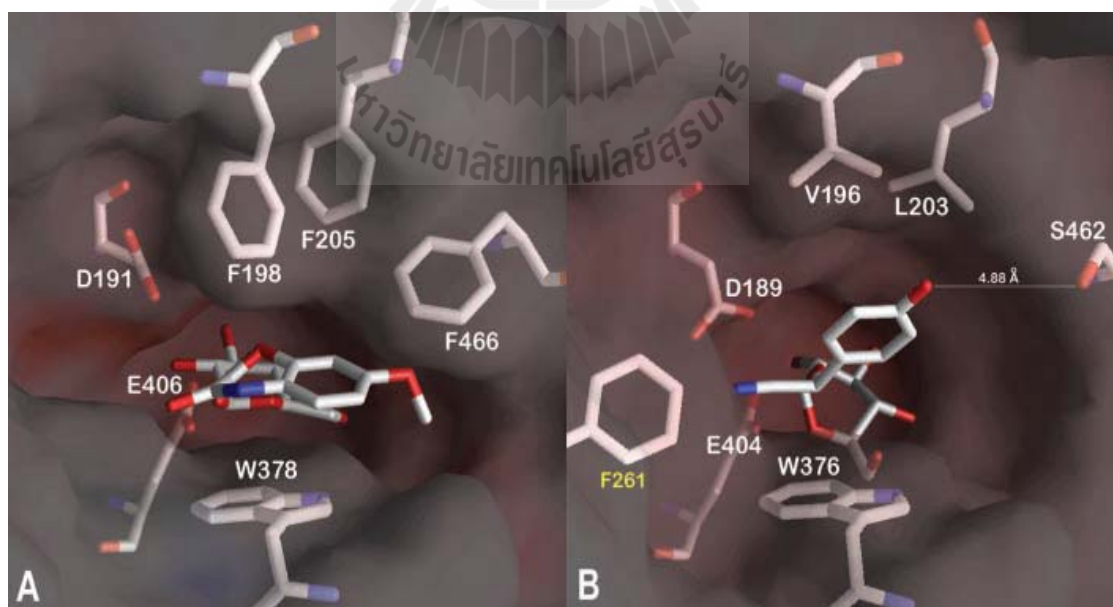
Figure 1.19 The aglycone-binding pockets of ZmGlu1 (A) and SbDhr1 (B). DIMBOA-Glc and dhurrin are shown in stick representation in A and B, respectively. The residues forming the aglycone pocket are visible underneath the surface (Verdoucq et al., 2004).

Rice GH1 β-glucosidases Os3BGlu7 (also called rice BGlu1) and Os4BGlu12 can both hydrolyze β-linked gluco-oligosaccharides (Opassiri et al., 2003, 2006). They have about 52% identical amino acid sequences, but have different specificities for glycones and substrate chain lengths. Os4BGlu12 hydrolyzes β-(1,4)-linked oligosaccharides and laminaribiose at higher rates than *p*NPGlc, and did not hydrolyze cellobiose, gentiobiose, *p*NP-β-D-mannoside, and *p*NP-β-D-cellobioside. Os3BGlu7 can hydrolyze *p*NP-β-D-mannoside and longer chain 1,3-linked oligosaccharides than Os4BGlu12. Another β-glucosidase, Os3BGlu6, hydrolyzed β-(1,2)- and β-(1,3)-linked disaccharides and alkyl glycosides, but barely hydrolyzed cello-oligosaccharides (Seshadri et al., 2009). The structures of Os3BGlu7, Os4BGlu12 and Os3BGlu6 and their mutants have been solved by X-ray crystallography recently (Chuenchor et al., 2008, 2011; Seshadri et al., 2009; Sansenya et al., 2011), so these different substrate specificities were able to be explained from the residue differences in the binding sites of the enzymes.

The structure of an inactive mutant Os3BGlu7 E178Q in complex with oligosaccharides showed that Asn245 hydrogen bonds to the second sugar in the +1 subsite for laminaribiose and the third sugar in the +2 subsite for cellotetraose and cellopentaose (Figure 1.20, Chuenchor et al., 2011). In Os3BGlu6, this residue is replaced with Met251, which appears to block the binding of cellooligosaccharides at the +2 subsite (Figure 1.21, Seshadri et al., 2009), whereas His252 in this position in Os4BGlu12 could hydrogen bond to oligosaccharides (Sansenya et al., 2011, 2012). Mutation of Os3BGlu6 Met251 to Asn resulted in a 15-fold increased k_{cat}/K_m value for hydrolysis of laminaribiose compared to wild type Os3BGlu6 and 9 to 24-fold increases for cellooligosaccharides with degrees of polymerization (DP) of 2-5 (Sansenya et al., 2012). On the other hand, mutation of Os3BGlu7 Asn245 to Met decreased the k_{cat}/K_m of hydrolysis by 6.5-fold for laminaribiose and 17 to 30-fold for cellooligosaccharides with DP >2, while mutation of Os4BGlu12 His252 to Met decreased the corresponding k_{cat}/K_m

values 2 to 6-fold. These results indicated that conversion of Met to Asn could generate an oligosaccharide binding site in Os3BGlu6, and the oligosaccharide binding was weakened if Asn or His was changed to Met at the corresponding positions in Os3BGlu7 and Os4BGlu12. This work also confirmed that the structure-based engineering of one active site cleft residue can dramatically alter the oligosaccharide specificity of plant GH1 enzymes.
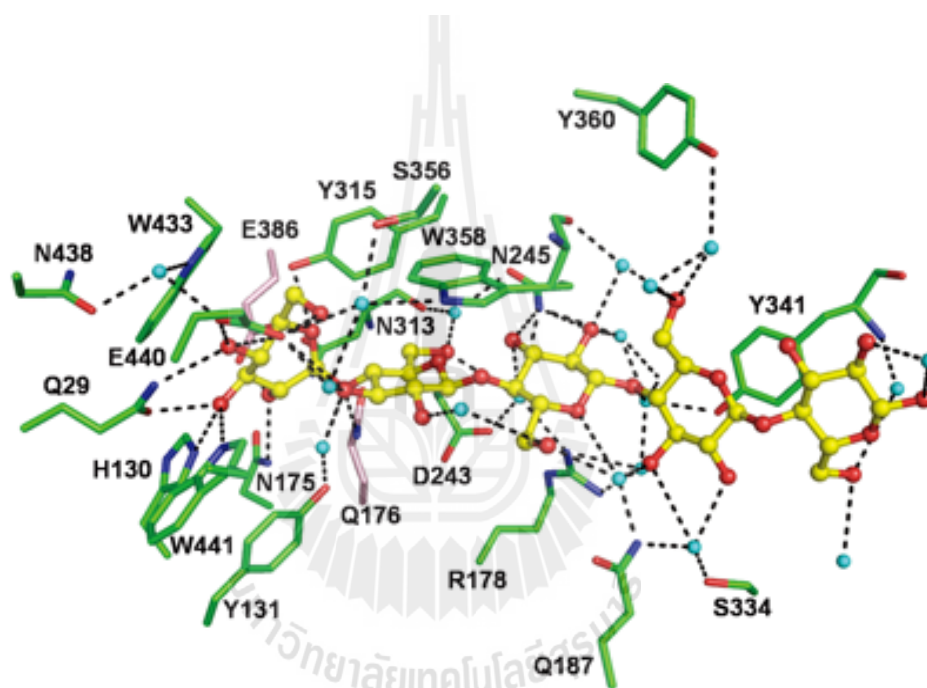
Figure 1.20 Binding of cellopentaose in the active site of rice Os3BGlu7 E176Q. The direct hydrogen bonds were observed between Asn245 and the Glc3 residue in the +2 subsite. This is consistent with the strong binding at the +2 subsite in kinetic subsite analysis (Chuenchor et al., 2011).
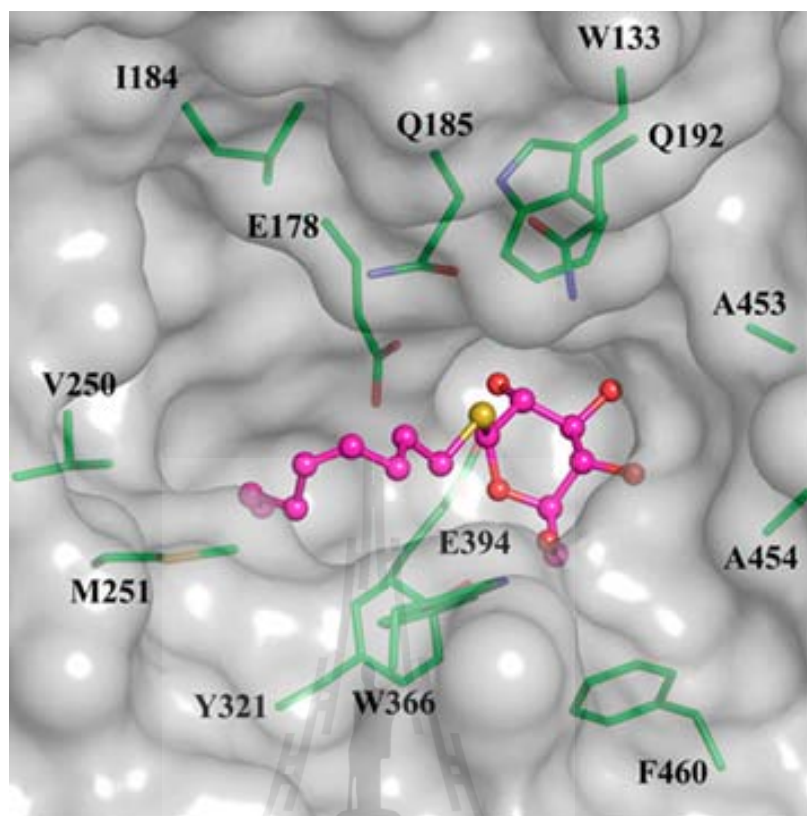
Figure 1.21 The active site of the Os3BGlu6/*n*-octyl-β-D-thioglucopyranoside complex structure. The side chain of Met251 in the mouth of the active site appears to block the binding of extended β-(1/4)-linked oligosaccharides and interact with the hydrophobic aglycone of *n*-octyl-β-D-thioglucopyranoside. This correlates with the preference of Os3BGlu6 for short oligosaccharides and hydrophobic glycosides (Seshadri et al., 2009).

1.3 Research Objectives

The objectives for this thesis project included:

1. Syntheses of GA-glucosyl conjugates, and confirmation of their structures by NMR and mass spectrometry;

2. Extraction, purification and characterization of rice β-glucosidases which are able to hydrolyze the GA-glucosyl conjugates to active GAs from suitable rice tissues;

3. Testing of the rice β-glucosidases which have been produced in our laboratory for hydrolysis activity toward GA-glucosyl conjugates;

4. Study of β-D-glucosidase's mechanism of glucosyl ester hydrolysis by comparing hydrolysis and transglycosylation activities of wild type and acid/base mutant enzymes with GA_4 glucosyl ester.

CHAPTER II

MATERIALS AND METHODS

2.1 Materials

2.1.1 Plant material

Rice (*Oryza sativa* cv. Suphan buri 1) was grown in a field in Sikiu district, Nakhon Ratchasima province during December, 2011. After 10 days, seedling shoots and leaves were collected and used for protein purification.

2.1.2 Chemicals

Gibberellic acid GA_3 and gibberellin GA_4 were purchased from Jiangsu Fengyuan Bioengineering Co. Ltd (Sheyang, P. R. China). *p*-toluenesulphonylmethylnitrosamide (Diazald) was purchased from Shanghai Jinglan Chemical Co. Ltd (Shanghai, P. R. China). Quinoline, α-aceto-bromoglucose, *p*-nitrophenyl-β-D-glucopyranoside (*p*NPGlc), peroxidase/glucose oxidase assay (PGO), phenylmethylsulfonyl fluoride (PMSF), sea sand, 2,2'-azino-bis(3-ethyl-benzothiazoline-6-sulphonic acid) (ABTS), ampicillin, DNase I, kanamycin, tetracyclin, isopropyl β-D-thiogalactoside (IPTG) and lysozyme were purchased from Sigma (St. Louis, USA). Silver oxide, methanol-d4, acetone-d6, chloroform-d, pyridine-d5, deuterium oxide and tetramethylsilane (TMS) were purchased from Aldrich (St. Louis, USA). Molecular sieve 4 Å, trifluoroacetic acid (TFA), polyethylene glycol (PEG), 2-morpholinoethanesulfonic acid (MES), Triton X-100, bovine serum albumin (BSA), calcium chloride, metal sodium and formic acid were

purchased from Fluka (Steinheim, Switzerland). 1,4-Dioxane was purchased from Fisher Scientific (Aalst, Belgium). Silica gel 60 F_{254} and TLC plates silica gel 60 F_{254} were purchased from Merck (Darmstad, Germany). HPLC-grade water and HPLC-grade methanol were purchased from RCI Labscan (Bangkok, Thailand). Trypsin (sequencing grade) was purchased from Promega (Madison, WI, USA). The Bradford assay kit was purchased from Bio-Rad (Hercules, CA, USA). Imidazole was purchased from USB Corporation (Cleveland, USA). Dichloroethane, benzene, ethyl acetate, dichloromethane, chloroform, acetic acid, sulfuric acid, hexane, methanol, ethanol, acetone, pyridine, isopropanol, *n*-propanol, acetonitrile, tetrahydrofuran, disodium ethlenediamine tetraacetate (EDTA), bromophenol blue, ammonium bicarbonate, calcium chloride (anhydrous), sodium sulfate (anhydrous), magnesium sulfate (anhydrous), ammonium sulfate, sodium bicarbonate, sodium chloride, sodium hydroxide, sodium carbonate, citric acid, disodium hydrogen phosphate, hydrochloric acid, Coomassie brilliant blue R250, Tris(hydroxymethyl)-aminomethane (Tris) and sodium dodecyl sulfate were purchased from CARLO ERBA (Rodano, Milano, Italy). Acrylamide, N,N′,N″,N‴-tetramethyl-ethyllenediamine (TEMED), ammonium persulphate, N,N'-methylenebisacrylamide, ConA-Sepharose resin, Superdex-75 and Superdex-200 gel filtration resin, immobilized metal affinity chromatography (IMAC) resin, HiPrep CM-Sepharose fast flow column (16/10, 20 ml), HiTrap SP Sepharose XL column (1 ml) and HiTrap Octyl Sepharose 4 fast flow column (1 ml) were purchased from GE Healthcare (Uppsala, Sweden). Dialysis bags (Cellu-SepT4, regenerated cellulose, 12,000-14,000 MWCO) were purchased from Membrane Filtration Products, Inc. (Seguin, TX, USA). QuikChange® Site-Directed Mutagenesis Kit was purchased from Stratagene (La Jolla, CA, USA). The ultra centrifugal filters (Amicon Ultra, regenerated cellulose, 30,000 MWCO) were purchased from Millipore Corporation (Bedford, MA, USA). Other chemicals and laboratory materials used but not listed here were purchased from a variety of suppliers.

2.2 Methods

2.2.1 Synthesis of gibberellin glucosyl conjugates

2.2.1.1 Synthesis of glucosyl esters of gibberellin GA_3 and GA_4

The GA_3-glucosyl ester (GA_3-Glc) and GA_4-glucosyl ester (GA_4-Glc) were synthesized following the method of Hiraga et al. (1974, Figure 2.1). Briefly, 3 mmol of gibberellin GA_3 or GA_4 was dissolved in 50 ml of dry dioxane (dried overnight with molecular sieves 4Å) in a 100 ml round bottom flask with three necks. Then, 3 mmol of α-acetobromo-glucose and 3 mmol silver oxide (Ag_2O) were added to the solution under nitrogen gas (N_2) flushing. The mixture was stirred overnight at room temp in darkness. Solids was filtered and washed with ethyl acetate (EtOAc) two times. The filtrate was extracted twice with 10% (w/v) of sodium bicarbonate ($NaHCO_3$). The organic phase was separated from the aqueous phase, dried with anhydrous sodium sulphate (Na_2SO_4, dried in the oven before use) and evaporated with a rotary evaporator at 40°C to get a solid. The solid was purified with ethyl acetate-hexane to get a white powder. Acetylated GA_4-Glc was produced with 43.7% yield (0.870 g), while acetylated GA_3-Glc was obtained in 18.3% yield.
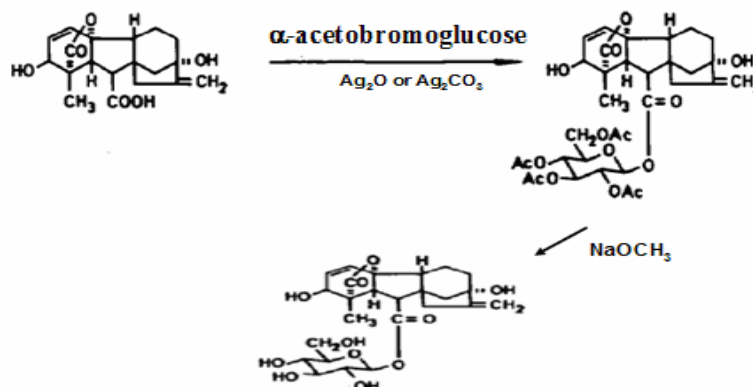
Figure 2.1 Reaction scheme for synthesis of gibberellin glucosyl esters (Hiraga et al., 1974).

Acetylated GA₄-Glc (0.733 g) was deacetylated by dissolving it in 15 ml of methanol (MeOH), cooling to -5°C, and adding 75 ml of 0.05 N sodium methoxide (NaOMe). After 2 hours reaction, the solution pH was adjusted to pH 7 with acetic acid, and the solvent was removed by concentration in a workstation -TurboVap® LV (Caliper life Science, USA) under N_2 flushing at room temperature. The solid obtained was purified by flash silica column chromatography with chloroform/methanol (CHCl₃/MeOH) to yield 0.504 g of GA₄-Glc (92.3% yield), while GA₃-Glc was obtained in 60% yield.

2.2.1.2 Synthesis of gibberellin methyl esters of GA₃ and GA₄

The methylation of GA₃ and GA₄ followed the procedures of Lombardi (1990, Figure 2.2) and was performed in the device shown in Figure 2.3.
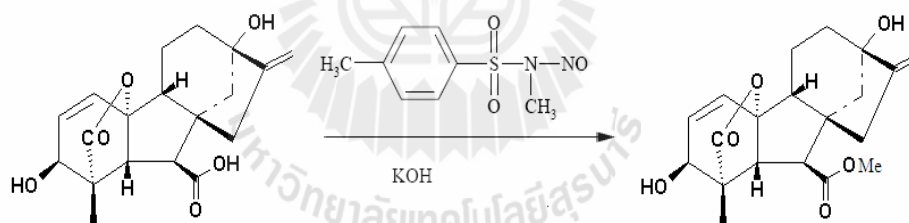
Figure 2.2 Reaction scheme for synthesis of gibberellin methyl esters.
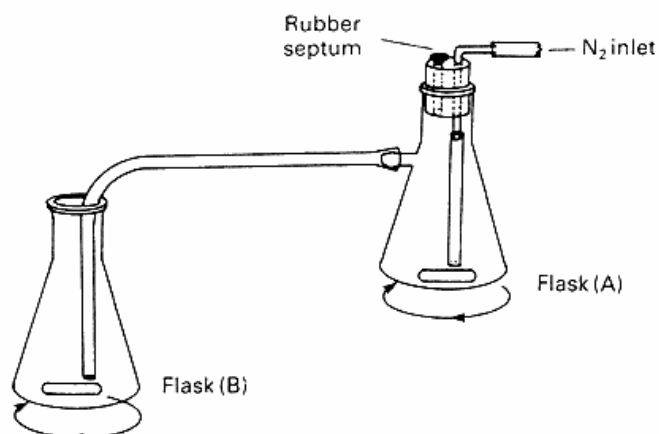
Figure 2.3 The device for methylation reaction (Lombardi, 1990).

In flask B, GA_3 or GA_4 (5 mmol) was dissolved in methylene dichloride (CH_2Cl_2, 40 ml) and ethanol (1 ml), and cooled to 0°C with stirring. *p*-Toluenesulphonylmethyl-nitrosamide (Diazald, 7.5 mmol) was suspended in ethanol (20 ml) in flask A, and the mixture was stirred while nitrogen was allowed to flow into the flask. Sodium hydroxide solution (30%, w/v) was added dropwise to the flask A. After a few seconds, yellow diazomethane began to evolve in flask A and passed into flask B where reaction with the substrate occurred. Sodium hydroxide solution was added dropwise to flask A at a rate of 2 ml/s until the yellow color in flask A was discharged. The solution in flask B was monitored by TLC using hexane/EtOAc (9:11, v:v) to check the completion of the methylation reaction.

The solvent was removed in a rotary evaporator to get the crude methylation products. The crude products were purified by Solid Phase Extraction (SPE) manifold (MACHEREY-NAGEL). The aminopropyl modified silica cartridge-Chromabond® NH_2 (3 ml, MACHEREY-NAGEL) was rinsed with 3 ml of EtOAc, then 3 ml of crude sample in EtOAc was loaded onto the cartridge, and the flow-through was collected. The cartridge was washed with 3 ml of hexane-EtOAc (1:1, v:v), 3 ml of EtOAc and 3 ml of MeOH, respectively; and the fractions were collected. The fractions were checked with TLC, the fractions with GA_3-OMe or GA_4-OMe were combined, and the solvents removed by TurboVap® LV to get white power. The yields for GA_3-OMe and GA_4-OMe were 90.0% and 67.4%, respectively.

2.2.1.3 Synthesis of β-D-glucopyranosyl gibberellin methyl esters of GA_3 and GA_4

β-D-glucopyranosyl gibberellin methyl esters of GA_3 and GA_4 were synthesized following the method of Scheiber et al. (1969) (Figure 2.4).
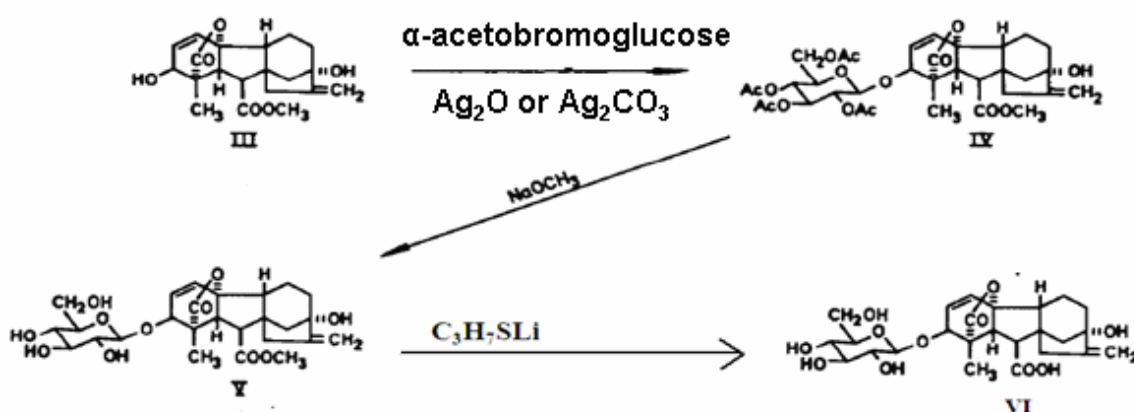
Figure 2.4 Reaction scheme for synthesis of β-D-glucopyranosyl gibberellin methyl ester (Scheiber et al., 1969).

One millimole of GA$_3$-OMe or GA$_4$-OMe, 3 ml of dry dioxane and 1.4 mmol of Ag$_2$O were added into a 100 ml round bottom flask with three necks. Then, 1.2 mmol of α-acetobromoglucose was dissolved in 10 ml of dry benzene and added to the flask dropwise under nitrogen gas (N$_2$) flushing. The flask was heated and 5 ml of benzene was distilled out. Then, the reaction solution was stirred at room temperature for 72 hrs. Forty milliliters of EtOAc was added into the reaction mix to dissolve the solid; the undissolvable solid was filtered and washed with EtOAc. The solvent from the filtrate was removed by evacuation in a rotary evaporator to get crude product. The crude product was then purified by flash column chromatograph over silica gel with hexane/EtOAc to get pure product. The yield for tetra acetylated β-D-glucopyranosyl gibberellin A$_3$ methyl ester (GA$_3$-OMe-Glc-Ac$_4$) was 54.3%, and for tetra acetylated β-D-glucopyranosyl gibberellin A$_4$ methyl ester (GA$_4$-OMe-Glc-Ac$_4$) was 50.0%.

The deacetylation followed the method described in section 2.2.1.1. The yields for β-D-glucopyranosyl gibberellin A$_3$ methyl ester (GA$_3$-OMe-Glc) and for β-D-gluco-pyranosyl gibberellin A$_4$ methyl ester (GA$_4$-OMe-Glc) were approximately 10%.

2.2.1.4 Identification of synthesized products with LC-MS and NMR

An Agilent 1100 HPLC equipped with a ZORBAX Eclipse XDB-C18, 4.6*150 mm, 5 micron column (Agilent, USA) was used to separate the samples. A gradient of 0-80% MeOH in 0.05% (v/v) formic acid was run over 20 min at a flow rate of 0.8 ml/min. The ion peaks and mass spectra were detected with an Agilent single quadrupole MSD mass spectrometer with the atmospheric pressure ionization-electro spray (API-ES) source in negative and positive ion modes. The scan range was 100-1000 *m/z*, and the fragmentor was 70. The flow rate of drying gas was 12.0 l/min and the temperature of the gas was 300°C. The VCap was 3000 V for both positive and negative modes.

The synthesized compounds were confirmed by NMR spectra on a 300 MHz NMR spectrometer (Unity INOVA, Varian, USA). Tetramethylsilane (TMS) was used as the reference standard. Deuterated chloroform ($CDCl_3$), acetone-d6 and methyl sulfoxide-d_6 (DMSO-d_6) were used as solvents, depending on the compound's solubility. The NMR spectra were collected with a Varian 300 ID/PFG probe at a frequency of 299.986 MHz. The software VNMR version 6.1 was used for data processing.

2.2.2 Extraction, purification and characterization of β-glucosidase from rice

2.2.2.1 Extraction of β-glucosidase from 10-day-old rice seedlings

Ten kilograms of 10-day-old rice seedling shoots and leaves (Suphan buri 1) were cut to small pieces with a blender, homogenized with McIlvaine buffer (0.1 M citric acid-0.2 M disodium hydrogen phosphate (Na_2HPO_4), pH 5.0) supplemented with 1 mM phenylmethylsulfonyl fluoride (PMSF) at 4°C overnight. The ratio of seedlings and buffer was 100 g per 600 ml. A crude extract was obtained by filtering through one layer of silk cloth and centrifugation at 12,000 g for 20 min at 4°C. To precipitate protein, 565 g of ammonium sulphate ($(NH_4)_2SO_4$) was added per one liter of crude extract (80% saturation) and stirred at 4°C for 3 h. The solution was centrifuged at 12,000 g for 20 min at 4°C to

collect the protein pellet. The protein pellet was suspended in 4-fold diluted McIlvaine buffer, pH 5, and dialyzed overnight against this buffer in dialysis bags (Cellu-SepT4, regenerated cellulose, 12,000-14,000 MWCO, USA). The dialysis solution was exchanged once. The dialyzed protein was centrifuged at 12,000 g for 20 min at 4°C again to remove precipitate. The supernatant was tested for hydrolysis activities toward pNPGlc and GA$_4$-Glc, and the fractions with the GA$_4$-Glc hydrolyzing activity were purified with the following procedures.

2.2.2.2 Purification of β-glucosidase by ion exchange chromatography with a CM-Sepharose fast flow column

A CM-Sepharose fast flow column (HiPrep CM FF 16/10, 20 ml, GE Healthcare) was equilibrated with 4-fold diluted McIlvaine buffer, pH 5 (buffer A). About 400 mg of dialyzed protein was loaded on to the column. The unbound proteins were washed out with buffer A, and then the bound proteins were eluted with a linear gradient of 0-1.0 M sodium chloride (NaCl) in buffer A at a flow rate of 2.0 ml/min. The column was cleaned with 1.0 M NaCl in buffer A, and then re-equilibrated with buffer A for the next purification. The fractions were collected and tested for hydrolysis activities toward pNPGlc and GA$_4$-Glc. The fractions with activities to GA$_4$-Glc were pooled and precipitated with (NH$_4$)$_2$SO$_4$ (80% saturation), followed by centrifugation at 16,000 g for 20 min at 4°C, then dialyzed against 20 mM Tris(hydroxymethyl)aminomethane hydrochloride (Tris-HCl), pH 7, containing 0.5 M NaCl (buffer B).

2.2.2.3 Purification of β-glucosidase by affinity chromatography with a Con A-Sepharose column

Ten milliliters of Con A-Sepharose 4B was packed in an empty glass column (GE Healthcare) and equilibrated with buffer B. Then, 200 mg of dialyzed protein was loaded

onto the column. The column was washed with 4 column volumes (CV) of buffer B, and then eluted with 4 CV of 0.5 M mannose in buffer B. Four CV of buffer B were used to wash the column again. Then, 20 mM Tris-HCl, containing 0.5 M of NaCl, pH 8.5 and pH 4.5 were used to clean and re-generate the Con A-Sepharose column. The collected fractions were tested for hydrolysis of pNPGlc as mentioned above; the active fractions were combined and concentrated with centrifugal filters (Amicon Ultra, regenerated cellulose, 30,000 MWCO) at 2,800 rpm, 4°C. The buffer of the concentrate was exchanged twice with 4-fold diluted McIlvaine buffer, pH 7, containing 0.2 M NaCl (buffer C), before testing activity with GA_4-Glc and further purification by gel filtration chromatography.

2.2.2.4 Purification of β-glucosidase by gel filtration chromatography with a Superdex-75 gel filtration column

A Superdex-75 gel filtration column (xk 26/40, 150 ml, GE Healthcare) was equilibrated with 2 CV of buffer C on an ÄKTA Protein Purifier system (GE Healthcare). Three milliliters of concentrated protein from the Con A-Sepharose column was loaded to the column with a super loop. Buffer C was used to elute the column at a flow rate of 1.0 ml/min. The fractions were tested for pNPGlc and GA_4-Glc hydrolysis activities and their purities checked with polyacrylamide gel electrophoresis (SDS-PAGE). The active fractions were pooled and concentrated with centrifugal filters as described above, then the buffer was exchanged with 4-fold diluted McIlvaine buffer, pH 5 (buffer A).

2.2.2.5 Purification of β-glucosidase by cation exchange chromatography with a HiTrap SP XL column

A 1 ml HiTrap SP Sepharose XL column (GE Healthcare) was equilibrated with buffer A on an ÄKTA Protein Purifier system. Five hundred microliters of concentrated

protein from the S-75 gel filtration column β-glucosidase pool was loaded onto the column. The column was eluted with a linear gradient of 0-1.0 M NaCl in buffer A at a flow rate of 1.0 ml/min. The fractions were tested for pNPGlc and GA$_4$-Glc hydrolysis activities. The purities of the active fractions were checked with SDS-PAGE and then similar fractions were pooled, concentrated with centrifugal filters as described above, and the buffer exchanged with 50 mM phosphate, pH 7, containing 1.7 M (NH$_4$)$_2$SO$_4$ (buffer D).

2.2.2.6 Purification of β-glucosidase by hydrophobic interaction chromatography with an Octyl Sepharose 4 column

Three milliliters of dialyzed protein from SP chromatography were loaded to a 1 ml HiTrap octyl FF column (Sepharose 4, GE Healthcare), which was pre-equilibrated with buffer D. The protein was eluted with a linear gradient of 1.7-0 M of (NH$_4$)$_2$SO$_4$ in 50 mM phosphate, pH 7. The buffer of the collected fractions was exchanged twice with 4-fold diluted McIlvaine buffer, pH 5. The fractions were then tested for pNPGlc and GA$_4$-Glc hydrolysis, and their protein components evaluated with SDS-PAGE.

2.2.2.7 Purification of β-glucosidase by gel filtration chromatography with a Superdex-200 gel filtration column

The active fractions from the octyl Sepharose 4 column were concentrated and loaded to the Superdex-200 gel filtration column (10/300, 24 ml, GE Healthcare) which was equilibrated with buffer C, as described for the S-75 gel filtration column, and eluted with the same buffer. The protein concentrations and GA$_4$-Glc hydrolysis activities of the fractions were measured, and their protein compositions checked with SDS-PAGE.

2.2.2.8 Identification of β-glucosidases with LC-MS

The protein from the Superdex-200 column purification was separated on an 8% SDS-PAGE. Two main bands were exercised separately and chopped to 5-8 pieces (1x1x1 mm), then destained with 25 mM ammonium bicarbonate (NH_4HCO_3)/50% methanol (v/v). Two hundred microliters of sterile water was added into the vials and they were shaken for 5 min at room temperature. Water was removed and 200 µl of 100% acetonitrile (ACN) was added and shaken for 5 min at room temperature. After the ACN was removed, the gel plugs were dried at room temperature for 5-10 min. In order to reduce disulfide bonds, the gels were immersed in 20 µl of 10 mM dithiothreitol in 10 mM NH_4HCO_3 and incubated at 56°C for 1 h. After removal of the 10 mM dithiothreitol in 10 mM NH_4HCO_3 solution, 20 µl of 100 mM iodoacetamide in 10 mM NH_4HCO_3 was added to the gels. The gels were kept in the dark at room temperature for 1 h, and then washed twice with 200 µl of 100% ACN.

Twenty microliters of 10 ng/µl trypsin (Promega, sequencing grade) was added to the gels for digestion. The gels were kept at 4°C or room temperature for 20 min then incubated at 37°C for 3 h. The solution was transferred to a new tube, extracted with 30 µL of 50% ACN/0.1% formic acid (v/v), and shaken at room temperature for 10 min. The extracted solution was dried in an incubator at 40°C for 3-4 h or overnight. The samples were kept at -80°C until analysis.

Nanoscale LC separation of tryptic peptides was performed with a NanoAcquity system (Waters Corp., Milford, MA) equipped with a Symmetry C_{18} 5 µm, 180 µm x 20 mm trap column and a BEH130 C_{18} 1.7 µm, 100 µm x 100 mm analytical reverse phase column (Waters Corp., Milford, MA). The samples were initially transferred with an aqueous 0.1% formic acid solution to the trap column with a flow rate of 15 µl/min for 1 min. Mobile phase A was 0.1% formic acid in water, while mobile phase B was 0.1%

formic acid in ACN. The peptides were separated with a gradient of 15–50% mobile phase B over 15 min at a flow rate of 600 nl/min followed by a 3-min rinse with 80% of mobile phase B. The column temperature was maintained at 35°C. The lock mass was delivered from the auxiliary pump of the NanoAcquity pump with a constant flow rate of 500 nl/min at a concentration of 200 fmol/μl of [Glu[1]]fibrinopeptide B to the reference sprayer of the NanoLockSpray source of the mass spectrometer. All samples were analyzed once. Analysis of tryptic peptides was performed on a SYNAPT[TM] HDMS mass spectrometer (Waters Corp., Manchester, UK). For all measurements, the mass spectrometer was operated in the V-mode of analysis with a resolution of at 9,000 full-width half-maximum. All analyses were performed in positive ion nanoelectrospray mode. The time-of-flight analyzer of the mass spectrometer was externally calibrated with [Glu[1]]fibrinopeptide B from m/z 50 to 1600 with acquisition lock mass corrected using the monoisotopic mass of the doubly charged precursor of [Glu[1]]fibrinopeptide B. The reference sprayer was sampled with a frequency of 20 s. Accurate mass LC-MS data were acquired in data direct acquisition mode. The energy of the trap was set at a collision energy of 6 V. In the transfer collision energy control, the low energy was set at 4 V. The quadrupole mass analyzer was adjusted such that ions from m/z 300 to 1800 were efficiently transmitted. The MS/MS survey was over the range of 50 to 1990 Da and the scan time was 0.5 s.

2.2.2.9 Determination of β-glucosidase activity

The activities of protein fractions to hydrolyze pNPGlc were tested in a manner similar to previously published methods (Opassiri et al., 2003, 2006; Seshadri et al., 2009; Kuntothom et al., 2009). Aliquots of enzyme solutions were incubated with 4 mM pNPGlc in 50 mM sodium acetate (NaOAc) buffer, pH 5.0, (total reaction volume 50 μl) at 30°C for 20 min. The reactions were stopped by adding 150 μl of 2 M sodium carbonate (Na_2CO_3). The released p-nitrophenol (pNP) was quantified by measuring the absorbance

at 405 nm (A_{405}) with a microplate reader (Thermo Labsystems, Finland), and comparing it to that of a *p*NP standard curve.

The hydrolysis of GA$_4$-glucosyl ester (GA$_4$-Glc) was determined with a peroxidase/glucose oxidase-based assay (PGO assay, Sigma). PGO reagent was prepared by dissolving one capsule of PGO enzymes in 100 ml of sterile distilled water. 2,2'-Azino-bis(3-ethylbenzothiazoline-6-sulphonic acid) (ABTS) was dissolved to 1 mg/ml in 50 mM NaOAc buffer, pH 5.0. The protein fractions were incubated with 1.72 mM GA$_4$-Glc in 50 mM NaOAc buffer, pH 5.0, at 30°C for 20 min. The reactions were stopped by boiling 1 min and cooled on ice immediately. Then, 100 μl of PGO and 50 μl of ABTS were added to the reaction mixes, mixed and incubated at 37°C for 30 min. The A_{405} was measured, and the amounts of glucose released were calculated from a glucose standard curve developed in the same manner.

Protein concentrations were determined with a Bio-Rad Bradford assay with bovine serum albumin (BSA) as a standard.

2.2.2.10 Determination of protein components, purity and size with SDS-PAGE

SDS-PAGE, sodium dodecyl sulfate polyacrylamide gel electrophoresis was performed according to Laemmli (1970). 12.5%, 10% and 8% (w/v) acrylamide separating gels were prepared in 0.375 M Tris-HCl buffer, pH 8.8, while 5% stacking gel was prepared in 0.065 M Tris-HCl buffer, pH 6.8. Fifteen microliters of protein was mixed with 10 μl of reducing loading buffer (0.05 M Tris-HCl buffer, pH 6.8; 50% glycerol (v/v); 10% SDS (w/v); 20% 2-mercaptoethanol (v/v) and 0.2 mg/ml bromophenol blue), boiled 5 min in a water bath, spun down a few minutes, and then loaded onto the gel. The protein standard marker, which included bovine α-lactalbumin (14 kDa), trypsin inhibitor (21.5 kDa), bovine carbonic anhydrase (31 kDa), ovalbumin (45 kDa), bovin serum

albumin (66 kDa) and phosphoryase (97.4 kDa), was loaded on to the same gel. The electrophoresis was run at 200 V for 50 min in 1X running buffer (0.3% (w/v) Tris-base, 1.4% (w/v) glycine, 1% (w/v) SDS). The gel was stained with Coomassie brilliant blue R-250 (CBB) solution for 40 min, which included 0.025% CBB, 40% methanol, 7% acetic acid, and then destained with destaining solution (40% methanol and 7% acetic acid) twice, followed by water. The gel was dried at 55°C for 90 min under vacuum.

Silver staining was also used to detect low amounts of protein. The silver staining kit from GE Healthcare was used following the company's protocol.

2.2.3 Screening of rice GH1 enzymes for GA$_4$-glucosyl ester hydrolysis

Five glycoside hydrolase family 1(GH1) enzymes that have been expressed in our lab, Os3BGlu6 (Seshadri et al., 2009), Os3BGlu7 (BGlu1, Opassiri et al., 2003), Os4BGlu12 (Opassiri et al., 2006), Os3BGlu18 (Baiya et al., unpublished) and Os9BGlu31 (Luang et al., unpublished) were tested for the hydrolysis activity to pNPGlc and GA$_4$-Glc according to method described in section 2.2.2.9.

2.2.4 Site-directed mutagenesis of Os3BGlu6

Mutagenesis of the pET32/Os3BGlu6 expression vector (Seshadri et al., 2009) to create the Os3BGlu6E178A, Os3BGlu6E178D, Os3BGlu6E178Q, Os3BGlu6E394D and Os3BGlu6E394Q mutations was performed with the QuikChange® Site-Directed Mutagenesis Kit (Stratagene, La Jolla, CA, USA) according to the supplier's instructions. The following oligonucleotides were used for mutagenesis: for E178A, 5'GATCA CGCTCAACGCGCCGCACACGGTG3' and its reverse complement; for E178D, 5'GATCACGCTCAACGATCCGCACACGGTGG 3' and its reverse complement; for E178Q, 5'GGATCACGCTCAACCAACCGCACACGGTGGC3' and its reverse complement; for E394D, 5'CCAGTGTACATCACTGATAACGGGATGGATGACA

GC3' and its reverse complement; and for E394Q, 5'CCACCAGTGTACATCACT CAGAACGGGATGGATGACAGC3' and its reverse complement. The cDNA were confirmed to include the desired mutations and be free of additional mutations by automated DNA sequencing (Macrogen Corp., Seoul, Rep. of Korea).

2.2.5 Recombinant expression and purification of Os3BGlu6 and its mutants

2.2.5.1 Recombinant expression of Os3BGlu6 and its mutants

The wild type rice Os3BGlu6 and its mutants M251N, E178Q, E178A and E178D were expressed in *Escherichia coli* strain Origami (DE3) as fusion proteins with N-terminal thioredoxin and His_6 tags, as described previously for Os3BGlu6 (Seshadri, et al., 2009).

The recombinant plasmids containing the Os3BGlu6 wild type, E178A, E178D, E178Q, and M251N were transformed into *E. coli* strain Origami (DE3) competent cells by heat shocking $CaCl_2$ competent cells and transformed cells were selected on an LB plate containing 15 μg/ml kanamycin, 12.5 μg/ml tetracycline and 50 μg/ml ampicillin at 37°C overnight. One colony of transformed cells was picked into 5 ml LB liquid media containing the same antibiotics and grown at 37°C overnight. The starter culture was added at a 1:100 dilution to a large scale culture in the same medium and grown continuously at 37°C with shaking at 220 rpm until the OD_{600} reached 0.6-0.8. Protein expression was induced with 0.4 mM IPTG (final concentration) at 20°C for 16-18 h. Cells were collected by centrifugation at 5,000 rpm for 10 min at 4°C and the pellet was stored at -80°C for 30 min or until protein extraction.

2.2.5.2 Extraction of recombinant Os3BGlu6 protein from induced cell

The pellets were thawed at room temperature. Cells were resuspended with extraction buffer (20 mM Tris-HCl, pH 8.0, 200 μg/ml lysozyme, 1% Triton-X100, 1 mM

PMSF and 0.25 mg/ml DNase I) and incubated at room temperature for 30 min. Soluble proteins were separated from cell debris by centrifugation at 12,000 rpm for 10 min at 4°C.

2.2.5.3 Purification of Os3BGlu6 and its mutants

Os3BGlu6 wild type, E178A, E178D, E178Q and M251N were purified with 2 steps of IMAC. The crude protein was mixed with pre-equilibrated cobalt (IMAC) resin with equilibration buffer (20 mM Tris-HCl, pH 8.0, and 150 mM NaCl) at 4°C for 30 min. The resin with crude protein was loaded into a column and unbound proteins were washed out with 5 CV of equilibration buffer, 5 CV of 5 mM imidazole in equilibration buffer and 5 CV of 10 mM imidazole in equilibration buffer, respectively. The bound proteins were eluted with 5 CV of 250 mM imidazole in equilibration buffer. The fractions with activity were combined, concentrated and imidazole removed by centrifugal ultrafiltration (Amico Ultra, 30k MWCO) at 2,800 rpm, 4°C; and the buffer exchanged with 50 mM Tris-HCl, pH 8.0, at 4°C. The concentrated proteins from the 1st IMAC step were incubated with Tobacco etch virus (TEV) protease at 4°C for 12-14 h to cut off the N-terminal thioredoxin, His$_6$ and S tags.

The N-terminal thioredoxin, His$_6$ and S tags were removed with a second IMAC purification. The proteins were mixed with cobalt (IMAC) resin equilibrated with equilibration buffer at 4°C for 30 min. The resin with protein was loaded into a column and unbound proteins were washed out with 10 CV of equilibration buffer, 10 CV of 5 mM imidazole in equilibration buffer, and 10 CV of 10 mM imidazole in equilibration buffer, respectively. Then bound proteins were eluted with 10 CV of elution buffer. The flow-through and wash fractions with activity were combined, concentrated and depleted of imidazole by centrifugal ultrafiltration (Amico Ultra, 30k MWCO) at 2,800 rpm, 4°C.

Protein concentrations were estimated by the Bradford protein assay (Bio-Rad) with BSA as the standard.

2.2.6 Characterization of Os3BGlu6 and its mutants

2.2.6.1 Determination of pH optima for Os3BGlu6 and its mutants

The pH optima of Os3BGlu6 and Os3BGlu6 M251N for hydrolysis of pNPGlc were determined by incubating 1 µg of enzyme with 2 mM pNPGlc, in 80 µl of universal buffer (0.1 M citric acid-0.1 M disodium hydrogen phosphate, final volume 100 µl), pH 2 to 11 in 0.5-pH-unit increments, at 30°C for 10 min. The reactions were stopped by adding 100 µl of 2 M sodium carbonate (Na_2CO_3). The released pNP was determined quantitatively by measuring the absorbance at 405 nm (A_{405}) and calculated by comparison to a pNP standard curve.

The optimum pH of Os3BGlu6 and its M251N, E178Q and E178A mutants for hydrolysis of GA$_4$-Glc were determined by incubating 1 µg of Os3BGlu6 or Os3BGlu6 M251N, or 5.0 µg of E178Q or E178A with 0.86 mM GA$_4$-Glc in 80 µl of 100 mM universal buffer (final volume was 100 µl), pH 2 to 11 in 0.5-pH-unit increments at 30° for 20 min. The reactions were stopped by boiling 1 min and cooled on ice immediately. Then, the amounts of glucose released were determined by the PGO assay as described in section 2.2.2.10.

The activity versus pH curves of the E178 Q and E178A mutants for hydrolysis GA$_4$-Glc were also determined in 50 mM MES buffer in the range of pH 5.0 to 7.5 in 0.5-pH-unit increments, following the same procedure as in universal buffer.

2.2.6.2 Measurement of wild type and mutant Os3BGlu6 activities for hydrolysis of gibberellin glucosyl ester and *p*NP-glucoside

The activities of Os3BGlu6 wild type and mutants to hydrolyze *p*NPGlc were analyzed. The enzymes were incubated with various concentrations of *p*NPGlc in 50 mM NaOAc buffer, pH 5.0, at 30°C and the reactions were stopped by adding 150 µl of 2 M sodium carbonate. The released *p*NP was measured as described above. To determine the kinetic parameters, variable reaction times, enzyme amounts and substrate concentrations were tested to obtain the initial velocities. The K_m and k_{cat} were calculated from nonlinear regression of Michaelis-Menten plots with Grafit 5.0 software.

To measure hydrolysis activities toward GA$_4$-Glc, Os3BGlu6 wild type and M251N mutant were incubated with GA$_4$-Glc in 50 mM NaOAc buffer, pH 5.0, but 50 mM MES buffer was selected for the E178Q and E178A mutants to avoid transglucosylation. The reactions were stopped by boiling 1 min and immediately cooled on ice. The amounts of glucose released were determined as described in section 2.2.2.10. The kinetic parameters were determined as described for *p*NPGlc.

2.2.6.3 Identification of transglucosylation products with TLC, LC-MS and NMR

Transglucosylation reactions were studied for Os3BGlu6 wild type and its M251N, E178Q and E178A mutants. For Os3BGlu6 wild type and E178Q mutant, *p*NPGlc or 2',4'-dinitrophenyl-2-deoxy-2-fluoro-β-D-glucopyranoside (2F-DNPG) donor was reacted with 1.0 µg of enzymes in 50 mM MES buffer, pH 5; and 40 mM sodium azide or 0.96 mM free GA$_4$ was used as acceptor. At different times, 10 µl aliquots of reaction mix were removed, boiled 1 min, and kept on ice for TLC analysis. Reactions without enzymes were used as controls. After overnight reactions, sample aliquots were spotted on TLC and the TLC plates developed with EtOAc-MeOH-H$_2$O (7.5:2.5:1.0, v:v:v) or CHCl$_3$-MeOH

(7:3, v:v). The products were detected by staining with 10% (v/v) sulfuric acid in ethanol followed by charring.

The new transglucosylation products of E178Q and E178A were analyzed with LC-MS. The column and LC-MS method was the same as that described in section 2.2.1.4.

The transglucosylation product was also manually collected from HPLC with multiple injections. The fractions were pooled and dried with a vacuum centrifuge. The product was dissolved in acetone-d6, and ^{1}H NMR and gCOSY spectra were collected with a 300 MHz NMR spectrometer (Unity INOVA, Varian, USA). TMS was used as the reference standard.

2.2.6.4 Transglucosylation kinetics of the acid/base mutants of Os3BGlu6

The pH optima of Os3BGlu6 E178Q and E178A for transglucosylation were determined in 50 mM MES, pH 5.0-7.5, and 50 mM NaOAc buffer, pH 4.0-6.0, in 0.5-pH-unit increments. Two micrograms of E178Q or E178A were incubated with 2 mM GA$_4$-Glc and 100 mM sodium azide, in the different pH buffers at 30°C for 30 min. The reactions without sodium azide were used to measure hydrolysis activities. The reactions were stopped by boiling 1 min and cooled on ice immediately. The reaction mixes were centrifuged at 6,000 rpm for 15 min and separated by LC-MS, as described in the preceding section. The gibberellin GA$_4$ released was detected with a DAD detector at 210 nm, and the amounts were calculated by comparison of the peak areas to a gibberellin GA$_4$ standard curve.

The concentrations of donor GA$_4$-Glc and acceptor sodium azide were varied to test their effects on transglucosylation kinetics. The concentration of sodium azide was varied from 0 to 400 mM, while the GA$_4$-Glc donor was fixed at 2 mM. The reactions were performed in 50 mM MES, pH 5, at 30°C for 20 min. The turnover rates of GA$_4$

release per minute per unit enzyme (V_0/E_0) were calculated based on the 210 nm peak area of GA$_4$. For the reactions varying the concentrations of GA$_4$-Glc donor, sodium azide was fixed at 50, 100, 200 and 400 mM, and reactions without sodium azide were used as controls.

CHAPTER III

RESULTS

3.1 Syntheses of GA-glucosyl Conjugates

3.1.1 Synthesis of the glucosyl ester of GA$_4$

Acetylated and deacetylated GA$_4$-Glc esters (Figure 3.1) were synthesized as described in section 2.2.1. Acetylated GA$_4$-Glc was dissolved in CDCl$_3$ and deacetylated GA$_4$-Glc in dimethyl sulfoxide-d6 (DMSO-d6) and NMR spectra were collected. A ^{1}H NMR spectrum was also acquired for the free gibberellin GA$_4$ (Figure 3.2) for comparison.

By comparing the spectra of acetylated GA$_4$-Glc ester (Figure 3.3) with free GA$_4$, the peaks for the glucosyl group attached to GA$_4$ were located on the NMR spectrum (enclosed in rectangular boxes in Figure 3.4). The gCOSY experiment confirmed the correlations within the protons on the glucosyl ring (Figures 3.5 and 3.6). The chemical shifts were assigned as δ5.78, H1, d, $J_{2,1}$=8.1 Hz; δ 5.14-5.30, m, H3, H4; δ5.15, H2, t, $J_{1,2}$=8.1 Hz; δ3.81, H5, m; δ4.11-4.23, H6, H6′, m. The coupling constant of H1 ($J_{2,1}$=8.1 Hz) confirmed that the acetylated GA$_4$-Glc ester had a β-configuration.
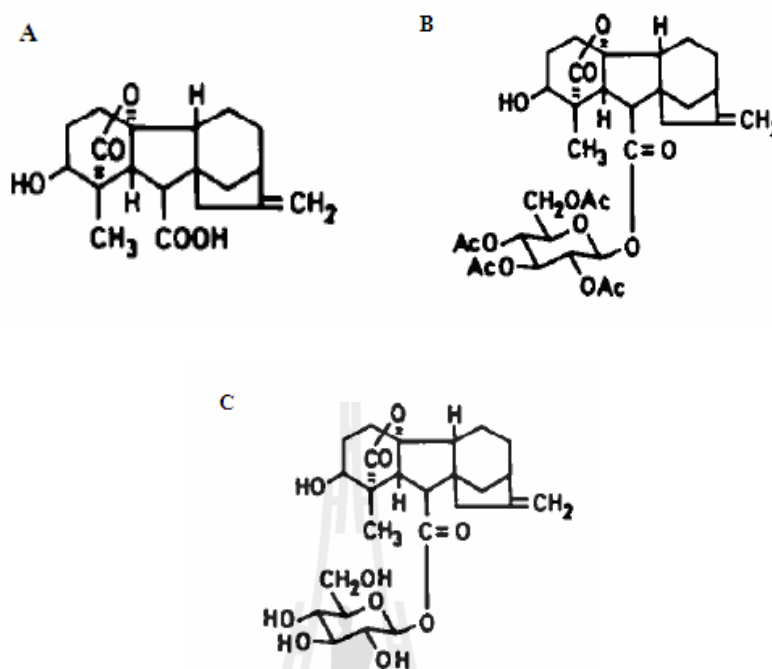
Figure 3.1 The structures of the gibberellin GA_4 and its derivatives. **A**. GA_4, $C_{19}H_{24}O_5$, molecular weight 332.39; **B**. Acetylated GA_4-Glc ester, $C_{33}H_{42}O_{14}$, molecular weight 662.68; **C**. GA_4-Glc ester, $C_{25}H_{34}O_{10}$, molecular weight 494.53.
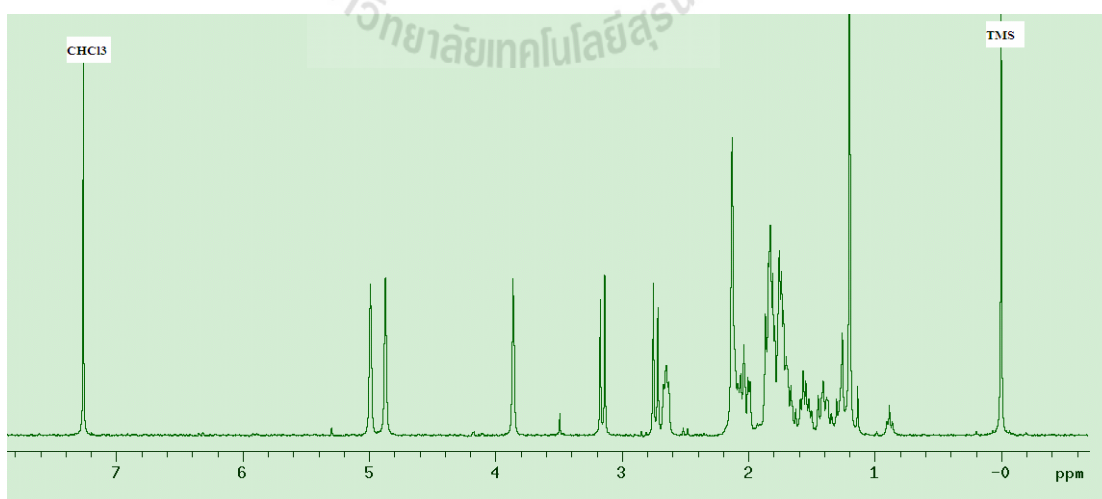
Figure 3.2 ^1H NMR spectrum of the gibberellin GA_4 in $CDCl_3$. TMS was used as reference standard. The spectrum was acquired at 299.986 MHz with a Varian 300 MHz NMR spectrometer.
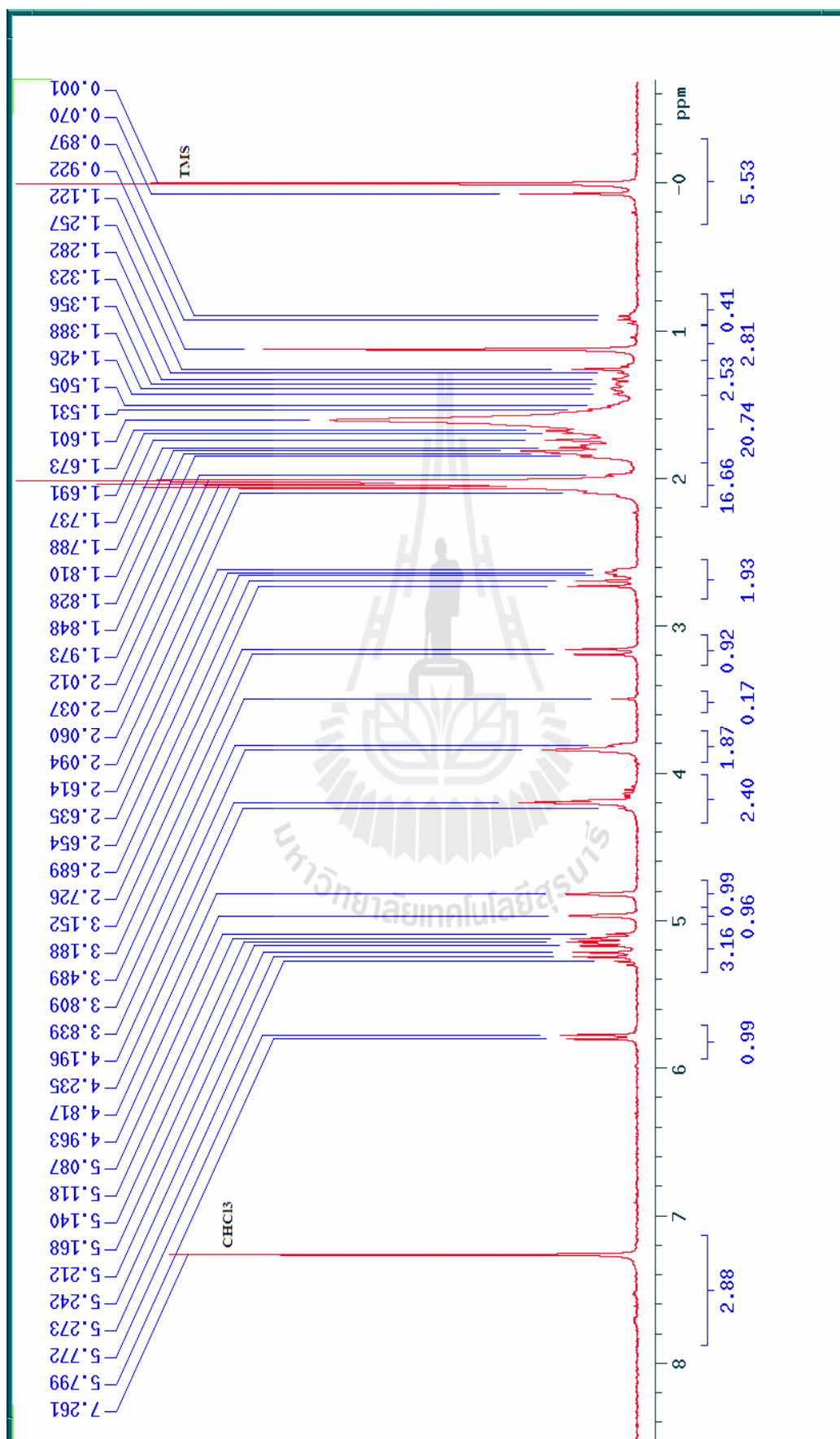
Figure 3.3 ^{1}H NMR spectrum of acetylated GA$_4$-Glc ester in CDCl$_3$.
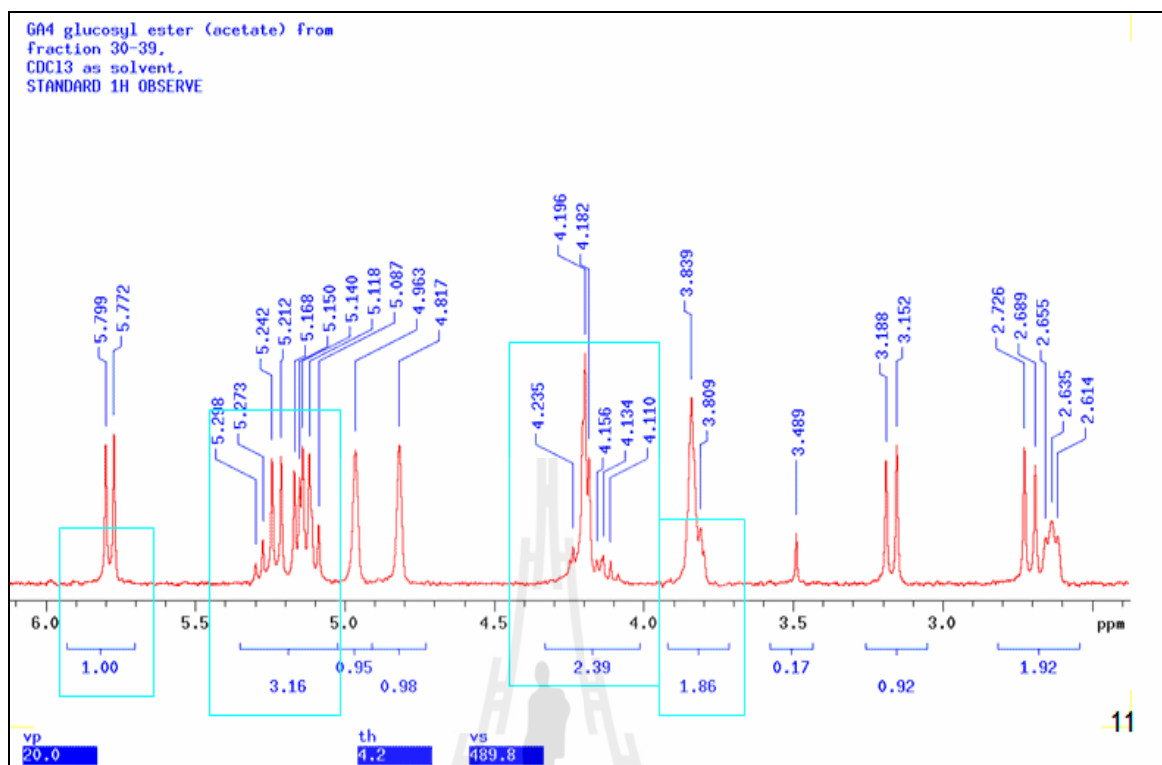
Figure 3.4 Expanded view of the ^{1}H NMR spectrum of acetylated GA$_4$-Glc ester in CDCl$_3$. The 7 protons on the glucosyl ring are boxed in rectangles (one proton from GA$_4$ was included at position δ3.839). The coupling constant of the H1 peak at δ5.786 (J$_{2,1}$=8.1 Hz) confirmed that the acetylated GA$_4$-Glc ester had a β-configuration.
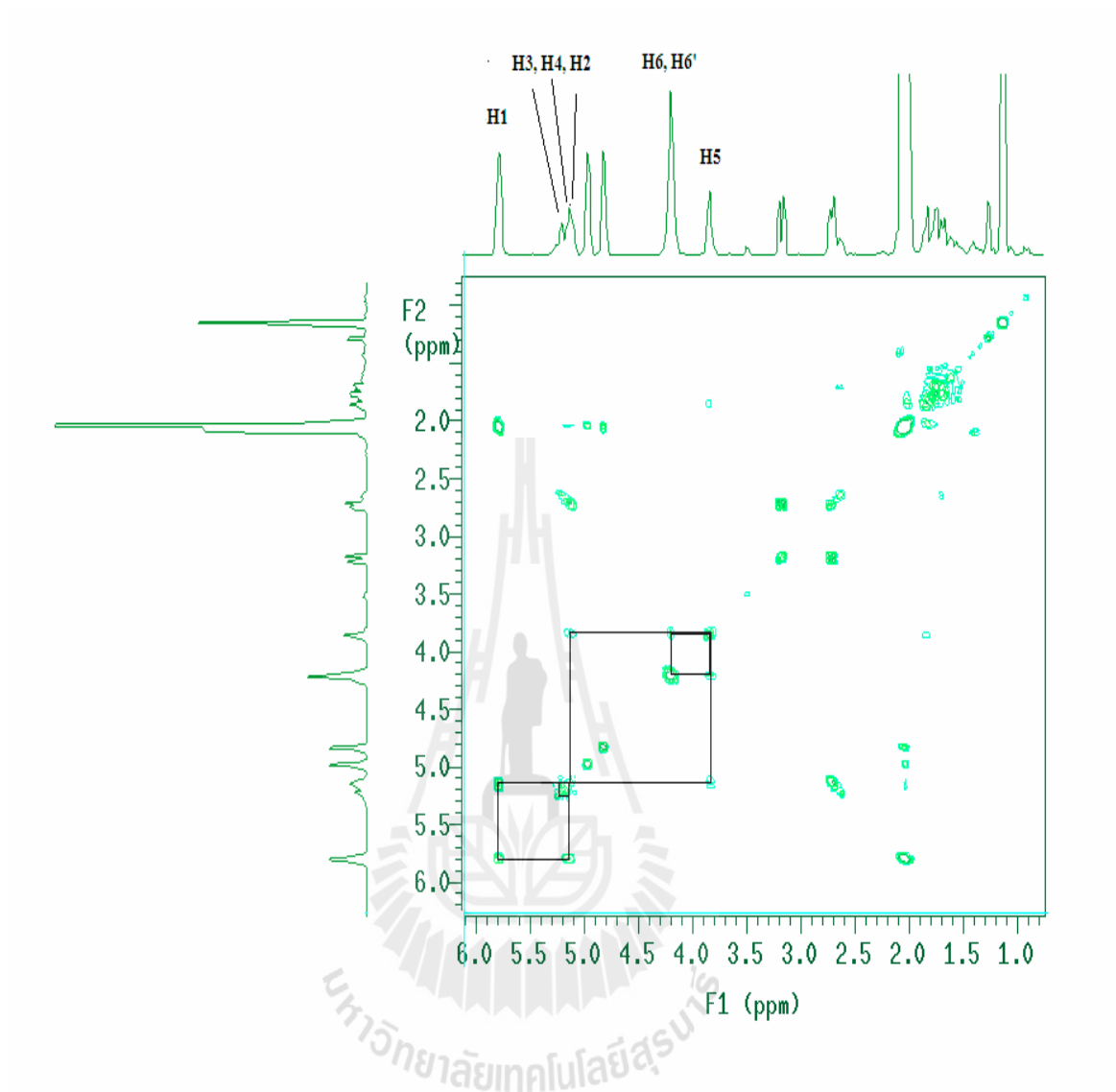
Figure 3.5 gCOSY spectrum of acetylated GA$_4$-Glc ester in CDCl$_3$. The 7 protons on the glucosyl ring are labeled on the top of the peaks. The boxes show the correlations between the 7 protons.
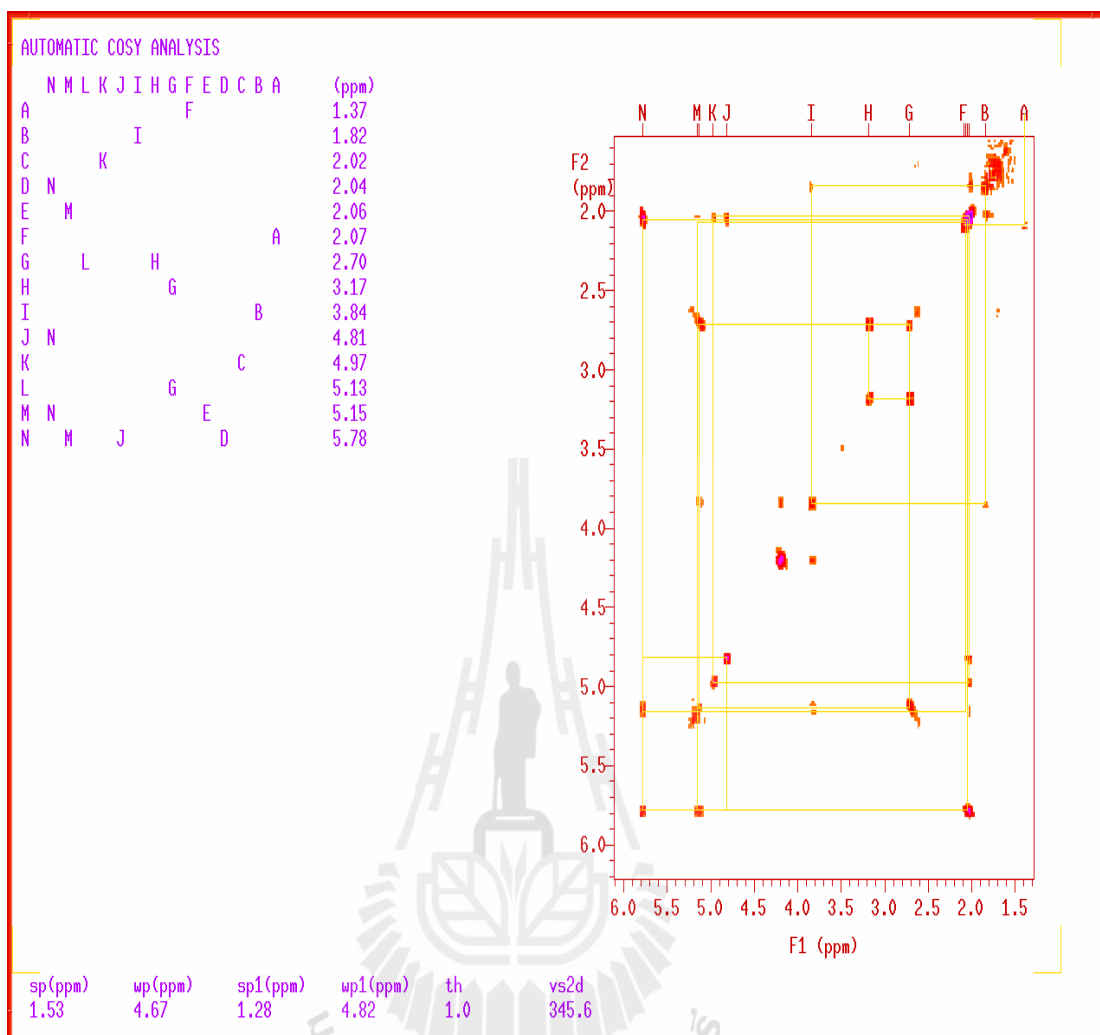
Figure 3.6 Analysis of gCOSY spectrum for acetylated GA_4-Glc ester.

The identity of the deacetylated GA_4-Glc ester was confirmed from its mass spectrum (Figure 3.7). In the positive mode, $[M+Na]^+$ at m/z 517.1, $[M+H-H_2O]^+$ at m/z 477.2, and $[M+H-Glc]^+$ at m/z 315.5 were detected. Based on ^1H and gCOSY NMR (Figures 3.8 and 3.9), δ5.32 was assigned as H1, d, $J_{2,1}$=8.1 Hz, and δ3.1 was assigned as H2. Other protons on the glucosyl ring were not assigned since they were overlapped at the range δ3.1-3.6 and not necessary for the structure confirmation. The NMR chemical shift and coupling constant of H1 confirmed the compound as a GA_4-β-D-Glc ester. The ^1H NMR was also consistent with the published data (Hiraga et al., 1974).
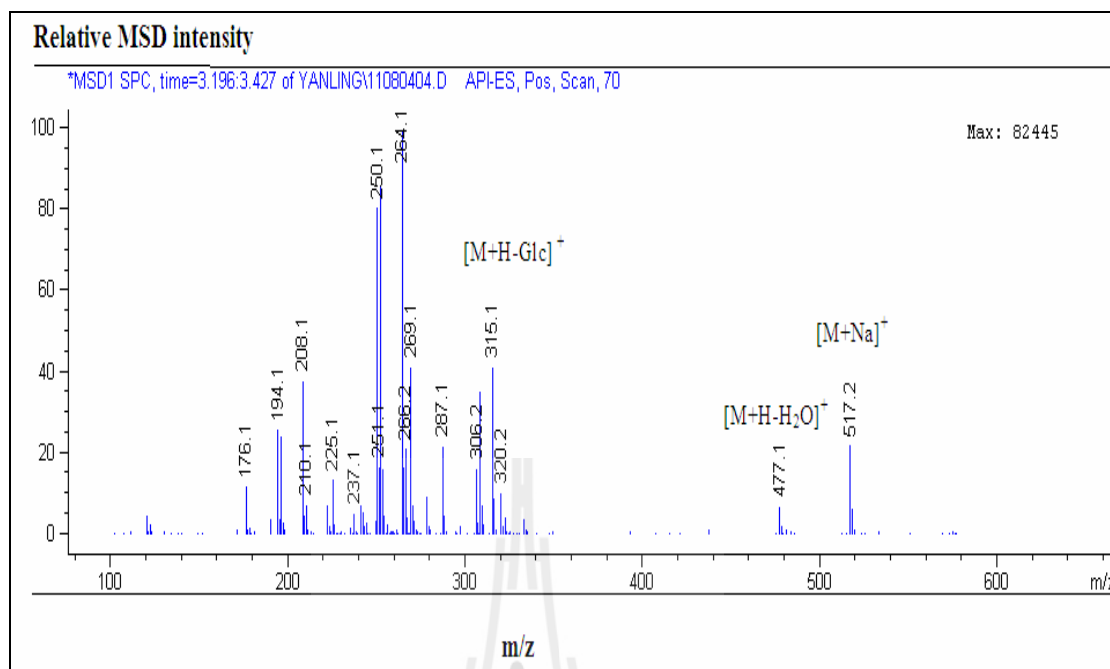
Figure 3.7 The mass spectrum of GA₄-Glc in the positive mode. $[M+Na]^+$, $[M+H-H_2O]^+$ and $[M+H-Glc]^+$ are marked on the mass spectrum.
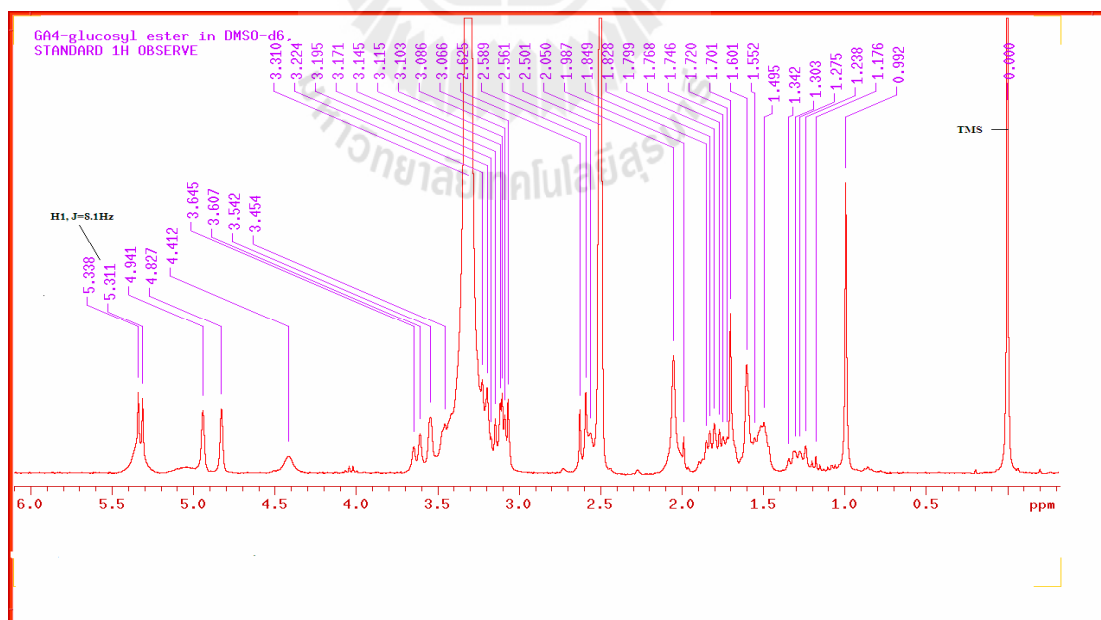
Figure 3.8 ^{1}H NMR spectrum of GA₄-Glc ester in DMSO-d6 with TMS as reference standard. δ5.32 was assigned as H1, d, $J_{2,1}$=8.1 Hz, which confirmed that the GA₄-Glc ester had a β-configuration.
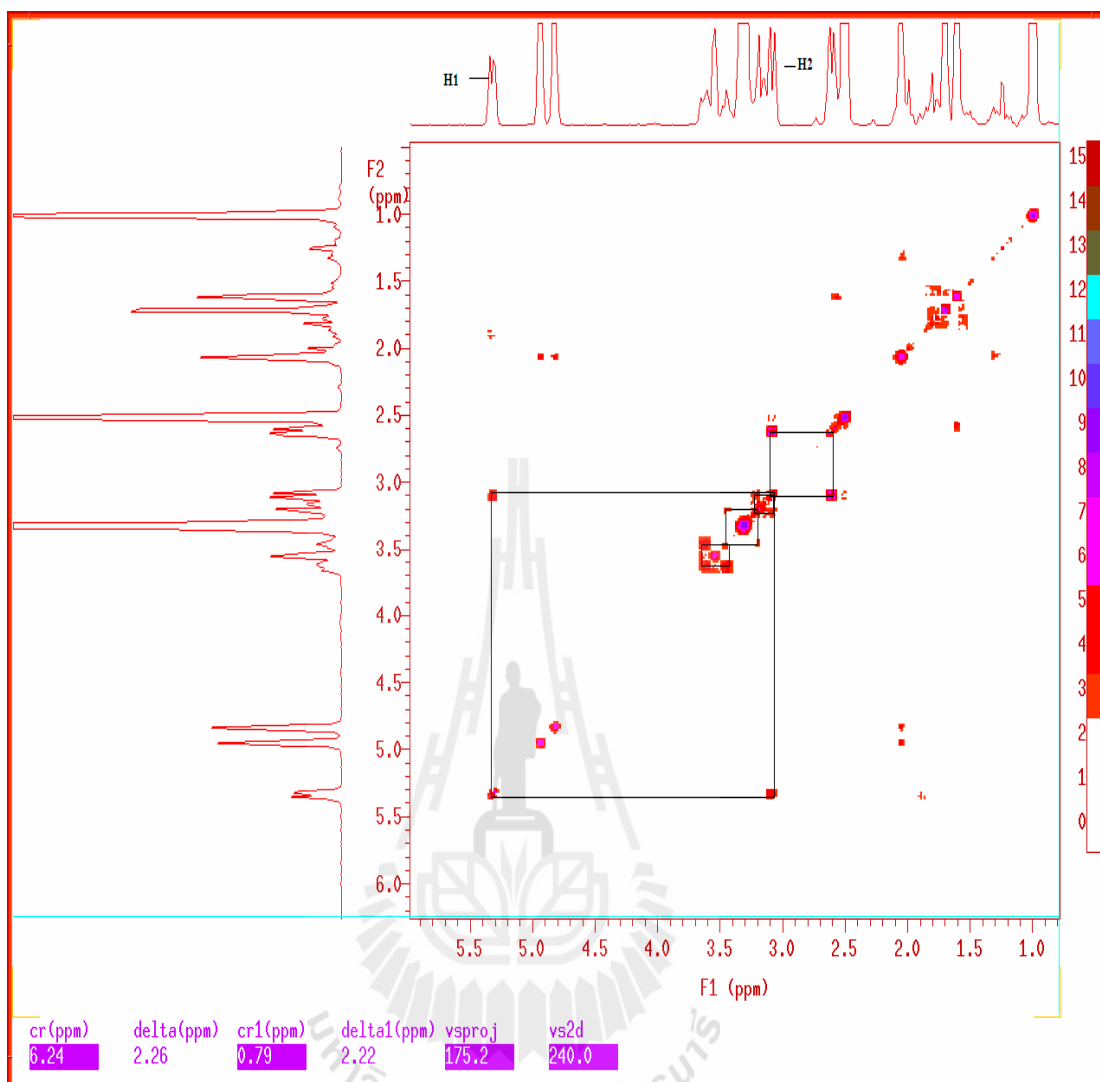
Figure 3.9 gCOSY NMR spectrum of GA$_4$-Glc ester in DMSO-d6 with TMS as reference standard. H1 and H2 on the glucosyl ring are marked beside the peaks. The boxes show the correlations between the protons.

3.1.2 Synthesis of the glucosyl ester of GA$_3$

The structures of acetylated and deacetylated GA$_3$-Glc esters (Figure 3.10) were confirmed by NMR and mass spectrometry. By comparing the ^{1}H NMR spectra of the GA$_3$ (Figure 3.11) with the acetylated GA$_3$-Glc ester (Figure 3.12), the peak for the H1 proton on the glucosyl ring was located at 5.81 ppm, with a coupling constant of 7.8 Hz, which confirmed that the acetylated GA$_3$-Glc ester had a β-configuration.
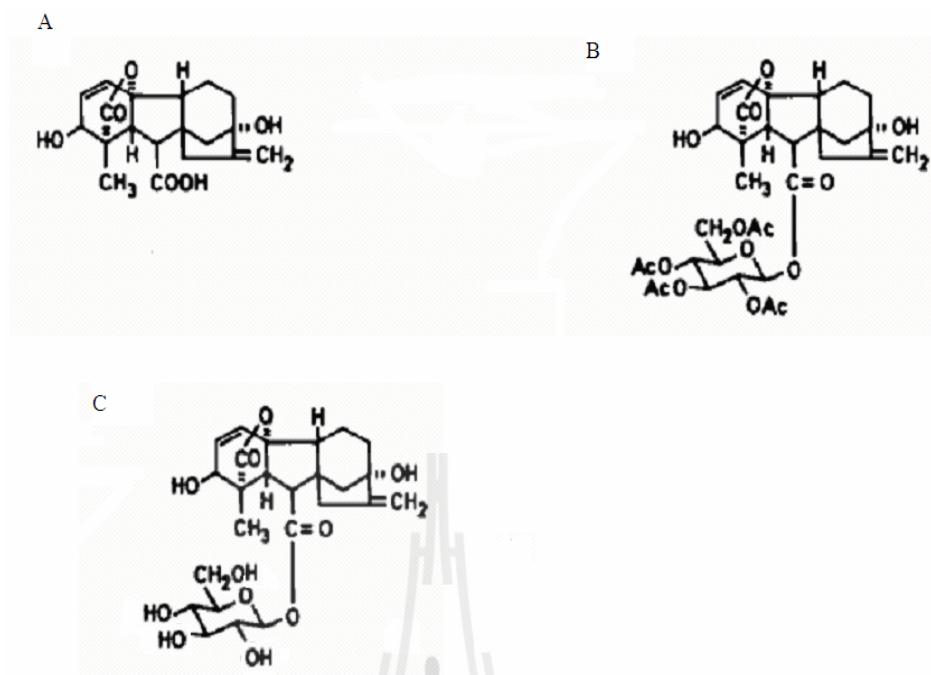
Figure 3.10 The structures of the gibberellin GA_3 and its derivatives. **A**. GA_3, $C_{19}H_{22}O_6$, molecular weight 346.37; **B**. Acetylated GA_3-Glc ester, $C_{33}H_{40}O_{15}$, molecular weight 676.36; **C**. GA_3-Glc ester, $C_{25}H_{32}O_{11}$, molecular weight 508.51.
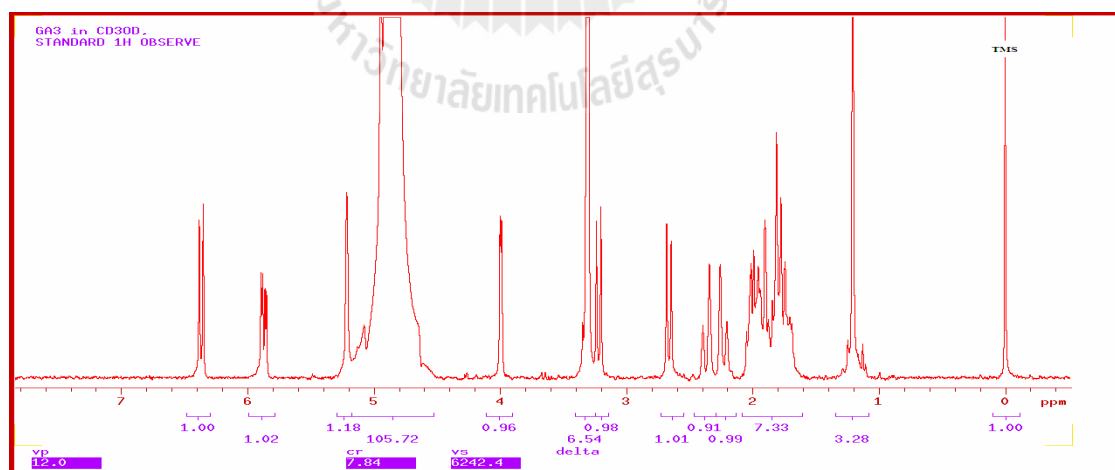
Figure 3.11 ^1H NMR spectrum of the gibberellin GA_3 in CD_3OD. TMS was used as reference standard. The spectrum was acquired at 299.986 MHz with a Varian 300 MHz NMR spectrometer.
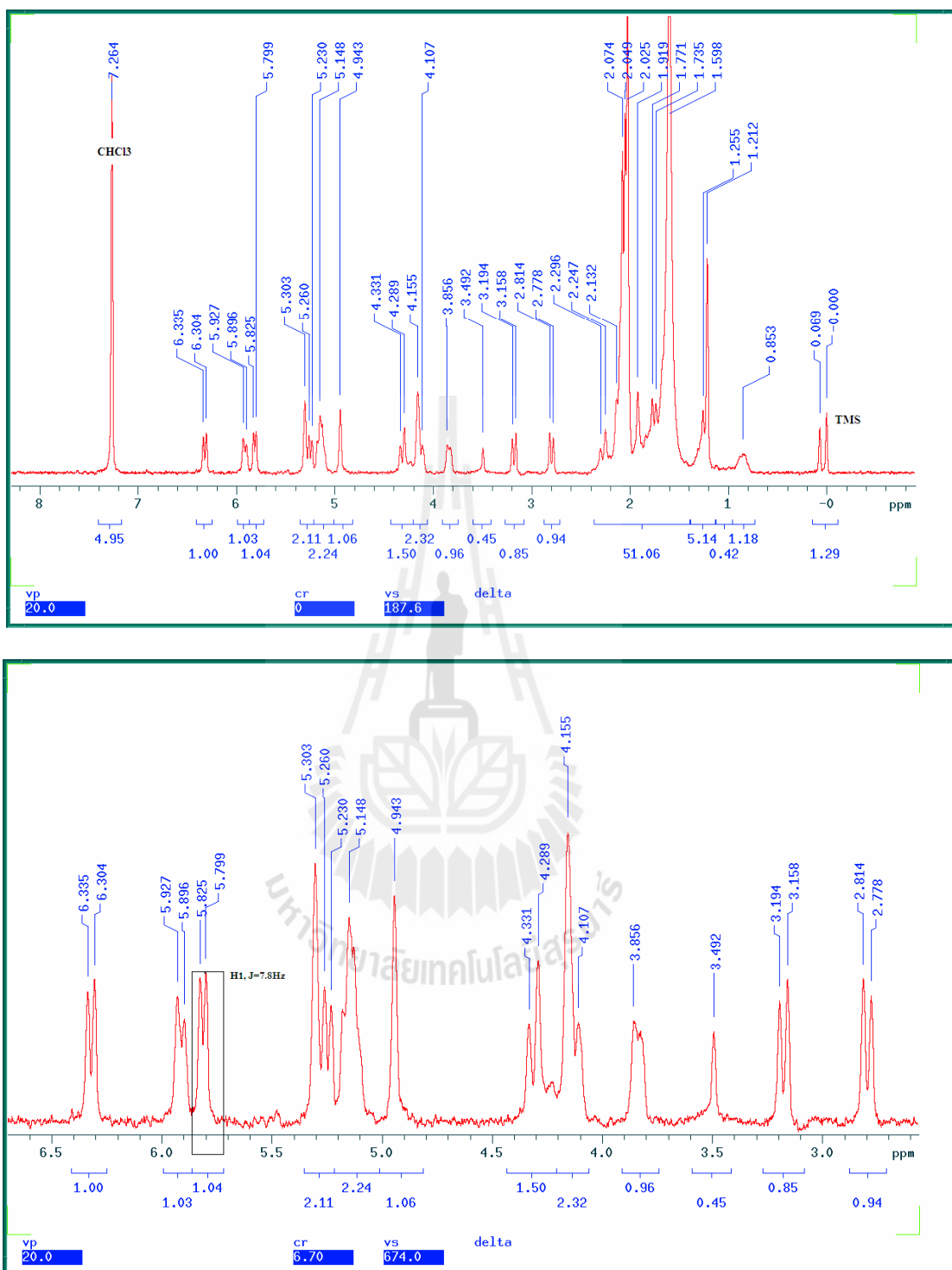
Figure 3.12 The full (top) and expanded (bottom) ^{1}H NMR spectra of the acetylated GA$_3$-

Glc ester in CDCl$_3$. TMS was the reference standard. The peak for the anomeric H1 proton

on the glucosyl ring is enclosed in the box.

The deacetylated GA₃-Glc ester was confirmed from its mass spectrum (Figure 3.13). In the negative mode, $[M+^{35}Cl]^-$ at m/z 543.4, $[M+^{37}Cl]^-$ at m/z 545.2 and $[M+HCO_2]^-$ at m/z 553.3 were detected. The β-configuration of the GA₃-Glc ester was confirmed from the peak for the anomeric H1 proton on the glucosyl ring, which was located at 5.55 ppm, with $J_{1,2}$=8.4 Hz (Figure 3.14). The gCOSY spectrum was acquired and the correlations between the sugar protons were observed, H1 and H2 were assigned at 5.55 and 3.42 ppm, respectively (Figure 3.15). The ^{1}H NMR of GA₃-Glc ester was also consistent with the published data (Hiraga et al., 1974).
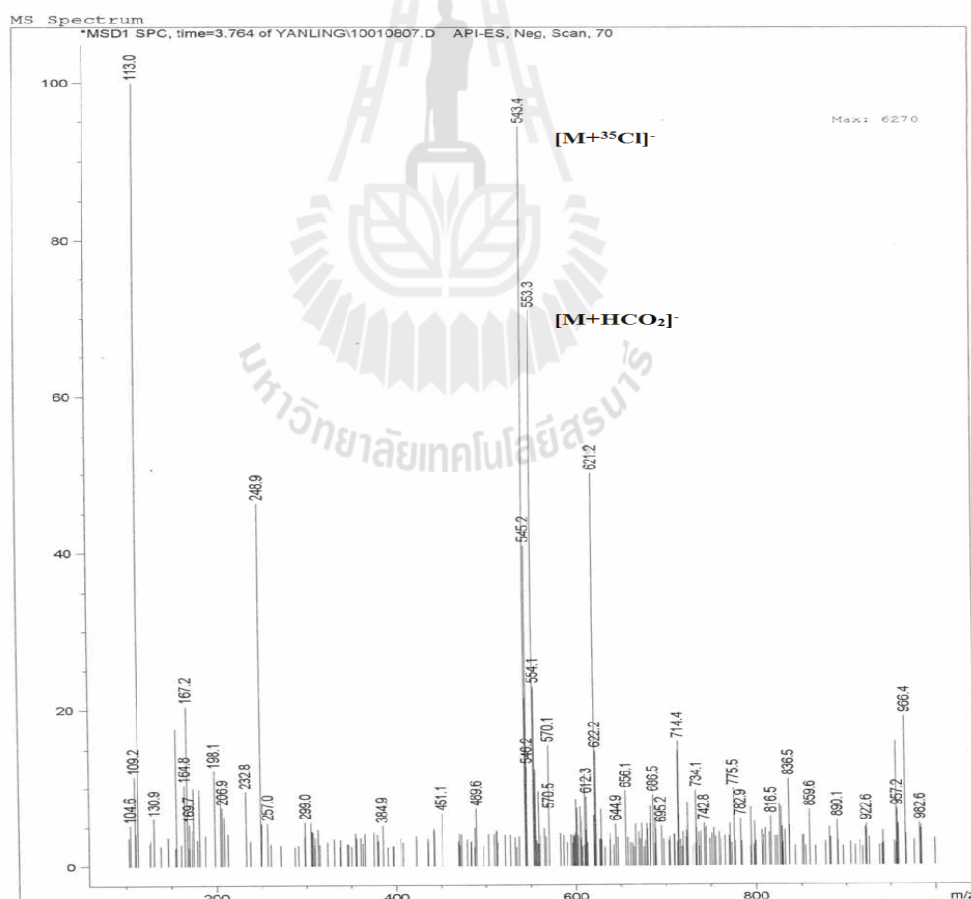
Figure 3.13 The mass spectrum of GA₃-Glc ester in the negative mode. Peaks for $[M+^{35}Cl]^-$ at m/z 543.4, $[M+^{37}Cl]^-$ at m/z 545.2 and $[M+HCO_2]^-$ at m/z 553.3 are found in the mass spectrum.
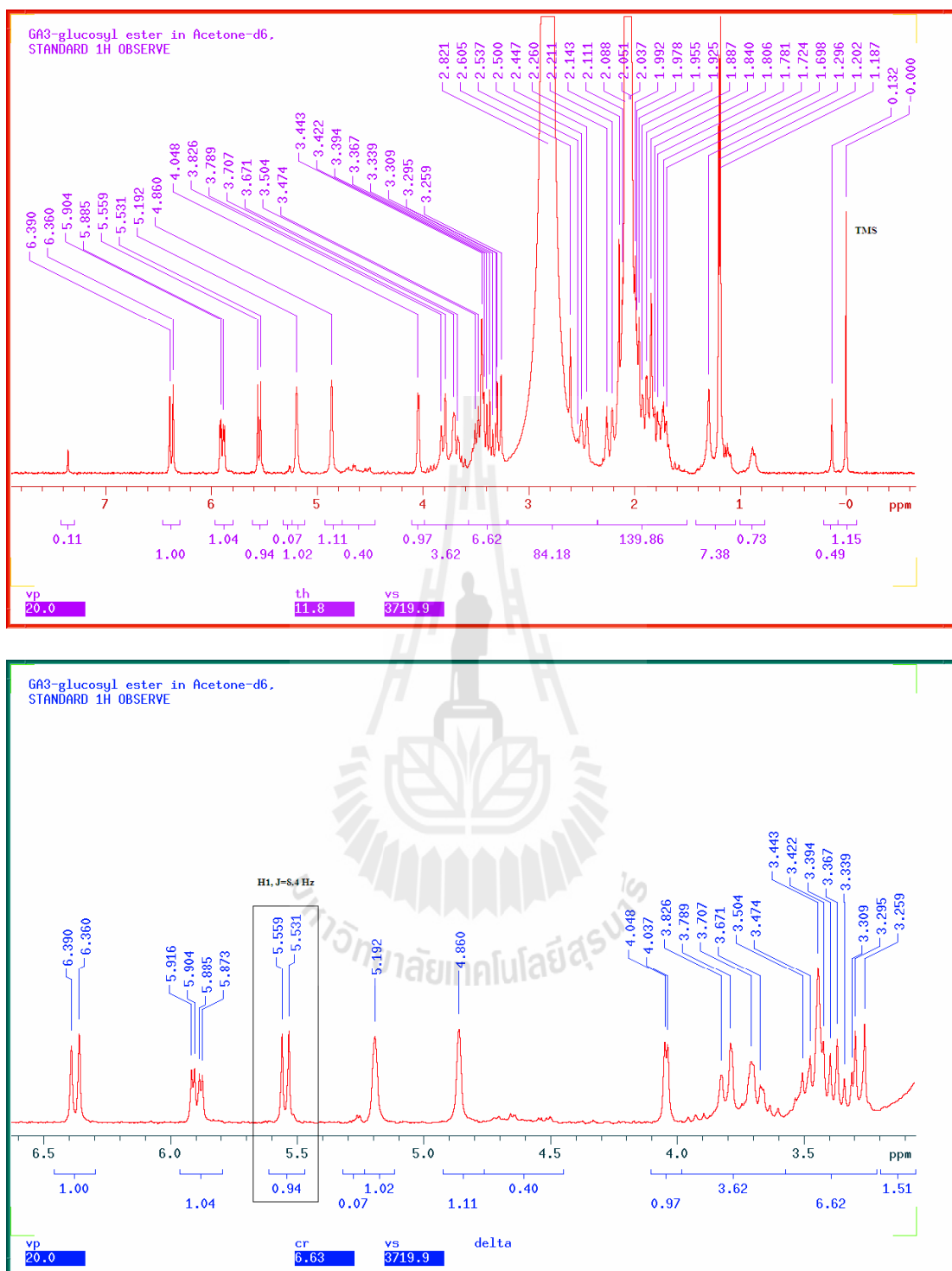
Figure 3.14 The full (top) and expanded (bottom) ^{1}H NMR spectra of the GA$_3$-Glc ester in acetone-d6. The doublet for the H1 proton on the glucosyl ring is boxed in the rectangle.
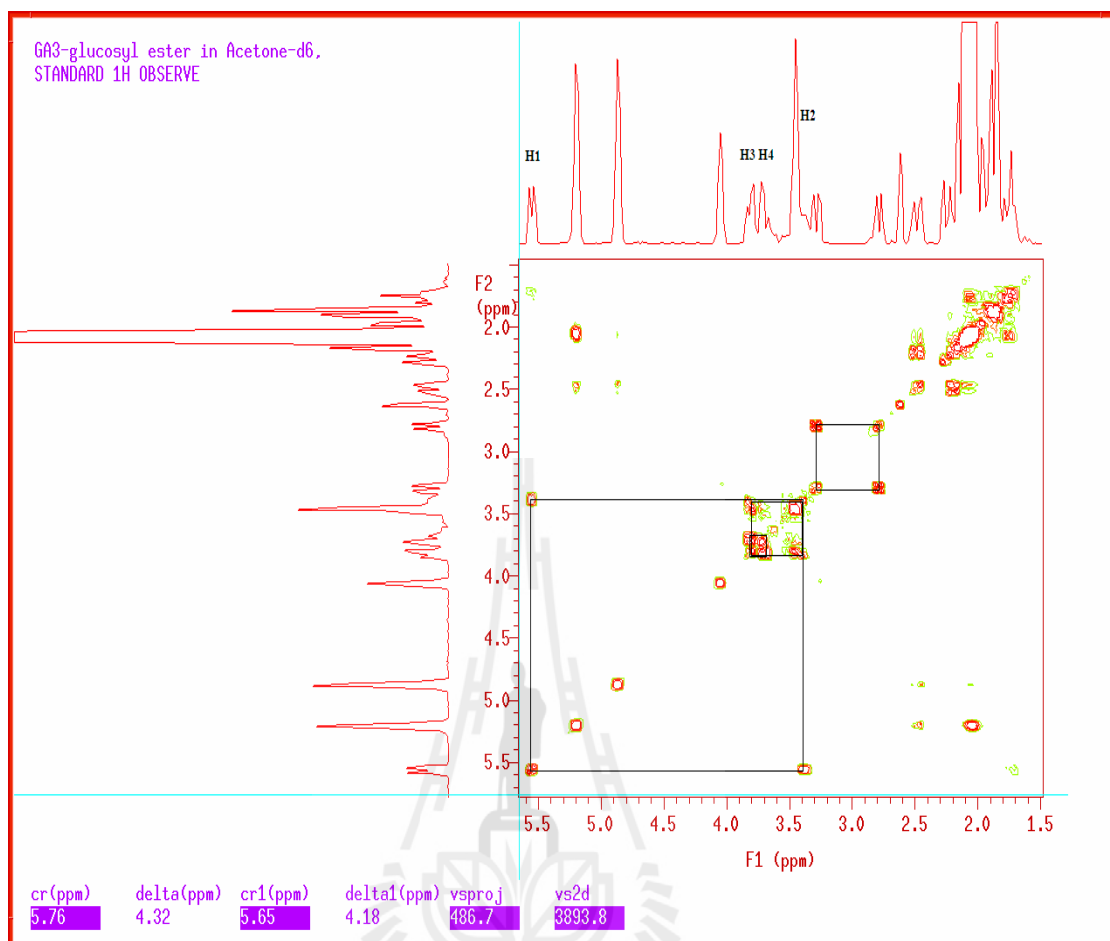
Figure 3.15 gCOSY NMR spectrum of the of GA₃-Glc ester in acetone-d6. The peaks for the four protons on the glucosyl ring, H1, H2, H3 and H4 are labeled.

3.1.3 Synthesis of gibberellin GA₃ methyl ester and its glucosides

GA₃-OMe and its two glucosides (Figure 3.16) were synthesized and identified with mass and NMR spectrometry as described in chapter 2. GA₃-OMe was confirmed from its mass spectrum (Figure 3.17). In the positive mode, [M+Na]⁺ was found as the base peak at m/z 383.3, [2M+Na]⁺ was found at m/z 743.5. The ¹H NMR spectrum (Figure 3.18) was acquired for GA₃-OMe for comparison.

The two GA₃-OMe glucosides were separated by LC-MS (Figure 3.19), and their molecular masses were confirmed in their mass spectra (Figure 3.20). [M+HCO₂]⁻ were found as the base peaks, m/z at 567.2, for both of them, although these two glucosides had different fragment patterns under the same ionization conditions.

The ^{1}H NMR spectra were collected for these two glucosides, and they were compared with the spectrum of GA$_3$-OMe. The differences were seen mainly for H2 and H17 on the skeleton of GA$_3$. HPLC peak 2 was assigned as GA$_3$-OMe-3-O-Glc, since its chemical shift value for the peak of H2 was higher than the one on GA$_3$-OMe and GA$_3$-OMe-13-O-Glc, because of the glucosyl linkage at carbon position 3.
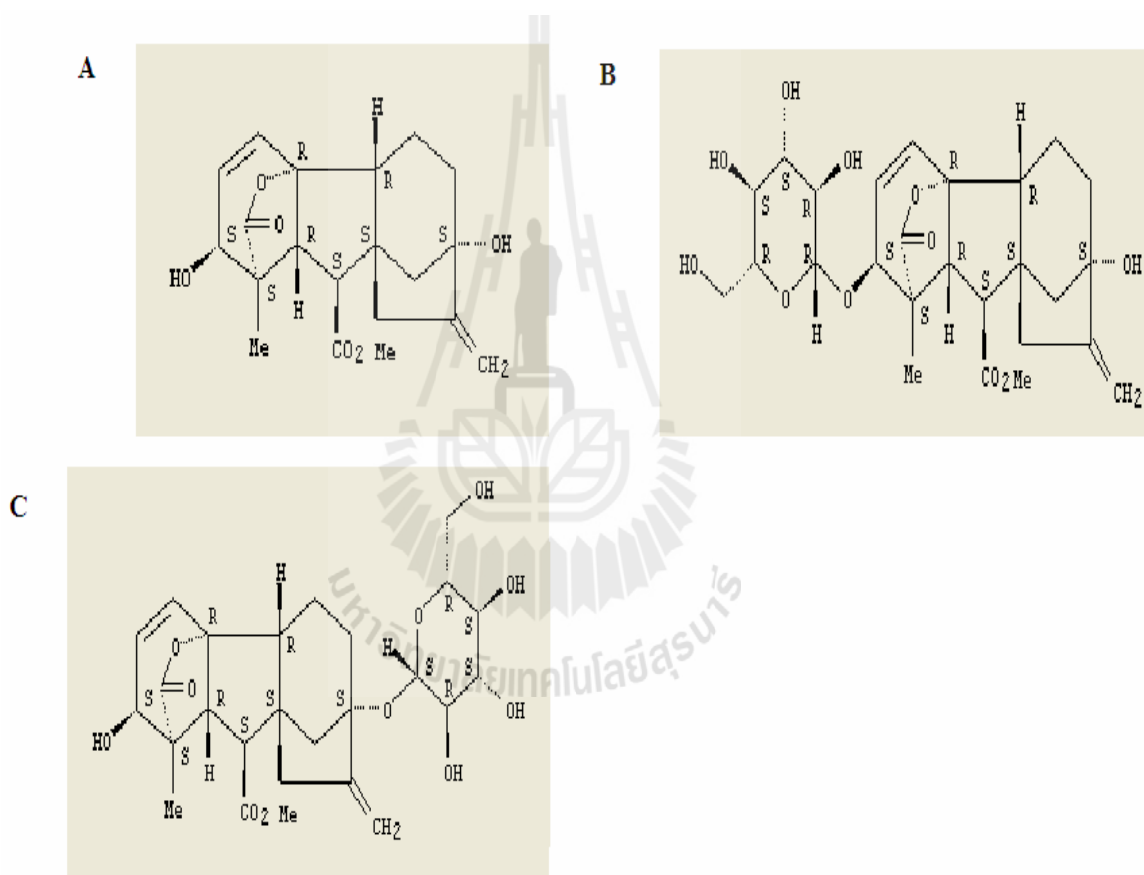
Figure 3.16 The structures of the GA$_3$-OMe (A), GA$_3$-OMe-3-O-Glc (B) and GA$_3$-OMe-13-O-Glc (C). **A**. GA$_3$-OMe, C$_{20}$H$_{24}$O$_6$, molecular weight 360.40; **B**. GA$_3$-OMe-3-O-Glc, C$_{26}$H$_{34}$O$_{11}$, molecular weight 522.54; **C**, GA$_3$-OMe-13-O-Glc, C$_{26}$H$_{34}$O$_{11}$, molecular weight 522.54.
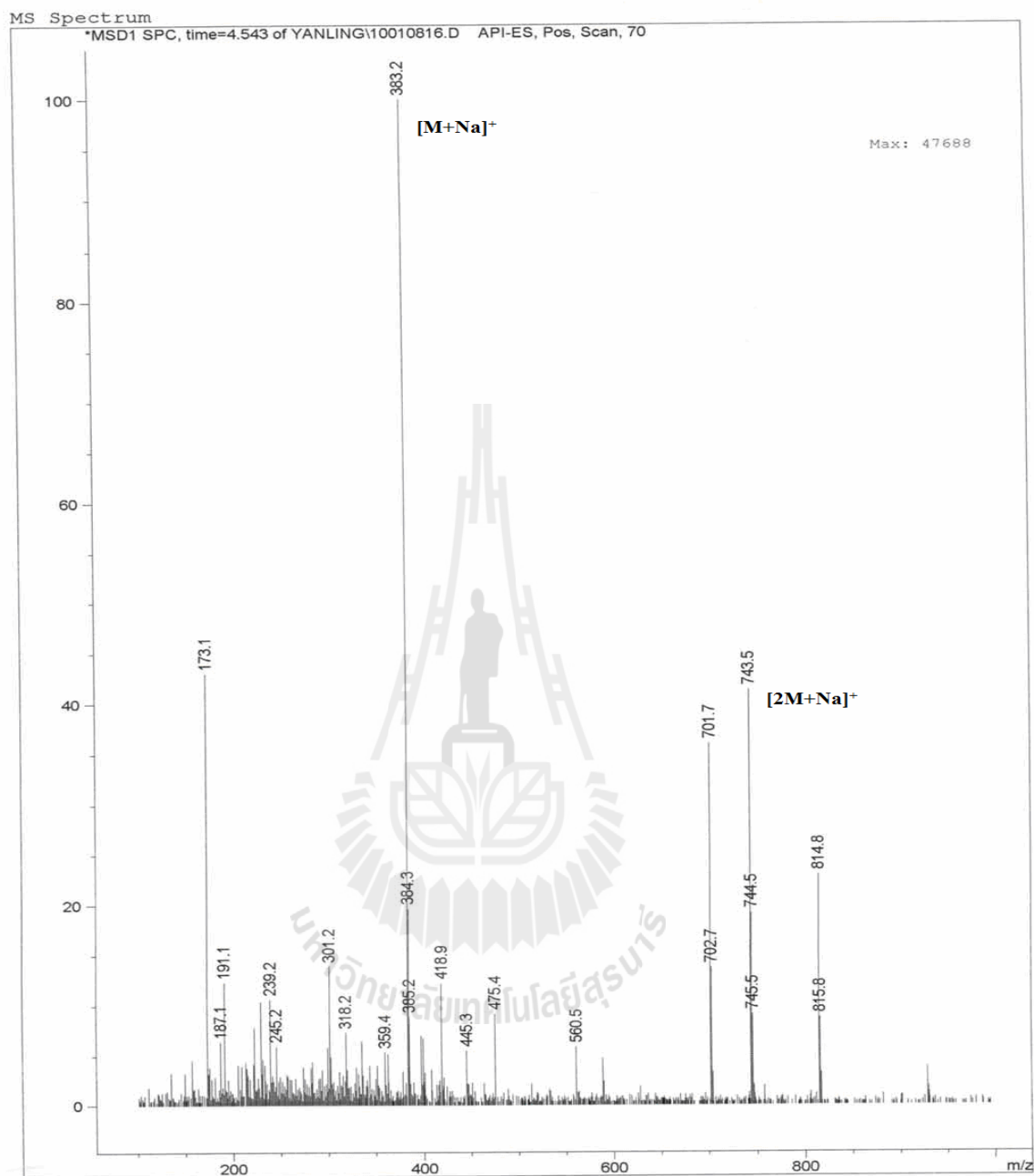
Figure 3.17 The mass spectrum of GA$_3$-OMe. The peak for [M+Na]$^+$ is found as the base peak at *m/z* 383.3, while [2M+Na]$^+$ is found at *m/z* 743.5.
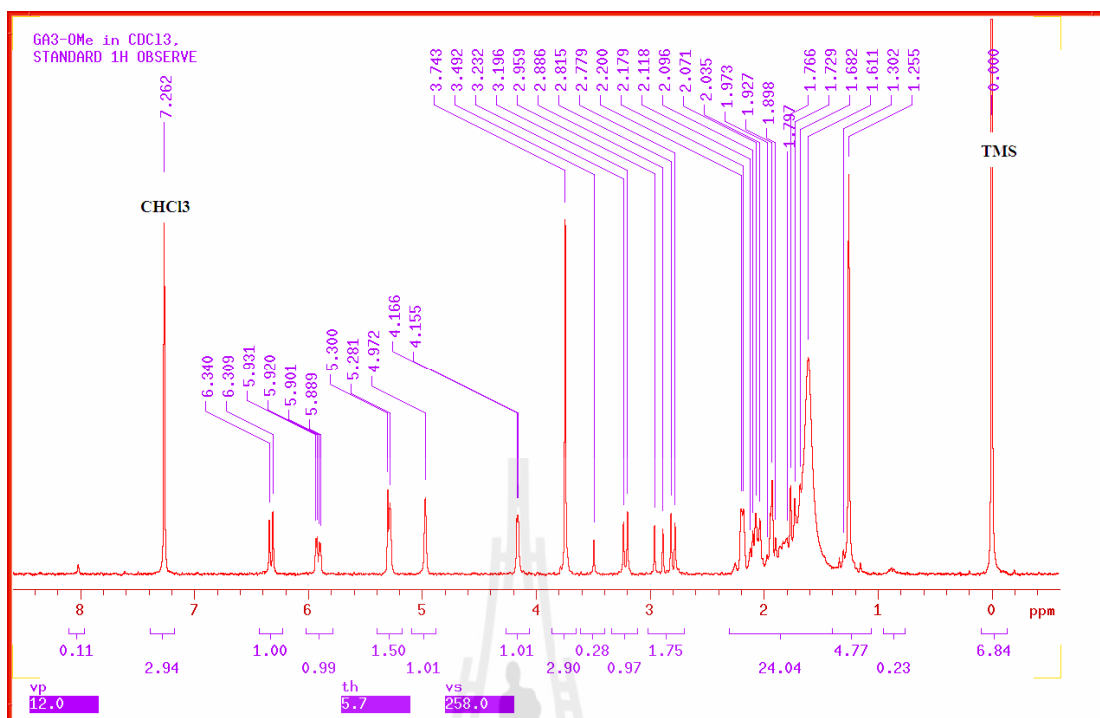
Figure 3.18 The ^{1}H NMR spectrum of GA$_3$-OMe in CDCl$_3$.
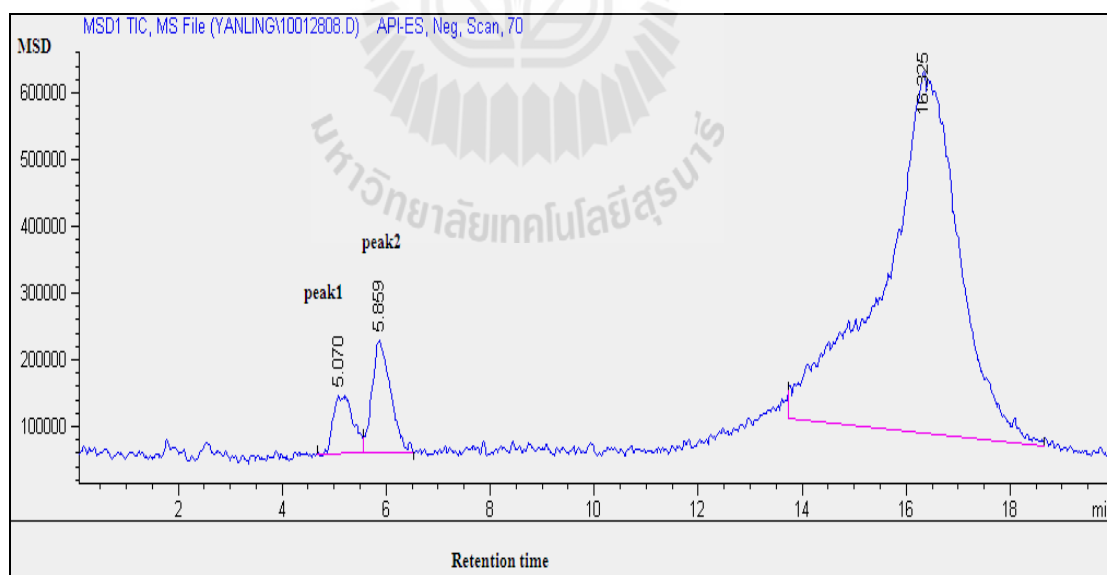
Figure 3.19 The LC-MS chromatogram of the GA$_3$-OMe-glucosides. The compounds were separated on a ZORBAX Eclipse XDB-C18, 4.6*150 mm, 5 Micron column (Aglient). Peak 1: GA$_3$-OMe-13-O-β-D-Glc; Peak 2: GA$_3$-OMe-3-O-β-D-Glc.
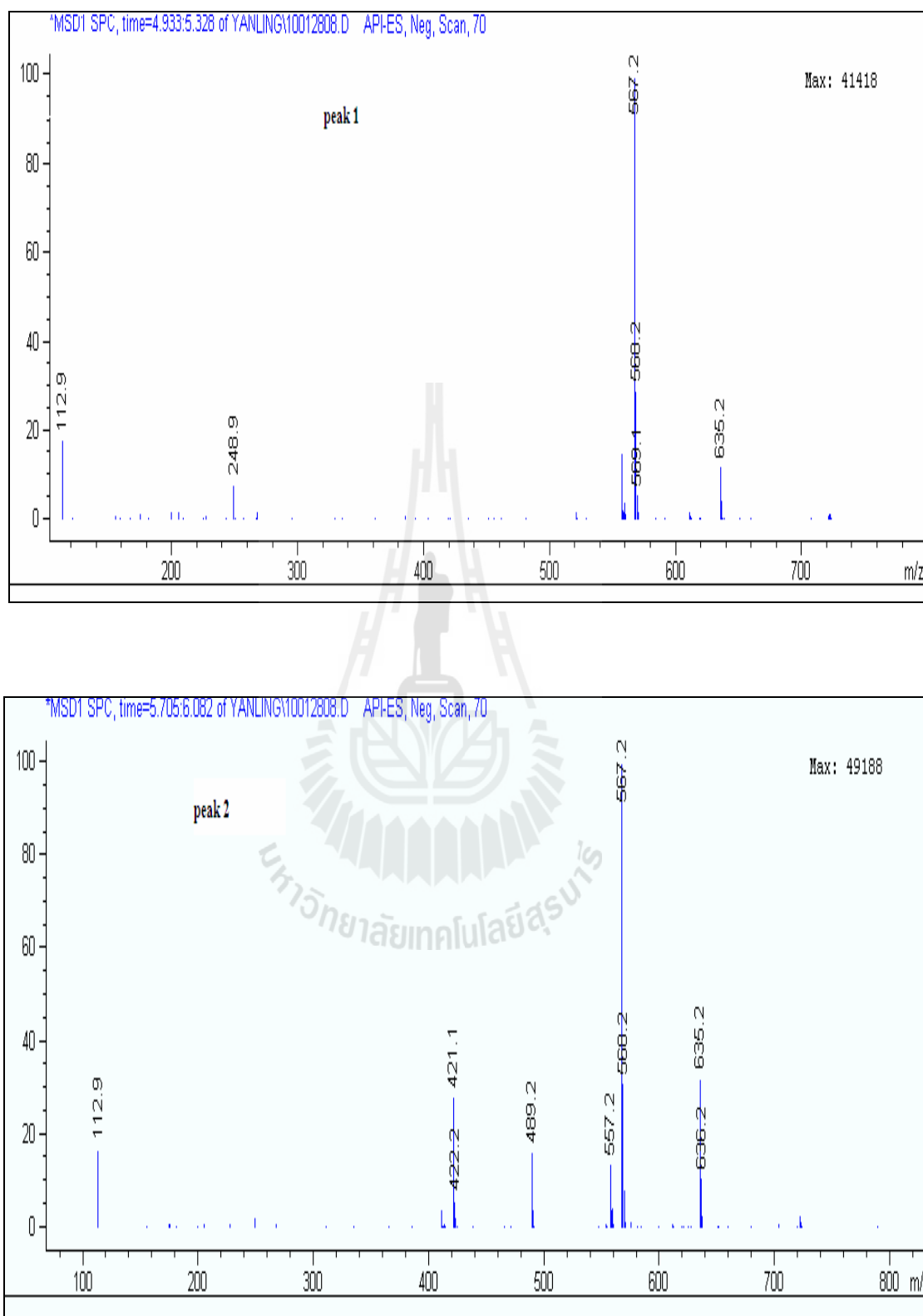
Figure 3.20 The mass spectra of the two GA$_3$-OMe-glucosides in the negative mode. The

peak at *m/z* 567.2 was assigned as [M+HCO$_2$]$^-$.
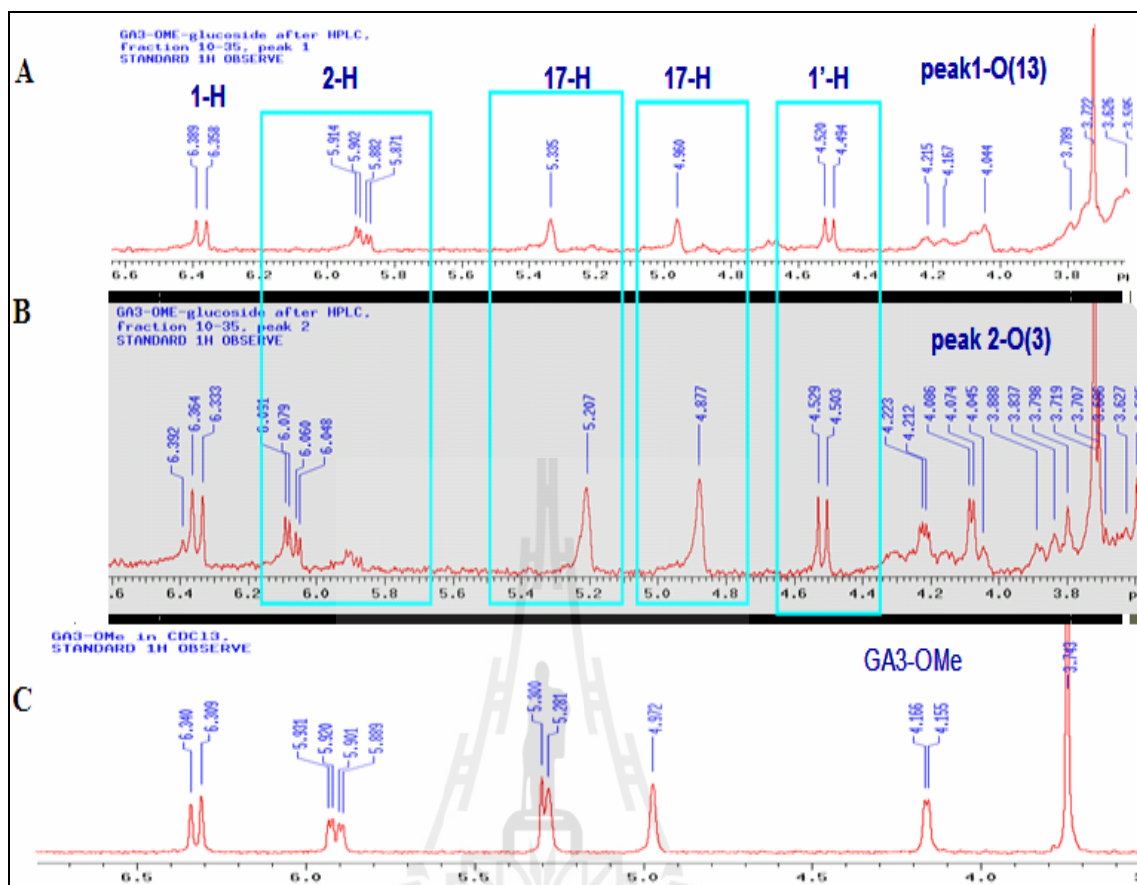
Figure 3.21 Overlay of the NMR spectra of GA$_3$-OMe and its glucosides. A, peak 1, GA$_3$-OMe-13-O-Glc; B, peak 2, GA$_3$-OMe-3-O-Glc; C, GA$_3$-OMe.

3.1.4 Synthesis of gibberellin GA$_4$ methyl ester and its glucosides

The structures of GA$_4$-OMe and GA$_4$-OMe-Glc were mainly confirmed by their mass spectra (Figures 3.22 and 3.23). The peaks for the GA$_4$-OMe and GA$_4$-OMe-Glc formate adducts [M+HCO$_2$]$^-$ were identified as the base peaks in their negative mode mass spectra, at m/z 391.1 and 553.3, respectively. The ^{1}H NMR of GA$_4$-OMe was acquired for its structure identification (Figure 3.24).
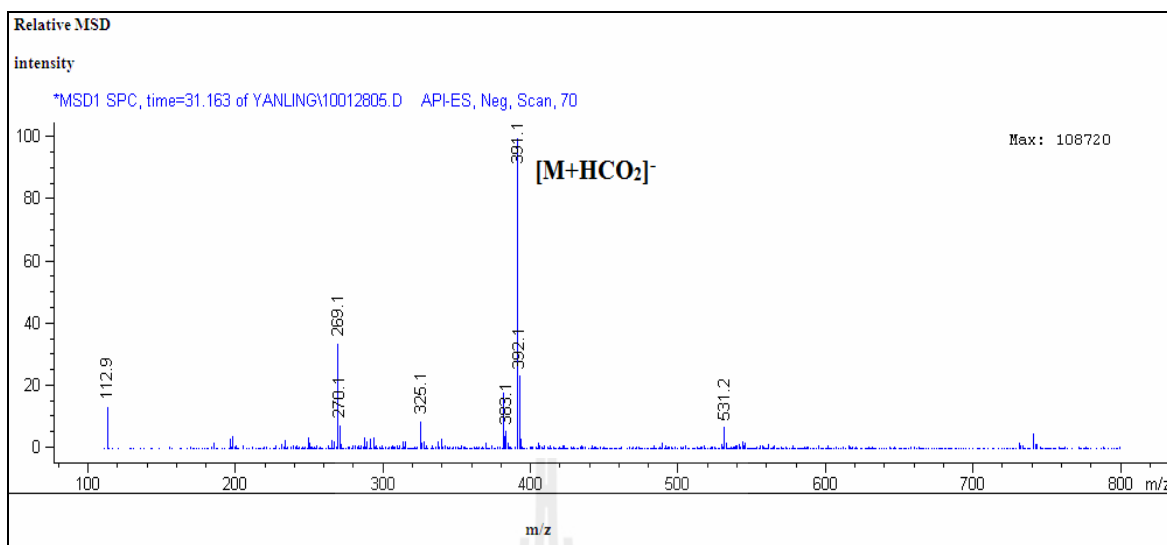
Figure 3.22 The mass spectrum of GA$_4$-OMe in the negative mode. The peak at *m/z* 391.1 was assigned as [M+HCO$_2$]$^-$.
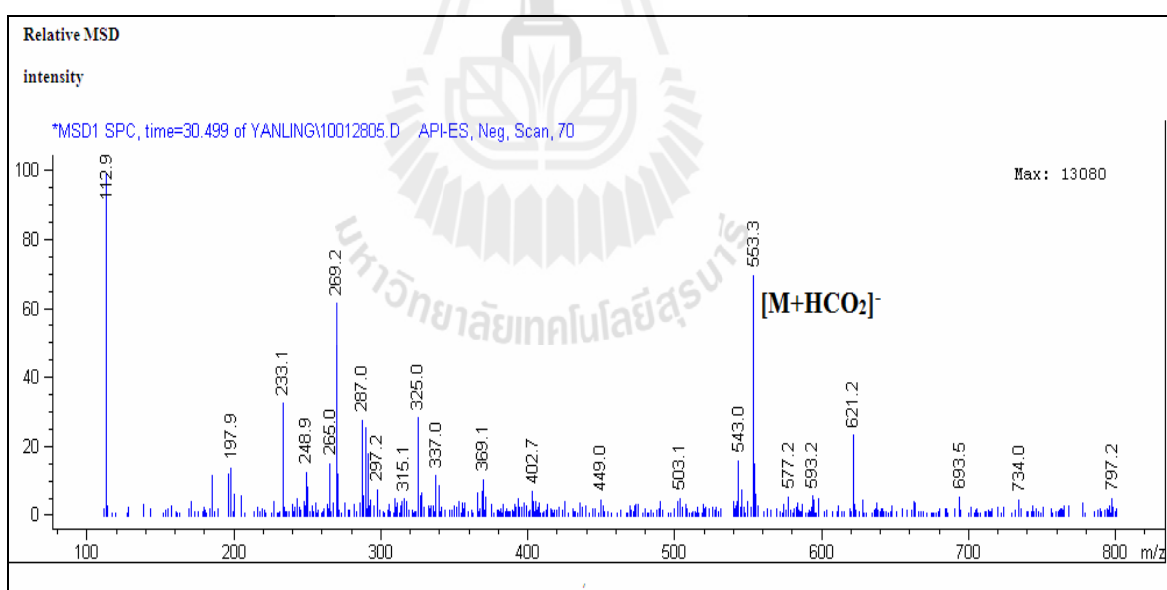
Figure 3.23 The mass spectrum of GA$_4$-OMe-Glc in the negative mode. The peak at *m/z* 553.3 was assigned as [M+HCO$_2$]$^-$.
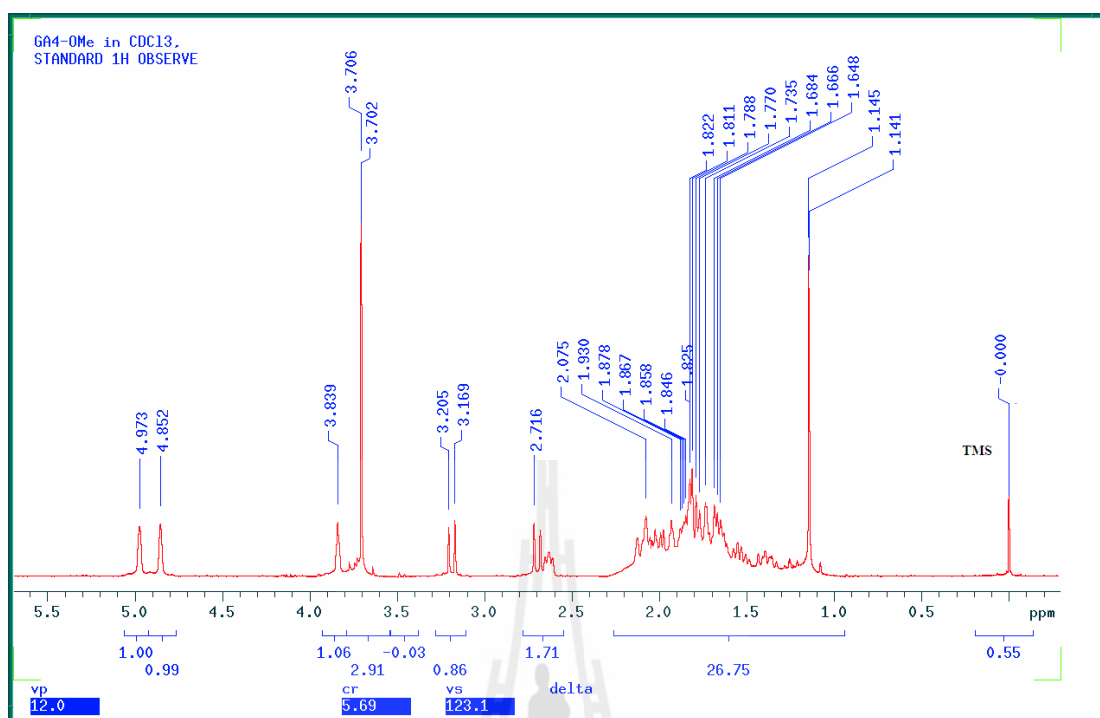
Figure 3.24 The ^{1}H NMR spectrum of GA$_4$-OMe in CDCl$_3$.

3.2 Extraction, Purification and Characterization of GA$_4$-glucosyl Ester β-glucosidase from Rice

Ten kilograms of 10-day rice seedling shoots and leaves were extracted and the crude proteins were purified with seven purification steps (Table 3.1 and Figure 3.25). *p*NPGlc and GA$_4$-Glc were used as substrates to test the β-D-glucosidase activities. The protein fractions with high hydrolysis activities toward GA$_4$-Glc were pooled, concentrated and used for the next purification step. Finally, 0.15 mg of protein was obtained after seven steps of purification. This protein included two major bands that were seen in 10% SDS-PAGE and identified.

Table 3.1 Summary of purification of β-glucosidase in rice.

Purification step	Total activity (μmol/min.)		Protein (mg)	Specific activity (μmol/min.mg)		Purification fold		Yield (%)
	pNP-Glc	GA$_4$-Glc		pNP-Glc	GA$_4$-Glc	pNP-Glc	GA$_4$-Glc	
1. Crude extract	5,710	11.0	27,200	0.21	$4.03*10^{-4}$	1	1	100
2. After (NH$_4$)$_2$SO$_4$ precipitation & dialysis	2,220	6.17	12,000	0.18	$5.12*10^{-4}$	0.9	1.3	44.3
3. CM-Sepharose 20 ml column	1,470	4.22	1,215	1.21	$3.47*10^{-3}$	5.8	8.6	4.47
4. Con A-Sepharose column	281	1.57	140	2.01	$1.12*10^{-2}$	9.6	27.8	0.51
5. Sephadex 75 column	157	1.50	57	2.73	$2.62*10^{-2}$	13	65	0.21
6. SP xl column	30.4	0.36	6	5.07	$6.0*10^{-2}$	24	149	0.02
7. Octyl column	3.07	0.05	0.63	4.88	$8.1*10^{-2}$	23	201	0.002
8. Superdex 200 column	1.63	0.02	0.15	10.9	0.136	52	337	$5.5*10^{-4}$

Yield was calculated based on the amount of the protein obtained in each purification steps.
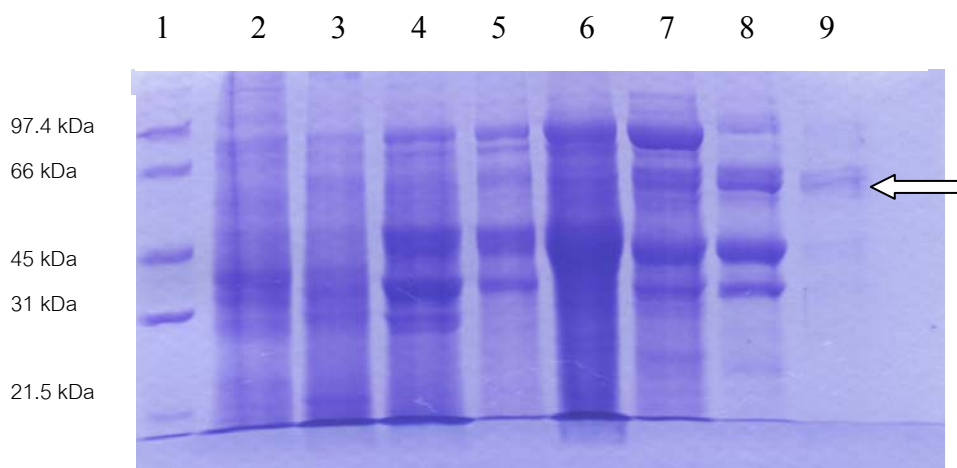
Figure 3.25 10% SDS-PAGE analysis of β-glucosidase purification from rice seedlings. Lane 1, protein marker; lane 2, crude extract; lane 3, crude extract after dialysis; lane 4, protein after CM column chromatography; lane 5, protein after Con A column chromatography; lane 6, protein after S75 column chromatography; lane 7, protein after SP column chromatography; lane 8, protein after octyl column chromatography; lane 9, protein after S200 column chromatography.

3.2.1 Purification of β-glucosidase from rice by ion exchange chromatography with a CM-Sepharose column

The crude protein after $(NH_4)_2SO_4$ precipitation & dialysis with McIlvaine buffer was fractionated with a CM-Sepharose column (20 ml), which was equilibrated with 4-fold diluted McIlvaine buffer, pH 5, and eluted with a linear gradient of 0-1.0 M NaCl in this buffer (Figure 3.26). Two peaks were detected in the bound proteins, and their activities were tested with *p*NPGlc and GA$_4$-Glc as described in Chapter II (Figure 3.27).
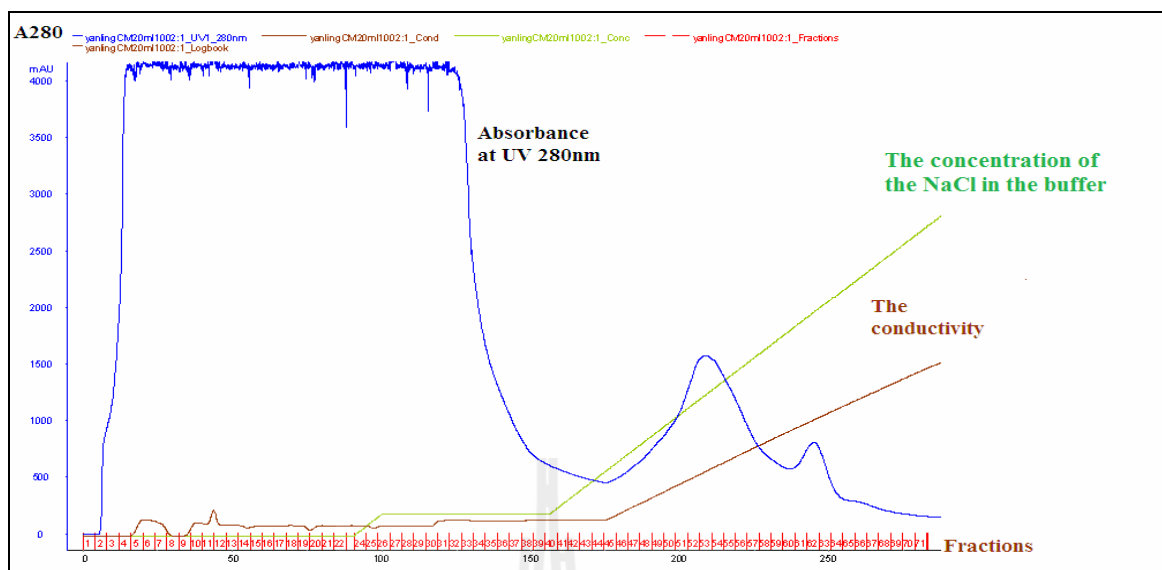
Figure 3.26 Protein elution profile from CM-Sepharose column**.** The unbound proteins were washed out with 4-fold diluted McIlvaine buffer, pH 5 (buffer A), and the bound proteins were eluted with a linear gradient of 0-1.0 M sodium chloride (NaCl) in buffer A at a flow rate of 2.0 ml/min. The fraction volume was 4 ml. The blue curve indicates the absorbance at 280 nm, the green curve indicates the relative theoretical concentration of the NaCl in the buffer, and the brown curve indicates the conductivity.
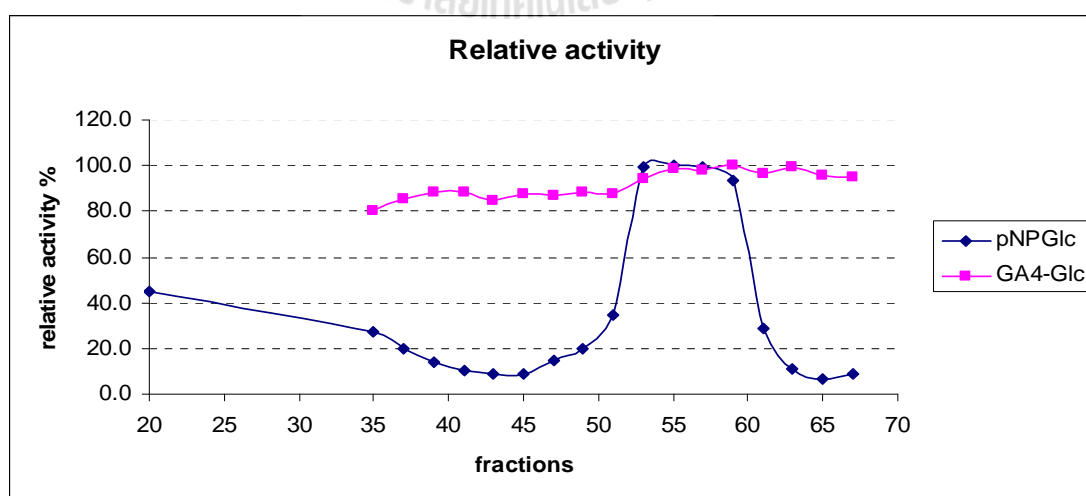
Figure 3.27 Relative β-glucosidase activities of eluting fraction from CM-Sepharose column with *p*NPGlc and GA$_4$-Glc as substrates. Relative activity (%) was based on the absorbance at 405 nm in the respective assays.

The activities of fractions from the CM-Sepharose column for hydrolysis of *p*NPGlc showed that there were two peaks in the bound proteins, peak 1 had higher hydrolysis activity than peak 2 and the unbound proteins peak. For the activities with GA$_4$-Glc, it was too low to conclude which peak had higher activity toward GA$_4$-Glc. So, based on the *p*NPGlc hydrolysis activity, two peaks from bound proteins were pooled, concentrated by $(NH_4)_2SO_4$ precipitation, dialyzed, and used for next step of purification.

3.2.2 Purification of β-glucosidase from rice by affinity chromatography with a ConA-Sepharose column

The fractions from ConA-Sepharose column were divided into four groups: flow-through 1, flow-through 2, eluate 1 and eluate 2. Eluate 1 & 2 showed higher activities than flow-through 1 & 2 for hydrolyzing GA$_4$-Glc (Figure 3.28), so these two fractions were pooled and used for further purification.
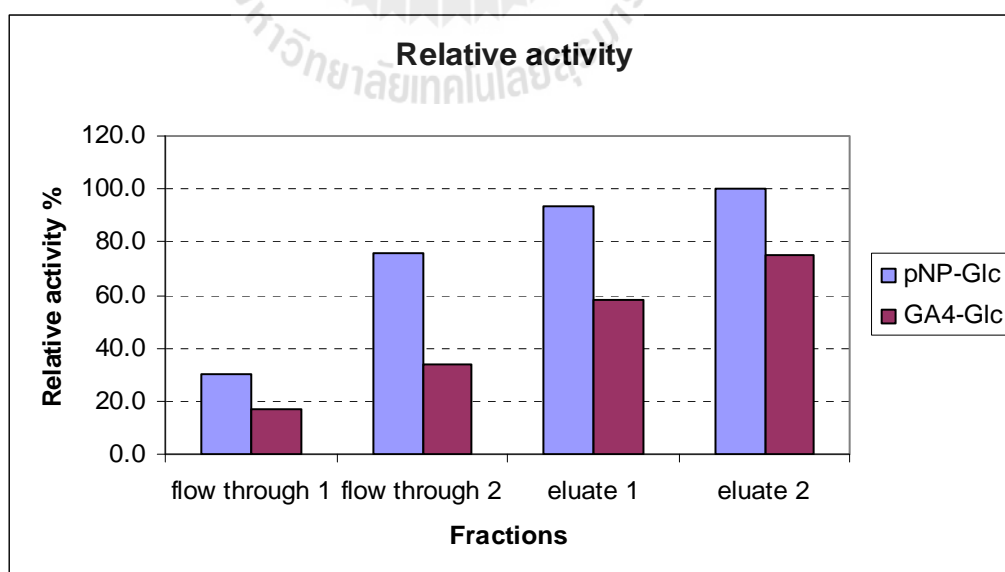
Figure 3.28 Relative activities of flow-through and eluting fractions from the ConA-Sepharose column. The relative activities were calculated based on the specific activities.

3.2.3 Purification of β-glucosidase in rice by gel filtration chromatography through a Superdex S75 column

The active fractions from the ConA-Sepharose column were concentrated and purified with a S75 gel filtration column (Figure 3.29). The eluting fractions were tested for hydrolysis of *p*NPGlc and GA$_4$-Glc (Figure 3.30). The fractions 62-74 showed the highest activities to hydrolyze GA$_4$-Glc. These fractions were run on SDS-PAGE to check their protein compositions (Figure 3.31), and then pooled for further purification.
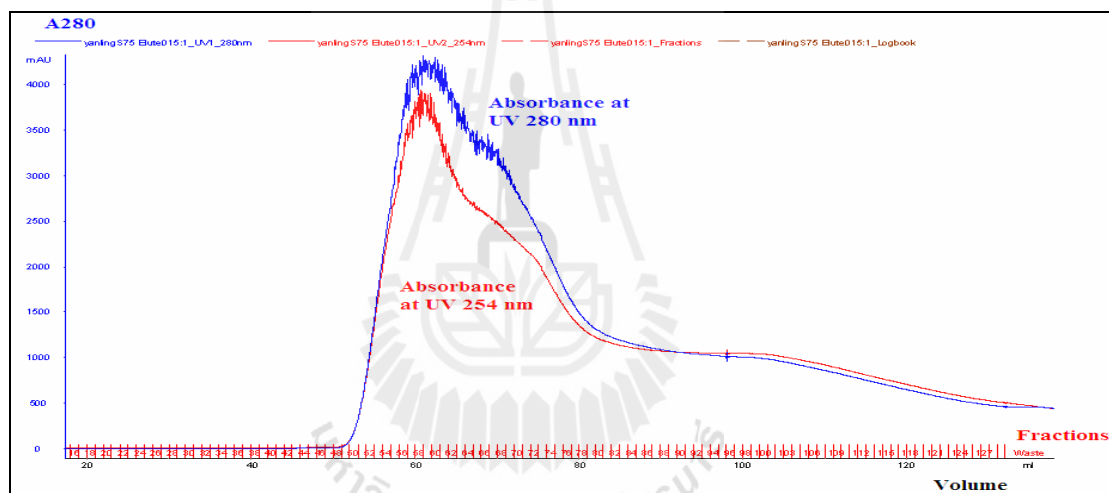
Figure 3.29 Protein elution profile of the Superdex S75 column. The protein was eluted with 4-fold diluted McIlvaine buffer, pH 7, containing 0.2 M NaCl at a flow rate of 1.0 ml/min, and the fraction volume was 1 ml.
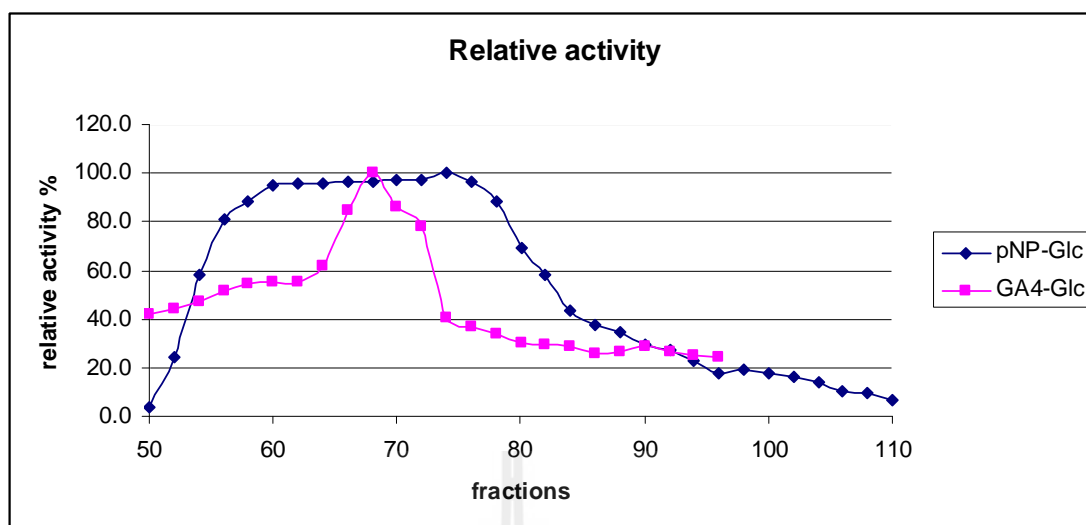
Figure 3.30 Activities of eluting fractions from S75 column with *p*NPGlc and GA₄-Glc.

♦ Hydrolysis activity against *p*NPGlc, ■ Hydrolysis activity against GA₄-Glc. Relative

activity (%) was calculated based on the absorbance at 405 nm obtained in the respective

assays.
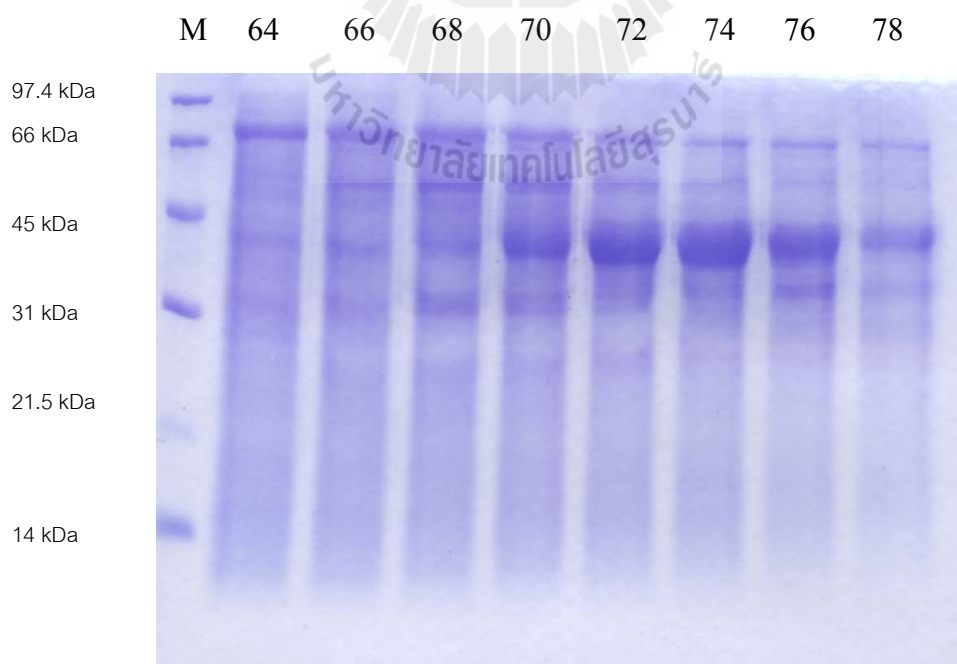
Figure 3.31 SDS-PAGE analyses of fractions after S75 column purification. Lane M,

marker; lane 64-78 represented fractions 64-78.

3.2.4 Purification of β-glucosidase from rice by cation exchange chromato-graphy with an SP XL column

The concentrated protein pool from the S-75 gel filtration column was purified with a HiTrap SP XL column (Figure 3.32). The eluting fractions were tested for hydrolysis of pNPGlc and GA$_4$-Glc. Figure 3.33 shows that fractions 1-2, 8-13 could hydrolyze pNPGlc, but only fractions 8-10 showed relatively high hydrolysis activities with GA$_4$-Glc. Therefore, fractions 8-10 were pooled and used for further purification.
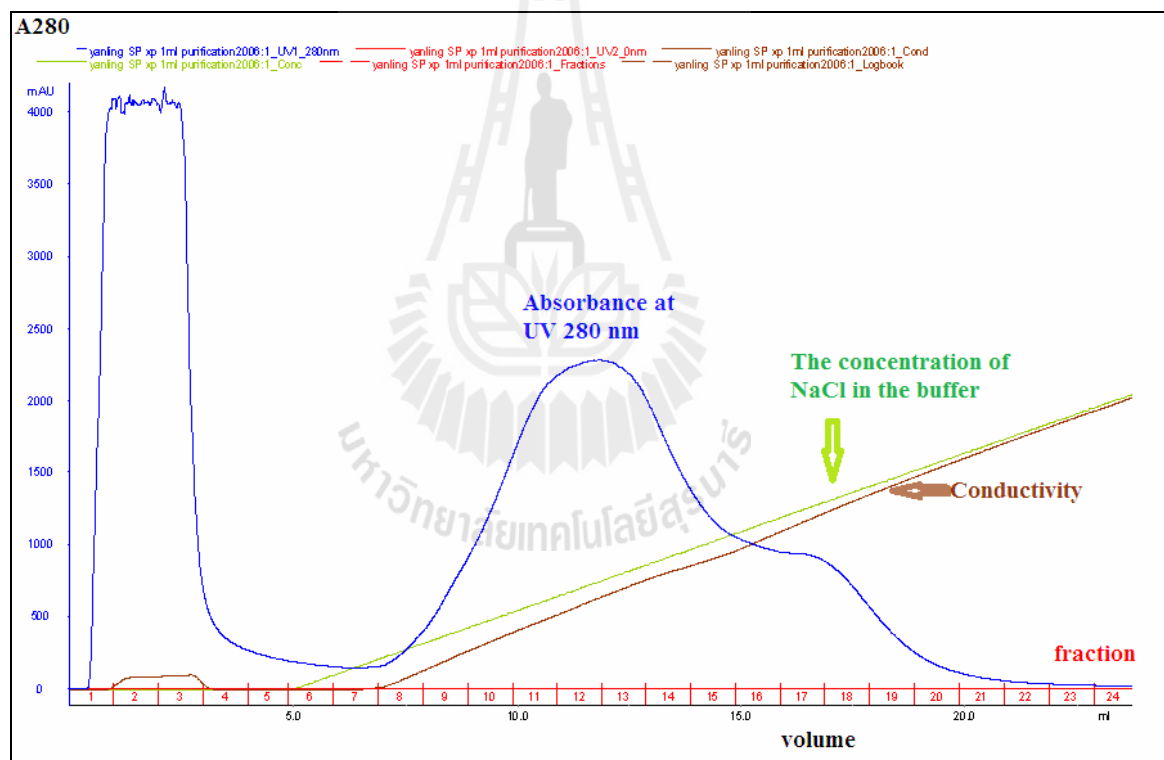
Figure 3.32 Protein elution profile of SP column. The column was eluted with a linear gradient of 0-1.0 M NaCl in 4-fold diluted McIlvaine buffer, pH 5, at a flow rate of 1.0 ml/min. The fraction volume was 1.0 ml.
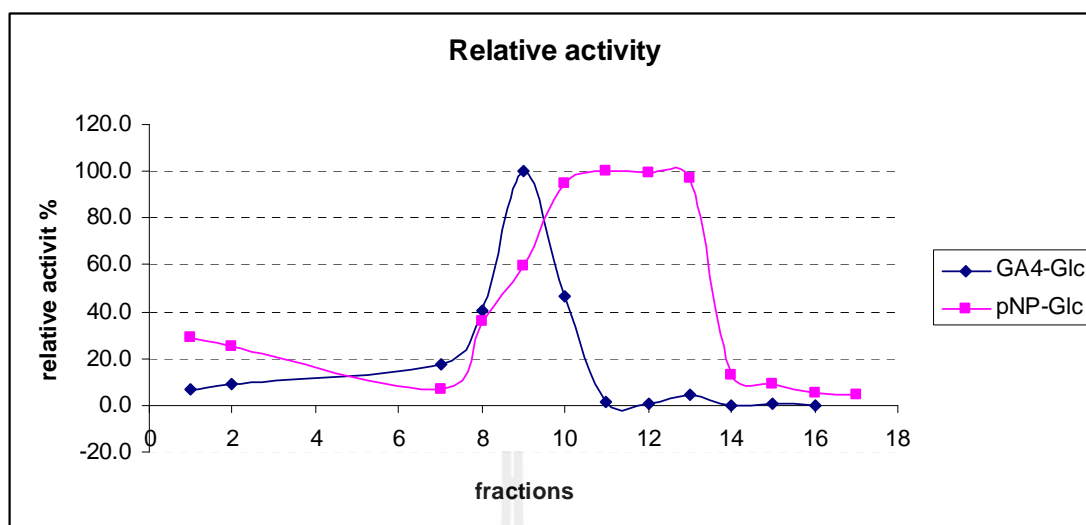
Figure 3.33 β-Glucosidase activities of eluting fractions from SP column with *p*NPGlc and GA$_4$-Glc substrates. ■ Hydrolysis activity with *p*NPGlc, ♦ Hydrolysis activity with GA$_4$-Glc. The relative activities (%) were calculated based on A$_{405}$.
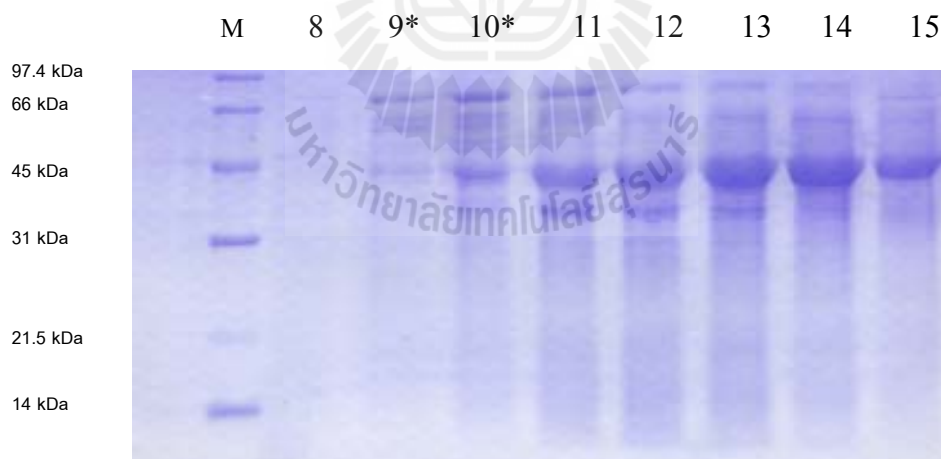
Figure 3.34 SDS-PAGE analysis of fractions containing high activity against GA$_4$-Glc after SP column chromatography. Lane M, marker; lanes 8-15 represented fractions 8-15. Two bands at size around 60 kDa appeared in fraction 9 and 10, and these two fractions had the highest hydrolysis activity against GA$_4$-Glc.

3.2.5 Purification of β-glucosidase by hydrophobic interaction chromatography over an Octyl Sepharose 4 column

The β-glucosidase pool obtained from the SP column purification was purified with hydrophobic Octyl-Sepharose 4 column. Most of proteins were bound to the column and eluted at reduced $(NH_4)_2SO_4$ concentration in phosphate buffer (Figure 3.35). The buffer of the collected fractions was exchanged twice with 4 times diluted McIlvaine buffer, pH 5, to remove $(NH_4)_2SO_4$; and then the fractions were tested for hydrolysis of GA$_4$-Glc (Figure 3.36) and aliquots were analyzed by SDS-PAGE to check protein components (Figure 3.37). Fractions 27-33 were found to have higher hydrolysis activities than other fractions. Three groups of bands were mainly seen in the fractions 27-33, at sizes of approximately 60 kDa, 45 kDa and 33 kDa. The bands at 45 kDa and 33 kDa were also evident in the fractions 11, 12 and 13 of the SP column purification (Figure 3.34) in high amounts, but these fractions did not have activities for hydrolysis of GA$_4$-Glc. Only two major bands at approximately 60 kDa size were highly correlated with the activity. So fractions 27-33 were pooled, concentrated and purified further by gel filtration chromatography.
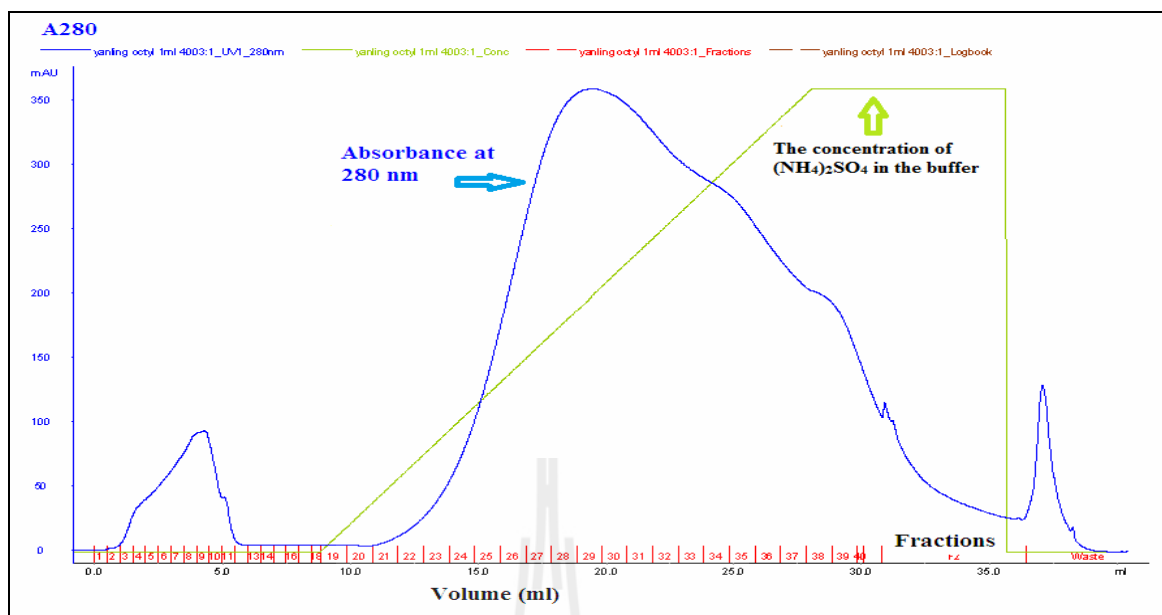
Figure 3.35 Protein elution profile of Octyl Sepharose 4 column. The protein was eluted with a linear gradient of 1.7-0 M of $(NH_4)_2SO_4$ in 50 mM phosphate, pH 7, buffer. The elution fraction volume was 1.0 ml each.
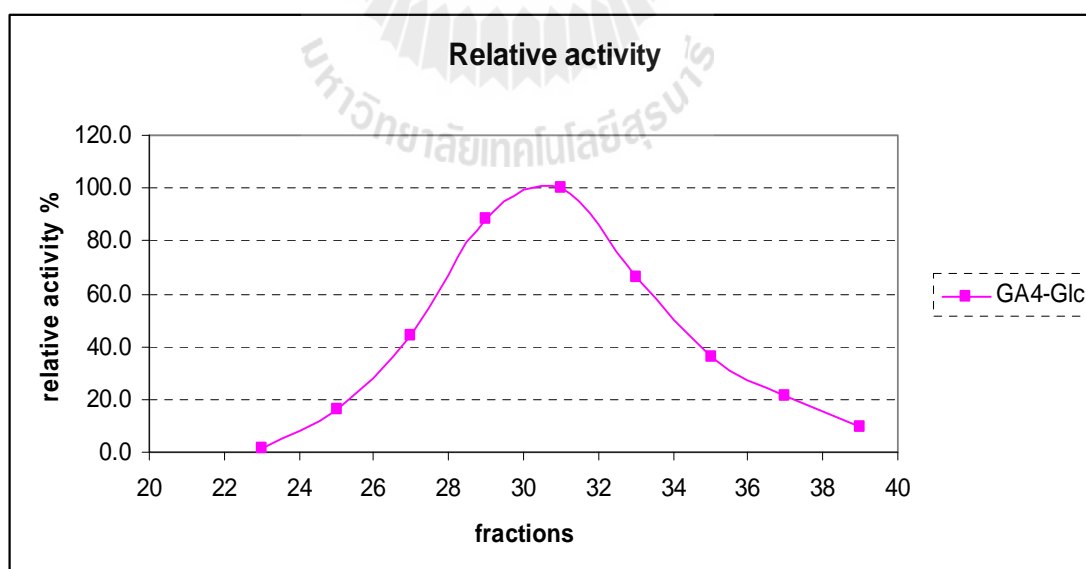
Figure 3.36 Activities of fractions eluted from the Octyl Sepharose column for hydrolysis of GA_4-Glc. The relative activities (%) were calculated based on A_{405}.
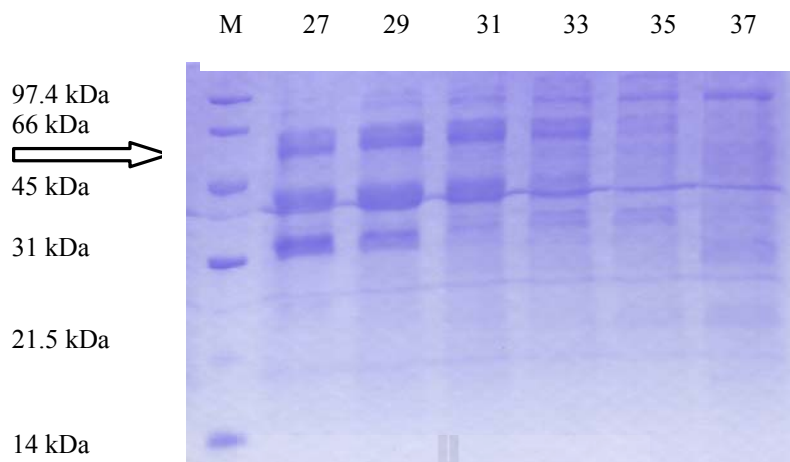
Figure 3.37 SDS-PAGE analysis of fractions after Octyl hydrophobic interaction chromatography. Lane M, marker; lanes 27-37 represent the corresponding fractions 27-37.

3.2.6 Purification of β-glucosidase with an S200 gel filtration column

The active fraction pool from the Octyl column purification was further purified with gel filtration over a Superdex S200 column (Figure 3.38). The buffer in the eluting fractions was exchanged to 4-fold diluted McIlvaine buffer, pH 5, with an ultra centrifugal filter before activity tests. Fractions 29 and 30 were found to have the highest hydrolysis activities with GA_4-Glc (Figure 3.39). In the 10% SDS-PAGE, two bands with size at approximately 60 kDa were evident as major bands in the fractions 29 and 30 (Figure 3.40).
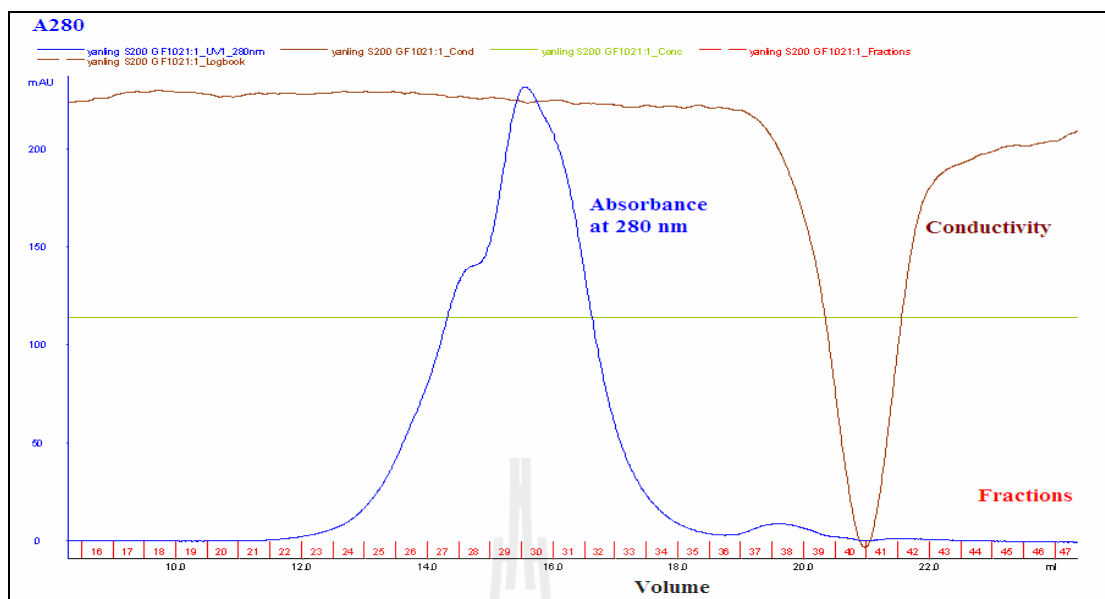
Figure 3.38 Protein elution profile of Superdex S200 gel filtration column. The protein was eluted with 4-fold diluted McIlvaine buffer, pH 7, containing 0.2 M NaCl at a flow rate of 0.5 ml/min; and the fraction volume was 0.5 ml.
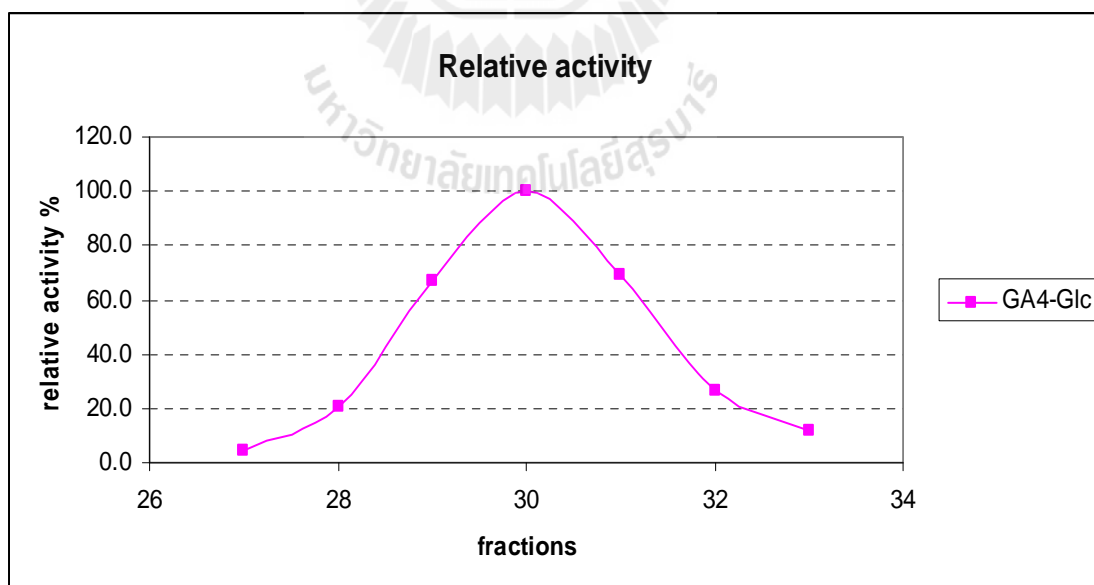
Figure 3.39 Activities of eluting fractions from Superdex S200 gel filtration chromatography for hydrolysis of GA_4-Glc. The relative activities (%) were calculated based on A_{405}.
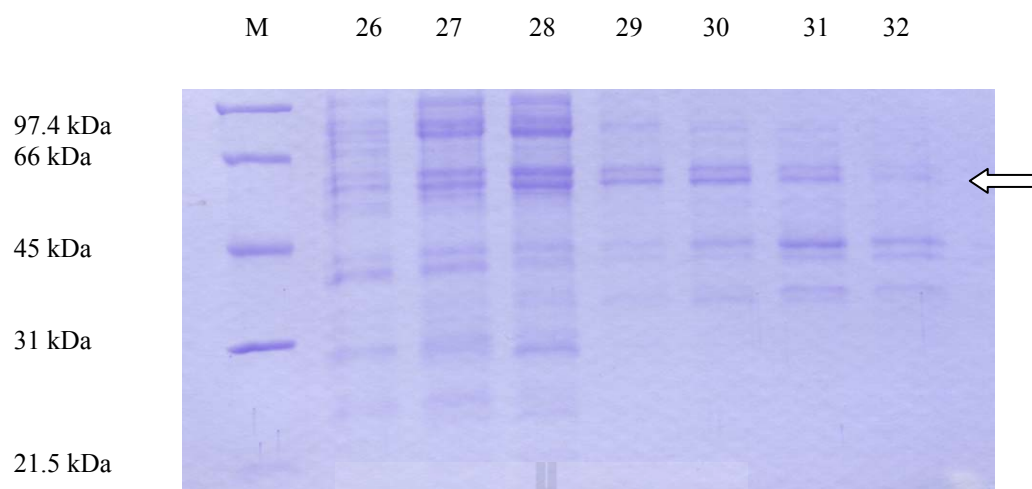
Figure 3.40 SDS-PAGE analysis of fractions after Superdex S200 gel filtration chromatography. Lane M, marker; lanes 26-32 represent fractions 26-32.

3.2.7 Identification of β-glucosidase with LC-MS

The two major protein bands from Superdex S200 column fraction 29 were identified by LCMS of tryptic peptides generated from their SDS-PAGE gel bands (Figure 3.41), as described in section 2.2.2.8. The peptide mass results were used in a MASCOT search of the Genbank non-redundant (nr) protein database. The peptide masses from the lower band matched the protein product from the Os04g0474900 gene locus [*Oryza sativa* Japonica Group], which corresponds to β-glucosidase Os4BGlu13, from glycoside hydrolase family 1 (Table 3.2). The peptide masses from the upper band matched a hypothetical protein OsI_23311 [*Oryza sativa* Indica Group] (Table 3.3).
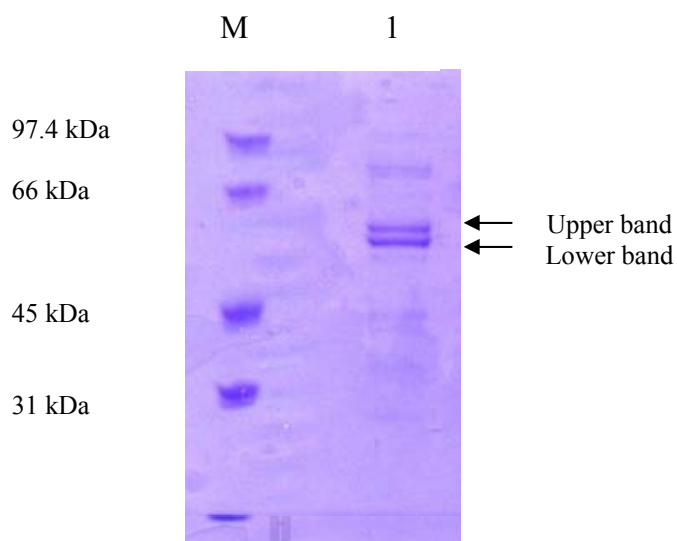
Figure 3.41 8% SDS-PAGE of fraction 29 in preparation for tryptic digestion and mass spectrometric analysis of derived peptides. Lane M, protein marker; lane 1, fraction 29. The two major bands were excised separately and submitted for tryptic digestion followed by LC-MS analysis.

Table 3.2 MASCOT search results for lower band.

Protein View:	**gi|115458942**
	Os04g0474900 [*Oryza sativa* Japonica Group]

Database:	NCBInr
Score:	1006
Nominal mass (M$_r$):	57,386
Calculated pI:	6.44
Taxonomy:	*Oryza sativa* Japonica Group

Search parameters

Enzyme:	Trypsin: cuts C-term side of K or R, unless next residue is P.
Fixed modifications:	Carbamidomethyl (C)
Variable modifications:	Oxidation (M)

Protein sequence coverage: 49%

Matched peptides are shown in ***bold red***.

1	MAAAGEVVML	GGILLPLLLV	VAVSGEPPPI	SR**RSFPEGFI**	**FGTASSSYQY**
51	**EGGAR**EGGR**G**	**PSIWDTFTHQ**	**HPDKIADKSN**	**GDVAADSYHL**	**YKEDVR**IMKD
101	MGVDAYR**FSI**	**SWTRILPNGS**	**LSGGINREGI**	**SYYNNLINEL**	**LLKGVQPFVT**
151	**LFHWDSPQAL**	**EDKYNGFLSP**	**NIINDYK**EYA	ETCFKEFGDR	VKHWITFNEP
201	LSFCVAGYAS	GGMFAPGRCS	PWEGNCSAGD	SGR**EPYTACH**	**HQLLAHAETV**
251	**R**LYKEKYQVL	QKGK**IGITLV**	**SNWFVPFSR**S	KSNIDAAR**RA**	**LDFMLGWFMD**
301	**PLIR**GEYPLS	MRELVR**NRLP**	**QFTK**EQSELI	KGSFDFIGLN	YYTSNYAGSL
351	PPSNGLNNSY	STDARANLTA	VR**NGIPIGPQ**	**AASPWLYIYP**	**QGFRELVLYV**
401	**K**ENYGNPTIY	ITENGVDEFN	NK**TLPLQEAL**	**KDDTR**IDYYH	K**HLLSLLSAI**
451	**R**DGANVKGYF	AWSLLDNFEW	SNGYTVR**FGI**	**NFVDYNDGAK**	RYPKMSAHWF
501	KEFLQK				

Table 3.3 MASCOT search results for upper band.

Protein View:	gi|125555680 **hypothetical protein OsI_23311 [*Oryza sativa* Indica Group]**
Database:	NCBInr
Score:	851
Nominal mass (M$_r$):	57,128
Calculated pI:	8.67
Taxonomy:	*Oryza sativa* Indica Group

Search parameters

Enzyme:	Trypsin: cuts C-term side of K or R, unless next residue is P.
Fixed modifications:	Carbamidomethyl (C)
Variable modifications:	Oxidation (M)

Protein sequence coverage: 35%

Matched peptides shown in **_bold red_**.

1	MAAAPMSFAF	TLLAACISFL	HHAPAAAAAA	PANQTAGFLD	CLAASLPAGV
51	VYTHASR**SYQ**	**SVLESSIKNL**	**LFDTPATPTP**	**VAVVEATDAS**	**HVQAAVR**CGV
101	GHGVSVRSRS	GGHDYEGLSY	RSLDAAR**AFA**	**VVDMAGGALR**	AVRVDVRGRA
151	AWVGSGATLG	EVYYAIANKT	SRLGFPGSVG	PTVGVGGFLS	GGGFGLMLRK
201	**HGLASDHVLD**	**ATMVDAK**GRL	LDR**AAMGEDL**	**FWAIRGGGGG**	**NFGIVLSWK**L
251	RLVPVPATVT	VFTVHRSRNQ	SATDLLAKWQ	R**VAPSLPSDA**	**FLRVVVQNQN**
301	**AQFESLYLGT**	**R**AGLVAAMAD	AFPELNVTAS	DCIEMTWVQS	VLYFAFYGTG
351	KPPEMLLDRG	TGRPDRYFKA	KSDYVQEPMP	SQVWETTWSW	LLK**DGAGLLI**
401	**LDPYGGEMAR**	VAPAATPFPH	RQALYNIQYY	GFWSESGEAA	AAKHMGWIR**G**
451	**VYGEMEPYVS**	**K**NPRGAYVNY	R**DLDLGVNDD**	**GGGVAR**ARYE	KATVWGRAYF
501	KANFERLAAV	K**AKVDPDNYF**	**KNEQSIPPLP**	**S**	

3.3 Screening of Rice GH1 enzymes for GA$_4$-glucosyl Ester Hydrolysis

Five rice GH1 enzymes that have been expressed in our lab were tested for the hydrolysis of pNPGlc and GA$_4$-Glc according to the methods described in section 2.2.2.9. As shown in Table 3.4, Os3BGlu6 was found to have the highest hydrolysis activity to GA$_4$-Glc among these enzymes. Although Os9BGlu31 had a higher ratio of activity toward GA$_4$-Glc compared to pNPGlc (0.267 vs. 0.07 for Os3BGlu6), it is primarily a transglycosidase and has very low activity toward both substrates.

Table 3.4 GA$_4$-Glc hydrolysis by recombinantly expressed rice GH1 enzymes.

Enzyme	Activity toward GA$_4$-Glc (µmol Glc released/min/mg)	Activity toward pNPGlc (µmol pNP released/min/mg)	Ratio of activity toward GA$_4$-Glc/pNPGlc
Os3BGlu6	0.185	2.6	0.07
Os3BGlu7 (BGlu1)	0.02	4.0	0.005
Os4BGlu12	0.035	130	0.003
Os4BGlu18	N.D.	0.94	-
Os9BGlu31	0.02*	0.075*	0.267

N.D. means not detectable.

* Activity is primarily transglycosylation, rather than hydrolysis (Luang et al., unpublished).

3.4 Recombinant Expression and Purification of the Mutants of Os3BGlu6

3.4.1 Purification of Os3BGlu6 wild type with IMAC

The Os3BGlu6 protein expressed in *E. coli* was purified with 2 steps of IMAC, as described in section 2.2.5.3. The fractions were analyzed by 12% SDS-PAGE (Figures 3.42-3.44). After the 2nd IMAC, the protein appeared as a single band on the gel with about 90% purity.
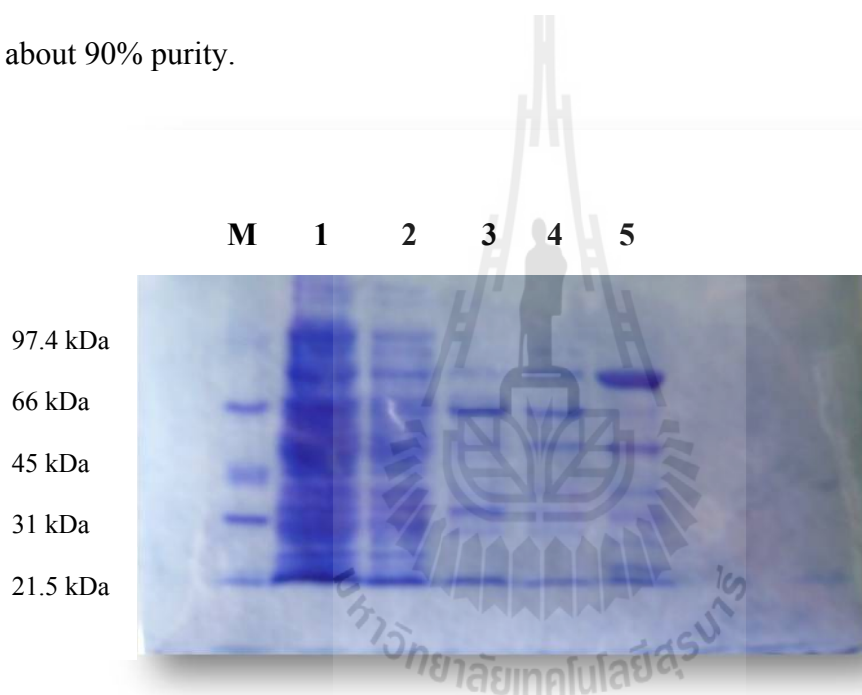
Figure 3.42 SDS-PAGE analysis of fractions from the 1st IMAC purification of Os3BGlu6. Lane M, marker; lane 1, flow-through fraction; lane 2, wash with equilibration buffer (20 mM Tris-HCl, pH 8.0); lane 3, wash with 5 mM imidazole in equilibration buffer; lane 4, wash with 10 mM imidazole in equilibration buffer; lane 5, protein eluted with elution buffer, 250 mM imidazole in equilibration buffer.
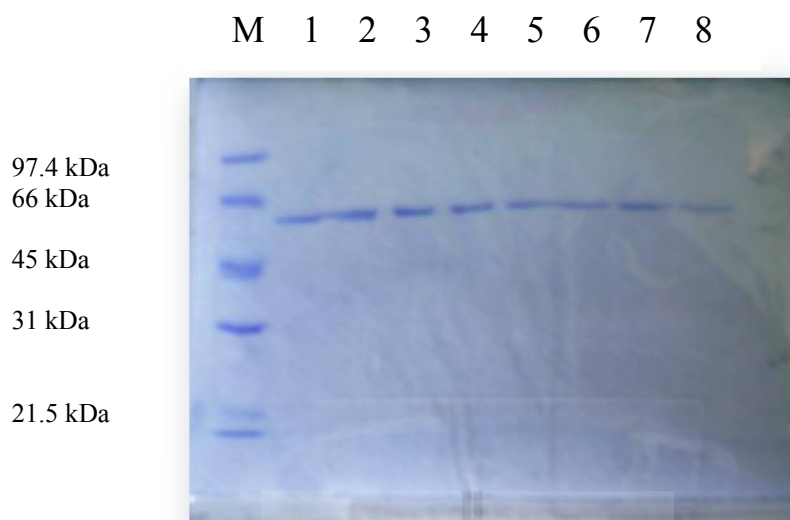
Figure 3.43 SDS-PAGE analysis of Os3BGlu6-containing fractions from the 2nd IMAC purification of Os3BGlu6. The protein from the 1st IMAC pool was digested with TEV protease and purified over a 2nd IMAC column. Lane M, protein marker; lanes 1, 2 and 3, flow-through fractions; lanes 4, 5 and 6, fractions from wash with equilibration buffer; lanes 7 and 8, fractions from wash with 5 mM imidazole in equilibration buffer.

Figure 3.44 Comparison of Os3BGlu6 after 1st and 2nd IMAC purifications. Lane M, protein marker; lane 1, protein after 1st IMAC; lane 2, protein after 2nd IMAC.

3.4.2 Purification of Os3BGlu6 M251N, E178Q and E178A with IMAC

Os3BGlu6 M251N, E178Q and E178A were purified by the same method as its wild type, and the protein fractions were analyzed with SDS-PAGE (Figures 3.45-3.48). The first IMAC step gave results similar to the wild type Os3BGlu6 for the three mutants, as shown for Os3BGlu6 M251N in Figure 3.45. After the 2nd IMAC step, the proteins were seen as a single major band and the purity were higher than 90%, as shown in Figures 3.46 (for Os3BGlu6 M251N), 3.47 (Os3BGlu6 E178Q) and 3.48 (Os3BGlu6 E178A).
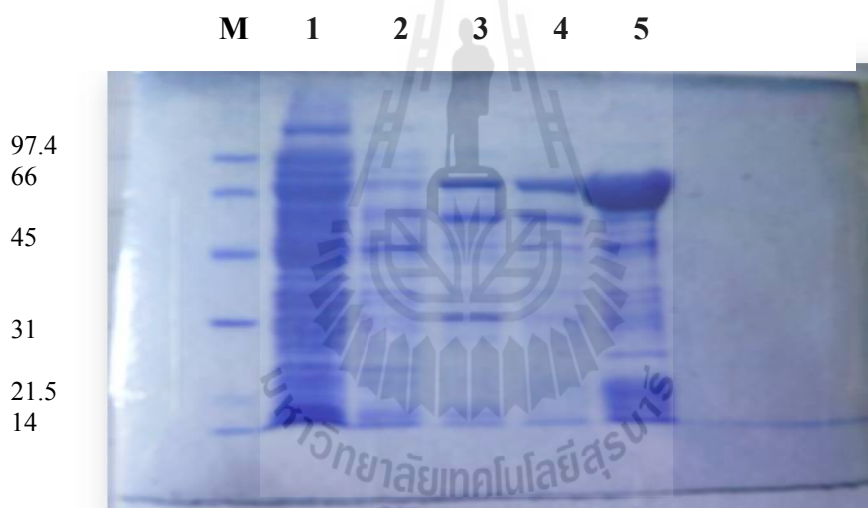
Figure 3.45 SDS-PAGE analysis of Os3BGlu6 M251N after 1st IMAC purification. Lane M, marker; lane 1, flow-through; lane 2, wash with equilibration buffer (20 mM Tris-HCl, pH 8.0); lane 3, wash with 5 mM imidazole in equilibration buffer; lane 4, wash with 10 mM imidazole in equilibration buffer; lane 5, protein eluted with elution buffer (250 mM imidazole in equilibration buffer).
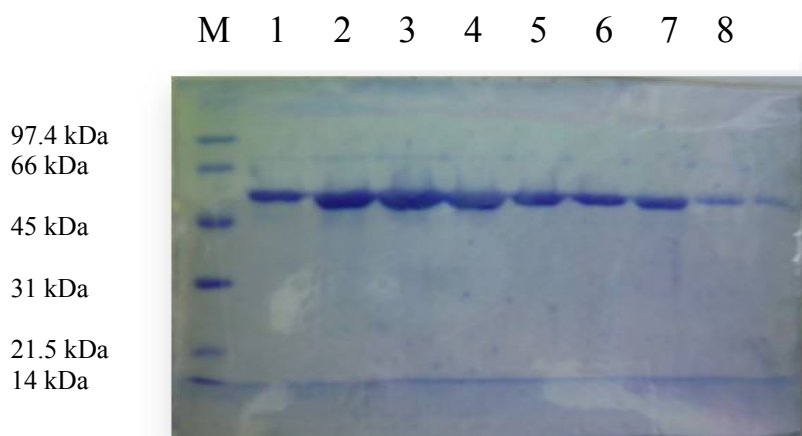
Figure 3.46 SDS-PAGE analysis of Os3BGlu6 M251N after 2nd IMAC purification. The protein from 1st IMAC was digested with TEV protease, and purified with a 2nd round of IMAC. Lane M, protein marker; lanes 1, 2 and 3, flow-through fractions; lanes 4, 5 and 6, fractions from wash with equilibration buffer; lanes 7 and 8, fractions from wash with 5 mM imidazole in equilibration buffer.

Figure 3.47 SDS-PAGE analysis of Os3BGlu6 E178Q after two steps of IMAC purification. Lane M, protein marker; lane 1, crude protein; lane 2, protein after 1st IMAC; lane 3, protein after 2nd IMAC.
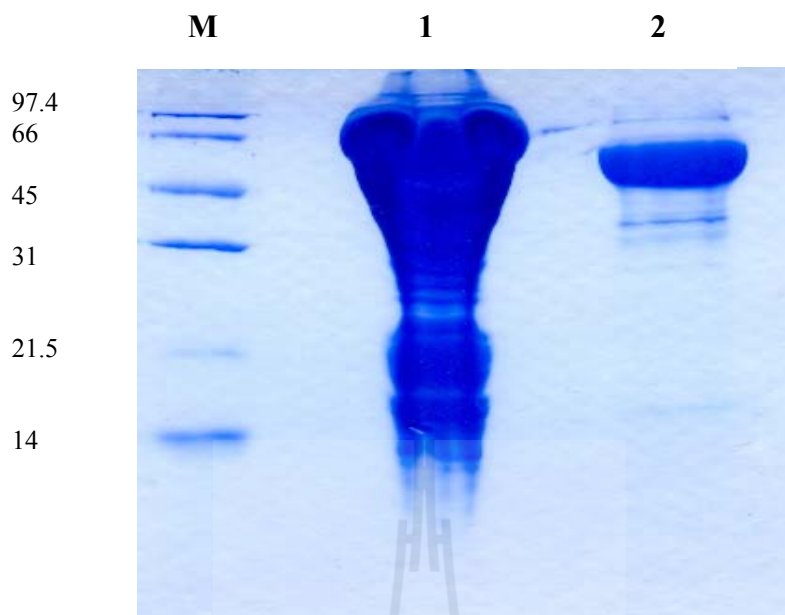
Figure 3.48 SDS-PAGE analysis of Os3BGlu6 E178A after two steps of IMAC purification. Lane M, protein marker; lane 1, protein after 1st IMAC purification; lane 2, protein after 2nd IMAC purification.

3.5 Characterization of Os3BGlu6 and Its Mutants

3.5.1 pH optimum for Os3BGlu6 and its mutants

The Os3BGlu6 wild type and M251N were found to have high pNPGlc hydrolysis activity between pH 4.0 and 5.0, with highest value at pH 4.5, while the activity quickly dropped above pH 5.5, with 50% of maximal activity at approximately pH 3.3 and 5.6 for wild type, and pH 3.5 and 5.5 for M251N (Figure 3.49). With GA$_4$-Glc substrate, Os3BGlu6 wild type and M251N, E178Q and E178A mutants also showed highest hydrolytic activities at pH 4.5 (Figure 3.50). The activities of Os3BGlu6 E178Q and E178A dropped slowly above pH 6.0, compared to Os3BGlu6 wild type and M251N, when hydrolyzing GA$_4$-Glc.
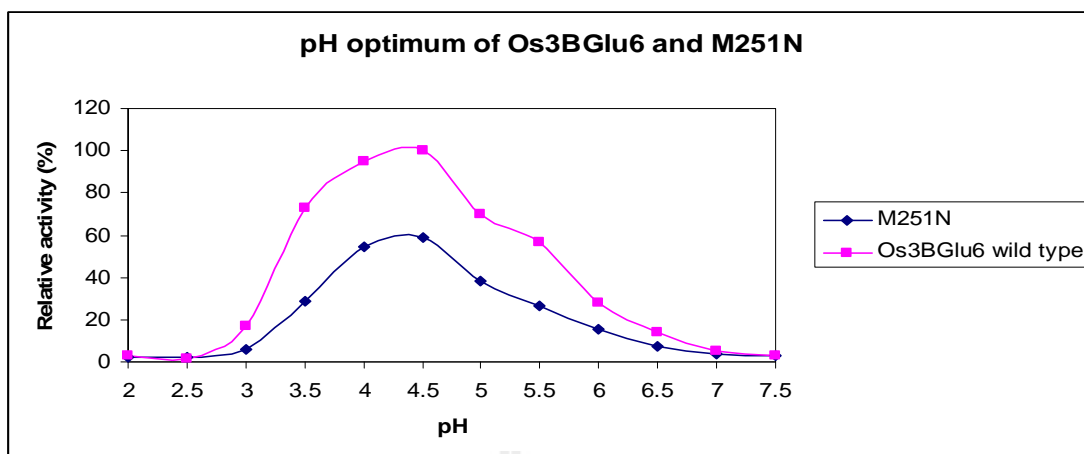
Figure 3.49 The pH-activity profiles of Os3BGlu6 and Os3BGlu6 M251N for hydrolysis of *p*NPGlc in universal buffer. One microgram of enzyme was incubating with 2 mM *p*NPGlc, in 80 µl of universal buffer (final volume was 100 µl), pH 2 to 11, in 0.5-pH-unit increments, at 30°C for 10 min. The reactions were stopped by adding 100 µl of 2 M Na_2CO_3. The relative activities were calculated based on $A_{405.}$
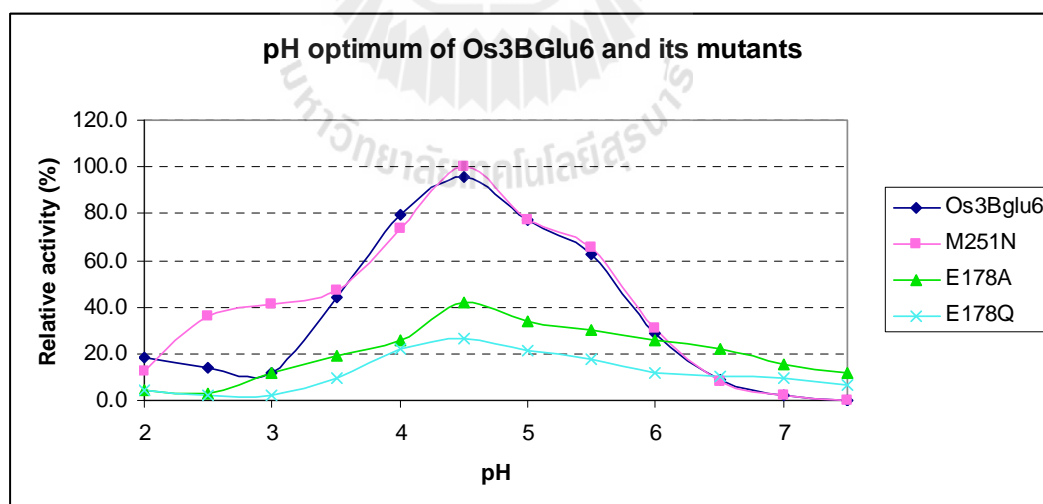
Figure 3.50 The pH-activity profiles of Os3BGlu6 and its mutants for hydrolysis of GA_4-Glc in universal buffer. This figure showed 1 µg of Os3BGlu6 or Os3BGlu6 M251N, E178Q or E178A was incubated with 0.86 mM GA_4-Glc in 80 µl of 100 mM universal buffer (final volume was 100 µl), pH 2 to 11, in 0.5-pH-unit increments, at 30° for 20 min. The relative activities are percentages of the highest activity observed, that of Os3BGlu6 M251N at pH 4.5.

3.5.2 Hydrolysis activities of Os3BGlu6 and its mutants

The structure of Os3BGlu6 wild type has been resolved by X-ray crystallography (Seshadri et al., 2009). The residue M251 was found playing an important role in the substrate binding. The mutation of M251 to Asn resulted a 15-fold increase in hydrolysis efficiency with laminaribiose and 9 to 24-fold increases for cellooligosaccharides compared to wild type Os3BGlu6 (Sansenya et al., 2012). In our study, the M251N mutant showed reduced hydrolytic activities for pNPGlc and GA$_4$-Glc compared to its wild type. The relative activities of M251N were 51.6% for pNPGlc, 88.9% for GA$_4$-Glc; the catalytic efficiencies (k_{cat}/K_m) for M251N were reduced to 2.6 from 6.2 mM^{-1}s^{-1} for pNPGlc, 0.08 from 0.13 for GA$_4$-Glc (Table 3.5) compared to its wild type. The mutation of the putative catalytic acid/base glutamate residue at 178 to alanine (E178A) and glutamine (E178Q) led to complete loss of hydrolytic activity toward pNPGlc; and the relative activities to GA$_4$-Glc were reduced to 22.2% and 12.5%, respectively, compared to its wild type. The mutation of the catalytic nucleophile glutamate residue at 394 to glutamine (E394Q) and aspartic acid (E394D) led to complete loss of hydrolytic activity toward both pNPGlc and GA$_4$-Glc.

Table 3.5 Hydrolysis activities of Os3BGlu6 and its mutants.

Enzyme	pNP-β-D-glucoside				GA$_4$-Glc ester			
	Relative activity (%)	K_m (mM)	k_{cat} (s^{-1})	k_{cat}/K_m (mM^{-1} s^{-1})	Relative activity (%)	K_m (mM)	k_{cat} (s^{-1})	k_{cat}/K_m (mM^{-1} s^{-1})
Os3BGlu6	100	6.3 ± 0.4*	38.9 ± 0.9*	6.2*	100	5.8 ± 0.6	0.75 ± 0.04	0.13
Os3BGlu6-M251N	51.6	6.5 ± 0.7	15.4 ± 0.9	2.6	88.9	14.6 ± 2.0	1.2 ± 0.1	0.08
Os3BGlu6-E178Q	0.3	n.m.	n.m.	n.m.	12.5	0.09 ± 0.01	0.03 ± 0.001	0.33
Os3BGlu6-E178A	0.7	n.m.	n.m.	n.m.	22.2	3.7 ± 0.4	0.09 ± 0.005	0.03
Os3BGlu6-E394D**	0.9	n.m.	n.m.	n.m.	1.4	n.m.	n.m.	n.m.
Os3BGlu6-E394Q**	0.8	n.m.	n.m.	n.m.	0.6	n.m.	n.m.	n.m.

n.m.: not measured. *Data from Seshadri et al. (2009). ** The mutants E394D and E394Q were supplied by Sompong Sansenya. For the relative activity with pNPGlc, 0.5 µg of Os3BGlu6 wild type or M251N, 3 µg of E178A, E178Q, E394D or E394Q was incubating with 4 mM pNPGlc in NaOAc buffer (final volume was 50 µl), at 30°C for 10 min. For the relative activity with GA$_4$-Glc, 1.0 µg of Os3BGlu6 wild type or M251N, 3 µg of E178A, E178Q, E394D or E394Q was incubating with 1.7 mM GA$_4$-Glc in NaOAc buffer (final volume was 50 µl), at 30°C for 20 min. The relative activities were calculated based on A$_{405}$ and the amount of the enzymes. For the kinetic activities, 50 mM NaOAc buffer was used for Os3BGlu6 wild type and M251N, for both substrates; but 50 mM MES buffer was selected for the E178Q and E178A mutants. Variable reaction times, enzyme amounts and substrate concentrations were tested to obtain the initial velocities.

3.5.3 Identification of transglucosylation product with TLC (Table 3.6), LC-MS and NMR

Os3BGlu6 hydrolyzed *p*NPGlc in MES buffer to *p*NP and glucose, and no transglucosylation products were formed when GA_4 (Figure 3.51) and azide were added as acceptors. Neither Os3BGlu6 wild type nor E178Q could hydrolyze dNP2FGlc, and no transglucosylation product was formed when GA_4 was used as an acceptor to try to rescue the reaction (Figures 3.52 and 3.53).

Table 3.6 Hydrolysis and transglucosylation activities of Os3BGlu6 and its mutants detected by TLC.

Enzyme	Donor	Acceptor	Hydrolysis	Trans-glucosylation
Os3BGlu6	*p*NPGlc	GA_4	✓	nd
Os3BGlu6	dNP2FGlc	GA_4	nd	nd
Os3BGlu6	*p*NPGlc	Na-azide	✓	nd
Os3BGlu6	GA_4-Glc	Na-azide	✓	nd
M251N	*p*NPGlc	Na-azide	✓	nd
M251N	GA_4-Glc	Na-azide	✓	nd
E178Q	*p*NPGlc	GA_4	nd	nd
E178Q	dNP2FGlc	GA_4	nd	nd
E178Q	*p*NPGlc	Na-azide	nd	✓
E178Q	*p*NPGlc	H_2O	✓	nd
E178Q	GA_4-Glc	Na-azide	✓	✓
E178A	*p*NPGlc	Na-azide	nd	✓
E178A	GA_4-Glc	Na-azide	✓	✓

nd: not detected. Overnight reaction products were spotted on TLC, developed with $CHCl_3$-MeOH (7.0:3.0), EtOAc-MeOH-NH_4OH (7.0:2.8:0.2) or EtOAc-MeOH-H_2O (7.5:2.5:1.0), and carbohydrate products were detected with sulfuric acid staining followed by charring.

GA$_4$

pNPGlc

GA$_4$-Glc

Glucose

1 2 3 4 5 6 7 8
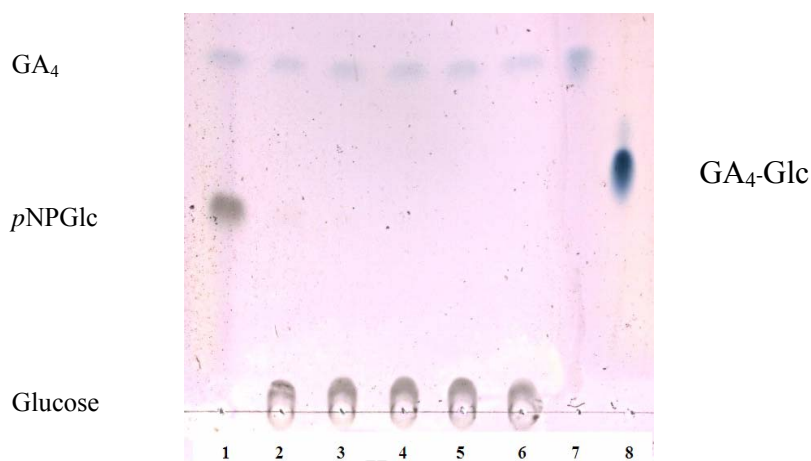
Figure 3.51 Thin layer chromatographic analysis of transglycosylation of GA$_4$ by Os3BGlu6 β-glucosidase. Here, 4 mM pNPGlc was reacted with 0.48 mM of GA$_4$, as the acceptor, and 1.0 µg of Os3BGlu6 in 50 mM MES buffer, pH 5. Sample aliquots were spotted on a silica gel 60 F$_{254}$ TLC plate and developed with CHCl$_3$-MeOH (7.0:3.0, v/v). The products were detected by staining with 10% sulfuric acid in ethanol followed by charring. Lane 1, control, GA$_4$ with pNPGlc without enzyme; Lane 2, reaction after 70 min; Lane 3, reaction after 120 min; Lane 4, reaction after 180 min; Lane 5, reaction after 7.5 h; Lane 6, reaction after 18 h; Lane 7, GA$_4$ in MES buffer; Lane 8, GA$_4$-Glc ester in water.
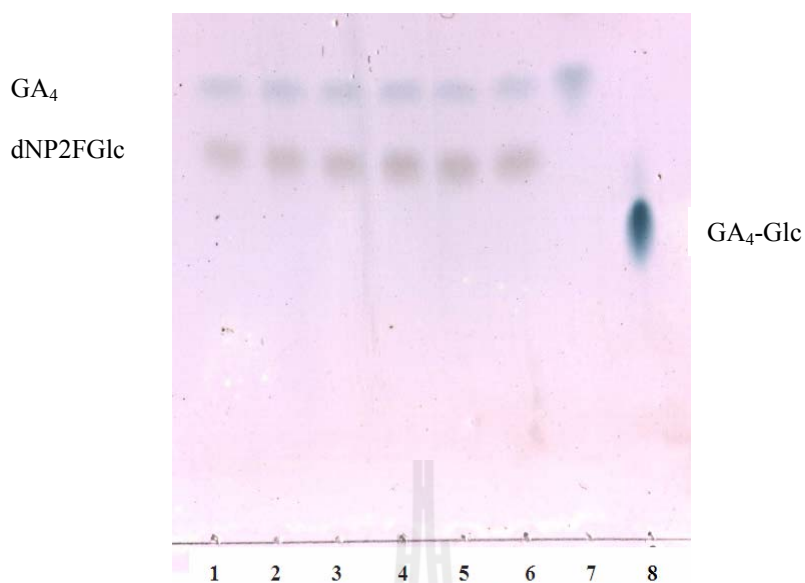
Figure 3.52 TLC analysis of attempted transglycosylation of GA$_4$ with dNP2FGlc by Os3BGlu6 β-glucosidase. In this experiment, 3.0 mM dNP2FGlc was reacted with 1.0 μg of Os3BGlu6 in 50 mM MES buffer, pH 5, and 0.48 mM of GA$_4$ was included as a possible acceptor. TLC conditions were the same as in Figure 3.51. Lane 1, control, GA$_4$ with dNP2FGlc without enzyme; Lane 2, reaction after 70 min; Lane 3, reaction after 120 min; Lane 4, reaction after 180 min; Lane 5, reaction after 7.5 h; Lane 6, reaction after 18 h; Lane 7, GA$_4$ in MES buffer; Lane 8, GA$_4$-Glc ester in water.
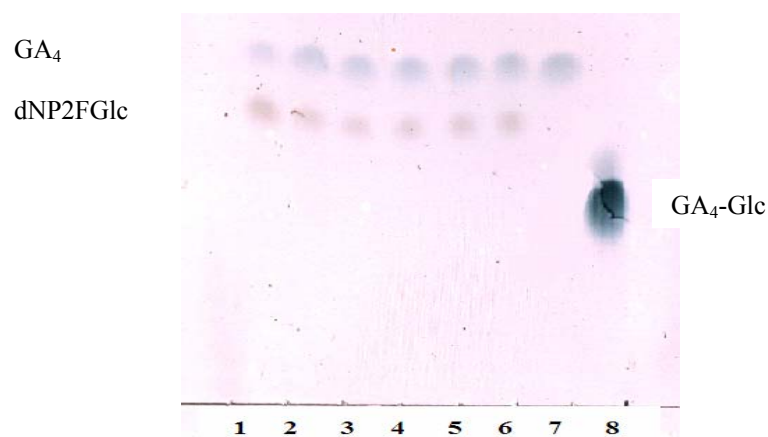
Figure 3.53 TLC analysis of attempted transglycosylation of GA_4 with dNP2FGlc by Os3BGlu6 E178Q. Here, 1.5 mM dNP2FGlc was reacted with 1.0 µg of Os3BGlu6 E178Q in 50 mM MES buffer, pH 5; 0.96 mM GA_4 was used as a possible acceptor. TLC conditions were the same as in Figure 3.51. Lane 1, control, GA_4 with dNP2FGlc without enzyme; Lane 2, reaction after 70 min; Lane 3, reaction after 120 min; Lane 4, reaction after 180 min; Lane 5, reaction after 7.5 h; Lane 6, reaction after 18 h; Lane 7, GA_4 in MES buffer; Lane 8, GA_4-Glc ester in water.

Os3BGlu6 E178Q and E178A showed negligible hydrolysis of pNPGlc within an hour, but hydrolysis products were detected after overnight reaction. When sodium azide was present, transglucosylation products were detected after overnight reaction, but no significant hydrolysis products were detected (Figure 3.54). However, when this E179Q mutant was used in an attempt to generate GA_4-Glc ester by transglycosylation of GA_4 acceptor with pNPGlc donor, no transglycosylation product was detected (Figure 3.55). When GA_4-Glc ester was used as donor and sodium azide as acceptor, both hydrolysis and transglucosylation products were detected in the reaction of Os3BGlu6 E178Q and E178A, but transglucosylation products were apparently the main products (Figure 3.56).
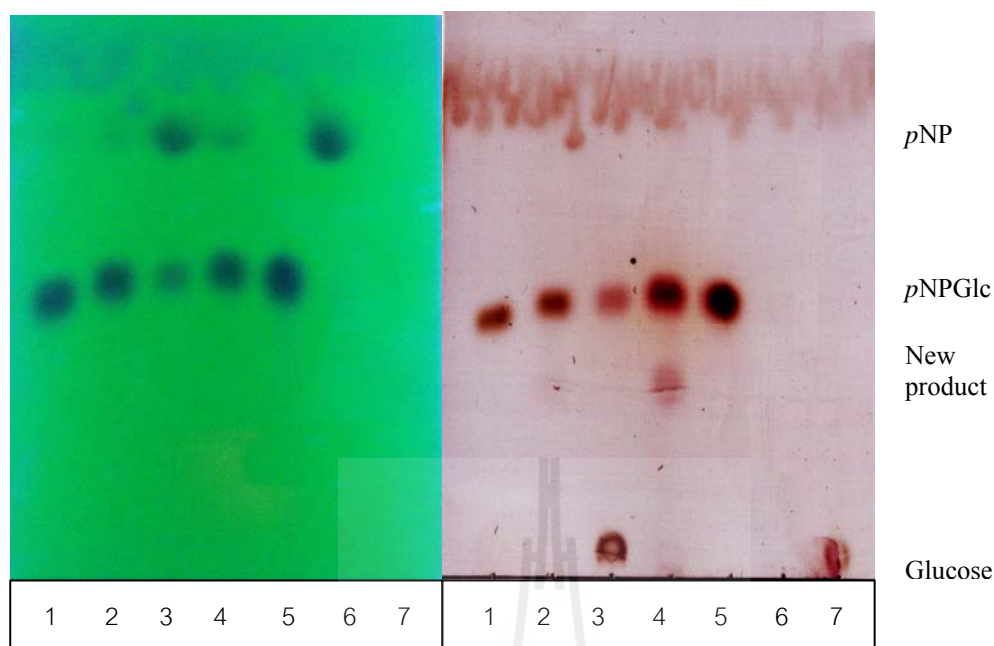
Figure 3.54 TLC analysis of the reaction of Os3BGlu6 E178Q with *p*NPGlc with and without sodium azide. In each reaction, 3.0 μg of Os3BGlu6 E178Q was reacted with 2 mM *p*NPGlc in 50 mM MES buffer at 30°C for 1 h or 24 h. The resulting reaction solutions were spotted onto a silica gel 60 F_{254} TLC plate, which was developed with EtOAc-MeOH-NH$_4$OH (7.0:2.8:0.2 v/v/v), and detected with UV$_{254}$ (plate A) and then sulfuric acid staining followed by charring (plate B). Lane 1, reaction of E178Q + *p*NPGlc in MES buffer, 1 h; Lane 2, reaction of E178Q + *p*NPGlc +50 mM Na-azide in 50 mM MES buffer, 1 h; Lane 3, reaction of E178Q + *p*NPGlc in MES buffer, 24 h; Lane 4, reaction of E178Q + *p*NPGlc +50 mM Na-azide in 50 mM MES buffer, 24 h; Lane 5, *p*NPGlc standard; Lane 6, *p*NP standard; Lane 7, Glucose standard.
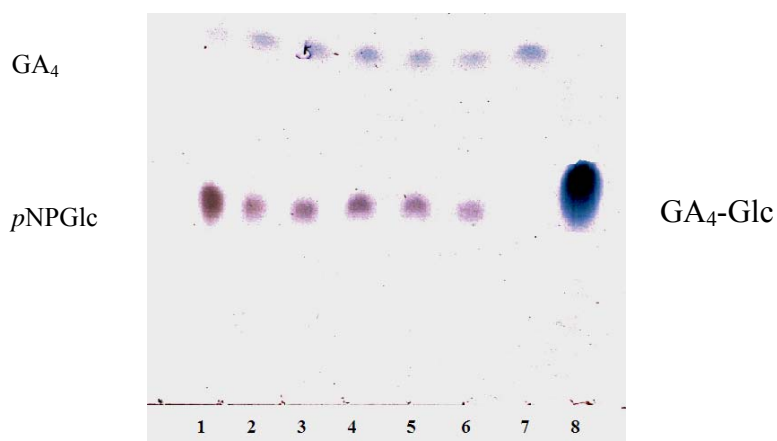
Figure 3.55 TLC analysis of attempted transglycosylation of GA$_4$ with pNPGlc by Os3BGlu6 E178Q. In this experiment, 2 mM pNPGlc was reacted with 1.0 μg of Os3BGlu6 E178Q in 50 mM MES buffer, pH 5; 0.96 mM GA$_4$ was used as a possible acceptor. TLC conditions were the same as in Figure 3.51. Lane 1, control, GA$_4$ with pNPGlc without enzyme; Lane 2, reaction after 70 min; Lane 3, reaction after 120 min; Lane 4, reaction after 180 min; Lane 5, reaction after 7.5 h; Lane 6, reaction after 18 h; Lane 7, GA$_4$ in MES buffer; Lane 8, GA$_4$-Glc ester in water.
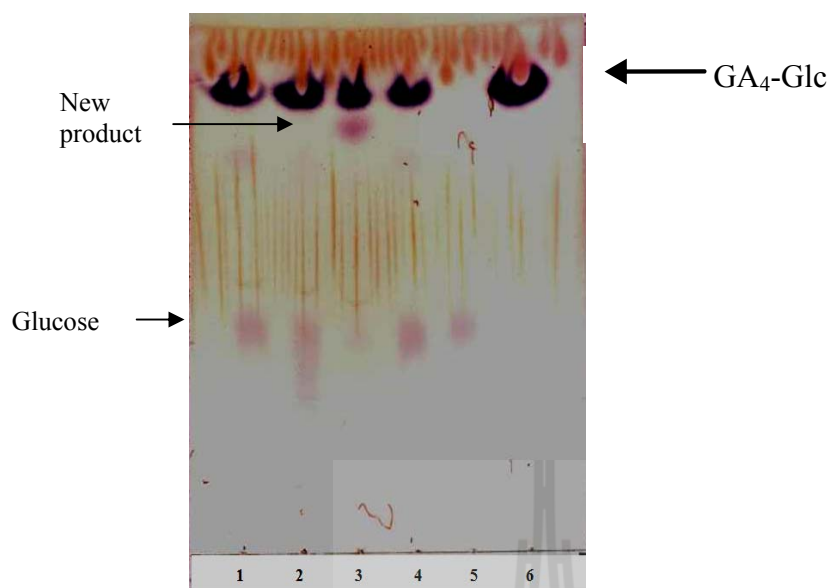
Figure 3.56 Reaction of Os3BGlu6 E178A with GA$_4$-Glc in different solutions. In each case, 3.5 μg of Os3BGlu6 E178A was reacted with 5 mM GA$_4$-Glc in a different buffer at 30°C for 60 min. The developing solvent was EtOAc-MeOH-H$_2$O (7.5:2.5:1.0 v/v/v), and carbohydrate products were detected with sulfuric acid staining followed by charring. Lane 1: reaction in 50 mM NaOAc; Lane 2: reaction in universal buffer; Lane 3: reaction with 50 mM Na-azide in 50 mM MES; Lane 4: reaction in 50 mM MES; Lane 5: Glucose standard; Lane 6: GA$_4$-Glc standard.

The transglucosylation products of Os3BGlu6 E178A with GA$_4$-Glc were identified with LC-MS (Figure 3.57). GA$_4$ was confirmed not only to match the retention time of the standard, but also the mass spectrum (Figure 3.58, Molecular Weight: 332.39). The peaks for [M-H]$^-$ and [M+M-H]$^-$ were the major ions in the mass spectra. The newly formed product observed in TLC (Figure 3.56) was expected to be β-D-glucopyranosyl azide (also called 1-azido-β-D-glucose) based on the retaining mechanism of the GH1 β-glucosidases. The peak at retention time 3.69 min in the LC-MS chromatogram (Figure 3.57) had a mass spectrum consistent with the molecular mass of 205.17 of β-D-glucopyranosyl azide (Figure 3.59). Since formic acid (HCO$_2$H) was used in the mobile

phase of LC-MS, its adduct ion $[M+HCO_2]^-$ was detected as the base peak. Other major peaks were identified as ion adducts with molecular masses for $[M-H]^-$, $[M+Cl]^-$, $[M+M-H]^-$ and $[M+113]^-$. The *m/z* of 113 was detected as an intensive peak, but its chemical composition has not yet been assigned.
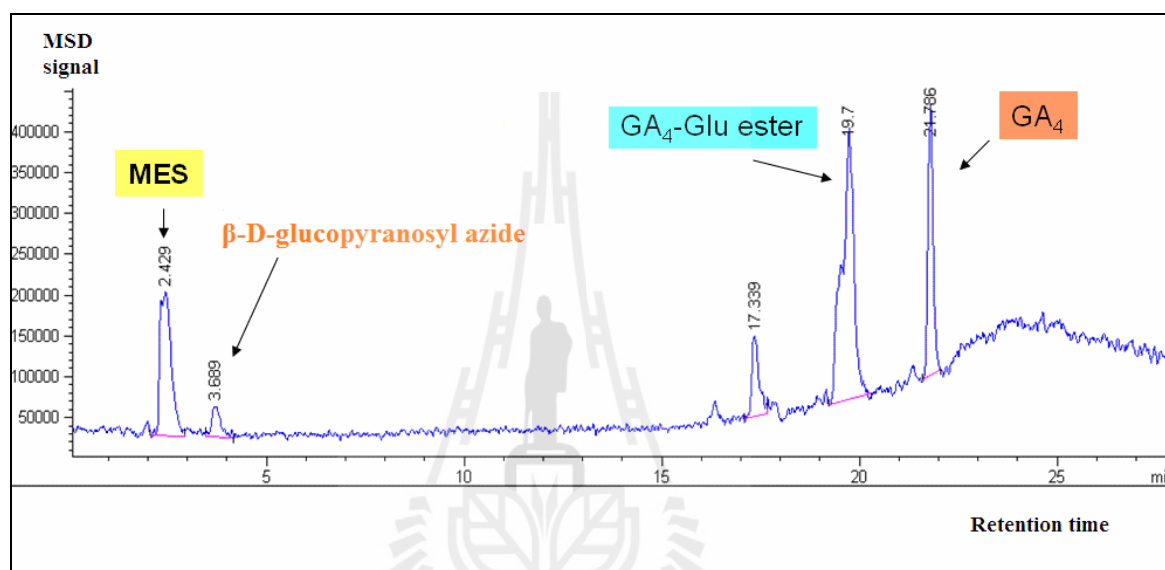
Figure 3.57 The LC-MS chromatogram of the transglucosylation reaction of Os3BGlu6 E178A with GA$_4$-Glc as donor and sodium azide as acceptor. The reaction components were separated on a ZORBAX Eclipse XDB-C18, 4.6*150 mm, 5 Micron column (Agilent). The mobile phases were A: water with 0.05% (v/v) formic acid and B: MeOH with 0.05% (v/v) formic acid, and the gradient was 0-80% B in 20 min, at a flow rate of 0.8 ml/min. The detector was an Agilent MSD single quadrupole mass spectrometer with an API-ES source in the negative ion mode cycled over a scan range of 50-800 *m/z*.
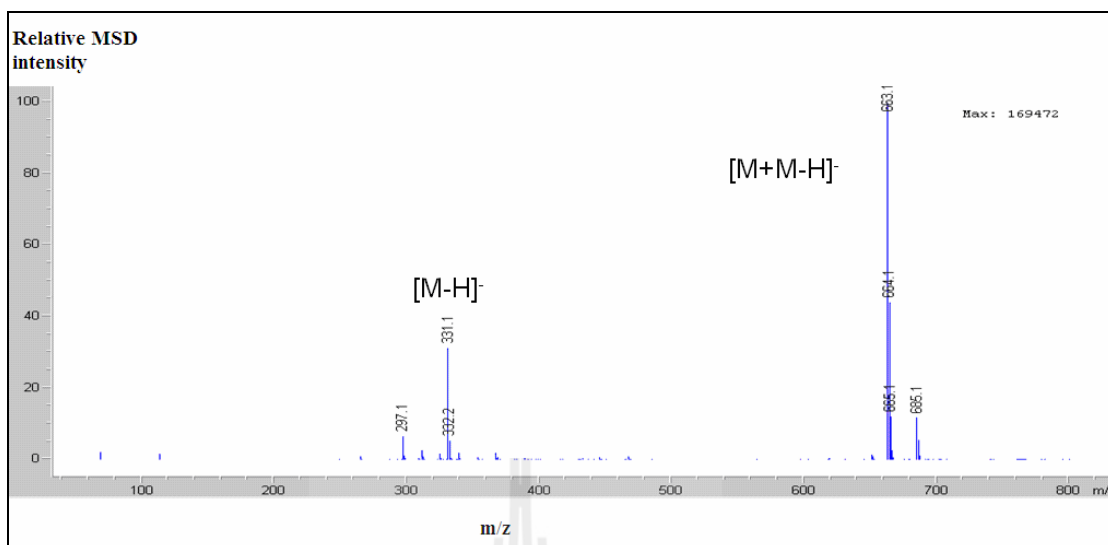
Figure 3.58 The mass spectrum of the HPLC peak at retention time 21.79 in the negative mode, identified as GA_4.
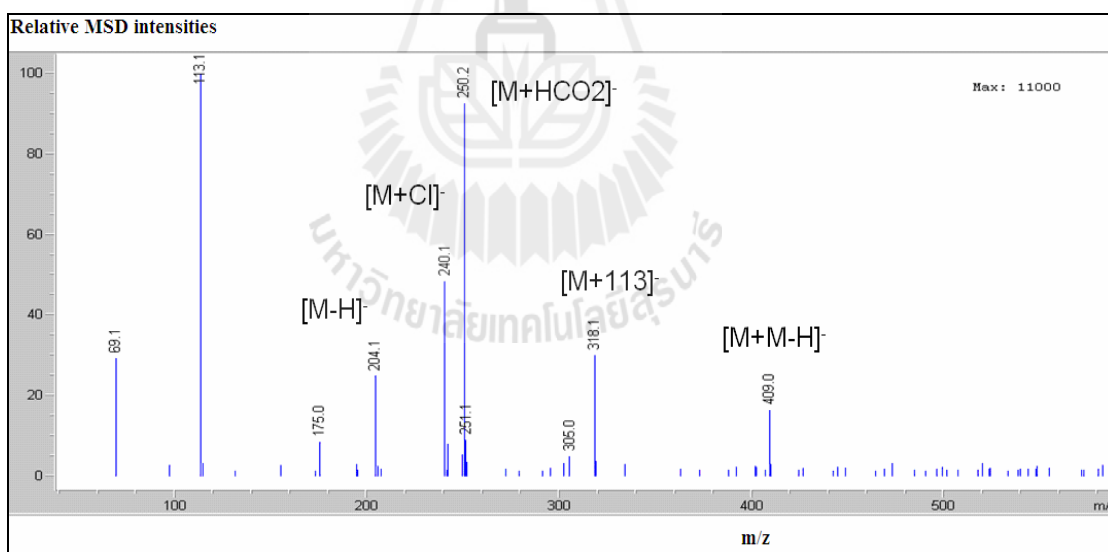
Figure 3.59 The mass spectrum of the HPLC peak at the retention time 3.69 min, identified as β-D-glucopyranosyl azide.

The structure of the β-D-glucopyranosyl azide was also confirmed from its ^1H (Figure 3.60) and gCOSY NMR spectra (Figure 3.61). The ^1H spectrum peaks were assigned as: δ4.53, H1, d, $J_{2,1}$=9.0 Hz; δ3.85, H6, dd, $J_{6,6'}$=11.1 Hz; δ3.678, H6′, dd, $J_{5,6'}$=4.8Hz, $J_{6,6'}$=11.1 Hz; δ3.364-3.458, H3,H4, H5, m; δ3.192, H2, t, $J_{1,2} = J_{3,2}$ =9.0 Hz.

The ^{1}H NMR spectrum matched the published data for β-D-glucopyranosyl azide (Wang et al., 1995). The coupling constant between H1 and H2 of 9.0 Hz, confirmed the β-D-glucopyranosyl azide had the "β" configuration.
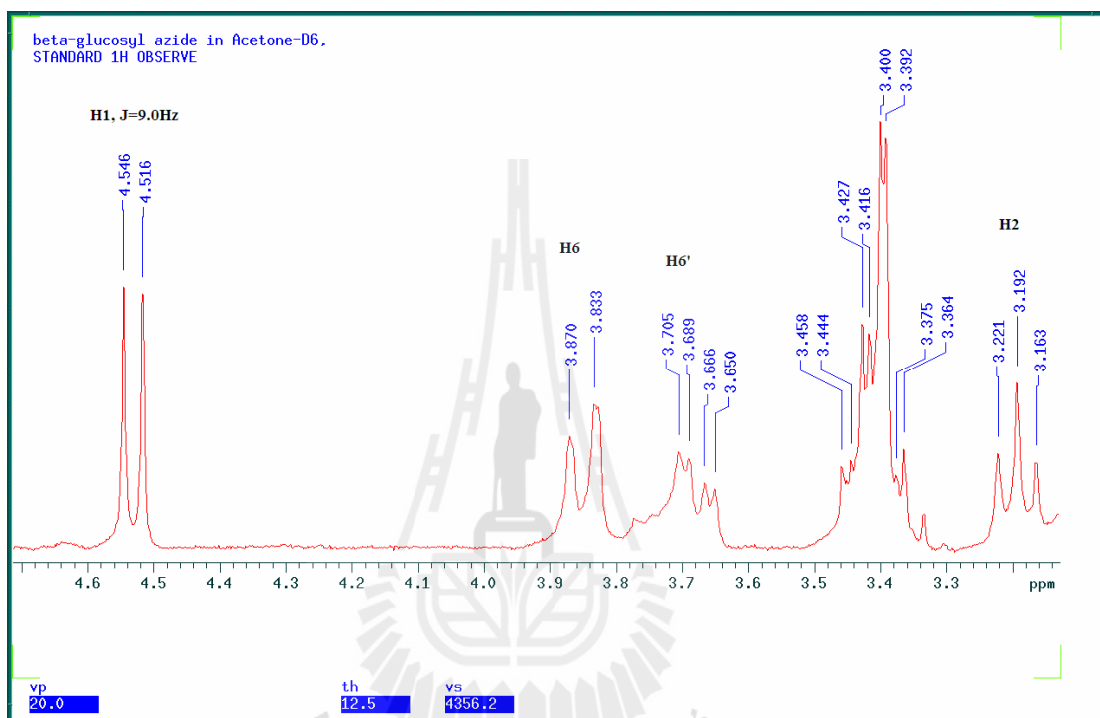
Figure 3.60 The expanded ^{1}H NMR spectrum of β-D-glucopyranosyl azide. The transglucosylation product was collected from HPLC and dried with a vacuum centrifuge. The white powder was dissolved in acetone-d6 and the ^{1}H NMR spectrum was acquired with a 300 MHz NMR spectrometer. TMS was used as the reference standard.
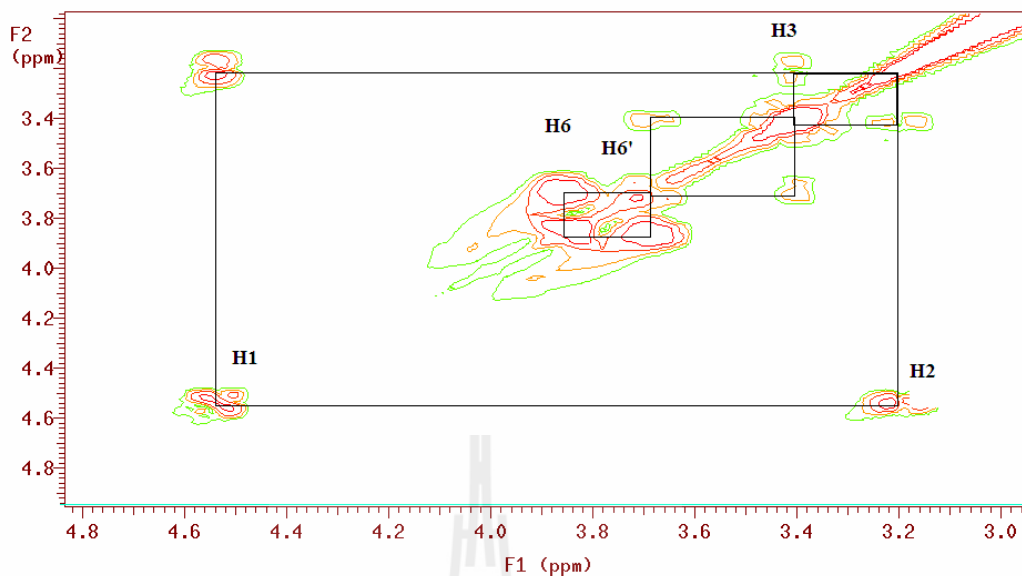
Figure 3.61 The gCOSY NMR spectrum of β-D-glucopyranosyl azide in acetone-d6. The protons on the glucosyl ring are marked beside the peaks. The boxes show the correlations between the protons.

3.5.4 Transglucosylation kinetics of the mutants of Os3BGlu6

The activity versus pH profiles for transglucosylation of azide with GA$_4$-Glc donor were determined in NaOAc and MES buffers. For the Os3BGlu6 E178Q mutant, its optimum pH range was 5.0 to 6.0 in both buffers (Figure 3.62), slightly higher than its optimum pH for hydrolysis of GA$_4$-Glc. The Os3BGlu6 E178A mutant showed a different pattern. Its transglucosylation activity was high at pH 5 in MES buffer, but high at pH 4.0 in NaOAc buffer. In NaOAc buffer, the transglucosylation activity of the Os3BGlu6 E178A was much higher than that in MES buffer, even without azide in the system. This indicated that NaOAc could act as a nucleophile or substitute acid/base to rescue the hydrolysis activity.
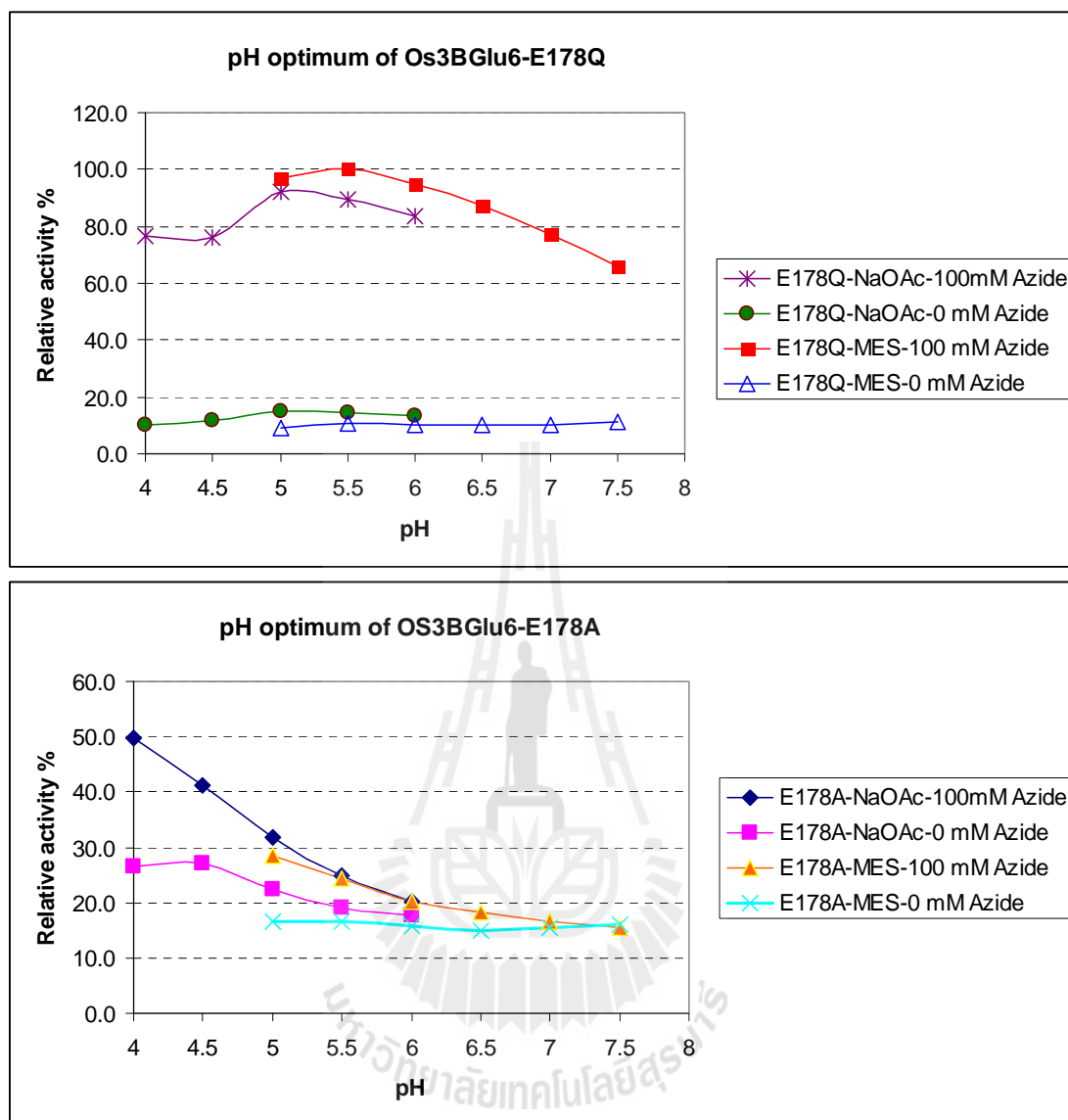
Figure 3.62 pH dependence of transglucosylation of azide with GA$_4$-Glc donor by Os3BGlu6 E178Q (Top) and E178A (Bottom) mutants. In each reaction, 2 µg of Os3BGlu6 E178Q or E178A was incubated with 2 mM GA$_4$-Glc and 100 mM Na-azide, in 50 mM MES (pH 5.0-7.5) and 50 mM NaOAc buffer (pH 4.0-6.0) at 30°C for 30 min. The relative activities were measured from the released GA$_4$. The highest activity of Os3BGlu6 E178Q with 100 mM azide in MES buffer at pH 5.5 was set as 100% for relative activities in both figures.

Figure 3.63 shows that when the concentration of donor GA$_4$-Glc was fixed at 2 mM, the turnover rates V_0/E_0 of GA$_4$ for Os3BGlu6 E178A slowly increased with increasing concentrations of Na-azide and reached its maximum at 400 mM Na-azide. However, for Os3BGlu6 E178Q, the turnover rates of GA$_4$ slowed down after reaching a maximum at 100 mM Na-azide. This indicates that the high concentration of Na-azide was inhibiting the reaction. Two methods were tried for calculating the kinetic parameters; one was calculated from the released GA$_4$ after subtracting hydrolysis product and another one without subtracting hydrolysis product. Since transglucosylation products were the main products and little glucose was evident when the acceptor azide was present compared to when it was not (as seen in the TLC in Figure 3.56), the parameters calculated from the released GA$_4$ without subtracting hydrolysis should yield a better estimate for these reactions. The k_{cat}/K_m values of Os3BGlu6 E178 A and Os3BGlu6 E178Q were 0.066 and 0.13 mM^{-1}s^{-1}, respectively, when they were calculated from the released GA$_4$ without subtracting hydrolysis product (Table 3.7).
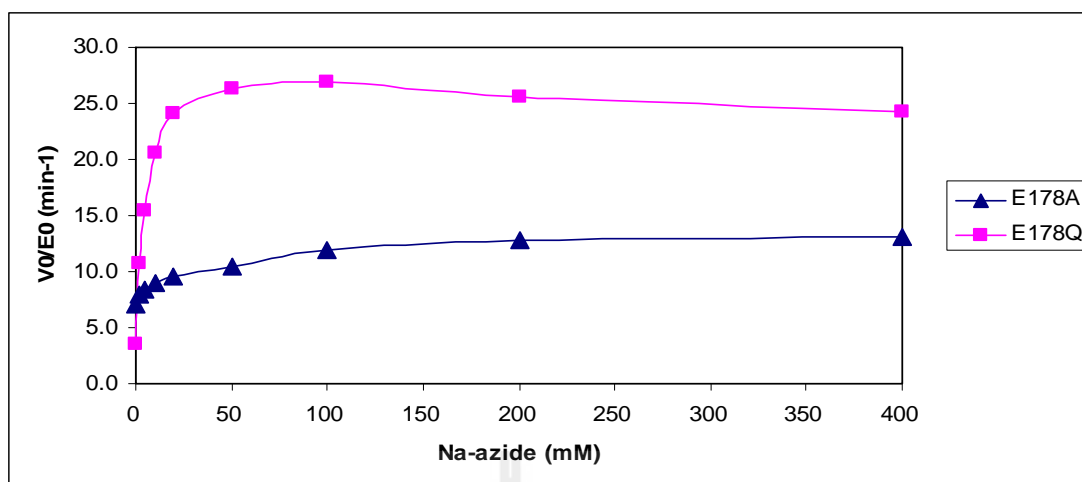
Figure 3.63 Kinetics for transglucosylation of azide acceptor with GA_4-Glc donor by the Os3BGlu6 E178A and E178Q acid/base mutants. The concentrations of Na-azide acceptor were varied from 0 to 400 mM, while donor GA_4-Glc was fixed at 2 mM. The reactions were performed in 50 mM MES, pH 5, at 30°C for 20 min. The turnover rates, V_0/E_0, of GA_4 (μmole of GA_4 release per minute per μmole of enzyme) were calculated based on the area of GA_4 HPLC peaks. The total area of GA_4 was used without subtracting the hydrolysis reaction.

Table 3.7 Transglucosylation kinetics of Os3BGlu6 E178Q and E178A for sodium azide acceptor with 2 mM GA_4-Glc donor.

Enzyme	Na-azide		
	K_m (mM)	k_{cat} (s^{-1})	k_{cat}/K_m (mM^{-1}s^{-1})
Os3BGlu6 E178Q (a)	5.78 ± 0.37	0.44 ± 0.01	0.075
(b)	3.71 ± 0.47	0.48 ± 0.01	0.13
Os3BGlu6 E178A (a)	30.1 ± 3.1	0.106 ± 0.003	0.0035
(b)	3.1 ± 0.5	0.204 ± 0.006	0.066

The transglucosylation rates were calculated from the released GA_4 after subtracting hydrolysis product from the reaction without azide (a) and without subtracting hydrolysis product (b).

The effects of the concentration of Na-azide on the transglucosylation kinetics were further studied by varying concentrations of donor GA$_4$-Glc, fixing the concentration of Na-azide at 50, 100, 200 and 400 mM, and measuring k_{cat} and K_m for GA$_4$-Glc. Figure 3.64 shows that 400 mM Na-azide did not inhibit the transglucosylation reaction of Os3BGlu6 E178A yet, but 200 mM and 400 mM Na-azide showed significant inhibition in the reactions catalyzed by Os3BGlu6 E178Q. The kinetic parameters also confirmed this inhibition (Table 3.8). For Os3BGlu6 E178Q, the k_{cat}/K_m of GA$_4$-Glc was 0.51 when the concentration of Na-azide was 100 mM, and reduced to 0.41 and 0.29 when the concentration of Na-azide was increased to 200 and 400 mM, respectively. For Os3BGlu6 E178A, the k_{cat}/K_m of GA$_4$-Glc was not changed when the concentration of Na-azide increased to 400 mM from 200 mM.
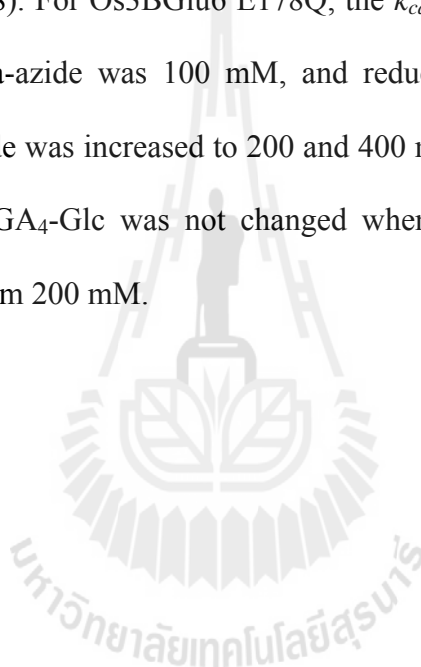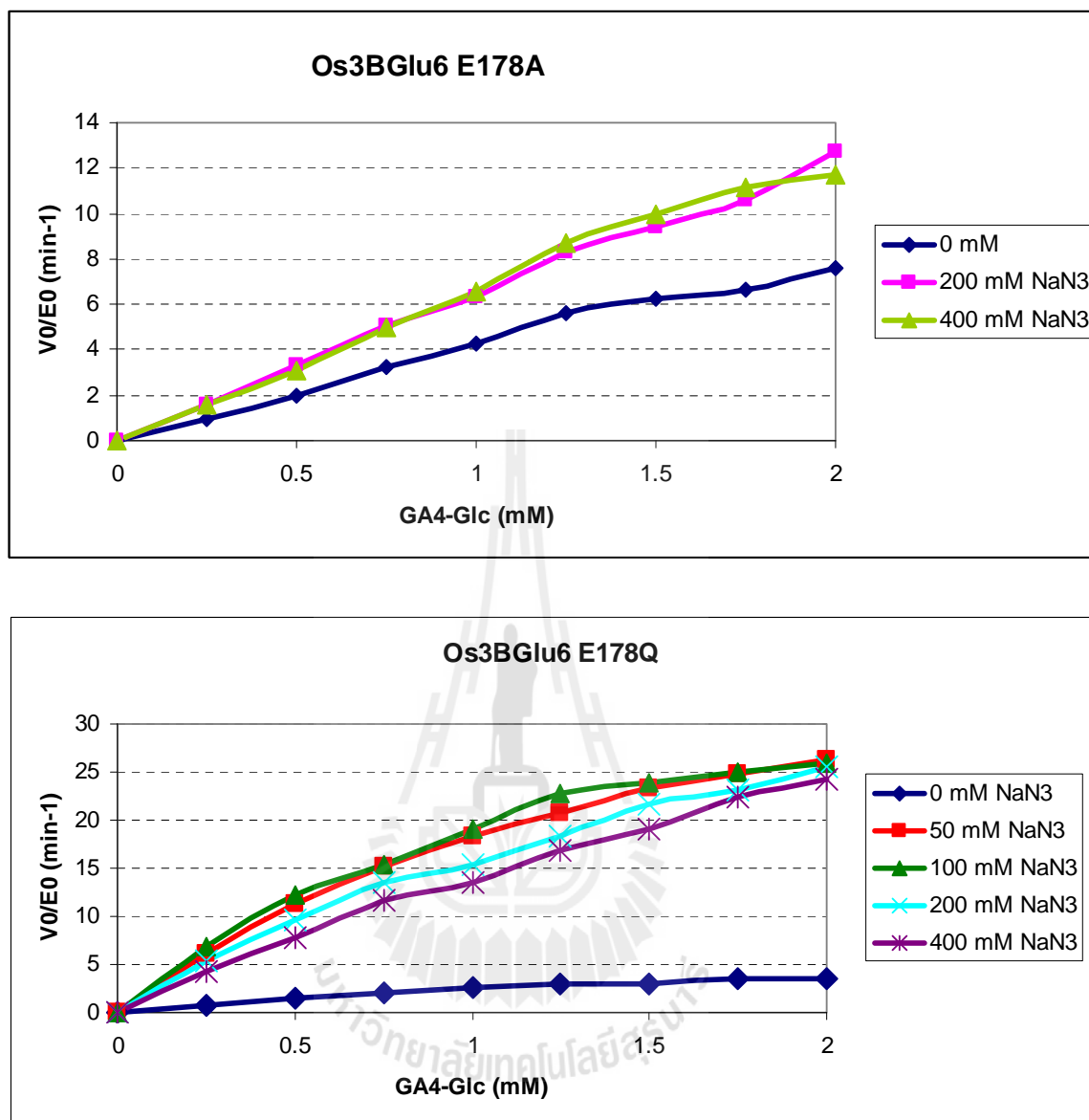
Figure 3.64 Reaction rates for transglucosylation of different concentrations of azide acceptor with GA_4-Glc donor by Os3BGlu6 acid/base mutants. Top, Os3BGlu6 E178A; bottom, Os3BGlu6 E178Q. The concentrations of donor GA_4-Glc were varied, while Na-azide was fixed at 50, 100, 200 and 400 mM, and reactions without Na-azide were used as controls. The reactions were performed in 50 mM MES, pH 5, at 30°C for 20 min. The turnover rates V_0/E_0 of GA_4 (μmole of GA_4 release per minute per μmole of enzyme) were calculated based on the areas of GA_4 HPLC peaks. The total area of GA_4 was used without subtracting hydrolysis product, since glucose was not readily detected when azide was present in the reaction.

Table 3.8 Transglucosylation kinetics of Os3BGlu6 E178Q and E178A for GA$_4$-Glc donor at various fixed concentrations of sodium azide acceptor.

Enzyme	Na-azide (mM)	K_m (mM)	k_{cat} (s^{-1})	k_{cat}/K_m (mM^{-1}s^{-1})
Os3BGlu6	0	0.09 ± 0.01	0.03 ± 0.001	0.33
E178Q	50	1.64 ± 0.15	0.81 ± 0.04	0.49
	100	1.69 ± 0.13	0.86 ± 0.04	0.51
	200	2.07 ± 0.31	0.84 ± 0.08	0.41
	400	3.97 ± 0.65	1.16 ± 0.14	0.29
Os3BGlu6	0	3.7 ± 0.4	0.09 ± 0.005	0.03
E178A	200	11.6	1.39	0.12
	400	13.36	1.56	0.12

The transglucosylation rates were calculated from the released GA$_4$ without subtracting hydrolysis product.

CHAPTER IV

DISCUSSION

4.1 Syntheses of Gibberellin Glucosyl Conjugates

Deacetylated GA$_4$-Glc and GA$_3$-Glc esters were synthesized with final yields of 40% and 10%, respectively. GA$_3$-OMe-3-O-Glc, GA$_3$-OMe-13-O-Glc and GA$_4$-OMe-Glc were synthesized with 3 steps; the final yields were less than 5% for all of them. GA$_3$-OMe-3-O-Glc and GA$_3$-OMe-13-O-Glc could not be separated by flash column chromatography, so they were separated by HPLC with multiple injections and manual collection, which was very time consuming. Furthermore, GA$_3$-OMe-3-O-Glc, GA$_3$-OMe-13-O-Glc and GA$_4$-OMe-Glc should be taken through one more reduction step to reduce -OMe to -OH, in order to obtain the natural substrates GA$_3$-3-O-Glc, GA$_3$-13-O-Glc and GA$_4$-Glc glucosides (Figure 1.5), and this reduction step is usually low yield. Therefore, it may be useful to explore an alternative synthesis method in the future.

Monitoring purification of β-glucosidase requires a lot of substrate, which must be custom synthesized for GA glucosyl conjugates. Considering the difficulty in synthesis of these conjugates and the fact that although GA$_4$ and its conjugates were discovered in rice, neither GA$_3$ nor its conjugates were found in rice (Tables 1.1 and 1.2), GA$_4$-Glc ester was chosen as the substrate to test the β-D-glucosidase activity. Therefore, I undertook purification of a β-glucosidase that can hydrolyze GA$_4$-Glc ester from rice.

4.2 Extraction, Purification and Characterization of β-glucosidase from Rice

Ten kilograms of 10-day rice seedling shoots and leaves were extracted and the crude proteins were purified with seven purification steps. pNPGlc and GA$_4$-Glc were used as substrates to test the β-D-glucosidase activities. Finally, 0.15 mg of protein was obtained, for which the specific activities to pNPGlc and GA$_4$-Glc were 10.9 and 0.14 μmol/min.mg, respectively. The purification of GA$_4$-Glc-hydrolyzing β-D-glucosidase was only 337 fold, which is quite low considering the low yield of the protein. The total activity of final protein was only 0.18% of the original protein. The purification work lasted one month and many steps had to be done at room temperature (25-30°C). During the purification, some of the enzyme molecules may have been degraded or lost their activity, which may be one main reason for the low purification yield. In addition, some isoenzymes that have GA$_4$-Glc ester hydrolyzing ability (many with lower specific activity than the purified protein) were likely to have been removed during the purification, resulting in a decrease in yield.

In the final protein, two major bands with size at approximately 60 kDa were observed in the 10% SDS-PAGE. They co-eluted in the SP cation exchange column at pH 5, octyl sepharose 4 hydrophobic interaction column and S200 gel filtration column. The final protein mix was submitted to two further purification attempts with SP Sephadex cation exchange chromatography in buffers at pH 5.5 and 6.0, respectively. The protein could not bind to the column at these two pH values; although previously they were bound to the SP column at pH 5.0. A Resource Q anion exchange column was also tested to see whether it could resolve the remaining bands. The column was eluted with a linear gradient of 0-1.0 M NaCl in 4-fold diluted McIlvaine buffer, pH 7 and pH 8, respectively, but the protein did not bind to the column at either pH.

The two major protein bands from the final purified protein fractions were identified by LCMS after tryptic digestion to peptides. The peptide mass results were used in a MASCOT search of the Genbank nr protein database. The peptide masses from the upper band matched a hypothetical protein OsI_23311 [*Oryza sativa* Indica Group] with the matching score of 851. The protein was predicted to have a molecular mass of 57,128 Da, and calculated pI of 8.67 for the precursor, including its signal peptide. The first 28 residues were predicted as a signal sequence in the precursor protein by SignalP 4.0 (Petersen et al., 2011); and 3 N-glycosylation sites at residues 33, 168 and 326 were predicted with NetNGlyc 1.0 (Gupta et al., 2004) in the amino acid sequence of the precursor protein (Figure 4.1).

```
  1 MAAAPMSFAF  TLLAACISFL  HHAPAAAAAA  PANQTAGFLD  CLAASLPAGV  VYTHASRSYQ
                                            ▲

 61 SVLESSIKNL  LFDTPATPTP  VAVVEATDAS  HVQAAVRCGV  GHGVSVRSRS  GGHDYEGLSY

121 RSLDAARAFA  VVDMAGGALR  AVRVDVRGRA  AWVGSGATLG  EVYYAIANKT  SRLGFPGSVG
                                                         ▲

181 PTVGVGGFLS  GGGFGLMLRK  HGLASDHVLD  ATMVDAKGRL  LDRAAMGEDL  FWAIRGGGGG

241 NFGIVLSWKL  RLVPVPATVT  VFTVHRSRNQ  SATDLLAKWQ  RVAPSLPSDA  FLRVVVQNQN

301 AQFESLYLGT  RAGLVAAMAD  AFPELNVTAS  DCIEMTWVQS  VLYFAFYGTG  KPPEMLLDRG
                                           ▲

361 TGRPDRYFKA  KSDYVQEPMP  SQVWETTWSW  LLKDGAGLLI LDPYGGEMAR  VAPAATPFPH

421 RQALYNIQYY  GFWSESGEAA AAKHMGWIRG VYGEMEPYVS KNPRGAYVNY RDLDLGVNDD

481 GGGVARARYE  KATVWGRAYF  KANFERLAAV  KAKVDPDNYF  KNEQSIPPLP S
```

Figure 4.1 The amino acid sequence of hypothetical protein OsI_23311 [*Oryza sativa* Indica Group]. The first 28 underlined residues compose a signal sequence; the closed triangles denote the predicted N-glycosylation sites.

The molecular mass and theoretical pI of the mature protein were predicted to be 54,150 Da and 8.74, respectively. Since this protein bound to the Con A column, it is likely to be glycosylated, which may easily account for its slightly larger apparent size of 60 kDa on the SDS-PAGE. Although this protein has a region homologous to an FAD binding domain, the function of this protein is not clear yet.

The peptide masses from the lower band matched the protein product from the Os04g0474900 gene locus [*Oryza sativa* Japonica Group], which corresponds to a GH1 β-glucosidase Os4BGlu13, with the matching score of 1006 and sequence coverage of 49%. This precursor protein was calculated to have a molecular mass of 57,386 Da and pI of 6.44 when its signal peptides were included. The first 25 residues were predicted to be a signal sequence (Figure 4.2) in the precursor protein by SignalP 4.0 (Petersen et al., 2011); the molecular mass and theoretical pI after the signal peptide was removed were predicted to be 54,761 Da and 6.66, respectively. Considering the fact that there are five putative N-linked glycosylation sites in the amino acid sequence of the precursor protein, this molecular mass matched the size seen in the 10% SDS-PAGE (Figure 3.40).

The β-D-glucosidase Os4BGlu13, also called OsTAGG1, was previously reported by Wakuta et al. (2010) as a β-D-glucosidase hydrolyzing tuberonic acid glucoside (TAG). The protein was purified from rice panicles by $(NH_4)_2SO_4$ fractionation and five different types of chromatography. The purified OsTAGG1 migrated as a single band on native PAGE, but was present as two polypeptides with molecular masses of 42 kDa and 26 kDa under denaturing conditions (Figure 4.3). They explained that the two apparent subunits were caused by proteolytic cleavage of the initial mature protein to produce two bands in SDS-PAGE, and they determined the two N-terminal sequences (Figure 4.2). The sum of the molecular masses of two polypeptides was 68 kDa, which is different from the predicted molecular mass of 55 kDa. This discrepancy was explained by authors as likely to be due to the fact that there are five N-linked glycosylation sites in the amino acid

sequence of the precursor protein, so the molecular size of the mature protein could be increased by addition of sugar chains.

```
   1  ATGGCAGCTGCAGGGGAAGTGGTGATGCTTGGTGGCATTCTCCTCCCTCTCCTCCTGGTTGTCGCCGTCTCCGGTGAGCCGCCGCCGATC
   1   M  A  A  A  G  E  V  V  M  L  G  G  I  L  L  P  L  L  L  V  V  A  V  S  G  E  P  P  P  I

  91  AGCCGGAGGAGCTTCCCCGAGGGGTTCATCTTCGGGACGGCCTCGTCGTCGTATCAGTATGAGGGTGGCGCCAGAGAGGGGGGCAGAGGA
  31   S  R  R  S  F  P  E  G  F  I  F  G  T  A  S  S  S  Y  Q  Y  E  G  G  A  R  E  G  G  R  G

 181  CCAAGCATCTGGGACACATTCACACACCAGCACCCAGATAAGATTGCTGACAAAAGCAATGGGACGTGGCTGCAGACTCCTACCATCTA
  61   P  S  I  W  D  T  F  T  H  Q  H  P  D  K  I  A  D  K  S  N  G  D  V  A  A  D  S  Y  H  L

 271  TACAAGGAAGATGTGCGCATCATGAAGGATATGGGAGTGGATGCATATAGGTTCTCCATCTCATGGACAAGAATTCTTCCAAATGGAAGT
  91   Y  K  E  D  V  R  I  M  K  D  M  G  V  D  A  Y  R  F  S  I  S  W  T  R  I  L  P (N) G  S

 361  CTGAGCGGTGGAATCAACAGAGAAGGCATCAGCTACTACAACAATTTGATCAATGAACTATTACTGAAAGGGGTGCAACCATTTGTTACC
 121   L  S  G  G  I  N  R  E  G  I  S  Y  Y  N  N  L  I  N  E  L  L  L  K  G  V  Q  P  F  V  T

 451  CTTTTCCACTGGGACTCGCCACAGGCATTAGAAGATAAATATAATGGATTTCTTAGCCCTAATATCATAAATGACTATAAGGAGTACGCT
 151   L  F  H  W  D  S  P  Q  A  L  E  D  K  Y  N  G  F  L  S  P  N  I  I  N  D  Y  K  E  Y  A

 541  GAAACCTGCTTCAAAGAGTTTGGTGACAGAGTGAAACATTGGATCACCTTCAATGAGCCTTTGAGCTTCTGTGTTGCGGGATATGCATCA
 181   E  T  C  F  K  E  F  G  D  R  V  K  H  W  I  T  F  N (E) P  L  S  F  C  V  A  G  Y  A  S

 631  GGTGGCATGTTTGCACCAGGCCGCTGTTCGCCTTGGGAGGGAAATTGCAGTGCTGGCGATTCAGGAAGGGAGCCTTACACCGCATGCCAT
 211   G  G  M  F  A  P  G  R  C  S  P  W  E  G (N) C  S  A  G  D  S  G  R  E  P  Y  T  A  C  H

 721  CATCAACTACTTGCTCATGCGGAAACTGTTCGGTTGTACAAAGAGAAATATCAGGTCTTACAAAAGGGGAAGATTGGAATAACTTTGGTC
 241   H  Q  L  L  A  H  A  E  T  V  R  L  Y  K  E  K  Y  Q  V  L  Q  K  G  K  I  G  I  T  L  V

 811  TCGAACTGGTTTGTTCCCTTCTCCCGCTCCAAATCCAACATCGATGCTGCAAGGCGTGCTTTAGACTTCATGCTTGGATGGTTTATGGAT
 271   S  N  W  F  V  P  F  S  R  S  K  S  N  I  D  A  A  R  R  A  L  D  F  M  L  G  W  F  M  D

 901  CCCCTAATTAGAGGCGAGTACCCCCTAAGCATGAGAGAATTGGTTCGGAATCGCTTGCCTCAGTTCACTAAAGAACAATCTGAGTTGATC
 301   P  L  I  R  G  E  Y  P  L  S  M  R  E  L  V  R  N  R  L  P  Q  F  T  K  E  Q  S  E  L  I

 991  AAGGGTTCATTCGATTTTATTGGACTTAATTACTACACTTCAAATTATGCTGGTAGCCTTCCTCCATCAAATGGCCTCAATAACAGCTAT
 331   K  G  S  F  D  F  I  G  L  N  Y  Y  T  S  N  Y  A  G  S  L  P  P  S  N  G  L (N) N  S  Y

1081  AGTACTGATGCTCGAGCTAATCTTACTGCTGTTCGAAACGGCATTCCCATAGGTCCTCAGGCTGCTTCGCCTTGGCTTTACATCTATCCT
 361   S  T  D  A  R  A (N) L  T  A  V  R  N  G  I  P  I  G  P  Q  A  A  S  P  W  L  Y  I  Y  P

1171  CAAGGGGTTCCGTGAATTGGTGCTTTATGTTAAGGAAAACTATGGCAATCCTACCATCTACATCACCGAAAATGGTGTTGATGAATTCAAC
 391   Q  G  F  R  E  L  V  L  Y  V  K  E  N  Y  G  N  P  T  I  Y  I  T (E) N  G  V  D  E  F  N

1261  AATAAGACCTTACCACTCCAGGAAGCCTTGAAGGATGACACTAGAATAGATTACTACCACAAGCACCTCCTTTCACTGCTAAGTGCAATA
 421  (N) K  T  L  P  L  Q  E  A  L  K  D  D  T  R  I  D  Y  Y  H  K  H  L  L  S  L  L  S  A  I

1351  AGGGACGGAGCAAATGTGAAGGGATACTTTGCATGGTCGCTGCTTGATAACTTCGAGTGGTCGAACGGCTATACTGTTCGCTTTGGGATA
 451   R  D  G  A  N  V  K  G  Y  F  A  W  S  L  L  D  N  F  E  W  S  N  G  Y  T  V  R  F  G  I

1441  AACTTTGTGGATTACAATGACGGAGCGAAGAGATACCCCAAAATGTCTGCCCATTGGTTCAAGGAGTTCCTCCAGAAGTGA
 481   N  F  V  D  Y  N  D  G  A  K  R  Y  P  K  M  S  A  H  W  F  K  E  F  L  Q  K  *
```

Figure 4.2 Nucleotide and deduced amino acid sequences of the cDNA encoding OsTAGG1 (Os4BGlu13). The circles and triangles denote the catalytic and sugar-binding residues that are highly conserved in GH1, respectively. The sequences corresponding to the N-terminal sequences of large and small subunits of purified OsTAGG1 (Figure 4.3) on SDS-PAGE are underlined. The circled highlighted residues are predicted N-glycosylation sites (figure from Wakuta et al., 2010).
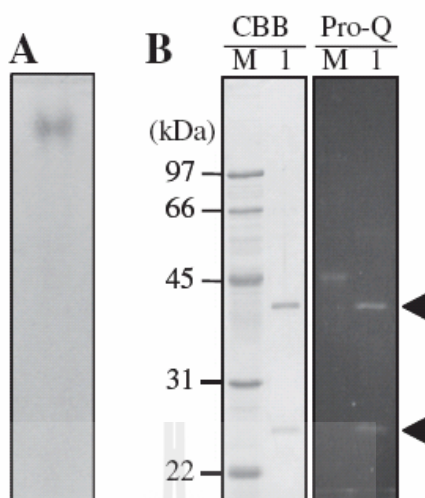
Figure 4.3 SDS–PAGE and native PAGE of purified OsTAGG1. (A) OsTAGG1 was loaded on 10% polyacrylamide and Coomassie brilliant blue (CBB)-stained native PAGE gels. (B) Total protein was stained with CBB (left panel) and Pro-Q emerald for glycoprotein detection (right panel). The arrow shows the 42- and 26-kDa polypeptides that match with β-glucosidase (AK070962) according to N-terminal amino acid and tryptic peptide MALDI-TOF MS analyses (figure from Wakuta et al., 2010).

The conclusion for this section is that β-D-glucosidase Os4BGlu13 was purified from rice seedling shoots and leaves, but with approximate 50% purity. This protein could hydrolyze GA_4-Glc to release GA_4, and also hydrolyze TAG to release TA with high activity. Our purification method produced the same protein as Wakuta et al. (2010), but with different molecular size, as judged by SDS-PAGE. From our purification, we observed a single protein band on SDS-PAGE, but Wakuta et al. reported two bands on SDS-PAGE. Our enzyme was extracted from 10-day old rice seeding shoots and leaves, while Wakuta's enzyme was extracted from rice panicles during grain filling. So, the different tissue sources may be the main cause for obtaining two different molecular sizes for the same mature protein, if the protein undergoes proteolytic processing in the panicle that does not occur in the seedling shoots and leaves, and different levels of glycosylation

occur in the different tissues. Since different purification methods were used, Wakuta's protein may have been proteolytically cleaved during the purification, while this proteolysis did not occur in the current work.

4.3 Hydrolysis of GA$_4$-Glc by Os3BGlu6 and Its Mutants

Five rice GH1 enzymes that have been expressed in our lab, Os3BGlu6, Os3BGlu7, Os4BGlu12, Os3BGlu18 and Os9BGlu31, were tested for the hydrolysis of pNPGlc and GA$_4$-Glc (Table 3.4). Os3BGlu6 was found to have the highest hydrolysis activity to GA$_4$-Glc among these enzymes. Although Os4BGlu12 could hydrolyze pNPGlc with high activity, its hydrolysis activity toward GA$_4$-Glc was only 20% that of Os3BGlu6. Since Os4BGlu12 is the isoenzyme most closely related to Os4BGlu13, which was identified as the GA$_4$-Glc β-glucosidase purified from the plant, this was a little surprising. Therefore, Os3BGlu6 hydrolyzes GA$_4$-Glc better and with a higher preference than Os4BGlu12 and other rice GH1 β-D-glucosidases, such as Os3BGlu7. We have not expressed Os4BGlu13 in the same system, so it is difficult to compare Os3BGlu6 and Os4BGlu13.

Although much characterization has been done for the hydrolysis kinetics of alkyl and aryl glycosides and oligosaccharides by β-D-glucosidases and their catalytic acid/base and nucleophile mutants (Wang et al., 1994, 1995; Mackenzie et al., 1998; Chuenchor et al., 2011), little or no description of glucosyl ester hydrolysis is available in the literature. Since Os3BGlu6 was identified as a β-D-glucosidase with relatively high ability to hydrolyze GA$_4$-Glc ester, it serves as a good model for investigation of β-glucosidic hydrolysis of glucosyl esters. It might be expected that the relatively low pK_a of the leaving group would make the glucosyl ester relatively insensitive to the presence of a catalytic acid for the initial glycosylation step, similar to 2,4-dinitrophenyl glycosides, but

other influences of having the ester bond in apposition to the glycosidic bond are not so clear. In order to study the properties of glucosyl ester hydrolysis and glucosyl transfer by a β-glucosidase, the wild type rice Os3BGlu6 and its catalytic acid/base mutants E178Q and E178A were expressed and purified, and their optimum pH and activities for hydrolysis of GA$_4$-Glc and pNPGlc were compared. The Os3BGlu6 active site cleft mutant M251N, which was previously created in our laboratory to improve hydrolysis of cellooligosaccharides by Os3BGlu6 (Sansenya et al., 2012), was also tested. The activity of two catalytic nucleophile mutants developed for possible production of Os3BGlu6 GA$_4$-Glc ester complexes for structural analysis, E394D and E394Q, were also tested, since loss of the nucleophile is expected to greatly decrease the enzyme activity regardless of the substrate, as described by Wang et al. (1994).

The Os3BGlu6 wild type and M251N mutant were found to have high pNPGlc hydrolysis activity between pH 4.0 and 5.0; and Os3BGlu6 wild type and its M251N, E178Q and E178A mutants also showed highest GA$_4$-Glc hydrolytic activities at pH 4.5. This optimum pH is in the range of commonly seen in plant β–glucosidases (Esen, 1993) and agreed with the previously reported pH optimum for wild type Os3BGlu6 (Seshadri et al., 2009). When hydrolyzing pNPGlc, the activity of Os3BGlu6 wild type and M251N quickly dropped above pH 5.5 (Figure 3.49). In contrast, the Os3BGlu6 E178Q, E178A, E394D and E394Q mutants had less than 1% of wildtype activity toward pNPGlc. Although the catalytic nucleophile mutants had little activity to GA$_4$-Glc as well, the activities of Os3BGlu6 E178Q and E178A were significant and dropped slowly above pH 6.0 when hydrolyzing GA$_4$-Glc, compared to wild type Os3BGlu6 and Os3BGlu6 M251N. The pH dependence of enzymatic reactions is generally considered to reflect ionizations of acid/base groups involved in catalysis (Kempton and Withers, 1992; McIntoch et al., 1996). The residue E178 in Os3BGlu6 acts as a general acid catalyst to protonate the glycosidic oxygen during the enzyme glycosylation step, and then as a

general base to deprotonate the attacking water during deglycosylation. The dual role of E178 places specific demands upon its ionization states, which has been seen for E172 in *Bacillus circulans* xylanase in McIntoch's work (1996). For Os3BGlu6 E178Q and E178A, the glutamate residue was mutated to glutamine and alanine, so the pH had no effect on ionization of the sidechain and its effect on the hydrolysis was reduced. This is why the activities of Os3BGlu6 E178Q and E178A were not very sensitive to the pH compared to Os3BGlu6 wild type and M251N when hydrolyzing GA_4-Glc.

The structures of the Os3BGlu6 apo enzyme, its complexes with 2-deoxy-2-fluoro glucoside and n-octyl-β-D-thioglucoside have been solved by X-ray crystallography (Figure 1.18, Seshadri et al., 2009). In the active site, E178 and E394 were positioned as the two catalytic residues. M251 was located at the mouth of active site cleft and appeared to block the binding of extended β-(1/4)-linked oligosaccharides and interact with the hydrophobic aglycone of n-octyl-β-D-thioglucopyranoside. A few nonpolar aromatic residues W366, W133 and F460 were located around the cleft. This correlates with the preference of Os3BGlu6 for short oligosaccharides and hydrophobic glycosides. Mutation of Os3BGlu6 Met251 to Asn resulted in a 15-fold increased k_{cat}/K_m value for hydrolysis of laminaribiose compared to wild type Os3BGlu6 and 9 to 24-fold increases for cellooligo-saccharides with degrees of polymerization (DP) of 2-5 (Sansenya et al., 2012). These results indicated that conversion of Met to Asn could generate an oligosaccharide binding subsite in Os3BGlu6, and increase its hydrolytic activity for oligosaccharide. In our study, the Os3BGlu6 M251N mutant showed reduced hydrolytic activities for pNPGlc and GA_4-Glc compared to its wild type. The relative activities of M251N compared to wildtype Os3BGlu6 were 51.6% for pNPGlc and 88.9% for GA_4-Glc, while the catalytic efficiencies (k_{cat}/K_m) for M251N were reduced to 2.6 from 6.2 mM^{-1}s^{-1} for pNPGlc, 0.08 from 0.13 for GA_4-Glc compared to wild type. The K_m to pNPGlc for both Os3BGlu6 and Os3BGlu6 M251N is almost the same; the smaller k_{cat} of Os3BGlu6 M251N is the main

cause for its lower k_{cat}/K_m compared to the wild type. This suggested that the two enzymes' affinities for pNPGlc are similar in the binding substrate step due to the smaller size of pNPGlc, which would not reach to the M251 residue from a position with it glycosidic bond in position for hydrolysis, but Os3BGlu6 M251N has lower k_{cat} than Os3BGlu6. In contrast, for GA$_4$-Glc, the higher K_m for Os3BGlu6 M251N is the main reason for its lower k_{cat}/K_m compared to the wild type. This suggested that N251 residue in Os3BGlu6 M251N reduced the affinity to GA$_4$-Glc due to the bulky size of the GA$_4$-Glc and the polarity of N251 residue. The higher K_m of Os3BGlu6 M251N led to its lower k_{cat}/K_m. This suggests that Met251 functions to stabilize hydrophobic aglycones of these substrates in the reaction processing.

The generally accepted catalytic mechanism of family 1 glycoside hydrolase was confirmed for Os3BGlu6 in this work. As with other GH Clan A families, GH1 enzymes act through a retaining mechanism, utilizing one conserved glutamate residue as a catalytic acid/base and a second as a nucleophile or base (Rye and Withers, 2000). The two-step mechanism with a covalent enzyme-α-glucoside intermediate (Figure 4.4) has been supported by the demonstration of covalent intermediates of 2-F-glucosides (Withers et al., 1990) and natural glucoside with an acid/base mutant (Noguchi et al., 2008). In the glycosylation step, the catalytic nucleophile of the enzyme displaces the aglycone with general acid-assistance from the catalytic acid/base to form the intermediate. The deglycosylation step is the reverse of the first step, with water or another nucleophile attacking from the opposite side, with basic assistance from the catalytic acid/base, to displace the enzyme from the glycone. If the displacing nucleophile is water, hydrolysis results; whereas with other nucleophiles, transglycosylation results. In our study, the mutation of the glutamate at residue 178 to alanine (E178A) and glutamine (E178Q) led to complete loss of hydrolytic activity toward pNPGlc; and the relative activities to GA$_4$-Glc were reduced to 22.2% and 12.5%, respectively, compared to its wild type. The mutation

of glutamate residue 394 to glutamine (E394Q) and aspartic acid (E394D) led to complete

loss of hydrolytic activity toward pNPGlc and GA$_4$-Glc. These data support the

identification of E178 as the acid/base catalyst and E394 as a nucleophile in the process.

Since the pK$_a$ of GA$_4$ and pNP are 4.3 and 7.2, respectively, the -COO attached on GA$_4$ is

a better leaving group than p-nitrophenolate (pNP). Without acid-assistance from residue

E178, pNP could not be released, so Os3BGlu6 E178A and Os3BGlu6 E78Q could not

hydrolyze pNPGlc. Without residue E178, the GA$_4$ will be released less in the

glycosylation step without general acid-assistance, and the water molecule cannot be

deprotonated in the deglycosylation step, so Os3BGlu6 E178A and Os3BGlu6 E78Q kept

partial activity to GA$_4$-Glc compared to their wild type.
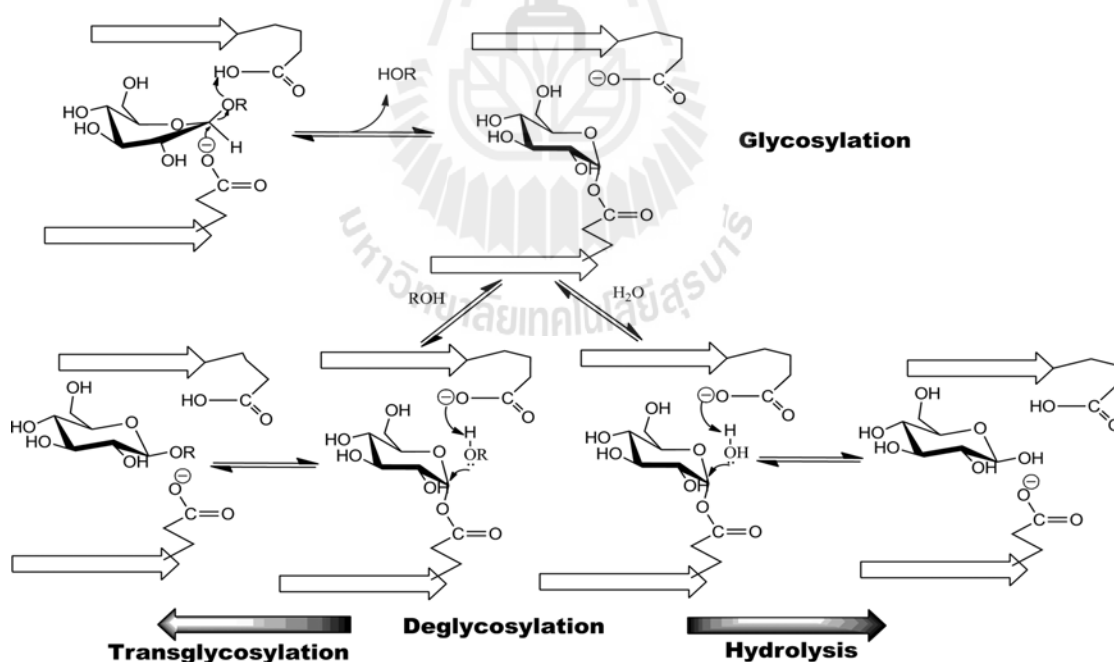
Figure 4.4 Double displacement mechanism proposed for retaining β-glycosidases, such

as those in glycoside hydrolase family 1. The first step of glycosylation is shown in the

top row, which forms a semi-stable glycosyl enzyme intermediate. The deglycosylation

step in the bottom row is split into hydrolysis to the right and transglycosylation to the

left, depending on whether water or another nucleophile acts as the acceptor substrate

(from Ketudat Cairns et al., 2012).

The transglucosylation activities were discovered for Os3BGlu6 E178Q and Os3BGlu6 E178A. Wild type Os3BGlu6 and Os3BGlu6 M251N hydrolyzed pNPGlc in MES buffer to pNP and glucose only, and no transglucosylation products were formed when GA_4 and azide were added as acceptors. For Os3BGlu6 E178Q and E178A, when pNPGlc or GA_4-Glc ester was used as donor and sodium azide as acceptor, both could produce transglucosylation products. Without sodium azide, only hydrolysis products were observed, while with sodium azide, the transglucosylation product β-glucosyl azide was the main product. This indicates that hydrolysis and transglucosylation are two competing reactions and that the strong nucleophile sodium azide is better at displacing the enzyme from the glycone in the absence of a catalytic base.

The transglucosylation kinetics were also studied for the acid/base mutants of Os3BGlu6. The activity versus pH profiles for transglucosylation of azide with GA_4-Glc donor were determined in NaOAc and MES buffers. For the Os3BGlu6 E178Q mutant, its optimum pH range was 5.0 to 6.0 in both buffers, slightly higher than its optimum pH for hydrolysis of GA_4-Glc. The E178A mutant showed a different pattern. Its transglucosylation activity was high at pH 5 in the MES buffer, but high at pH 4.0 in the NaOAc buffer. In the NaOAc buffer, the GA_4 releasing activity of the E178A was much higher than the one in MES buffer, even without azide in the system. This indicated that acetate could act as a nucleophile or substitute acid/base to rescue the hydrolysis activity. The work of Wang et al. (1995) also showed that the rate of hydrolysis of 2,4-dinitrophenyl β-D-glucopyranoside (2,4-DNPG) by the *Agrobacterium* β-glucosidase acid/base mutant AbgE178G could be increased by nucleophiles, such as azide, acetate, formate, benzoate, and thiophenyl to 292, 159, 150, 67 and 15 fold, respectively, compared to the reaction without nucleophile present. This is also one reason why we selected MES buffer for the transglucosylation kinetic studies instead of acetate and McIlvaine buffer, to avoid rescue of the cleavage activity by nucleophiles from the buffer.

When the transglucosylation activities of Os3BGlu6 E178Q and Os3BGlu6 E178A were compared with GA$_4$-Glc donor fixed at 2 mM and varying concentrations of sodium azide as acceptor, the k_{cat}/K_m values for Os3BGlu6 E178Q and Os3BGlu6 E178A were 0.13 and 0.066 mM^{-1}s^{-1}, respectively. These indicate that the polar glutamine at residue 178 in Os3BGlu6 E178Q supported transglycosylation by azide better than the nonpolar alanine residue at the same position in Os3BGlu6 E178A. Since the k_{cat}/K_m value is generally thought to reflect the first covalent step, the energy of glycosyl enzyme intermediate formation at the glycosylation step (Figure 4.4) is lower for Os3BGlu6 E178Q than Os3BGlu6 E178A, likely due to hydrogen bonding to the leaving group.

Another phenomenon is that the transglucosylation turnover rate, V_0/E_0, of GA$_4$ was increased very significantly as the concentration of azide was increased. The maximum of V_0/E_0 for Os3BGlu6 E178Q was seen at 100 mM of azide, and this specific activity gradually decreased when the concentration of azide increased further. In contrast, for Os3BGlu6 E178A, this inhibition was observed when the concentration of azide reached 400 mM. The rate increase with increasing concentration of azide was also observed by Wang et al. (1995). They concluded that addition of azide as a competitive nucleophile increased k_{cat} values 100-300 fold for substrates whose rate-limiting step is deglycosylation, but had no effect on the wild type enzyme. For the hydrolysis of GA$_4$-Glc with Os3BGlu6 E178Q and Os3BGlu6 E178A, the rate-limiting step is deglycosylation. As the concentration of azide is increased, the rate of deglycosylation increases, until glycosylation becomes rate determining. The inhibition of transglucosylation of Os3BGlu6 E178Q by high concentrations of azide might be due to the high concentrations of azide interfering with the nucleophile E394 in the process of attacking the anomeric carbon during glycosylation, thus reducing the reaction rate. Actually, high concentrations of azide were also observed to inhibit hydrolysis of GA$_4$-Glc by wild type Os3BGlu6.

4.4 Comparison of the Protein Structures and Substrate Binding for Os3BGlu6, Os3BGlu7, Os4BGlu12 and Os4BGlu13

To study the relationship between the protein's structure and their substrate binding, the amino acid sequences of Os3BGlu6, Os3BGlu7 and Os4BGlu12 were aligned with Os4BGlu13. The alignment results (Figure 4.5) show that Os4BGlu12 and Os4BGlu13 have 85% identity; Os3BGlu6 and Os3BGlu7 have 49% identity with Os4BGlu13. The identity between Os3BGlu6 and Os3BGlu7 is also 49%.

```
Os4Bglu13    YRFSISWTRILPNGSLSGGINREGISYYNNLINELLLKGVQPFVTLFHWDSPQALEDKYN 165
Os4Bglu12    YRFSISWTRILPNGSLRGGVNKEGIKYYNNLINELLSKGVQPFITLFHWDSPQALEDKYN 169
Os3Bglu6     YRFSIAWSRIYPNG--VGQVNQAGIDHYNKLIDALLAKGIQPYVTLYHWDLPQALEDKYK 177
Os3Bglu7     YRFSISWSRIFPDG--EGRVNQEGVAYYNNLINYLLQKGITPYVNLYHYDLPLALEKKYG 170
             *****:*:** *:*   * :*: *: :**:**: ** **: *::.*:*:* * ***.**

Os4Bglu13    GFLSPNIINDYKEYAETCFKEFGDRVKHWITFNEPLSFCVAGYASGGMFAPGRCSPWE-G 224
Os4Bglu12    GFLSPNIINDFKDYAEICFKEFGDRVKNWITFNEPWIFCSNGYATG-LFAPGRCSPWEKG 228
Os3Bglu6     GWLDRQIVDDFAAYAETCFREFGDRVKHWITLNEPHIVAIQGYDAG-LQAPGRCSVLLHL 236
Os3Bglu7     GWLNAKMADLFTEYADFCFKTFGNRVKHWFTFNEPRIVALLGYDQG-TNPPKRCTKCA-- 227
             *:*. :: : :  **: **: **:***:*:.:**** ..   ** *   .* **:

Os4Bglu13    NCSAGDSGREPYTACHHQLLAHAETVRLYKEKYQVLQKGKIGITLVSNWFVPFSRSKSNI 284
Os4Bglu12    NCSVGDSGREPYTACHHQLLAHAETVRLYKAKYQALQKGKIGITLVSHWFVPFSRSKSND 288
Os3Bglu6     YCKAGNSGTEPYVVAHHFILAHAAAASIYRTKYKATQNGQLGIAFDVMWFEPMSNTTIDI 296
Os3Bglu7     --AGGNSATEPYIVAHNFLLSHAAAVARYRTKYQAAQQGKVGIVLDFNWYEALSNSTEDQ 285
               *:*. ***.***:  ** *.*:** .  :* **: *:*::**.:  *: .:*.:. :

Os4Bglu13    DAARRALDFMLGWFMDPLIRGEYPLSMRELVRNRLPQFTKEQSELIKGSFDFIGLNYYTS 344
Os4Bglu12    DAAKRAIDFMFGWFMDPLIRGDYPLSMRGLVGNRLPQFTKEQSKLVKGAFDFIGLNYYTA 348
Os3Bglu6     EAAKRAQEFQLGWFADPFFFGDYPATMRARVGERLPRFTADEAAVKGALDFVGINHYTT 356
Os3Bglu7     AAAQRARDFHIGWYLDPLINGHYPQIMQDLVKDRLPKFTPEQARLVKGSADYIGINQYTA 345
             **:** :* :**: **:: *.** *:  * :***:** ::: ::**: *::*:* **:

Os4Bglu13    NYAGSLPP---SNGLNNSYSTDARANLTAVRNGIPIGPQAASPWLYIYPQGFRELVLYVK 401
Os4Bglu12    NYADNLPP---SNGLNNSYTTDSRANLTGVRNGIPIGPQAASPWLYVYPQGFRDLLLYVK 405
Os3Bglu6     YYTRHNNTNIIGTLLNNTLADTGTVSLP-FKNGKPIGDRANSIWLYIVPRGMRSLMNYVK 415
Os3Bglu7     SYMKGQQL---MQQTPTSYSADWQVTYVFAKNGKPIGPQANSNWLYIVPWGMYGCVNYIK 402
             *           .: :    ..    :** *** :* * ***: * *:   : *:*

Os4Bglu13    ENYGNPTIYITENGVDEFNNKTLPLQEALKDDTRIDYYHKHLLSLLSAIR-DGANVKGYF 460
Os4Bglu12    ENYGNPTVYITENGVDEFNNKTLPLQEALKDDARIEYYHKHLLSLLSAIR-DGANVKGYF 464
Os3Bglu6     ERYNSPPVYITENGMDDSNNPFISIKDALKDSKRIKYHNDYLTNLAASIKEDGCDVRGYF 475
Os3Bglu7     QKYGNPTVITENGMDQPAN--LSRDQYLRDTTRVHFYRSYLTQLKKAID-EGANVAGYF 459
             :.*..*.:*:  ***** *:  *  :. .: *:*  *:.::..:* .*  :*  :*.:* ***
```

Figure 4.5 Sequence alignment for four rice β-glycosidases, Os3BGlu6, Os3BGlu7, Os4BGlu12 and Os4BGlu13 with Clustal 2.1 software. Only portions of each polypeptide are shown. The regions surrounding the two catalytic amino acids are boxed in rectangles.

The sequence alignment of four β-glycosidases showed that there are two conserved amino acid residue regions near the catalytic amino acids, one is T(F/L)NEP, another one is ITENG (Figure 4.5). The glutamate residues at positions 199 and 413 (Os4BGlu13 numbering) were predicted to be the acid-base catalyst and catalytic nucleophile, respectively, based on previous studies on Os3BGlu6 (Seshadri et al., 2009), Os3BGlu7 (Opassiri et al., 2003) and Os4BGlu12 (Sansenya et al., 2011). Though Os4BGlu12 and Os4BGlu13 have 85% amino acid sequence identity, these two enzymes have shown different specific activity, especially to GA_4-Glc ester. The ratio of hydrolysis activities to GA_4-Glc and pNPGlc for partially purified Os4BGlu13 (approximately 50% purity from SDS-PAGE) was 0.01, for Os4BGlu12 was 0.0003, for Os3BGlu6 was 0.07, and for Os3BGlu7 (BGlu1) was 0.005, respectively. These indicated that for the hydrolysis of GA_4-Glc, Os4BGlu13 and Os3BGlu6 are much better than Os4BGlu12 and Os3BGlu7. In contrast, for the hydrolysis of pNPGlc, Os4BGlu12 is the best enzyme among the four enzymes.

By comparing the active sites of Os3BGlu6, Os4BGlu12, and Os4BGlu13 (Figure 4.6), we can see that the residues at the -1 site are well conserved for the three enzymes, but the residues at the +1 and +2 sites are different. For Os4BGlu12 (shown with green carbons), two residues at the +2 site, W181 and H252, are bulkier and occupy more space than the residues at the same positions in Os3BGlu6 and Os4BGlu13, so they may lead to a smaller binding cleft. This may have resulted in poor binding of GA_4-Glc for Os4BGlu12, so that it was hydrolyzed poorly. Since pNPGlc is relatively small in size and the interactions between the aromatic residues in the active site and pNP ring favored the binding, the binding to pNPGlc for Os4BGlu12 may be the best among the three enzymes, resulting in its high ratio of hydrolysis of pNPGlc comparing to GA_4-Glc. In contrast, the binding clefts within Os4BGlu13 and Os3BGlu6 are likely bigger than Os4BGlu12 which may make it is easier for GA_4-Glc to bind at the binding cleft, so Os4BGlu13 and

Os3BGlu6 were found to have higher hydrolysis activity toward GA$_4$-Glc relative to pNPGlc, compared to the other enzymes.
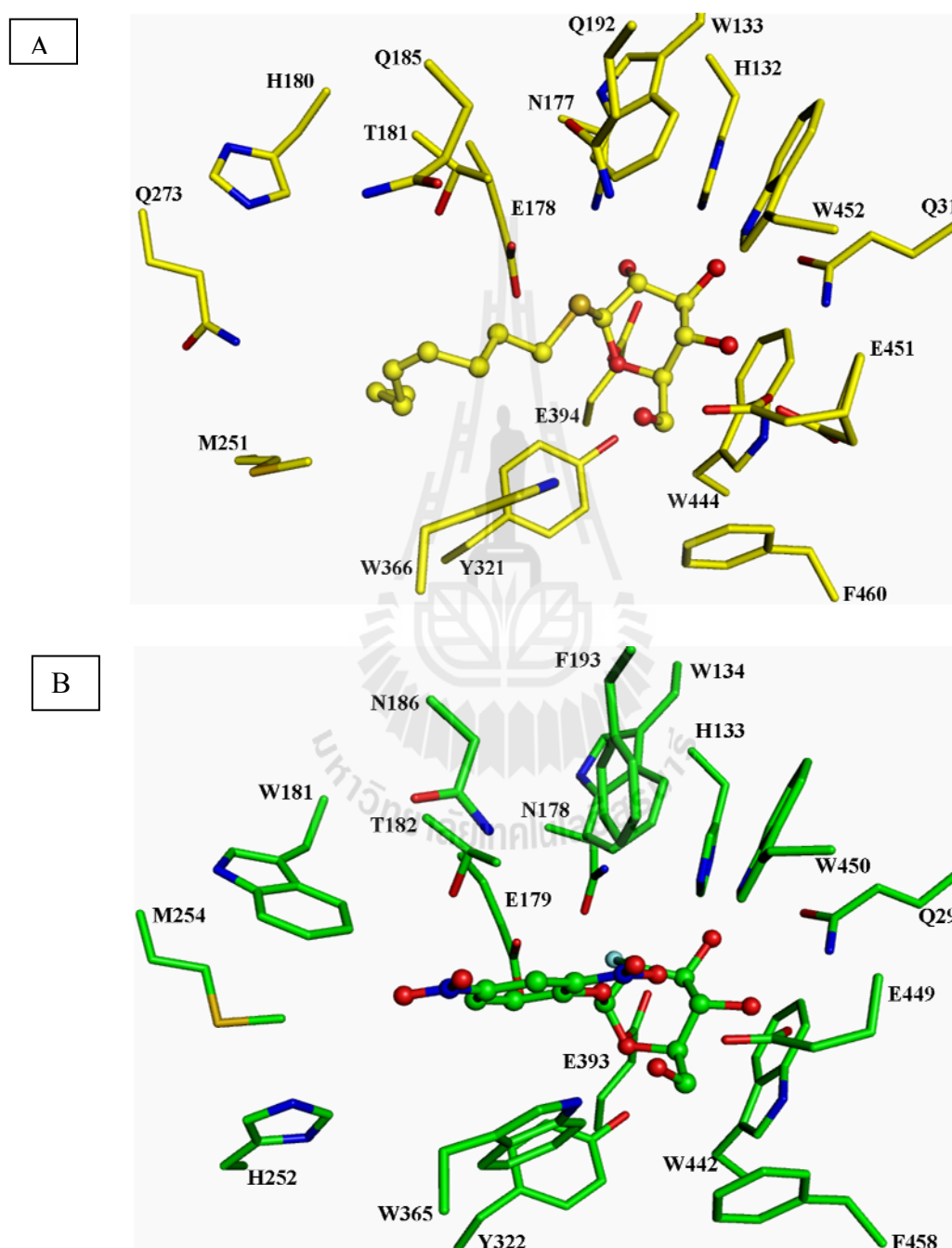
Figure 4.6 Comparison of the active sites of Os3BGlu6, Os4BGlu12 and Os4BGlu13.

(A) The active site of the Os3BGlu6/n-octyl-β-D-thioglucopyranoside complex structure (PDB code 3GNP_A). **(B)** The active site of Os4BGlu12 with DNP2FG (PDB code 3PTQ_B).
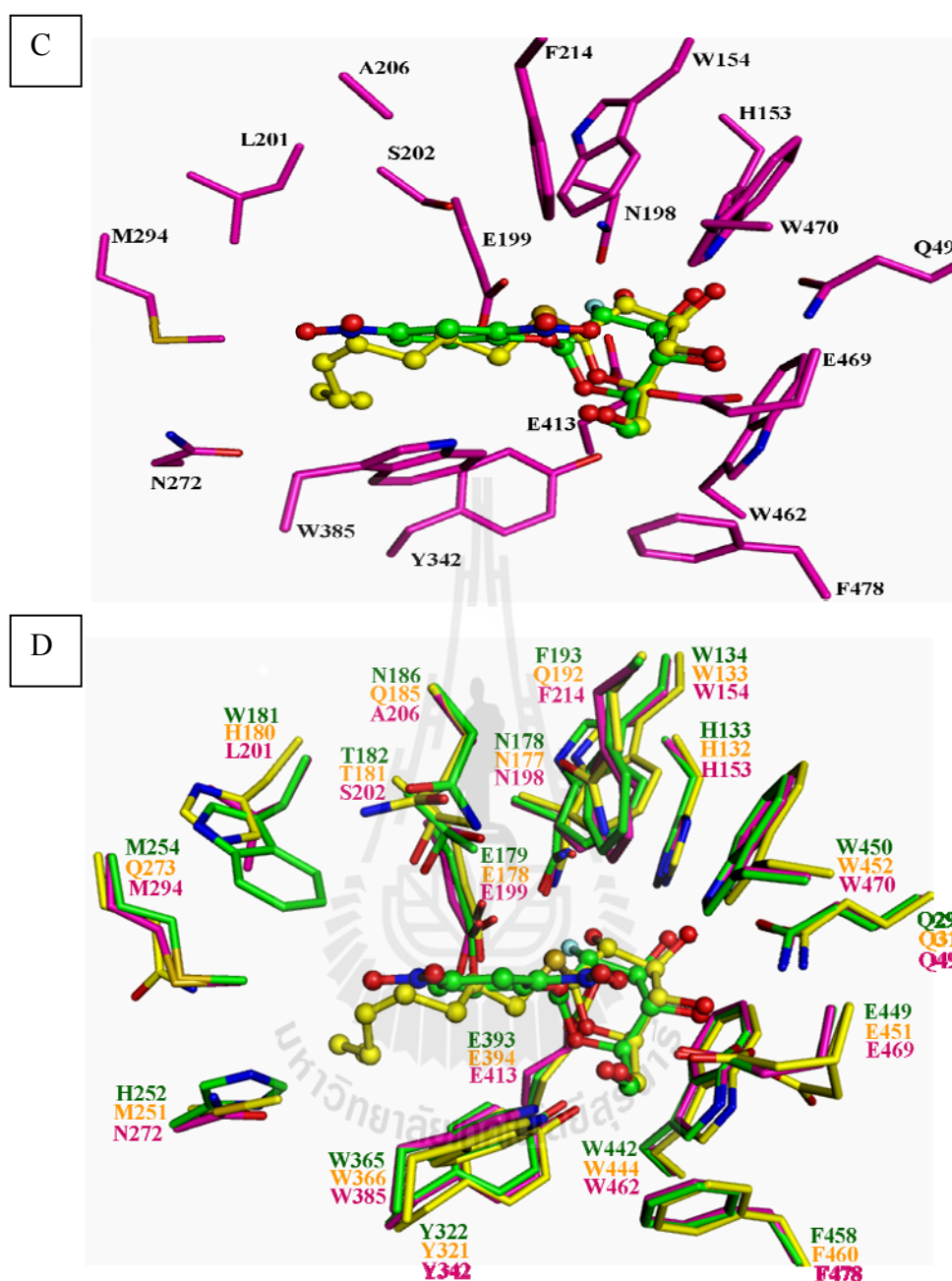
Figure 4.6 (Continued) (C) The superimposition of the active site of a homology model of Os4BGlu13 with DNP2FG from the Os4BGlu12 complex structure (PDB code 3PTQ_B) & n-octyl-β-D-thioglucopyranoside from the Os3BGlu6 complex structure (PDB code 3GNP_A). **(D)** The superimposition of the active sites of the Os3BGlu6 complex with n-octyl-β-D-thiogluco-pyranoside, the Os4BGlu12 complex with DNP2FG and the Os4BGlu13 homology model. The residues with green carbons are from Os4BGlu12, those with yellow carbons are from Os3BGlu6, and those with pink carbons are from Os4BGlu13. The figures were generated by Pymol (Schrödinger LLC).

This section suggested that the amino acid residues around binding cleft are very important for the substrate binding; the charge, the polarity and the sizes of the amino acid residues all contribute to the enzyme's substrate specificity.

CHAPTER V

CONCLUSIONS

Nine GA conjugates, which included acetylated and deacetylated GA_4-Glc esters, acetylated and deacetylated GA_3-Glc esters, GA_4-OMe, GA_3-OMe, GA_3-OMe-3-O-Glc, GA_3-OMe-13-O-Glc and GA_4-OMe-Glc were synthesized following the published methods or with modification. Their structures were identified with ^{1}H and gCOSY NMR and LC-MS spectrometry. The β-configuration of the H1 on the glucosyl ring were confirmed with the coupling constant of H1 ($J_{2,1}$ = approx. 8 Hz) for all glucosyl conjugates.

Ten kilograms of 10-day rice seedling shoots and leaves were extracted and the crude proteins were purified with seven purification steps. pNPGlc and GA_4-Glc were used as substrates to test the β-D-glucosidase activities. Finally, 0.15 mg of protein was obtained, and this protein contained two major bands seen on 10% SDS-PAGE. The LC-MS analysis of these two bands after trypsin digestion indicated one protein was Os4BGlu13 β-glucosidase, the product of the Os04g074900 gene locus, which belongs to glycoside hydrolase family 1, while the other one was OsI_23311, a putative FAD binding protein.

Five rice GH1 enzymes that have been expressed in our lab, Os3BGlu6, Os3BGlu7 (BGlu1), Os4BGlu12, Os3BGlu18 and Os9BGlu31 were tested for the hydrolysis of pNPGlc and GA_4-Glc. Os3BGlu6 was found to have the highest hydrolysis activity to GA_4-Glc among these enzymes. The activity of Os4BGlu12 to hydrolyze pNPGlc was 50 times higher than Os3BGlu6, but the activity to hydrolyze GA_4-Glc of Os4BGlu12 was

only 20% of that of Os3BGlu6.

The wild type rice Os3BGlu6 and its mutants M251N, E178A and E178Q were expressed in *Escherichia coli* strain Origami (DE3) as fusion proteins with N-terminal thioredoxin and His$_6$ tags, and purified with 2 steps of IMAC. The proteins after the 2nd IMAC were seen as single bands and their purities were higher than 90%. The purified proteins were characterized by determination of their pH optima for hydrolysis of *p*NPGlc and GA$_4$-Glc. The Os3BGlu6 wild type and M251N mutant were found to have high *p*NPGlc hydrolysis activity between pH 4.0 and 5.0, with highest value at pH 4.5, while the activity quickly dropped above pH 5.5. The Os3BGlu6 E178A and E178Q mutants showed little or no hydrolysis of *p*NPGlc. With GA$_4$-Glc substrate, Os3BGlu6 wild type and M251N, E178Q and E178A mutants also showed highest hydrolytic activities at pH 4.5. The activities of Os3BGlu6 E178Q and E178A dropped slowly above pH 6.0 compared to Os3BGlu6 wild type and M251N mutant, when hydrolyzing GA$_4$-Glc.

The activities of Os3BGlu6 wild type and its mutants to hydrolyze *p*NPGlc and GA$_4$-Glc were analyzed. The Os3BGlu6 M251N mutant showed reduced hydrolytic activities for *p*NPGlc and GA$_4$-Glc compared to its wild type. The relative activities of Os3BGlu6 M251N were 51.6% for *p*NPGlc, 88.9% for GA$_4$-Glc, while the catalytic efficiencies (k_{cat}/K_m) for M251N were reduced to 2.6 from 6.2 mM^{-1}s^{-1} for *p*NPGlc and to 0.08 from 0.13 for GA$_4$-Glc compared to wild type Os3BGlu6. The mutation of the glutamate at residue 178 to alanine (E178A) and glutamine (E178Q) led to complete loss of hydrolytic activity toward *p*NPGlc; and the relative activities to GA$_4$-Glc were reduced to 22.2% and 12.5%, respectively, compared to its wild type. The mutation of the glutamate residue at 394 to glutamine (E394Q) and aspartic acid (E394D) led to complete loss of hydrolytic activity toward *p*NPGlc and GA$_4$-Glc. This work confirmed the roles of

Os3BGlu6 E178 as an acid/base catalyst and E394 as a nucleophile in the retaining catalytic mechanism of family 1 glycoside hydrolases.

The transglucosylation activities were studied for Os3BGlu6 and its mutants. Os3BGlu6 hydrolyzed pNPGlc in MES buffer to pNP and glucose, and no transglucosylation products were formed when GA$_4$ and azide were added as acceptors. Neither Os3BGlu6 wild type nor E178Q could hydrolyze DNP2FG, and no transglucosylation product was formed when GA$_4$ was used as an acceptor to try to rescue the reaction. When pNPGlc or GA$_4$-Glc ester was used as donor and sodium azide as acceptor, both Os3BGlu6 E178Q and E178A could produce transglucosylation products. The prominent transglucosylation product was identified by NMR and mass spectra as β-D-glucopyranosyl azide.

The transglucosylation kinetics were also studied for the acid/base mutants of Os3BGlu6. The activity versus pH profiles for transglucosylation of azide with GA$_4$-Glc donor were determined in NaOAc and MES buffers. The Os3BGlu6 E178Q and E178A mutants showed similar optimum pH range in MES buffer, but different optimum pH in NaOAc buffer, since the acetate ion was acting as a nucleophile in the reaction to rescue the hydrolysis activity of Os3BGlu6 E178A.

The concentrations of donor GA$_4$-Glc and acceptor sodium azide were varied to test their effects on transglucosylation kinetics. When the concentrations of Na-azide acceptor were varied from 0 to 400 mM, while donor GA$_4$-Glc was fixed at 2 mM, the turnover rates, V_0/E_0, of GA$_4$ for Os3BGlu6 E178A slowly increased with the increasing concentration of Na-azide and reached its maximum at 400 mM Na-azide. However, for Os3BGlu6 E178Q, the turnover rates of GA$_4$ slowed down after reaching its maximum at 100 mM Na-azide, indicating that the high concentration of Na-azide was inhibiting the reaction. For Os3BGlu6 E178Q, the k_{cat}/K_m of GA$_4$-Glc was 0.51 when the concentration of Na-azide was 100 mM, and reduced to 0.41 and 0.29 when the concentration of Na-

azide was increased to 200 and 400 mM, respectively. For Os3BGlu6 E178A, the k_{cat}/K_m of GA$_4$-Glc was not changed when the concentration of Na-azide changed to 200 mM from 400mM.

In summary, this work discovered Os4BGlu13 as a β-glucosidase with the relatively high activity to hydrolyze GA$_4$-Glc in the extract of rice seedlings, while Os3BGlu6 was identified to have similar activity by testing recombinant rice β-D-glucosidases expressed in the laboratory. The hydrolysis and transglucosylation activities for Os3BGlu6 and its mutants confirmed its retaining catalysis mechanism and the roles of the residues M251, E178 and E394 in the catalytic process.
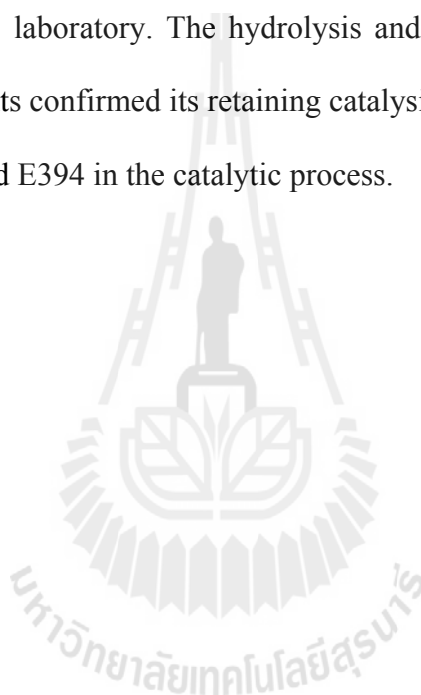
REFERENCES
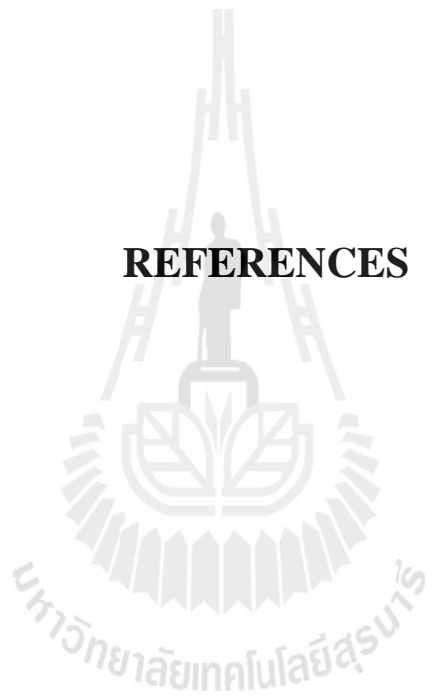
REFERENCES

Asano, N. (2003). Glycosidase inhibitors: Update and perspectives on practical use. **Glycobiology.** 13: 93R-104R.

Barleben, L., Ma, X., Koepke, J., Peng, G., Michel, H. and Stöckigt, J. (2005). Expression, purification, crystallization and preliminary X-ray analysis of strictosidine glucosidase, an enzyme initiating biosynthetic pathways to a unique diversity of indole alkaloid skeletons. **Biochim. Biophys. Acta.** 1747: 89-92.

Brzobohatý, B., Moore, I., Kristoffersen, P., Bako, L., Campos, N., Schell, J. and Palme, K. (1993). Release of active cytokinin by a β-glucosidase localized to the maize root meristem. **Science.** 262: 1051-1054.

Berrin, J.G., Czjzek, M., Kroon, P.A., McLauchlan, W.R., Puigserver, A., Williamson, G. and Juge, N. (2003). Substrate (aglycone) specificity of human cytosolic beta-glucosidase. **Biochem. J.** 373: 41-48.

Berrin, J.G., McLauchlan, W.R., Needs, P., Williamson, G., Puigserver, A., Kroon, P.A. and Juge, N. (2002). Functional expression of human liver cytosolic beta-glucosidase in *Pichia pastoris* insights into its role in the metabolism of dietary glucosides. **Eur. J. Biochem.** 269: 249-258.

Butters, T.D., Dwek, R.A. and Platt, F.M. (2003). Therapeutic applications of imino sugars in lysosomal storage disorders. **Curr. Top. Med. Chem.** 3: 561-574.

Cassán, F., Bottini, R., Schneider, G. and Piccolo, P. (2001). *Azospirillum brasilense* and *Azospirillum lipoferum* hydrolyze conjugates of GA_{20} and metabolize the resultant aglycones to GA_1 in seedlings of rice dwarf mutants. **Plant Physiol.** 125: 2053-2058.

Cantarel, B.L., Coutinho, P.M., Rancurel, C., Bernard, T., Lombard, V. and Henrissat, B. (2009). The Carbohydrate-Active EnZymes database (CAZy): an expert resource for glycogenomics. **Nucleic. Acids Res.** 37: D233-D238.

Chuankhayan, P., Rimlumduan, T., Tantanuch, W., Mothong, N., Kongsaeree, P.T., Metheenukul, P., Svasti, J., Jensen, O.N. and Ketudat Cairns, J.R. (2007). Functional and structural differences between isoflavonoid β-glycosidases from *Dalbergia* sp. **Arch. Biochem. Biophys.** 468: 205-216.

Chuenchor, W., Pengthaisong, S., Robinson, R.C., Yuvaniyama, J., Oonanant, W., Bevan, D.R., Esen, A., Chen, C.J., Opassiri, R., Svasti, J. and Ketudat Cairns, J.R. (2008). Structural insights into rice BGlu1 β-glucosidase oligosaccharide hydrolysis and transglycosylation. **J. Mol. Biol.** 377: 1200-1215.

Chuenchor, W., Pengthaisong, S., Robinson, R.C., Yuvaniyama, J., Svasti, J. and Ketudat Cairns, J.R. (2011). The structural basis of oligosaccharide binding by rice BGlu1 beta-glucosidase. **J. Struct. Biol.** 173: 169-179.

Cicek, M., Blanchard, D., Bevan, D.R. and Esen, A. (2000). The aglycone specificity-determining sites are different in 2,4-dihydroxy-7-methoxy-1,4-benzoxazin-3-one (DIMBOA)-glucosidase (Maize beta-glucosidase) and dhurrinase (Sorghum beta-glucosidase). **J. Biol. Chem.** 275 (26): 20002-20011.

Cobucci-Ponzano, B., Aurilia, V., Riccio, G., Henrissat, B., Coutinho, P.M., Strazzulli, A., Padula, A., Corsaro, M.M., Pieretti, G., Pocsfalvi, G., Fiume, I., Cannio, R., Rossi, M. and Moracci, M. (2010). A new archaeal-glycosidase from *Sulfolobus solfataricus*. **J. Biol. Chem.** 285 (27): 20691-20703.

Czjzek, M., Cicek, M., Zamboni, V., Bevan, DR., Henrissat, B. and Esen, A. (2000). The mechanism of substrate (aglycone) specificity in β-glucosidase is revealed by crystal structures of mutant maize β-glucosidase-DIMBOA, -DIMBOAGlc, and -dhurrin complexes. **Proc. Natl. Acad. Sci**. **USA.** 97: 13555-13560.

Czjzek, M., Cicek, M., Zamboni, V., Burmeister, W.P., Bevan, D.R., Henrissat, B. and Esen, A. (2001). Crystal structure of a monocotyledon (maize ZMGlu1) β-D-glucosidase and a model of its complex with *p*-nitrophenyl β-D-thioglucoside. **Biochem. J.** 354: 37-46.

Dathe, W., Sembdner, G., Kefeli, V.I. and Vlasov, P.V. (1978). Gibberellins, abscisic acid, and related inhibitors in branches and bleeding sap of birch (*Betula pubescens Ehrh*). **Biochem. Physiol. Pflanzen.** 173: 238-248.

Dathe, W., Sembdner, G., Yamaguchi, I. and Takahashi, N. (1982). Gibberellins and growth inhibitors in spring bleeding sap, roots and branches of *Juglans regia* L. **Plant Cell Physiol.** 123: 115-123.

Davies, P.J. (1995). **Plant Hormones: Physiology, Biochemistry and Molecular Biology.** Publisher: Kluwer Academic Publishes, ISBN: 0792329848

de Melo, E.B., Gomes, A.D., Carvalho, I. (2006). Alpha- and beta-glucosidase inhibitors: Chemical structure and biological activity. **Tetrahedron.** 62: 10277-10302.

Dharmawardhana, D.P., Ellis, B.E. and Carlson, J.E. (1995). A β-glucosidase from lodgepole pine specific for the lignin precursor coniferin. **Plant Physiol.** 107: 331-339.

Duroux, L., Delmotte, F.M., Lancelin, J.M., Keravis, G. and Jay-Alleand, C. (1998). Insight into naphthoquinone metabolism: β-glucosidase-catalysed hydrolysis of hydrojuglone β-D-glucopyranoside. **Biochem. J.** 333: 275-283.

Esen, A. (1993). **β-Glucosidase: Biochemistry and Molecular Biology**. Edited by Esen, A. American Chemical Society, Washington DC, 259pp.

Falk, A. and Rask, L. (1995). Expression of a zeatin-O-glucoside-degrading β-glucosidase in *Brassica napus*. **Plant Physiol.** 108: 1369-1377.

Fan, X., Mattheis, J.P., Fellman, J.K. (1998). A role for jasmonates in climacteric fruit ripening. **Planta.** 204: 444-449.

Fowler, T. (1993). Deletion of the *Trichoderma reesei* β-glucosidase gene, *bgl1*. In **β-glucosidases: Biochemistry and Molecular Biology** Edited by Esen, A. Washington DC: American Chemical Society; 56-65. [ACS Symposium Series 533]

Fuchs, P. and Schneider, G. (1996). Synthesis of glucosyl conjugates of [17-^{2}H$_2$] labelled and unlabelled gibberellin A$_{34}$. **Phytochemistry.** 42: 7-10.

Hayashi, Y., Okino, N., Kakuta, Y., Shikanai, T., Tani, M., Narimatsu, H. and Ito, M. (2007). Klotho-related protein is a novel cytosolic neutral beta-glycosyl-ceramidase. **J. Biol. Chem.** 282: 30889-30900.

Hemphill, D.D., Baker, L.R. and Sell, H.M. (1973). Isolation of novel conjugated gibberellins from *Cucumis sarivus* seed. **Can. J. Biochem.** 51: 1647-1653.

Henrissat, B. (1991). A classification of glycosyl hydrolases based on amino acid sequence similarities. **Biochem. J.** 280: 309-316.

Henrissat, B. and Davies, G. (1997). Structural and sequence-based classification of glycosyl hydrolases. **Curr. Opin. Struct. Biol.** 7: 637-644

Hiraga, K., Yokota, T. and Takahashi, N. (1974). Biological activity of some synthetic gibberellin glucosyl esters. **Phytochemistry.** 13: 2371-2376.

Hommalai, G., Chaaiyen, P. and Svasti, J. (2005). Studies on the transglucosylation reactions of cassava and Thai rosewood β-glucosidases using 2-deoxy-2-fluoro-glycosyl-enzyme intermediates. **Arch. Biochem. Biophy.** 442: 11-20.

Hommalai, G., Withers, S.G., Chuenchor, W., Ketudat Cairns, J.R. and Svasti, J. (2007). Enzymatic synthesis of cello-oligosaccharides by mutated rice β-glucosidases. **Glycobiology.** 17: 744-753.

Kai, K., Wakasa, K. and Miyagawa, H. (2007). Metabolism of indole-3-acetic acid in rice: Identification and characterization of N-β-D-glucopyranosyl indole-3-acetic acid and its conjugates. **Phytochemistry.** 68: 2512-2522.

Kempton, J.B. and Withers, S.G. (1992). Mechanism of Agrobacterium β-glucosidase: Kinetic studies. **Biochemistry.** 31: 9961-9969.

Ketudat Cairns, J.R. and Esen, A. (2010). β-Glucosidases. **Cell. Mol. Life Sci.** 67: 3389-3405.

Kobayashi, M., Yamaguchi, I., Murofushi, N., Ota, Y., Takahashi. N. (1984). Endogenous gibberellins in immature seeds and flowering ears of rice. **Agric. Biol. Chem.** 48: 2725-2729.

Kobayashi, M., Yamaguchi, I., Murofushi, N., Ota, Y., Takahashi. N. (1988) Fluctuation and localization of endogenous gibberellins in rice **Agric. Biol. Chem.** 52: 1189-1194.

Koda, Y., Omer, E.A., Yoshihara, T., Shibata, H., Sakamura, S. and Okazawa, Y. (1988). Isolation of a specific potato tuber-inducing substance from potato leaves. **Plant Cell Physiol.** 29: 1047-1051.

Kojima, M., Kamada-Nobusada, T., Komatsu, H., Takei, K., Kuroha, T., Mizutani, M., Ashikari, M., Ueguchi-Tanaka, M., Matsuoka, M., Suzuki, K. and Sakakibara, H. (2009). Highly sensitive and high-throughput analysis of plant hormones using MS-probe modification and liquid chromatography–tandem mass spectrometry: an application for hormone profiling in *Oryza sativa*. **Plant Cell Physiol.** 50: 1201-1214.

Koshioka, M., Yamada, T., Takeno, K., Beall, F.D., Janzen, L.M., Pharis, R.P. and Mander L.N. (1988). Gibberellin & metabolism in rice plant seedlings. In: Abstr.

13th Intern Conf Plant Growth Substances. Edited by Pharis R.P. and Rood S.B. Calgary. No. 217.

Koshland, D.E. (1953). Stereochemistry and mechanism of enzymatic reactions. **Biol. Rev. Camb. Philos. Soc.** 28: 416-436.

Kuntothom, T., Luang, S., Harvey, A.J., Fincher, G.B., Opassiri, R., Hrmova, M. and Ketudat Cairns, J.R. (2009). Rice family GH1 glycosyl hydrolases with β-D-glucosidase and β-D-mannosidase activities. **Arch. Biochem. Biophys.** 491(1-2): 85-95.

Kurogochi, S., Murofushi, N., Ota, Y., Takahashi, N. (1979). Identification of gibberellins in rice plant and quantitative changes of gibberellin A$_{19}$ throughout its life circle. **Planta**. 146: 185-191.

Laemmli, U.K. (1970). Cleavage of structural proteins during the assembly of the head of bacteriophage T4. **Nature.** 227 (5259): 680-685.

Lee, K.H., Piao, H.L., Kim, H.Y., Choi, S.M., Jiang, F., Hartung, W., Hwang, I., Kwak, J.M., Lee, I.J. and Hwang, I. (2006). Activation of glucosidase via stress-induced polymerization rapidly increases active pools of abscisic acid. **Cell.** 126: 1109-1120.

Lenton, J.R. and Appleford, N.E.J. (1991). Gibberellin production and action during germination of wheat. In: **Gibberellins.** Edited by Takahashi, N., Phinney, B.O. and MacMillan, J. New York: Springer. 125-135.

Lenton, J.R., Appleford, N.E.J. and Crokers, J. (1993). Gibberellin dependent α-amylase production in germinating wheat (*Triticum aestivum*) grain. **Frontiers of Gibberellin Research Abstr.** 19. Tokyo Riken.

Lombardi, P. (1990). A rapid, safe and convenient procedure for the preparation and use of diazomethane. **Chem. Ind. London.** 21: 708.

Ly, H.D. and Withers, S.G. (1999). Mutagenesis of glycosidases. **Annu. Rev. Biochem.** 68: 487-522.

Mackenzie, L., Sulzenbacher, G., Divne, C., Jones, T.A., Woldike, H.F., Schulein, M., Withers, S.G. and Davies, G. (1998). Crystal structure of the family 7 endoglucanase (Cel7B) from *Humicola insolens* at 2.2 Å resolution and identification of the catalytic nucleophile by trapping of the covalent glycosyl-enzyme intermediate. **Biochem. J.** 335: 409-416.

MacMillan, J. (2002). Occurrence of gibberellins in vascular plants, fungi, and bacteria. **J. Plant Growth Regul.** 20: 387-442.

MacMillan, J. and Suter, P.J. (1958). The occurrence of gibberellin A1 in higher plants: isolation from the seed of runner bean (*Phaseolus multiflorus*). **Naturwiss.** 45: 46-47.

Mauseth, J.D. (1991). **Botany: An Introduction to Plant Biology.** Philadelphia: Saunders. 348-415.

McCarter, J.D., Yeung, W., Chow, J., Dolphin, D., and Withers, S.G. (1997). Design and synthesis of 2'-deoxy-2'-fluorodisaccharides as mechanism-based glycosidase inhibitors that exploit aglycon specificity. **J. Am. Chem. Soc.** 119: 5792-5797.

McConn, M., Creelman, R.A., Bell, E., Mullet, J.E., Browse, J. (1997). Jasmonate is essential for insect defense in Arabidopsis. **Proc. Natl. Acad. Sci. USA.** 94: 5473-5477.

McIntosh, L.P., Hand, G., Johnson, P.E., Joshi, M., Korner, M., Plesniak, L.A., Ziser, L., Wakarchuk, W.W. & Withers, S.G. (1996). The pKa of the general acid/base

carboxyl group of a glycosidase cycles during catalysis: A 13 C-NMR study of *Bacillus circulans* xylanase. **Biochemistry.** 35: 9958-9966.

Miersch, O., Neumerkel, J., Dippe, M., Stenzel, I., Wasternack, C. (2007). Hydroxylated jasmonates are commonly occurring metabolites of jasmonic acid and contribute to a partial switch-off in jasmonate signaling. **New Phytologist.** 177: 114-127.

Mizutani, M., Nakanishi, H., Ema, J., Ma, S., Noguchi, E., Inohara-Ochiai, M., Fukuchi-Mizutani, M., Nakao, M. and Sakata, K. (2002). Cloning of β-primeverosidase from tea leaves a key enzyme in tea aroma formation. **Plant Physiol.** 130: 2164-2176.

Noguchi, J., Hayashi, Y., Baba, Y., Okino, N., Kimura, M., Ito, M., Kakuta, Y. (2008). Crystal structure of the covalent intermediate of human cytosolic beta-glucosidase. **Biochem. Biophys. Res. Commun.** 374: 549-552.

Opassiri, R., Hua, Y., Wara-Aswapati, O., Akiyama, T., Svasti, J., Esen, A. and Ketudat Cairns, J.R. (2004). β-Glucosidase, exo-β-glucanase and pyridoxine transgluco-sylase activities of rice BGlu1. **Biochem. J.** 379: 125-131.

Opassiri, R., Ketudat Cairns, J.R., Akiyama, T., Wara-Aswapati, O., Svasti, J. and Esen, A. (2003). Characterization of a rice β-glucosidase genes highly expressed in flower and germinating shoot. **Plant Sci.** 165: 627-638.

Opassiri, R., Pomthong, B., Onkoksoong, T., Akiyama, T., Esen, A and Ketudat Cairns, J.R. (2006). Analysis of rice glycosyl hydrolase family I and expression of Os4BGlu12 β-glucosidase. **BMC Plant Biol.** 6: 33.

Park, J.K., Wang, L.X., Patel, H.V., Roseman, S. (2002). Molecular cloning and character-rization of a unique β-glucosidase from *Vibrio cholorae*. **J. Biol. Chem.** 277: 29555-29560.

Phinney, B.O. (1983) The history of gibberellins. In: **The Biochemistry and Physiology of Gibberellins** Edited by Crozier A. Praeger Publishers. USA. 1: 19-52.

Poulton, J.E. (1990). Cyanogenesis in plants. **Plant Physiol.** 94: 401-405.

Qi, M., Jun, H.S. and Forsbert, C.W. (2008). Cel9D, an atypical 1,4-β-D-glucan gluco-hydrolase from *Fibrobacter succinogenes*: characteristics, catalytic residues, and synergistic interactions with other cellulases. **J. Bacteriol.** 109: 1976-1984.

Raven, P.H., Evert, R.F. and Eichhorn, S.E. (1992). **Biology of Plants.** New York: Worth. 545-572.

Rempel, B. and Withers, S. (2008). Covalent inhibitors of glycosidases and their applications in biochemistry and biology. **Glycobiology.** 18: 570-586.

Rivier, L., Gaskin, P., Albone, K.Y.S. and MacMillan, J. (1981). GC-MS Identification of endogenous gibberellins and gibberellin conjugates as their permethylated derivatives. **Phytochemistry.** 20: 687-692.

Rye, C.S. and Withers, S.G. (2000). Glycosidase mechanisms. **Curr. Opin. Chem. Biol.** 4: 573-580.

Salisbury, F.B. and Ross, C.W. (1992). **Plant Physiology.** Belmont, CA: Wadsworth. 357-407, 531-548.

Sansenya, S., Maneesan, J. and Ketudat Cairns, J.R. (2012). Exchanging a single amino acid residue generates or weakens a +2 cellooligosaccharide binding subsite in rice beta-glucosidases. **Carbohydr. Res**. 351: 130-133.

Sansenya, S., Opassiri, R., Kuaprasert, B., Chen, C.J. and Ketudat Cairns, J.R. (2011). The crystal structure of rice (*Oryza sativa* L.) Os4BGlu12, an oligosaccharide and tuberonic acid glucosidehydrolyzing β-glucosidase with significant thiogluco-hydrolase activity. **Arch. Biochem. Biophys.** 510: 62-72.

Sasaki, Y., Asamizu, E., Shibata, D., Nakamura, Y., Kaneko, T., Awai, K., Amagai, M., Kuwata, C., Tsugane, T., Masuda, T., Shimada, H., Takamiya, K., Ohta, H. and Tabata, S. (2001). Monitoring of methyl jasmonate-responsive genes in

Arabidopsis by cDNA macroarray: self-activation of jasmonic acid biosynthesis and crosstalk with other phytohormone signaling pathways. **DNA Res.** 8: 153-161.

Schliemann, W. (1984). Hydrolysis of conjugated gibberellins by β-glucosidases from dwarf rice (*Oryza sativa* L. cv. Tan-ginbozu). **J. Plant Physiol.** 116: 123-132.

Schmidt, J., Schneider, G. and Jensen, E. (1988). Capillary gas chromatography/mass spectrometry of permethylated gibberellin glucosides. **Biomed. Environ. Mass Spectrom.** 17: 7-13.

Schneider, G. (1983). Gibberellin conjugates. In: **The Biochemistry and Physiology of Gibberellins.** Edited by Crazier A. Praeger Publishers. New York. 1: 389-456.

Schneider, G., Jensen, E., Spray, C.R. and Phinney, B.O. (1992). Hydrolysis and reconjugation of gibberellin A_{20} glucosyl ester by seedlings of *Zea mays* L. **Proc. Natl. Acad. Sci. USA.** 89: 8045-8048.

Schneider, G., Fuchs, P. and Schmidta, J. (2002). Evidence for the direct 2beta- and 3beta-hydroxylation of [2H2]GA_{20}-13-O-[6′-2H2]glucoside in seedlings of *Phaseolus coccineus*. **Physiol Plant.** 116: 144-147.

Schneider, G. and Schmidt, J. (1996). Liquid chromatography electrospray ionization mass spectrometry for analyzing plant hormone conjugates. **J. Chromato. A** 728: 371-375.

Schneider, G. and Schliemann, W. (1994). Gibberellin conjugates: an overview. **Plant Growth Regul.** 15: 247-260.

Schneider, G. and Schmidt, J. (1994). Synthesis of 13-O-β-D-glucopyranosylgibberellin A5 β-D-glucopyranosyl ester. **Liebigs. Ann. Chem.** 1994: 1149-1151.

Schneider, G., Schmidt, J. and Phinney, B.O. (1987). GC-MS Identification of GA_{20}-13-O-glucoside formed from GA_{20} in normal plants and dwarf-l mutants of *Zea mays* L. **Plant Growth Regul.** 5: 217-223.

Schneider, G., Schreiber, K., Jensen, E. and Phinney, B.O. (1990). Synthesis of gibberellin A$_{29}$-β-D-glucosides and β–D-glucosyl derivatives of [17-^{13}C, T2] gibberellin A$_5$, GA$_{20}$, and A$_{29}$. **Liebigs. Ann. Chem.** 1990: 491-494.

Schneider, G., Sembdner, G., Jensen, E., Bernhard, U. and Wagenbreth, D. (1992). GC-MS identification of native gibberellin-O-glucosides in pea seeds. **Plant Growth Regul.** 11: 15-18.

Schneider, G., Sembdner, G. and Schreiber, K. (1974). Zur Synthese von Gibberellin-A3-/3-D-glucopyranosiden. **Z. Chem.** 14: 474-475.

Schneider, G., Sembdner, G. and Schreiber, K. (1977). Synthese von O(3)- und O(13)-glucosylierten Gibberellinen. **Tetrahedron.** 33: 1391-1397.

Schneider, G., Sembdner, G. and Phinney, B.O. (1984). Synthesis of GA$_{20}$ glucosyl derivatives and the biological activity of some gibberellin conjugates. **J. Plant Growth Regul.** 3: 207-215.

Schneider, G., Sembdner, G., Schreiber, K. and Phinney, B.O. (1989). Partial synthesis of some physiologically relevant gibberellin glucosyl conjugates. **Tetrahedron.** 45: 1355-l364.

Schneider, G., Schaller, B. and Jensen, R. (1993). Reverse phase high pressure chromato-graphic separation of permethylated free and glucosylated gibberellins - a method for the analysis of gibberellin metabolites. **Phytochem. Anal.** 5: 111-115.

Schreiber, K., Weiland, J. and Sembdner, G. (1967). Isolierung und Struktur eines Gibberellin-glucosides. **Tetrahedron Lett.** 4285-4288.

Schreiber, K., Weiland, J. and Sembdner, G. (1970). Isolierung von Gibberellin-A$_8$-O(3)-β-D-glucopyranosid aus Früchten von *Phaseolus coccineus.* **Phytochemistry.** 9: 189-198.

Schreiber, K., Schneider, G., Sembdner, G. and Focke, I. (1966). Gibbereline-X. Isolierung von O-Acetyl-Gibberellinsaure als Stoffwechselprodukt von *Fusaium moniliforme* Sheld. **Phytochemistry.** 5: 1221-1225.

Schreiber, K., Weiland, J. and Sembdner, G. (1969). Synthese von O(2)-β-D-Glucopyranosyl-gibberellin-A3-methylester. **Tetrahedron.** 25: 5541-5545.

Sembdner, G., Weiland, J., Aurich, O. and Schreiber, K. (1968). Isolation, structure and metabolism of a gibberellin glucoside. **Plant Growth Regul. S.C.I. Monograph.** 31: 70-86. London.

Sembdner, G., Atzorn, R. and Schneider, G. (1994). Plant hormone conjugation. **Plant Mol. Biol.** 26: 1459-1481.

Senns, B., Fuchs, P. and Schneider, G. (1998). GC-MS quantification of GA_{20}-13-O-glucoside and GA_8-2-O-glucoside in developing barley caryopses. **Phytochemistry.** 48: 1275-1280.

Seshadri, S., Akiyama, T., Opassiri, R., Kuaprasert, B. and Cairns, J.K. (2009). Structural and enzymatic characterization of Os3BGlu6, a rice beta-glucosidase hydrolyzing hydrophobic glycosides and (1→3)- and (1→2)-linked disaccharides. **Plant Physiol.** 151(1): 47-58.

Seto, Y., Hamada, S., Matsuura, H., Matsushige, M., Satou, C., Takahashi, K., Masuta, C., Ito, H., Matsui, H. and Nabeta, K. (2009). Purification and cDNA cloning of a wound inducible glucosyltransferase active toward 12-hydroxy jasmonic acid. **Phytochemistry.** 70: 370-379.

Sponsel, V.M. and Hedden, P. (2004). Gibberellin biosynthesis and metabolism In: **Plant Hormones: Biosynthesis, Signal Transduction, Action!** Edited by Davies, P.J. Kluwer, Dordrecht. 62-98.

Staswick, P.E., Su, W. and Howell, S.H. (1992). Methyl jasmonate inhibition of root growth and induction of a leaf protein are decreased in an *Arabidopsis thaliana* mutant. **Proc. Natl. Acad. Sci**. **USA.** 89: 6837-6840.

Stintzi, A. and Browse, J. (2000). The Arabidopsis male-sterile mutant, opr3, lacks the 12-oxophytodienoic acid reductase required for jasmonate synthesis. **Proc. Natl. Acad. Sci. USA.** 97: 10625-10630.

Stoddart, J.L. and Venis, M.A. (1980). Molecular and subcellular aspects of hormone action. In: **Encyclopedia of Plant Physiology.** Edited by MacMillan, J. Springer-Verlag, Berlin/Heidelberg/New York. New Series, 9: 445-510.

Sue, M., Yamazaki, K., Yajima, S., Nomura, T., Matsukawa, T., Iwamura, H. and Miyamoto, T. (2006). Molecular and structural characterization of hexameric beta-D-glucosidases in wheat and rye. **Plant Physiol.** 141: 1237-1247.

Suzuki, Y., Kurogochi, S., Murofushi, N., Ota, Y., Takahashi, N. (1981). Seasonal changes of GA_1, GA_{19} and abscisic acid in three rice cultivars. **Plant Cell Physiol.** 22: 1085-1093.

Tamura, S. 1990. Historical aspects of gibberellins. In: **Gibberellins** Edited by Takahashi, N., Phinney, B.O. and Macmillan, J. Springer-Verlag New York. 1-8.

Tribolo, S., Berrin, J.G., Kroon, P.A., Czjzek, M. and Juge, N. (2007). The crystal structure of human cytosolic beta-glucosidase unravels the substrate aglycone specificity of a family 1 glycoside hydrolase. **J. Mol. Biol.** 370: 964-975.

Verdoucq, L., Czjzek, M., Moriniere, J., Bevan, D.R. and Esen, A. (2003). Mutational and structural analysis of aglycone specificity in maize and sorghum β-glucosidases. **J. Biol. Chem.** 278: 25055- 25062.

Verdoucq, L., Morinie, J., Bevan, D.R., Esen, A., Vasella, A., Henrissat, B. and Czjzek, M. (2004). Structural determinants of substrate specificity in family 1 β-D-glucosidases. **J. Biol. Chem.** 279: 31796-31803.

Vijayan, P., Shockey, J., Lévesque, C.A., Cook, R.J. and Browse, J. (1998). A role for jasmonate in pathogen defense of Arabidopsis. **Proc. Natl. Acad. Sci. USA.** 95: 7209-7214.

Vocadlo, D.J., Davies, G.J., Laine, R. and Withers, S.G. (2001). Catalysis by hen egg-white lysozyme proceeds via a covalent intermediate. **Nature.** 412: 835-838.

Wakuta, S., Hamada, S., Ito, H., Matsuura, H., Nabeta, K. and Matsui, H. (2010). Identification of a β-glucosidase hydrolyzing tuberonic acid glucoside in rice (*Oryza sativa L.*) **Phytochemistry.** 71: 1280-1288.

Wang, Q., Graham, R.W., Trimbur, D., Warren, R.A.J. and Withers, S.G. (1994). Changing enzymic reaction mechanisms by mutagenesis: conversion of a retaining glucosidase to an inverting enzyme. **J. Am. Chem. Soc.** 116: 11594-11595.

Wang, Q., Trimbur, D., Graham, R., Warren, R.A.J. and Withers, S.G. (1995). Identification of the acid/base catalyst in *Agrobacterium faecalis* β-glucosidase by kinetic analysis of mutants. **Biochemistry.** 34: 14554-14562.

Wasternack, C. (2007). Jasmonates: an update on biosynthesis, signal transduction and action in plant stress response, growth and development. **Ann. Bot.** 100: 681-697.

Wierstra, I. and Kloppstech, K. (2000). Differential effects of methyl jasmonate on the expression of the early light-inducible proteins and other light-regulated genes in barley. **Plant Physiol.** 124: 833-844.

Withers, S.G., Warren, R.A.J., Street, I.P., Rupitz, K., Kempton, J.B. and Aebersold, R. (1990). Unequivocal demonstration of the involvement of a glutamate residue as

a nucleophile in the mechanism of a retaining glycosidase. **J. Am. Chem. Soc.** 112: 5887-5889.

Yokota, T., Hiraga, K., Yamane, H. and Takahashi, N. (1975). Mass spectrometry of trimethylsilyl derivatives of gibberellin glucosides and glucosyl esters. **Phytochemistry.** 14: 1569-1574.

Yoshihara, T., Omer, E.A., Koshino, H., Sakamura, S., Kikuta, Y., Koda, Y. (1989). Structure of a tuber-inducing stimulus from potato leaves (*Solanum tuberosum L.*). **Agric. Biol. Chem.** 53: 2835-2837.

Zechel, D.L. and Withers, S.G. (2000). Glycosidase mechanisms: Anatomy of a finely tuned catalyst. **Acc. Chem. Res.** 33: 11-18.

Zhu, S., Jiang, Z.Q., Liu, J.C., Shen, S.H., Cao, S.S. and Chen. M.Y. (1999). Genetic analysis on response of new dwarf to gibberellic acid and its sensitivity to gibberellic acid. **Guizhou Agric. Sci.** 27: 12-15.

CURRICULUM VITAE

NAME   Mrs Yanling Hua

DATE OF BIRTH   April 28, 1965

PLACE OF BIRTH   Hebei Province, P.R. China

EDUCATION

2007-Present   Ph.D. Candidate in School of Biochemistry, Institute of
                      Science, Suranaree University of Technology, Nakhon
                      Ratchasima, Thailand

1986-1989   **Master of Science**, Institute of Element -Organic
                      Chemistry, Nankai University, Tianjin, P.R.China

1982-1986   **Bachelor of Science**, Department of Chemistry, Nankai
                      University, Tianjin, P.R.China

WORK EXPERIENCE:

September 1997-Present: Scientist, Instrumental Analysis Division, Center for
                         Scientific and Technological Equipment, Suranaree
                         University of Technology, Thailand.

September 2003-September 2007:

                         Lecturer, part time. School of English, Institute of Science,
                         Suranaree University of Technology, Thailand.

September 1989-December 1994:

                         Researcher, Institute of Element-Organic Chemistry,
                         Nankai University, Tianjin, P.R.China